



**UNIVERSIDADE FEDERAL DO PARÁ
INSTITUTO DE GEOCIÊNCIAS
PROGRAMA DE PÓS-GRADUAÇÃO EM GEOLOGIA E GEOQUÍMICA**

TESE DE DOUTORADO N° 114

**SOLEIRAS E ENXAMES DE DIQUES MÁFICOS DO SUL-
SUDOESTE DO CRÁTON AMAZÔNICO**

Tese apresentada por:

GABRIELLE APARECIDA DE LIMA

Orientador: Prof. Dr. Moacir José Buenano Macambira (UFPA)

Co-orientadora: Prof^ª. Dr^ª. Maria Zélia Aguiar de Sousa (UFMT)

**BELÉM
2016**

Dados Internacionais de Catalogação-na-Publicação (CIP)
Sistema de Bibliotecas da UFPA

Lima, Gabrielle Aparecida de, 1987-
Soleiras e enxames de diques máficos do sul-sudoeste do
Cráton Amazônico / Gabrielle Aparecida de Lima. - 2016.

Orientador: Moacir José Buenano Macambira;
Coorientadora: Maria Zélia Aguiar de
Sousa.

Tese (Doutorado) - Universidade Federal do
Pará, Instituto de Geociências, Programa de Pós-
Graduação em Geologia e Geoquímica, Belém, 2016.

1. Magmatismo. 2. Geologia estrutural. 3.
Geocronologia. 4. Petrologia. I. Título.

CDD 22. ed. 552.1



UNIVERSIDADE FEDERAL DO PARÁ
INSTITUTO DE GEOCIÊNCIAS
PROGRAMA DE PÓS-GRADUAÇÃO EM GEOLOGIA E GEOQUÍMICA

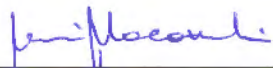
**SOLEIRAS E ENXAMES DE DIQUES MÁFICOS DO SUL-
SUDOESTE DO CRÁTON AMAZÔNICO**

TESE APRESENTADA POR:
GABRIELLE APARECIDA DE LIMA

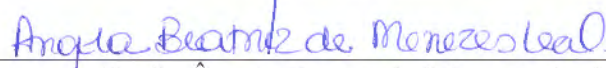
Como requisito parcial à obtenção do Grau de Doutor em Ciências na Área de
GEOQUÍMICA E PETROLOGIA

Data da Aprovação: 19/08/2016

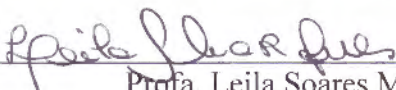
Banca Examinadora:



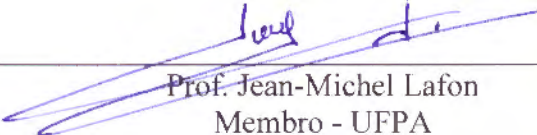
Prof. Moacir José Buenano Macambira
Orientador - UFPA



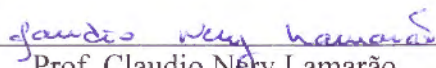
Profa. Ângela Beatriz de Menezes Leal
Membro - UFPA



Profa. Leila Soares Marques
Membro - USP



Prof. Jean-Michel Lafon
Membro - UFPA



Prof. Claudio Nery Lamarão
Membro - UFPA

À minha doce e encantadora Alice.

AGRADECIMENTOS

Ao Criador pela vida e por me agraciar com saúde e sabedoria suficientes para cumprir mais esta etapa.

Aos meus orientadores, Prof. Dr. Moacir Buenano Macambira e Prof^ª. Dr^ª. Maria Zélia Aguiar de Sousa, pelos ensinamentos, disponibilidade, dedicação, amizade e afetuosidade.

Ao Programa de Pós-Graduação em Geologia e Geoquímica (UFPA) e à Faculdade de Geociências (UFMT) pela infraestrutura disponibilizada.

Aos professores da UFMT e UFPA que contribuíram com minha formação acadêmica e científica.

Ao Grupo de Pesquisa em Evolução Crustal e Tectônica (Guaporé) pelo suporte à pesquisa, e a seus membros pelas ricas trocas de experiências que tanto me engrandecem.

Aos colegas de trabalho do Instituto de Engenharia (UFMT) pelo convívio e por possibilitarem meu afastamento para conclusão da tese.

Ao Conselho Nacional de Desenvolvimento Científico e Tecnológico - CNPq pela concessão de bolsa de doutorado. À Fundação de Amparo à Pesquisa do Estado de Mato Grosso - FAPEMAT (Proc. 222473/2015), à Fundação de Amparo à Pesquisa do Estado de São Paulo - FAPESP (Proc. 2011/50887-6), ao Conselho Nacional de Desenvolvimento Científico e Tecnológico - CNPq (Proc. 479779/2011-2) e ao Instituto Nacional de Ciência e Tecnologia de Geociências da Amazônia - GEOCIAM pelo suporte financeiro ao desenvolvimento da pesquisa.

A todos meus familiares, em especial aos meus pais, Luiz e Maria, que sempre me deram suporte e serviram de base e aos meus queridos sobrinhos, amo vocês.

Ao meu esposo, Amarildo, pelo carinho, incentivo, companheirismo e encorajamento, durante todo este período e por ser um exemplo de Pai. Te amo infinitamente.

À minha filha Alice, luz da minha vida. A você dedico todos os momentos. Amor incondicional.

Por fim, agradeço a todos que contribuíram de alguma forma para a construção deste trabalho.

RESUMO

Soleiras e enxames de diques máficos constituem importante ferramenta para o entendimento dos processos geodinâmicos, especialmente por marcarem o início de grandes eventos tectônicos extensionais, além de serem indicadores importantes da natureza e evolução das fontes mantélicas no tempo geológico. Na porção S-SW do Cráton Amazônico, ocorrências de soleiras e enxames de diques proterozoicos são relatadas no oriente boliviano, em Mato Grosso e Mato Grosso do Sul. Como exemplos têm-se os enxames de diques das suítes intrusivas Huanchaca, Rancho de Prata e Rio Perdido, bem como as soleiras máficas Huanchaca, Salto do Céu e Rincón del Tigre. O objetivo desta pesquisa é caracterizar natureza, evolução petrológica e tectônica do episódio magmático máfico, relacionado a eventos tafrogênicos responsáveis pela ruptura ou tentativa de ruptura da crosta continental. Para tal propósito foi feita uma abordagem multidisciplinar, envolvendo o mapeamento geológico, a realização de análises petrográfica, litoquímica e geocronológica (U-Pb ID-TIMS e Ar-Ar). As unidades estudadas estão localizadas nos municípios de Vila Bela da Santíssima Trindade, Nova Lacerda, Conquista D'Oeste e Salto do Céu, em Mato Grosso, Porto Murtinho e Caracol, no Mato Grosso do Sul. As rochas da Suíte Salto do Céu ocorrem na região dos municípios de Salto do Céu e Rio Branco (MT) e afloram como soleiras e derrames. As soleiras encontram-se alojadas em rochas pelíticas, até então inseridas como parte do Grupo Aguapeí, com baixos valores de mergulho, quase sempre para WSW. Os derrames recobrem a mesma unidade sedimentar e apresentam estruturas verticais internas e de topo, típicas de fluxos basálticos de pequena espessura. Vesículas e amígdalas, além de feições como dobras de fluxo e brechas são comumente observadas. Petrograficamente, essas rochas são mesocráticas a melanocráticas, cinza-esverdeadas a pretas, equigranulares variando, em geral, de muito finas até médias. As soleiras são compostas por diabásios e gabros maciços que ao microscópio apresentam texturas ofítica, subofítica, intergranular e coronítica. Constituem-se, essencialmente, por plagioclásio e piroxênio, tendo como minerais acessórios: opacos, cristais aciculares de apatita e subédricos de titanita. Os derrames constituem-se de basaltos e diabásios com texturas ofítica, subofítica, hialofítica, porfirítica ou amigdaloidal em matriz pseudo-traquítica e, em alguns exemplares, vitrofírica. Os componentes principais correspondem a cristais de plagioclásio e piroxênio, além de vidro reliquiar. As amígdalas são arredondadas a elipsoidais, preenchidas por material fibroso a fibro-radiado, composto por zeólitas, clorita, fluorita e opacos. As soleiras e derrames têm

afinidade toleítica, sendo classificadas como basaltos gerados em ambiente intraplaca continental. Essa unidade apresenta idade U-Pb (ID-TIMS), obtida em badeleíta, de 1439 ± 4 Ma. Dados geocronológicos Ar-Ar em plagioclásio e anfibólio, forneceram idades plateau de 1021 ± 5 Ma e integrada de 1385 ± 9 Ma, respectivamente. Os diques máficos da Suíte Intrusiva Rancho de Prata foram identificados em diversos sítios nas regiões de Nova Lacerda e Conquista D'Oeste (MT), ao longo de uma faixa com direção NNW, de aproximadamente 30 km de largura e 150 km de extensão, se apresentando como enxame de intrusões paralelas, orientadas segundo a direção $N30^{\circ}-40^{\circ}W$ com mergulhos íngremes. Exibem-se isentos de deformação e metamorfismo e mantêm contato intrusivo com as rochas gnáissicas, graníticas e metavulcanossedimentares do embasamento. As rochas dessa unidade caracterizam-se como gabros, diabásios e basaltos, faneríticos, afaníticos a porfíricos, de granulação muito fina a média. Apresentam-se melanocráticas de cor cinza-escuro a preta, exibindo estrutura maciça, por vezes com foliação discreta paralela às paredes do dique. Microscopicamente, essas rochas são holo a hipocristalinas, e apresentam textura porfírica, intergranular, sub-ofítica a ofítica, sendo constituídas, predominantemente, por plagioclásio, clino e ortopiroxênio, olivina e anfibólio. Nos basaltos encontra-se esporadicamente vidro intergranular de cor marrom-escuro. Litoquimicamente classificam-se como basaltos e andesi-basaltos. O magmatismo é do tipo subalcalino e toleítico que, pelas características químicas, se assemelham a basaltos continentais. Os padrões de distribuição dos elementos terras raras (ETR) estão em dois grupos: um fortemente fracionado e enriquecido em ETR leves e outro com pouco fracionamento, com razões médias La/Yb, respectivamente, iguais a 3,22 e 1,26. Idade U-Pb (ID-TIMS), em badeleíta, de 1387 ± 17 Ma foi obtida para este enxame. Dados Ar-Ar em plagioclásio apresentam idades plateaus de 967 ± 5 Ma e 980 ± 7 Ma. Já os dados em anfibólio são heterogêneos, com idades integradas de 1495 ± 8 Ma e 1509 ± 7 Ma. As soleiras e os diques máficos da Suíte Intrusiva Huanchaca estão inseridos no contexto geológico do Terreno Paraguá, em sua porção não afetada pelos efeitos da Orogenia Sunsás (1,1 a 0,9 Ga). Os diques têm como encaixantes rochas do embasamento do Grupo Aguapeí, representadas pelos granitos mesoproterozoicos do Complexo Granitoide Pensamiento, e ortognaisses paleoproterozoicos Shangri-lá e Turvo, do Complexo Metamórfico Chiquitania; enquanto as soleiras encontram-se alojadas nos pelitos e arenitos da Formação Vale da Promissão, Grupo Aguapeí. As soleiras afloram como blocos e lajedos com contatos sempre abruptos e paralelos ao acamamento das rochas sedimentares. Os diques afloram em pequenas e descontínuas

cristas orientadas segundo a direção ENE ou como blocos arredondados a angulosos, isolados no terreno granítico-gnáissico, cuja direção preferencial varia entre N70°-90°E. As soleiras, caracterizadas por gabros e diabásios, exibem cor cinza-esverdeado a preta e granulação fina a média. Opticamente, são rochas holocristalinas de textura sub-ofítica a ofítica e, mais raramente, intergranular. Rochas cumuláticas, de ocorrência restrita, foram identificadas com paragênese e texturas semelhantes diferenciando-se pela presença de olivina e grande quantidade de minerais máficos. As rochas das soleiras consistem, essencialmente, de plagioclásio, piroxênio, anfibólio, opacos, e em algumas delas, feldspato alcalino e quartzo com intercrescimento gráfico. Os diques apresentam cor cinza-escuro a cinza-esverdeado, granulação variando da margem para a porção central do corpo de muito fina ou vítrea a média, respectivamente. Classificam-se como diabásios e basaltos, respectivamente holo e hipocristalinos, constituídos essencialmente por plagioclásios, piroxênios e olivina. Ao exame óptico, os diabásios apresentam texturas inequigranular, sub-ofítica e subordinadamente ofítica, granulação fina a média, enquanto nos basaltos domina textura porfirítica, glomeroporfirítica, vitrofírica e, mais raramente, intersertal e hialofítica. Litoquimicamente, os diques e soleiras classificam-se como basaltos andesíticos de magmatismo subalcalino do tipo toleítico, de ambiente intraplaca continental. Os ETR mostram que as rochas das soleiras são mais enriquecidas em ETRtotais do que as dos diques e apresentam uma considerável variação vertical ao envelope, no entanto a ele paralelizada. Idades plateaus Ar-Ar foram obtidas para as soleiras, tanto para o plagioclásio (948 ± 5 Ma) como para o anfibólio (1113 ± 11 Ma). Ainda para as soleiras, foi conseguida uma idade U-Pb (ID-TIMS), em badeleíta, de $1111,5 \pm 1,9$ Ma. O exame de diques da Suíte Intrusiva Rio Perdido ocorre encaixado em rochas paleoproterozoicas, ao longo do Terreno Rio Apa (SW do MS) e no Paraguai. Os diques são tabulares a lenticulares, com espessura entre 1 e 30 m, são preferencialmente paralelos segundo as direções N70°-90°E e N70°-90°W, exibem contatos abruptos e discordantes ao trend geral NS. São compostos por diabásios de granulação muito fina a fina e microgabros finos a médios, isotrópicos, sem quaisquer vestígios de deformação dúctil e metamorfismo. Ao microscópio, classificam-se como holocristalinos, com textura ofítica a subofítica, intergranular, por vezes porfirítica, e localmente quenching, com morfologia do tipo “cauda de andorinha”. Constituem-se essencialmente por plagioclásio, piroxênios e olivina. Apresentam trend toleítico, com enriquecimento em FeO_t em relação ao MgO para valores de álcalis relativamente constantes. Classificam-se como basaltos e basaltos

andesíticos e quanto à ambiência tectônica, se assemelham à basaltos intraplaca fanerozoicos. O comportamento dos ETR, mostra forte fracionamento de ETR pesados em relação aos ETR leves, com razões La/Yb entre 2,8 e 6,2, com anomalia pouco expressiva ou inexistente de Eu. Dados recentes U-Pb (ID-TIMS), em badeleíta, forneceram idade de 1110 Ma. O Complexo Ígneo Rincón del Tigre corresponde a uma intrusão acamadada, espessa, alojada em rochas do Grupo Sunsás (abaixo) e Grupo Vibosi (acima). Foi denominado na região de Rincón del Tigre (Bolívia), e caracterizado como um registro ígneo relacionado à Orogenia Sunsás. As rochas que compõem esse complexo foram litoestratigraficamente divididas em três unidades: Ultramáfica (basal), Máfica (intermediária) e Félsica (superior). A Unidade Ultramáfica constitui-se por dunito serpentizado, harzburgito, olivina bronzitito, bronzita picrito e melanorito, enquanto a Unidade Máfica por norito e gabro. A Unidade Félsica está representada por granófiro. Idade U-Pb (ID-TIMS), em badeleíta, de $1110,4 \pm 1,8$ Ma, obtida a partir de amostra coletada da Unidade Félsica, demonstram similaridade cronológica com rochas de suítes graníticas sin e pós-orogênicas que ocorrem na província Sunsás-Aguapeí, na Bolívia e no Brasil. Com base em dados K-Ar com valores entre 875 e 1006 Ma, todas as unidades acima descritas eram agrupadas a um evento magmático e interpretadas como uma LIP associada à tentativa de ruptura do supercontinente Rodínia. Com base nos novos dados geocronológicos de precisão (U-Pb TIMS em badeleíta e Ar-Ar em anfibólio e plagioclásio) e informações de campo e petrológicas, essa hipótese não se confirma. Existem dois episódios de magmatismo fissural anteriores a aglutinação desse supercontinente: o mais antigo entre 1387 e 1439 Ma e o mais jovem em torno de 1110 Ma. Considerando a evolução do sudoeste do Cráton Amazônico, o episódio mais velho, marcado pelo enxame de diques Rancho de Prata e derrames e soleiras Salto do Céu, provavelmente esteja associado aos estágios pós-orogênicos do Arco Magmático Santa Helena do Terreno Jauru; o evento mais jovem, restrito aos Terrenos Paraguá e Rio Apa, representado pelas suítes Huanchaca, Rio Perdido e pelo Complexo Rincón del Tigre, integra uma LIP esteniana na porção sul-sudoeste do Cráton Amazônico, evoluída durante uma tentativa de ruptura continental responsável pelo desenvolvimento do Aulacógeno Aguapeí. As Faixas Sunsás e Aguapeí, marcam o período de aglutinação do supercontinente Rodínia e afetam metamórfica e deformacionalmente parte desta LIP esteniana.

Palavras-chave: Magmatismo Máfico. Tectônica Distensiva. Geocronologia U-Pb e Ar-Ar. Petrologia.

ABSTRACT

Sills and mafic dyke swarms are an important tool for understanding geodynamic processes once they mark the beginning of large extensional tectonic events, but also they are fundamental indicators of nature and evolution of mantle sources through geological time. In the S-SW Amazon Craton, Proterozoic sills and dyke swarms are reported in Eastern Bolivia, and in the Brazilian states of Mato Grosso and Mato Grosso do Sul. There are examples, such as the dyke swarms of the Huanchaca, Rancho de Prata, and Rio Perdido intrusive suites as well as mafic sills of the Huanchaca, and Salto do Céu suites, and Rincón del Tigre Complex. This work aims to characterize the nature, petrological evolution and tectonics of the mafic magmatic event related to tectogenetic events that are responsible for the break-up or attempted break-up of continental crust. Several tools were used in order to clarify this issue, such as geological mapping, petrographic, litho-geochemical and geochronological (U-Pb ID-TIMS and Ar-Ar) analysis. The studied units are sited in the municipalities of Vila Bela da Santíssima Trindade, Nova Lacerda, Conquista D'Oeste, and Salto do Céu in Mato Grosso, and in Porto Murtinho and Caracol in Mato Grosso do Sul. Rocks of the Salto do Céu suite occur in the municipalities of Salto do Céu and Rio Branco (MT), and outcrop as sills and lava flows. Sills are emplaced into pelitic rocks of the Aguapeí Group usually with shallow dips towards WSW. Lava flows overly the same sedimentary unit and show internal vertical structures and flow-top structures that are typical of thin basaltic flows. Vesicles and amygdaloids are commonly observed along with flow-folds and breccias. Petrographically, these rocks are mesocratic to melanocratic, greenish-gray to black, and equigranular varying from very fine- to medium-grained. Sills consist of diabases and massif gabbros that under the microscope show ophitic, sub-ophitic, intergranular, and coronitic textures. They are essentially composed of plagioclase and pyroxene having its accessory assemblage represented by opaques, acicular apatite and subhedral sphene. Lava flows, in turn, consist of basalts and diabases that commonly displays ophitic, sub-ophitic, hyalophitic, porphyritic or amygdaloidal textures in a pseudo-trachytic groundmass; some samples exhibit vitrophyric texture. The main components are plagioclase, pyroxene, and relict glass. Amygdaloids are rounded to ellipsoidal filled with fibrous to fibro-radiated material which is composed of zeolites, chlorite, fluorite, and opaques. Sills and lava flows have tholeiitic affinity, and are classified as intraplate basalts. This suite shows a U-Pb (ID-TIMS) baddeleyite age of 1439 ± 4 Ma. ^{40}Ar - ^{39}Ar analysis of plagioclase and amphibole provided a plateau age of 1021 ± 5

Ma, and an integrated age of 1385 ± 9 Ma, respectively. Numerous mafic dykes of the Rancho de Prata Intrusive Suite occur in the surroundings of Nova Lacerda and Conquista D'Oeste (MT) along an array about 30 km-wide and 150 km-long trending NNW. They occur as parallel dyke swarms striking $N30^{\circ}\text{--}40^{\circ}\text{W}$ with steep dips. There are no records of deformation or metamorphism on these rocks which occur in intrusive contact with gneissic, granitic and metavolcanosedimentary rocks of the basement. These mafic dykes consist of gabbros, diabases, and basalts, very fine to medium-grained, which exhibit phaneritic, aphanitic to porphyritic textures. They are melanocratic dark-gray to black, with massive structure, in places with discrete foliation parallel to the dyke walls. Microscopically, these rocks are holo- to hypocrystalline, and show porphyritic, intergranular, and subophitic to ophitic textures, and are essentially composed of plagioclase, clinopyroxene and orthopyroxene, olivine and amphibole. Dark-brown intergranular glass is seldom observed in basalts. Lithochemical studies allow us to classify these rocks as basalts and andesitic-basalts. The magmatism is sub-alkaline to tholeiitic whose chemical affinity is compatible with continental basalts. Two groups are observed in rare earth elements distribution patterns: one strongly fractionated and enriched in light ETR, and another one weakly fractionated with medium La/Yb ratios, respectively, 3.22 and 1.26. A U-Pb (ID-TIMS) baddeleyite age of 1387 ± 17 Ma was obtained for the dyke swarms. $^{40}\text{Ar}\text{--}^{39}\text{Ar}$ analysis of plagioclase provided plateau ages of 967 ± 5 Ma and 980 ± 7 Ma. However, $^{40}\text{Ar}\text{--}^{39}\text{Ar}$ age-spectrum data for amphibole is heterogeneous, therefore provide integrated ages of 1495 ± 8 Ma and 1509 ± 7 Ma. Sills and mafic dykes of the Huanchaca Intrusive Suite are sited in the portion of the Paraguá Terrane which is not affected by the Sunsás Orogeny (1.1 to 0.9). Dykes occur emplaced into the basement rocks underlying the Aguapeí Group that are represented by the Mesoproterozoic granites Guaporeí and Passagem that form part of the Pensamiento Granitoid Complex, as well as by the Paleoproterozoic orthogneisses Shangri-lá and Turvo that occur within the Chiquitania Metamorphic Complex; sills, in turn, are emplaced into the pelites and sandstones of the Vale da Promissão Formation (Aguapeí Group). Sills outcrop as blocks and low-lying outcrops in abrupt and parallel contacts to the layering of sedimentary rocks. On the other hand, dykes outcrop as small and discontinuous trending-ENE crests, or as single, rounded and angular blocks in the granitic-gneissic terrane whose main orientation varies between $N70^{\circ}\text{--}90^{\circ}\text{E}$. Sills consist of gabbros and diabases, are greenish-gray to black in colour, and fine- to medium-grained. Optically, these are holocrystalline with sub-ophitic to

ophitic texture, and rare intergranular texture. Cumulate rocks of restricted occurrence were identified with paragenesis and textures similar to each other whose difference is the presence of olivine and high content of mafic minerals. These rocks are essentially composed of plagioclase, pyroxene, amphibole, opaques, and in a few of them, alkali-feldspar and quartz displaying graphic intergrowth are also observed. Dykes are dark-gray to greenish-gray with grain size decreasing from the rock wall towards the center of the body from very fine-grained or glassy to medium-grained, respectively. They are classified as diabases and basalts, respectively, holo to hypocrySTALLINE, and have an essential composition of plagioclase, pyroxene and olivine. Under the microscope, diabases show inequigranular, sub-ophitic, and subordinate ophitic textures, and are fine- to medium-grained, while basalts display porphyritic, glomeroporphyritic, and textures vitrophyric, and rarely intersertal to hyalophitic textures. Chemically, dykes and sills are classified into sub-alkaline andesitic basalts (tholeiitic) formed in intraplate settings. REE patterns show that sills are richer in total REE relative to the dykes, as well as show significant vertical variation with respect to the REE pattern envelope, yet parallel to it. Ar-Ar plateau ages were obtained for the sills both from plagioclase (948 ± 5 Ma), and amphibole (1113 ± 11 Ma). A U-Pb (ID-TIMS) baddeleyite age of 1111.5 ± 1.9 Ma was also obtained for sills. The dyke swarms that form part of the Rio Perdido Intrusive Suite occur emplaced into Paleoproterozoic rocks sited in the Rio Apa Terrane (SW of Mato Grosso do Sul), and Paraguay. Dykes are tabular to lenticular, 1 to 30 m thick, generally striking N70°-90°E and N70°-90°W. They exhibit abrupt and discordant contact with respect to the general NS trend. Dykes consist of very fine- to fine-grained diabases, and fine- to medium-grained microgabbros, both with no evidence of ductile deformation and metamorphism. Under the microscope, they are holocrystalline with ophitic to sub-ophitic, intergranular, and, in places, porphyritic textures, as well as quench textures in which they display swallow-tail shape. They contain essential plagioclase, pyroxenes and olivine, and show a tholeiitic trend with FeO_t enrichment relative to MgO for relatively constant alkali contents. They are classified as basalts and andesitic basalts that are similar to Phanerozoic intraplate basalts. REE patterns show strong fractionation of light REE relative to the heavy, with La/Yb ratios varying between 2.8 and 6.2 and Eu anomalies subtly negative or absent. Recent U-Pb (ID-TIMS) data on baddeleyite provided an age of 1110 Ma. The Rincón del Tigre Igneous Complex is a thick layered intrusion that intrudes into the Sunsás Group (below), and into the Vibosi Group (above). Its name is due to the region of Rincón del Tigre

in Bolivia, and is characterized as an igneous event related to the Sunsás Orogeny. It is divided into three units: Ultramafic (basal), Mafic (intermediate), and Felsic (superior). The Ultramafic Unit is composed of serpentinized dunite, harzburgite, olivine bronzite, bronzite picrite, and melanorite, while the Mafic Unit is composed of norite and gabbro. The Felsic Unit is represented by granophyres. A U-Pb (ID-TIMS) baddeleyite age of 1110.4 ± 1.8 Ma was obtained from the Felsic Unit, and show chronological similarity to the syn- and post-orogenic granitic suites that occur in the Sunsás-Aguapeí province sited in Bolivia, and Brazil. Based on K-Ar ages varying between 1006 and 875 Ma, the units above were attributed to a single magmatic event and interpreted as a LIP that formed during an attempted breakup of Rodinia. Now, based on new precise geochronologic data (U-Pb TIMS on baddeleyite, and Ar-Ar on amphibole and plagioclase), and field and petrological data, this hypothesis is not supported anymore. There were two fissural magmatic events prior to the agglutination of this supercontinent: the older one with ages of 1439 and 1387 Ma, and the younger one around 1110 Ma old. By taking into account the evolution of the Amazon Craton, the older episode is marked by dyke swarms of the Rancho de Prata suite as well as lava flows and sills of the Salto do Céu suite, likely associated with post-orogenic stages of the Santa Helena Magmatic Arc in the Jauru Terrane; the younger event, which have occurrence restricted to the Paraguá and Rio Apa Terranes, is represented by the Huanchaca, and Rio Perdido suites and Rincón del Tigre Complex, and form part of a Stenian LIP sited in the south-southwestern Amazon Craton. This LIP evolved from an attempted break-up of continental crust that resulted in the formation of the Aguapeí Aulacogen. The Sunsás and Aguapeí Belts mark the period of agglutination of Rodinia, and are responsible for the metamorphism and deformation observed in part of this Stenian LIP.

Keywords: Mafic magmatism. Distensive tectonics. Ar-Ar and U-Pb Geochronology. Petrology.

LISTA DE ILUSTRAÇÕES

Figura 1.1 -	Mapa tectônico do Sul/Sudoeste do Cráton Amazônico.....	1
Figura 2.1 -	Províncias Geotectônicas da América do Sul.....	11
Figura 2.2 -	Províncias geocronológicas do Cráton Amazônico.....	14
Figura 2.3 -	Províncias geocronológicas do Cráton Amazônico.....	15
Figura 2.4 -	Compartimentação geocronológica e tectônica do Cráton Amazônico, considerando o Maciço Rio Apa como seu extremo meridional.....	16
Figura 2.5 -	A. Mapa simplificado do SW de Mato Grosso ilustrando a distribuição dos terrenos; B. Províncias Geocronológicas do Cráton Amazônico.....	18
Figura 2.6 -	Esboço geológico do Terreno Rio Apa no sudoeste do estado de Mato Grosso do Sul (Brasil) e noroeste do Paraguai.....	25
Figura 1 -	Mapa tectônico do Sul/Sudoeste do Cráton Amazônico.....	30
Figura 2 -	Esboço geológico do Terreno Rio Apa e a localização aproximada dos principais diques identificados.....	33
Figura 3 -	A e B) Diques da SIRP alojados em gnaiss do Complexo Rio Apa; C) dique de diabásio da SIRP de cor cinza-claro e granulação muito fina; D) detalhe de amostra de dique de microgabro da SIRP de textura intergranular a sub-ofítica.....	35
Figura 4 -	Diagrama de rosetas obtido para os diques da SIRP (20 medidas).....	35
Figura 5 -	Fotomicrografias de amostras da SIRP, ilustrando: A) textura ofítica a subofítica, plagioclásio com morfologia do tipo “cauda de andorinha” indicando textura quenching; B) textura predominantemente ofítica formada por augita incluindo cristais tabulares de plagioclásio, pseudomorfos de olivina envolvidos por augita. Polarizadores paralelos à esquerda e cruzados à direita.....	37

Figura 6 -	Fotomicrografias de amostras da SIRP, ilustrando: A) textura intergranular, presença de orto e clinopiroxênio; B) detalhe de ortopiroxênio rosa com inclusão de ripas de plagioclásio (textura ofítica) e clinopiroxênio branco prismático. Polarizadores paralelos à esquerda e cruzados à direita.....	38
Figura 7 -	Fotomicrografias de amostras da SIRP ilustrando: A) textura subofítica, cristais hexagonais de olivina com fraturas serpentinizadas e coroa de reação para piroxênio; B) cristais de olivina com bordas de reação para piroxênio; C) textura intergranular com plagioclásio tabular e cristal pseudo-hexagonal zonado de olivina com núcleo substituído por opaco, anfibólio, iddingsita e boulingita, com coroa de reação de piroxênio. Polarizadores paralelos à esquerda e cruzados à direita.....	39
Figura 8 -	Diagramas de variação MgO versus óxidos de elementos maiores (% em peso) para as rochas da SIRP.....	43
Figura 9 -	Diagramas de variação MgO versus elementos traço (% em peso) para as rochas da SIRP.....	44
Figura 10 -	Diagramas classificatórios para as rochas da SIRP.....	45
Figura 11 -	Diagramas classificatórios de ambiência tectônica.....	46
Figura 12 -	A) Diagrama de distribuição dos ETR para as rochas da SIRP, B) Diagrama multi-elementar para as rochas da SIRP.....	47
Figure 1 -	Tectonic Map of the South/Southwestern Amazonian Craton highlighting the fissural mafic magmatism (dykes of the intrusive suites Rio Perdido, Rancho de Prata and Huanchaca; and sills of the intrusive suites Salto do Céu and Huanchaca), and felsic magmatism (plutons of the Guapé Intrusive Suite and granitic dykes of the Vila Bela Granite).....	57
Figure 2 -	Location of the study area in the geological map of Salto do Céu and Rio Branco region – MT.....	61

- Figure 3 - Field aspects of sills from SCS: A) mafic enclave likely from the SCS enclosed in rocks of the RBIS; B) hybridized areas resulting from interaction between felsic (RBIS) and mafic (SCS) magmas; C) concordant contact between sills of SCS and laminated pelites of Vale da Promissao Formation; D) macroscopic aspect of sills, with emphasis on subophitic texture marked by interstitial plagioclase laths between pyroxene crystals..... 62
- Figure 4 - Field aspects of lava flows from SCS: A) e B) large amount of round vesicles in the flow top; C) and D) flow folds; E) and F) brecciated aspect resulting from flow lava fragmentation as deformation occurs during its motion; G) and H) alkali feldspar phenocryst displaying rapakivi texture and partially resorbed, respectively..... 63
- Figure 5 - Photomicrographs of sills from SCS displaying: A) ophitic texture featured by pseudomorph augite (titanoaugite) crystal consisting of opaque minerals and actinolite, including intensely altered plagioclase laths; B) Tabular plagioclase between prisms and grains of pyroxene characterizing subophitic texture; C) intergranular texture consisting of saussuritized tabular plagioclase crystals and partially uralitized interstitial pyroxene. Parallel polarizers to the left and crossed polarizers to the right..... 66
- Figure 6 - Photomicrographs of sills from the SCS showing: A) fractured plagioclase crystals, pyroxene and opaque minerals partially altered to amphibole, biotite and chlorite; B) subophitic texture consisting of tabular plagioclase and augite crystals, some pseudomorphized by amphibole; C) Pseudomorph of amphibole (hornblende) after pyroxene associated with plagioclase, quartz and opaques. Parallel polarizers to the left and crossed polarizers to the right..... 67
- Figure 7 - Photomicrographs of sills from SCS illustrating: A) detail of opaque minerals with biotite corona and plagioclase showing normal zoning; B) opaque mineral with symplectite texture associated with pyroxene, amphibole and plagioclase. Parallel polarizers to the left and crossed polarizers to the right..... 68

- Figure 8 - Photomicrographs of lava flows from SCS displaying: A) ophitic to intergranular texture featured by plagioclase laths and dark-pink titanogaugite with partial to complete replacement by green-coloured hornblende; B) porphyritic texture formed by tabular plagioclase enclosed into a subophitic to intergranular groundmass; C) fluidal groundmass showing pseudo-trachytic texture delineated by the arrangement of deformed plagioclase laths intercalated with mafic minerals, and amphibole pseudomorphs of original pyroxene. Parallel polarizers to the left and crossed polarizers to the right..... 70
- Figure 9 - Photomicrographs of lava flows from SCS showing: A) amygdale enclosed in subophitic groundmass with plagioclase laths and amphibole; B) amygdale filled with zeolite and chlorite surrounded by a halo consisting of a mixture of biotite, rutile, and iron oxides/hydroxides; C) amygdale filled with zeolite, chlorite, biotite, and iron oxides/hydroxides in fluidal groundmass; D) vitrophyric texture formed by elongate laths of plagioclase phenocrysts and amygdales enclosed in glassy groundmass; E) round and ellipsoidal amygdales in glassy groundmass; F) Detail of rounded amygdale filled with zeolite and chlorite. Parallel polarizers in (C) and crossed polarizers in (A), (B), (D), (E) and (F)..... 71
- Figure 10 - Photomicrographs of lava flows from SCS showing: A) fine-grained groundmass with pseudo-trachytic texture marked by alignment of plagioclase laths and mafic minerals, and amygdale filled with secondary phases, such as fluorite, opaques, chlorite and zeolite; B) details of previous image highlighting the purple colour of fluorite; C) detail of groundmass composed of plagioclase laths, pyroxene grains and amphibole; D) sphalerite and pyroxene phenocrysts in a trachytoid groundmass consisting of submillimetre-sized laths of plagioclase and mafic minerals; E) detail of euhedral sphalerite crystal with magmatic corrosion and reaction rim of calcite. Parallel polarizers to the left and crossed polarizers to the right in (A), parallel in (B) and (C), and crossed polarizers in (D) and (E)..... 72

Figure 11 -	MgO variation diagrams versus major-elements (% weight) for rocks from SCS.....	75
Figure 12 -	MgO variation diagrams (% weight) versus trace-elements (ppm) for rocks from SCS.....	76
Figure 13 -	Classification diagrams for rocks from SCS.....	77
Figure 14 -	REE (A) and multi-element spidergrams for rocks from SCS.....	78
Figure 1 -	South/Southwest Tectonic Map of Amazonian Craton highlighting U-Pb (ID-TIMS) baddeleyite ages for the suites Santo do Céu, Rancho de Prata and Huanchaca, and the Rincón del Tigre Complex.....	92
Figure 2 -	Field aspects. A – Concordant contact between sill of the Salto do Céu Suite and pelitic rocks of the Vale da Promissão Formation. B – Magmatic flow-folds in lava flows of the Salto do Céu Suite. C – Massif structure in sample of the Rancho de Prata Intrusive Suite. D – Contact between dyke of the Rancho de Prata Intrusive Suite and granitic rocks. E – Contact between sill of the Huanchaca Intrusive Suite, and pelites of the Vale da Promissão Formation. F – Angular block of dyke of the Huanchaca Intrusive Suite emplaced into rocks of the Guaporeí Granite.....	96
Figure 3 -	Photomicrography of samples of the Salto do Céu (A and B), Rancho de Prata (C and D), and Huanchaca suites (E and F) illustrating: A – Sill: ophitic texture formed by titanite with lath-shaped plagioclase intensely altered, pseudomorphized by opaque minerals and actinolite. B – Lava flow: rounded and ellipsoidal amygdales in glassy groundmass. C – Intergranular texture formed by tabular plagioclase and interstitial pyroxene. D – Subophitic texture highlighting orthopyroxene crystals. E – Dyke: microphenocrysts of pyroxene showing coronitic texture, relict olivine, and swallow-tail plagioclase. F – Sill: ophitic texture formed by augite crystal enclosing tiny euhedral to subhedral laths of plagioclase. Parallel polarizers in (D) and (E), and crossed polarizers in (A), (B), (C) e (F).	97

Figure 4 -	Molecular proportion ratio diagrams for the studied units (logarithmic scale). ▲ Salto do Céu Suite, ■ Rancho de Prata Intrusive Suite, ● Huanchaca Intrusive Suite (dykes), ○ Huanchaca Intrusive Suite (sills).....	99
Figure 5 -	Variation diagrams mg# versus major elements (% weight) for rocks of the Salto do Céu, Rancho de Prata, and Huanchaca suites. ▲ Salto do Céu Suite, ■ Rancho de Prata Intrusive Suite, ● Huanchaca Intrusive Suite (dykes), ○ Huanchaca Instrusive Suite (sills).....	100
Figure 6 -	Variation diagrams mg# versus trace elements (ppm) for rocks of Salto do Céu, Rancho de Prata and Huanchaca suites. ▲ Salto do Céu Suite, ■ Rancho de Prata Intrusive Suite, ● Huanchaca Intrusive Suite (dykes), ○ Huanchaca Intrusive Suite (sills).....	101
Figure 7 -	Classification diagrams for rocks of the Salto do Céu, Rancho de Prata and Huanchaca suites. ▲ Salto do Céu Suite, ■ Rancho de Prata Intrusive Suite, ● Huanchaca Intrusive Suite (dykes), ○ Huanchaca Intrusive Suite (sills).....	103
Figure 8 -	Rare Earth Elements (REE) diagrams normalized to CI Chondrite values for Salto do Céu, Rancho de Prata and Huanchaca suites. ▲ Salto do Céu Suite, ■ Rancho de Prata Intrusive Suite, ● Huanchaca Intrusive Suite (dykes), ○ Huanchaca Intrusive Suite (sills).....	104
Figure 9 -	Primitive mantle normalized multi-element diagrams for the Salto do Céu, Rancho de Prata and Huanchaca suites. OIB, E- and N-MORB patterns are presented for comparison issues. ▲ Salto do Céu Suite, ■ Rancho de Prata Intrusive Suite, ● Huanchaca Intrusive Suite (dykes), ○ Huanchaca Intrusive Suite (sills).....	105
Figure 10 -	$^{40}\text{Ar}/^{39}\text{Ar}$ (mineral) diagrams for the Salto do Céu Suite. A – Amphibole (hornblende). B – Plagioclase.....	107
Figure 11 -	$^{40}\text{Ar}/^{39}\text{Ar}$ (mineral) diagrams of the Rancho de Prata Intrusive Suite. A – Plagioclase. B – Amphibole (hornblende).....	107
Figure 12 -	$^{40}\text{Ar}/^{39}\text{Ar}$ (mineral) diagrams for the Huanchaca Intrusive Suite. A – Plagioclase. B – Amphibole (hornblende).....	108

Figure 13 -	Tectonic evolution scheme for the mafic dyke swarms, and mafic and acid sills sited in the south and southwestern Amazonian Craton.....	110
-------------	---	-----

LISTA DE TABELAS

Tabela 2.1 -	Equivalência entre a compartimentação em terrenos e as propostas tectônicas anteriores feitas para o SW do Cráton Amazônico em Mato Grosso.....	19
Tabela 1 -	Dados litoquímicos das rochas da SIRP [elementos maiores (% em peso), traço e terras raras (ppm)].....	40
Table 1 -	Geochronological and isotopic database for the acid to intermediate rocks (Rio Branco Suite) and basic rocks (Salto do Céu Suite). (Z) zircon; (S) sphene; (B) baddeleyite; (WR) whole-rock; (P) plagioclase.....	59
Table 2 -	Lithochemical data of rocks from Salto do Céu Suite [major elements (% weight), trace-elements (ppm)]. # Sills e * Lava flows.....	73
Table 1 -	Lithochemical data of rocks from Salto do Céu Suite [major elements (% weight), trace-elements (ppm)].....	114
Table 2 -	Lithochemical data of rocks from Rancho de Prata Intrusive Suite [major elements (% weight), trace-elements (ppm)].....	115
Table 3 -	Lithochemical data of rocks from Huanchaca Intrusive Suite [major elements (% weight), trace-elements (ppm)].....	116
Table 4 -	$^{39}\text{Ar}/^{40}\text{Ar}$ analytical data obtained from plagioclase and amphibole of the Salto do Céu Suite (SC-100).....	118
Table 5 -	$^{39}\text{Ar}/^{40}\text{Ar}$ analytical data obtained from plagioclase and amphibole of the Rancho de Prata Intrusive Suite (RP-W3).....	119
Table 6 -	$^{39}\text{Ar}/^{40}\text{Ar}$ analytical data obtained from plagioclase and amphibole of the Huanchaca Intrusive Suite (LG-70).....	120

SUMÁRIO

DEDICATÓRIA.....	iv
AGRADECIMENTOS.....	v
RESUMO.....	vi
ABSTRACT.....	x
LISTA DE ILUSTRAÇÕES.....	xiv
LISTA DE TABELAS.....	xx
1 INTRODUÇÃO.....	1
1.1 APRESENTAÇÃO DO TEMA.....	1
1.1.1 Suíte Salto do Céu.....	2
1.1.2 Suíte Intrusiva Rancho de Prata.....	3
1.1.3 Suíte Intrusiva Huanchaca.....	4
1.1.4 Suíte Intrusiva Rio Perdido.....	4
1.1.5 Complexo Ígneo Rincón del Tigre.....	5
1.2 PROBLEMÁTICA.....	5
1.3 OBJETIVOS.....	6
1.4 MATERIAIS E MÉTODOS.....	7
1.4.1 Revisão Bibliográfica.....	7
1.4.2 Trabalhos de Campo.....	8
1.4.3 Análises Petrográficas.....	8
1.4.4 Análises Litoquímicas.....	8
1.4.5 Análises Geocronológicas.....	9
1.4.5.1 Método U-Pb (ID-TIMS)	9
1.4.5.2 Método Ar-Ar.....	10
2 CONTEXTO GEOLÓGICO REGIONAL.....	11
2.1 O CRÁTON AMAZÔNICO.....	12
2.2 O SW DO CRÁTON AMAZÔNICO.....	16
2.2.1 Província Rondoniana-San Ignacio.....	17
2.2.1.1 Terreno Paraguá.....	19
2.2.1.2 Terreno Jauru.....	20
2.2.1.3 Terreno Rio Alegre.....	21
2.2.2 Província Sunsás-Aguapeí.....	22
2.2.2.1 Faixa Móvel Aguapeí.....	22
2.3 A PARTE SUL DO CRÁTON AMAZÔNICO.....	24
3 ARTIGOS SUBMETIDOS.....	26
3.1 SUÍTE INTRUSIVA RIO PERDIDO: MAGMATISMO INTRAPLACA NO SUL DO CRÁTON AMAZÔNICO – TERRENO RIO APA.....	26
3.2 GEOLOGY AND PETROLOGY OF THE SALTO DO CÉU SUITE: TECTONIC AND STRATIGRAPHIC IMPLICATIONS ON THE SW AMAZONIAN CRATON.....	53
3.3 FISSURAL MAFIC MAGMATISM ON SOUTHWESTERN AMAZONIAN CRATON: PETROGENESIS AND ⁴⁰ AR- ³⁹ AR GEOCHRONOLOGY.....	85

4 CONCLUSÕES E CONSIDERAÇÕES FINAIS.....	121
REFERÊNCIAS.....	126
ANEXOS – ARTIGOS PUBLICADOS.....	131

1 INTRODUÇÃO

1.1 APRESENTAÇÃO DO TEMA

Enxames de diques e *sills* máficos constituem importante ferramenta para o entendimento dos processos geodinâmicos, especialmente por marcar o início de grandes eventos tectônicos extensionais, e são indicadores essenciais da natureza e evolução das fontes mantélicas no tempo geológico.

Na porção S-SW do Cráton Amazônico, ocorrências de enxames de diques e *sills* máficos proterozoicos são relatadas no oriente boliviano, em Mato Grosso e Mato Grosso do Sul. Como exemplos, têm-se os enxames de diques das suítes intrusivas Huanchaca, Rancho de Prata e Rio Perdido, bem como os *sills* máficos Huanchaca, Salto do Céu e Rincón del Tigre (Fig. 1.1).

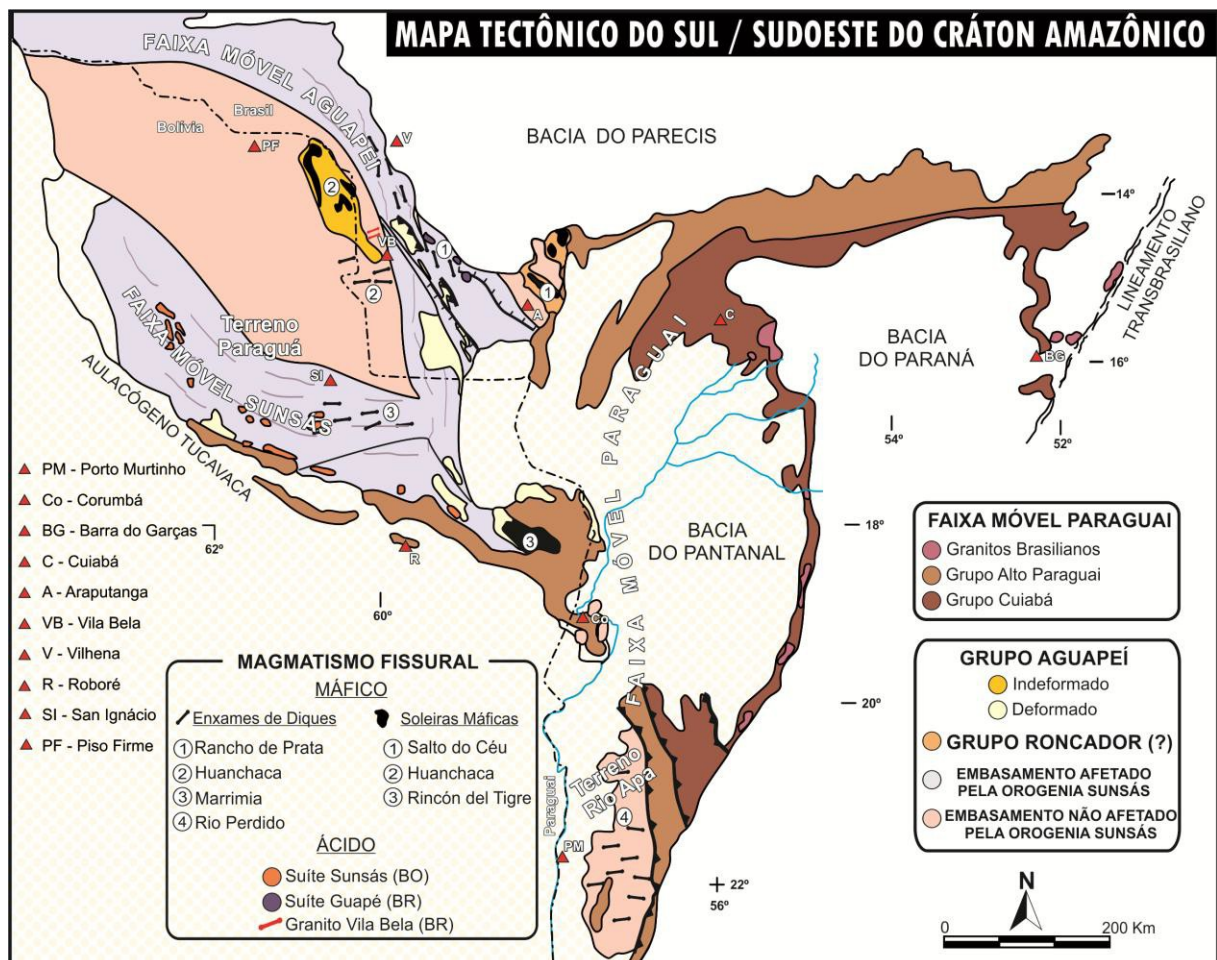


Figura 1.1. Mapa tectônico do Sul/Sudoeste do Cráton Amazônico (Extraído e modificado de Ruiz *et al.*, 2010a).

1.1.1 Suíte Salto do Céu

As rochas que ocorrem na região de Salto do Céu e Rio Branco, sudoeste de Mato Grosso, foram reportadas inicialmente por Oliva (1979). Posteriormente, Barros *et al.* (1982) descrevem os gabros e diabásios, que afloram nessa região, como parte do Grupo Rio Branco, e Leite *et al.* (1985) interpretam essas ocorrências de rochas básicas como exposições da porção meso-melanocrática da Suíte Intrusiva Rio Branco, caracterizando-as como um complexo ígneo estratiforme diferenciado, de caráter bimodal, que poderia indicar um magmatismo anorogênico, possivelmente desenvolvido em ambiente de *rift*.

Segundo Geraldès (2000) e Geraldès *et al.* (2001, 2004) os termos máficos constituíam a base da Suíte Intrusiva Rio Branco, a qual engloba uma associação pluto-vulcânica dominada por rochas ácidas a intermediárias no topo. Esses autores apresentam idades U-Pb de 1471 ± 8 Ma para os termos básicos e 1427 ± 10 Ma para os termos ácidos, interpretando-os como magmatismo extensional intracratônico, reflexo do arco magmático Santa Helena (1,47–1,42 Ga).

Araújo *et al.* (2005) individualizam o conjunto de intrusões paralelas ao acamamento das rochas da Formação Vale da Promissão, constituído por soleiras máficas de espessuras entre 1 a 5 m, denominando-o Suíte Intrusiva Salto do Céu. Araújo *et al.* (2007) definem que o Batólito Rio Branco é constituído por duas séries plutônicas principais, uma básica de distribuição descontínua, localizada nas bordas da intrusão, e outra ácida/intermediária, composta por três fácies petrográficas. Concluem que as exposições de rochas gabroicas representam dois eventos magmáticos independentes: as básicas plutônicas (gabros e dioritos) pertencendo à Suíte Intrusiva Rio Branco e as rochas hipoabissais (diabásios, microgabros), constituindo a Suíte Intrusiva Salto do Céu.

Segundo Araújo (2008), o magmatismo bimodal do Batólito Rio Branco é plenamente evidenciado. Um de natureza básica, gerado por derivação mantélica e outro, de composição ácida/intermediária, formado por processos de fusão e participação de material crustal, e através de processo de diferenciação magmática, geram-se os litotipos intermediários/ácidos distintos. Essa autora define, para as rochas intermediárias a ácidas, idades U-Pb de $1403 \pm 0,6$ Ma e 1382 ± 49 Ma, interpretando-as como sendo de cristalização dos magmas félsicos que deram origem à Suíte Ácida Intrusiva Rio Branco.

O Batólito Rio Branco, de acordo com Araújo *et al.* (2009, 2011), é constituído por duas suítes plutônicas principais: a Suíte Básica Intrusiva Rio Branco, formada por rochas básicas/intermediárias, e a Suíte Ácida Intrusiva Rio Branco de composição

intermediária/ácida. Ainda segundo esses autores, a associação gabroica constitui dois eventos magmáticos temporalmente independentes: as rochas básicas/intermediárias plutônicas, constituídas por microgabros a diabásios, monzogabros e quartzo monzonitos a quartzo dioritos, pertencentes à Suíte Básica Intrusiva Rio Branco, e os litotipos hipoabissais, diabásios e microgabros, agrupados sob a designação Suíte Básica Intrusiva Salto do Céu, alojada concordantemente aos estratos do Grupo Aguapeí.

Sousa *et al.* (2011), a partir de mapeamento geológico mais detalhado, restringem a denominação de Suíte Intrusiva Rio Branco apenas aos termos ácidos a intermediários, englobando todas as ocorrências gabroicas na Suíte Intrusiva Salto do Céu.

Teixeira *et al.* (2015a) apresentam idade U-Pb em badeleíta de 1439 ± 4 Ma para os *sills* Salto do Céu, interpretando-os como um episódio magmático associado à evolução do Supercontinente Columbia.

Lima *et al.* (subm.), com base em trabalhos de campo e novos dados geocronológicos disponíveis na literatura, descrevem além de soleiras, derrames básicos na Suíte Salto do Céu e a interpretam como uma suíte bimodal, onde a porção ácida corresponde à Suíte Intrusiva Rio Branco. Segundo esses autores, essa unidade foi gerada em ambiente intraplaca, em regime tectônico distensivo, anorogênico que reflete, possivelmente, um marco tectônico associado à evolução do Supercontinente Columbia/Nuna.

1.1.2 Suíte Intrusiva Rancho de Prata

Os diques máficos da região de Nova Lacerda (MT), foram inicialmente descritos por Ruiz *et al.* (2005) e denominados Suíte Intrusiva Rancho de Prata para individualizar um enxame de diques, tabulares, alojados nas rochas do embasamento do Terreno Jauru, reconhecidos primeiramente em afloramentos na fazenda homônima.

Corrêa da Costa *et al.* (2009) identificam um enxame de diques máficos, de direção NNW, alojados no Granito Nova Lacerda, na região homônima e de Conquista D'Oeste. Esses autores caracterizam três litotipos nesse enxame: diabásios, metadiabásios e anfibolitos e apresentam idades Rb-Sr de 1380 ± 32 Ma para os diabásios e de 1330 ± 120 Ma para os metadiabásios. Girardi *et al.* (2012) atribuem a origem das rochas dessa suíte à cristalização fracionada de líquidos evoluídos derivados de uma fonte mantélica heterogênea. Com base em dados geoquímicos e isotópicos, esses autores sugerem um ambiente tectônico do tipo arco continental para a colocação desses diques.

Teixeira *et al.* (2015a) apresentam idade U-Pb em badeleíta de 1387 ± 17 Ma para o enxame de diques máficos Nova Lacerda, interpretando-os como um episódio magmático associado à evolução do Supercontinente Columbia.

1.1.3 Suíte Intrusiva Huanchaca

Os diques e soleiras máficos que ocorrem no leste da Serra de Huanchaca, na fronteira da Bolívia com o Brasil, intrudidos em rochas do Grupo Sunsás e embasamento, foram inicialmente denominados, por Litherland *et al.* (1986), de Suíte Dolerítica Huanchaca.

Lima (2008, 2011) e Lima *et al.* (2012) descrevem pela primeira vez as ocorrências de soleiras alojadas no Grupo Aguapeí, na porção norte da Serra Ricardo Franco/Huanchaca, em território brasileiro, no SW do estado de Mato Grosso. Da mesma forma, Sécolo *et al.* (2008, 2012) e Sécolo (2011) apresentam resultados de estudos do enxame de diques máficos alojados em rochas do embasamento, na região de Vila Bela da Santíssima Trindade-MT.

Tanto as soleiras quanto os diques identificados em território brasileiro, foram correlacionados aos descritos por Litherland *et al.* (1986) no território boliviano, e agrupados sob a designação Suíte Intrusiva Huanchaca (Lima 2008, 2011; Lima *et al.* 2012; Sécolo *et al.* 2008, 2012; Sécolo 2011; Ruiz *et al.* 2010b).

Teixeira *et al.* (2015b) apresentam idade U-Pb em badeleíta de $1111,5 \pm 1,9$ Ma, para as soleiras desta unidade, e sugerem que estas rochas, juntamente com as do Complexo Ígneo Rincón del Tigre, pertencem a uma LIP até então desconhecida no Cráton Amazônico.

1.1.4 Suíte Intrusiva Rio Perdido

O enxame de diques, que representa a Suíte Intrusiva Rio Perdido, ocorre na porção sul do Cráton Amazônico, encaixado em rochas paleoproterozoicas, em toda a extensão do Terreno Rio Apa no Brasil (sudoeste do estado de Mato Grosso do Sul) e no Paraguai.

Os diques máficos foram descritos, inicialmente, por Araújo *et al.* (1982) que apresentam uma idade K/Ar, em plagioclásio, de 914 ± 9 Ma, admitida como a de sua formação. Godoi *et al.* (2001) posicionam os diques mapeados na região de Porto Murtinho e Corumbá como pertencentes ao Complexo Rio Apa, na Formação Serra Geral (Grupo São Bento).

Lacerda Filho *et al.* (2006) descrevem a ocorrência de diques e soleiras máficas, indeformados, que cortam a maioria das unidades paleoproterozoicas do Bloco Rio Apa.

Ruiz *et al.* (2010b) denominam esse enxame de diques como Suíte Intrusiva Rio Perdido e, com base na idade de 914 ± 9 Ma (Araújo *et al.*, 1982), o relacionam ao magmatismo intraplaca responsável pela ruptura do supercontinente Rodínia.

Faleiros *et al.* (2016) apresentam resultado U-Pb (LA-ICP-MS) em zircões de um dique de gabronorito, maciço, cujo intercepto superior em 1589 ± 44 Ma foi interpretado como a idade de sua formação.

Teixeira *et al.* (2016) obtêm idade U-Pb (ID-TIMS) de 1110 Ma, em badeleíta, e a correlacionam à LIP Rincón del Tigre-Huanchaca.

1.1.5 Complexo Ígneo Rincón del Tigre

O Complexo Ígneo Rincón del Tigre corresponde a uma intrusão acamadada, espessa, alojada em rochas dos grupos Sunsás e Vibosi. Inicialmente descrita por Hess (1960), foi denominado por Litherland *et al.* (1986), na região de Rincón del Tigre (Bolívia), e caracterizada como um registro ígneo relacionado à Orogenia Sunsás. Esses últimos autores obtiveram idades K-Ar de 1099 ± 37 Ma e 1002 ± 22 Ma, além de idade Rb-Sr de 993 ± 139 Ma, todas interpretadas como sendo de cristalização dessa unidade.

As rochas que compõem esse complexo acamadado foram, litoestratigraficamente, divididas em três unidades (Litherland *et al.*, 1986): Ultramáfica (basal), Máfica (intermediária) e Félsica (superior).

A Unidade Ultramáfica constitui-se por dunito serpentizado, harzburgito, olivina bronzitito, bronzita picrito e melanorito, enquanto a Unidade Máfica por norito e gabro, e Unidade Félsica está representada por granófiro.

Teixeira *et al.* (2015b) apresentam idade U-Pb em badeleíta de $1110,4 \pm 1,8$ Ma, obtida a partir de amostra coletada da Unidade Félsica (granófiro), e descrevem similaridade cronológica com rochas de suítes graníticas sin e pós-orogênicas que ocorrem na Província Sunsás-Aguapeí, na Bolívia e no Brasil.

1.2 PROBLEMÁTICA

O desenvolvimento da pesquisa buscou obter dados geológicos, goequímicos, geocronológicos e isotópicos que permitissem elucidar algumas dúvidas ou questionamentos relativos ao magmatismo básico, manifesto sob a forma de enxames de diques e soleiras, localizados no setor sul e sudoeste do Cráton Amazônico.

Apesar de algumas dessas unidades terem sido identificadas nas décadas de 70 e 80, apenas a partir da primeira década desse século, o magmatismo investigado foi criteriosamente cartografado e principiaram os estudos sob o ponto de vista petrológico, geocronológico e paleomagnético, restando ainda vários questionamentos, entre tantos, destacamos os seguintes:

- a) Há um controle estratigráfico e estrutural para a colocação desses diques e soleiras?
- b) Essas rochas máficas foram afetadas por eventos deformacionais e metamórficos posteriores?
- c) Trata-se de um único evento magmático fissural que afetou o sul e sudoeste do Cráton Amazônico, ou são distintos eventos magmáticos-tectônicos?
- d) Qual a idade desses enxames diques e soleiras máficas?
- e) Quais processos petrológicos foram responsáveis pela geração desses magmas básicos? São os mesmos para todas as unidades descritas?
- f) Qual a natureza do manto gerador desses magmas?
- g) Considerando a natureza fissural do magmatismo básico, qual a orientação dos esforços trativos que afetaram essa porção da crosta continental? Houve interferência das rochas hospedeiras na orientação dos diques e soleiras?
- h) Em termos de evolução magmática, há algum evento ígneo global a que esses diques e soleiras possam ser correlacionados?
- i) Em relação aos eventos tectônicos, é possível correlacionar esse(s) episódio(s) ou evento(s) tafrogênico(s) a ciclos tectônicos distensivos globais?
- j) Considerando o Ciclo dos Supercontinentes, os diques e soleiras estudados podem ser associados a evolução geológica/tectônica de algum supercontinente?
- h) Há elementos estruturais que permitam, além dos dados geocronológicos, relacionar esse magmatismo a processos tectônicos distensivos de natureza global?

1.3 OBJETIVOS

O objetivo geral desta pesquisa é caracterizar a natureza, evolução petrológica e tectônica do episódio magmático máfico que ocorre nos municípios de Vila Bela da Santíssima Trindade, Nova Lacerda, Conquista D'Oeste e Salto do Céu, em Mato Grosso, Porto Murtinho e Caracol, em Mato Grosso do Sul, expresso na forma de diques e *sills*, e elucidar seu significado para os processos de extensão e ruptura crustal que afetaram o SW do cráton Amazônico. Para tal propósito, foi feita uma abordagem multidisciplinar, envolvendo

mapeamento geológico e aplicação de análises petrográfica, litoquímica e geocronológica (U-Pb ID-TIMS e Ar-Ar).

Os objetivos específicos são os seguintes:

- Reconhecer geologicamente os *sills* e enxames de diques e suas encaixantes em Vila Bela da Santíssima Trindade, Nova Lacerda, Conquista D'Oeste, Salto do Céu, Porto Murtinho e Caracol;
- Caracterizar a maneira de colocação dos *sills* e diques, com destaque para a relação de campo entre eles e as encaixantes;
- Caracterizar petrograficamente as rochas dos *sills* e diques, na tentativa de individualizar litotipos distintos;
- Investigar a petrogênese dos *sills* e diques, com a utilização de dados litoquímicos (elementos maiores, traço, incluindo terras raras);
- Definir, com o emprego dos métodos isotópicos U-Pb e Ar-Ar, a idade de colocação/resfriamento dos *sills* e diques, fixando um intervalo de idades absolutas desse episódio magmático.

1.4 MATERIAIS E MÉTODOS

Para alcançar os objetivos propostos foram utilizados vários métodos e técnicas de investigação, detalhadas a seguir.

1.4.1 Revisão Bibliográfica

Essa etapa consistiu no levantamento da literatura disponível, visando o entendimento geológico das unidades estudadas, com objetivo de sumarizar dados de âmbito regional e local.

O levantamento bibliográfico foi feito a partir de trabalhos de conclusão do curso de geologia da Universidade Federal de Mato Grosso, dissertações e teses, Projeto RADAMBRASIL (Folhas Guaporé e Campo Grande), artigos de importante contribuição como Bettencourt *et al.* (2010) e Teixeira *et al.* (2010, 2015a, 2015b), além de alguns trabalhos publicados sobre o pré-cambriano boliviano (e.g. Litherland *et al.*, 1986; Boger *et al.*, 2005; Matos *et al.*, 2009).

Ademais, são de interesse direto da pesquisa temas referentes à evolução, petrogênese, geocronologia, assinatura isotópica e geoquímica de diques e *sills* máficos no mundo.

1.4.2 Trabalhos de Campo

Foram realizadas quatro etapas de campo, uma em cada unidade geológica pesquisada (Suítes Salto do Céu, Rancho de Prata, Huanchaca e Rio Perdido). Além disso, foram aproveitados dados obtidos, com a participação direta da autora, durante o desenvolvimento de dissertações de mestrado (Sécolo, 2011; Lima, 2011) e Trabalhos de Conclusão de Curso (Zenardi, 2011; Santos, 2010), todos ligados ao Grupo de Pesquisa em Evolução Crustal e Tectônica (Guaporé) da UFMT.

O reconhecimento geológico foi efetuado na escala 1:100.000, com descrição de afloramentos e coleta sistemática de amostras. Foram utilizadas imagens de satélite e produtos de levantamentos aereogeofísicos para auxiliar no reconhecimento das unidades geológicas.

Nessa fase de campo, buscou-se obter uma caracterização preliminar das rochas de cada unidade, com descrição de feições que definissem as relações de contato entre as unidades litológicas mapeadas.

Juntamente com as descrições feitas em campo, foram realizadas coletas de amostras de rochas para os estudos em laboratórios (análises macroscópicas, microscópicas, litoquímicas e geocronológicas).

1.4.3 Análises Petrográficas

As análises petrográficas foram iniciadas com o estudo macroscópico que serviu de base para a escolha de amostras para confecção de lâminas delgadas e posteriores exames microscópicos. Foram selecionadas amostras dos diques e *sills* de todas as unidades e descritos os principais aspectos, tais como, texturas, estruturas, processos de alteração, composição mineralógica, dentre outros.

As seções delgadas foram confeccionadas no Laboratório de Laminação da Faculdade de Geociências/UFMT e descritas no Laboratório de Microscopia, do PPGG/UFGA. As fotomicrografias das seções delgadas foram feitas com polarizadores paralelos e cruzados, com objetivas de aumento 2,5; 4 e 10x, usando uma câmera acoplada ao microscópio.

1.4.4 Análises Litoquímicas

Após a descrição microscópica das amostras das diversas unidades, foi feita a seleção das mesmas para análises litoquímicas de elementos maiores (%), traço e terras raras (ppm).

As amostras foram tratadas no Laboratório de Preparação de Amostras da Faculdade de Geociências da Universidade Federal de Mato Grosso.

Após a preparação, as amostras foram encaminhadas para o Laboratório Acme Analytical Laboratories (Vancouver - Canadá), onde foi empregada a técnica de ICP-ES (*Inductively Coupled Plasma Emission Spectrometry*) para análises dos elementos maiores e menores, expressos em óxidos (SiO_2 , Al_2O_3 , MgO , CaO , TiO_2 , MnO , Na_2O , K_2O , P_2O_5 , $\text{Fe}_2\text{O}_{3(\text{t})}$) e ICP-MS (*Inductively Coupled Plasma-Mass Spectrometry*) para os elementos traço (Ba, Sc, Be, V, Co, Zn, Ga, As, Rb, Sr, Cr, Ni, Zr, Y, Ce, , Nb, Mo, Ag, Sn, Sb, Cu e Cs) e terras raras (La, Ce, Pr, Nd, Sm, Eu, Gd, Tb, Dy, Ho, Er, Tm, Yb e Lu).

O tratamento dos dados foi feito utilizando o *software* GCDkit (versão 2.3, *Geochemical Data Toolkit for Windows*; Janousek *et al.*, 2006).

1.4.5 Análises Geocronológicas

1.4.5.1 Método U-Pb (ID-TIMS)

As análises U-Pb (ID-TIMS), em grãos de badeleíta (ZrO_2), foram feitas no Laboratório de Geocronologia Jack Satterly da Universidade de Toronto (Canadá). O procedimento analítico foi semelhante ao descrito por Söderlund e Johansson (2002).

A badeleíta é considerada o mineral mais adequado para datações precisas de soleiras e diques máficos, mesmo com toda a dificuldade encontrada na sua separação, principalmente pelo pequeno tamanho e formato laminar, devido a sua ocorrência comum nesse tipo de rocha e por raramente apresentar herança isotópica.

Para a concentração desse mineral foram utilizados, aproximadamente, 200 g de amostra, finamente moída, passada em uma mesa vibratória (Wilfley), produzindo um concentrado de minerais pesados. A seleção dos melhores grãos de badeleíta, de cada amostra, para as análises, foi feita com o auxílio de um microscópio binocular.

As frações foram lavadas e depositadas em cápsulas de Teflon com ácido fluorídrico e traçador isotópico ^{205}Pb - ^{235}U , e dissolvido a uma temperatura acima de 200°C no período de 3 a 4 dias, conforme procedimentos reportados por Krogh (1973). O peso das frações foi estimado utilizando-se imagem digital e densidade da badeleíta.

As amostras foram convertidas em sais usando HCl 3N e colocadas em filamentos de Re desgaseificados em espectômetro de massa VG354, utilizando-se sílica gel e ácido

fosfórico. As razões isotópicas foram medidas através de detector tipo Daly, equipado com contador iônico digital.

As correções de *deadtime* do sistema durante esse período foram de 20 ns para Pb e U. Para as correções de desvios de massa do detector Daly e para as correções do efeito de discriminação de massa térmica foram utilizados, respectivamente, os fatores 0,07%/ u.m.a e 0,10%/ u.m.a.

Os “brancos” do procedimento químico U-Pb no laboratório é, em média, 0,5 pg para Pb e 0,1 pg para U. A plotagem e as regressões foram feitas utilizando-se os algoritmos e *software* (Isoplot 3.0) desenvolvido por Ludwig (2003). Todos os erros descritos nos diagramas (incluindo o erro das elipses e a idade calculada) são com base no nível 2- σ . Detalhes sobre a separação e dados analíticos foram fornecidos por Reis *et al.* (2013).

1.4.5.2 Método Ar-Ar

As amostras selecionadas para análises isotópicas $^{40}\text{Ar}/^{39}\text{Ar}$ foram trituradas, até alcançarem granulação inferior a 2 mm, sendo em seguida lavadas em banho ultrassônico. Depois disso, voltam a ser lavadas por um período mínimo de 15 minutos, em água destilada e etanol absoluto e, posteriormente, secas ao ar. Os grãos minerais (plagioclásio e anfibólio), com granulação entre 0,5 e 2 mm, foram selecionados com auxílio de um microscópio binocular a partir do material limpo. Os minerais foram acondicionados em discos de alumínio junto com um padrão internacional (Fish Canyon Sanidine - idade $28,201 \pm 0,046$ Ma; Kuiper *et al.*, 2008), para monitoramento do fluxo de nêutrons, seguindo a geometria ilustrada em Vasconcelos *et al.* (2002). Os discos de irradiação foram fechados com tampas de alumínio, envolvidos em papel alumínio, selados em tubos de quartzo, dispostos num recipiente colunar de cádmio e posteriormente irradiados, em um reator tipo TRIGA na Universidade do Estado de Oregon - EUA, por 42 horas.

Cada amostra foi aquecida gradualmente com um feixe de laser contínuo com tamanho de 2 mm, para extração do Ar por fusão por etapas (*step-heating*) das amostras irradiadas. Esse procedimento resulta em extrações de várias frações de gás a temperaturas crescentes analisadas individualmente no espectrômetro de massa MAP-215-50, utilizando-se o *software* "MassSpec Versão 7.527", desenvolvido pelo Centro de Geocronologia de Berkeley - EUA. Os dados analíticos foram obtidos no Laboratório da Universidade de Queensland – Austrália e todos os procedimentos encontram-se descritos por Deino & Potts (1990) e Vasconcelos *et al.* (2002).

2 CONTEXTO GEOLÓGICO REGIONAL

O Continente Sulamericano constitui-se por três unidades geotectônicas, conforme proposta de Almeida *et al.* (1981), sendo elas: Plataforma Sulamericana, Cinturão Andino e Plataforma Patagônica. A Plataforma Sulamericana é representada por três escudos pré-cambrianos: das Guianas, Brasil Central e Atlântico, e por Coberturas Fanerozoicas representadas pelas Bacias do Solimões, Amazonas, Parnaíba e Paraná (Figura 2.1).

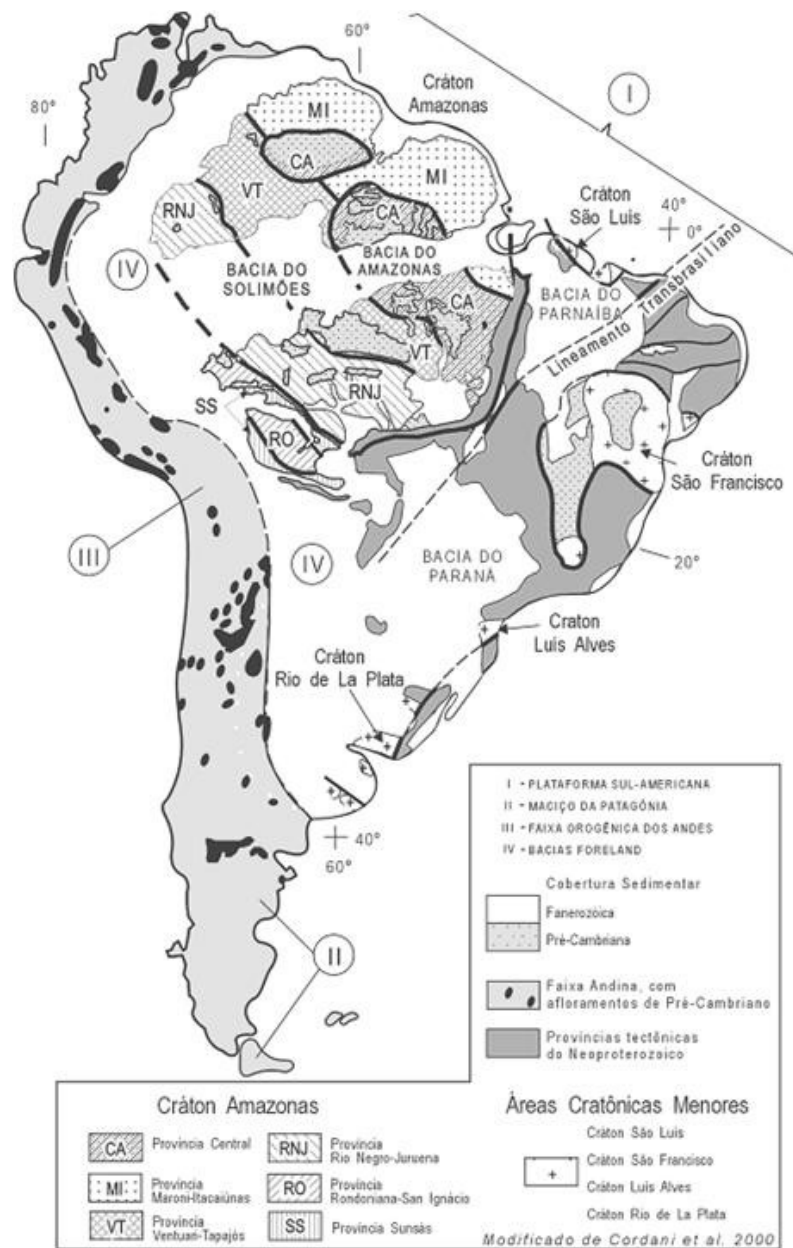


Figura 2.1. Províncias Geotectônicas da América do Sul (Almeida *et al.* 1981, *in*: Cordani *et al.*, 2000).

2.1 O CRÁTON AMAZÔNICO

O Cráton Amazônico, localizado na porção norte da América do Sul, corresponde a uma das principais entidades geotectônicas pré-cambrianas da Plataforma Sulamericana. Tem como limite oriental os cinturões neoproterozoicos Paraguai, a sudeste, a leste, o Araguaia, a sul, a Bacia do Pantanal, estando os limites norte e oeste recobertos pelas rochas sedimentares das bacias subandinas. Abrange uma área de aproximadamente 4.500.000 km², aflorando no Brasil, Bolívia, Colômbia, Guiana, Guiana Francesa e Suriname, e está dividido, pela Sinéclise do Amazonas, em dois escudos: o Escudo Brasil Central e o Escudo das Guianas.

No Brasil, a primeira síntese sobre a geologia/tectônica do Cráton Amazônico deve-se a Almeida (1974), quando o autor delinea os primeiros esboços do então denominado Cráton do Guaporé. Amaral (1974), em levantamento de dados geológicos e geocronológicos (K-Ar e raros Rb-Sr), propõe a divisão do cráton em províncias, baseando-se, nos trabalhos de mapeamento geológico executado pela CPRM e RADAMBRASIL, nos anos 70.

Os levantamentos efetuados pela CPRM, principalmente na década de 70, e pelo Projeto RADAMBRASIL, iniciado em 1970 e concluído na primeira metade dos anos 80, constituem o primeiro acervo integrado de dados geológicos, geoquímicos e geocronológicos sobre o cráton. Ao serem gradativamente sintetizados e publicados (Montalvão, 1976; Issler, 1977; Montalvão *et al.*, 1979; Montalvão & Bezerra, 1980; Santos *et al.*, 1979; entre outros) proporcionam um quadro mais realista de sua constituição litoestratigráfica e evolução tectônica.

As décadas de 80 e 90 caracterizam-se pelos escassos projetos de mapeamento geológico, salvo os realizados por empresas privadas de mineração e Serviço Geológico Nacional (CPRM) e as pesquisas acadêmicas com programas de mapeamento geológico de algumas universidades. No entanto, nesse período deu-se a intensificação da utilização da geologia isotópica, especialmente as sistemáticas Rb-Sr, K-Ar U-Pb e Sm-Nd.

Nas últimas décadas, firmam-se os modelos geodinâmicos baseados nos fundamentos da Teoria da Tectônica Global ou de Placas, entendidos como um processo de evolução crustal balizado em sucessivas acreções de crosta juvenil, do Arqueano até o limiar do Neoproterozoico, em torno de um núcleo arqueano, aplicados tanto para o cráton como um todo, quanto para setores restritos desse. Entre as muitas contribuições sobre o tema ressaltam-se, no primeiro caso, as de Teixeira *et al.* (1989), Tassinari (1996), Tassinari & Macambira (1999, 2004), Tassinari *et al.* (2000), Santos *et al.* (2000), Almeida *et al.* (2000) e, para o setor SW do Estado de Mato Grosso destacam-se entre outros, Saes & Fragoço César

(1996), Pinho *et al.* (1997), Saes (1999), Geraldés (2000), Leite & Saes (2000), Geraldés *et al.* (2001), Matos *et al.* (2004), Ruiz (2005, 2009), Bettencourt *et al.* (2010) e Teixeira *et al.* (2010). Concomitantemente, são efetuadas as primeiras tentativas de correlação global, por exemplo, Sadowski & Bettencourt (1996), que sugerem a justaposição da Amazônia e Laurentia durante a amalgamação do Supercontinente Rodínia.

Os modelos de compartimentação tectônico-geocronológica do Cráton Amazônico continuam em aprimoramento. Três principais modelos permanecem em debate e enriquecem a discussão sobre a história evolutiva deste cráton: Tassinari & Macambira (1999, 2004), Santos *et al.* (2000, 2008) e Ruiz (2005).

A compartimentação sugerida por Tassinari & Macambira (2004; Figura 2.2), evoluída a partir de Cordani *et al.* (1979), retrata sucessivas acreções de crostas juvenis em cinturões móveis proterozoicos (províncias Maroni-Itacaiúnas, 2,2 a 1,9 Ga; Ventuari-Tapajós, 1,9 a 1,8 Ga; Rio Negro-Juruena, 1,8 a 1,55 Ga; Rondoniano-San Ignácio, 1,55 a 1,3 Ga e Sunsás-Aguapeí, 1,2 a 0,9 Ga), situados ao redor de um núcleo proto-cratônico arqueano (Província Amazônia Central, > 2,5 Ga).

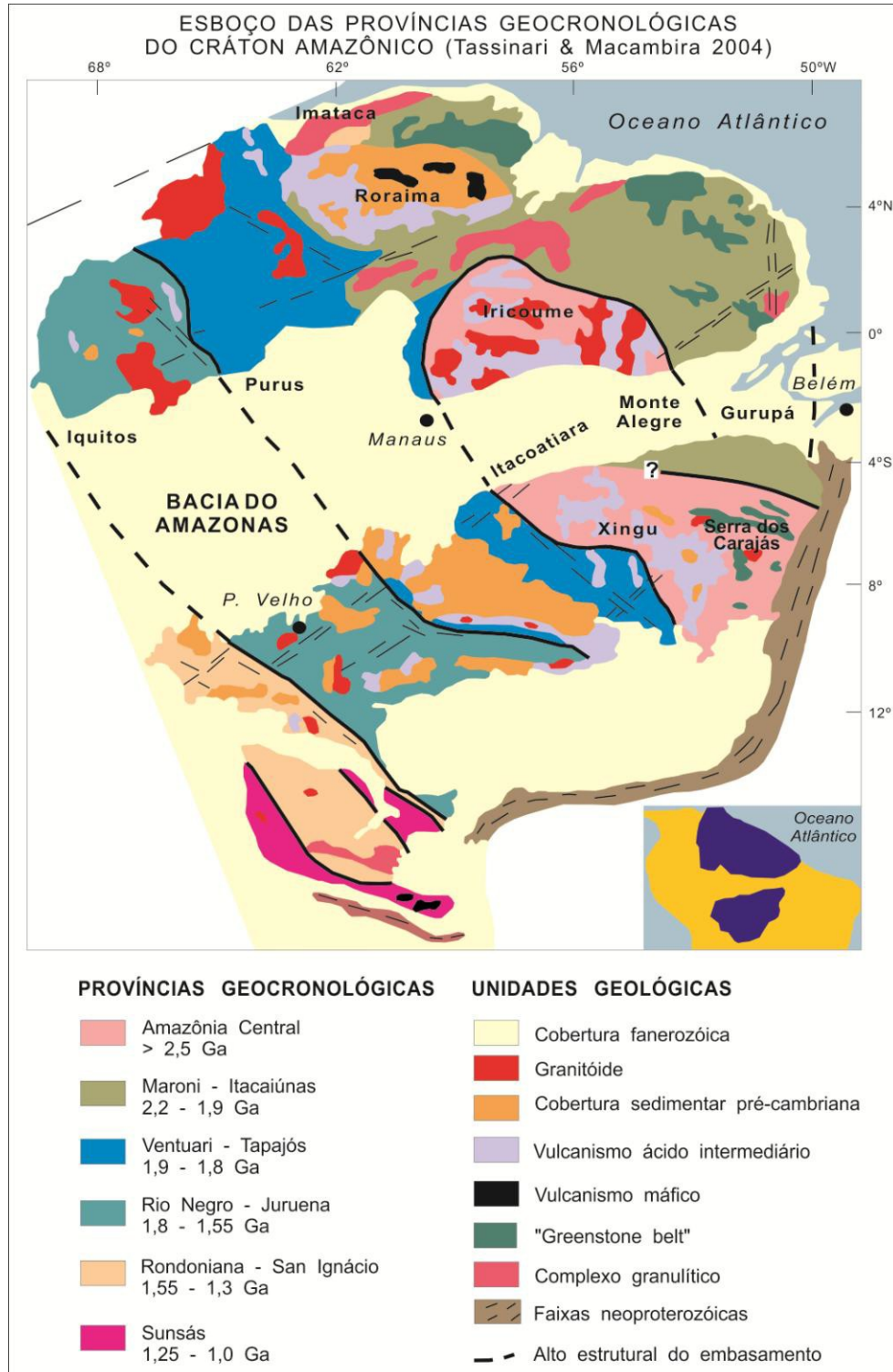


Figura 2.2. Províncias geocronológicas do Cráton Amazônico (Extraído de Tassinari & Macambira, 2004).

Santos *et al.* (2000, 2008) identificam oito províncias tectônicas com base, principalmente, nos dados geocronológicos obtidos pelo método U-Pb (SHRIMP). Em sequência cronológica, têm-se as províncias: Carajás (3,0-2,5 Ga), Transamazônica (2,26-2,01

Ga), Tapajós-Parima (2,03-1,88 Ga), Amazônia Central (Arqueana?), Rio Negro (1,82-1,52 Ga), Rondônia-Juruena (1,82-1,54 Ga) e Sunsás (1,45-1,10 Ga; Figura 2.3).

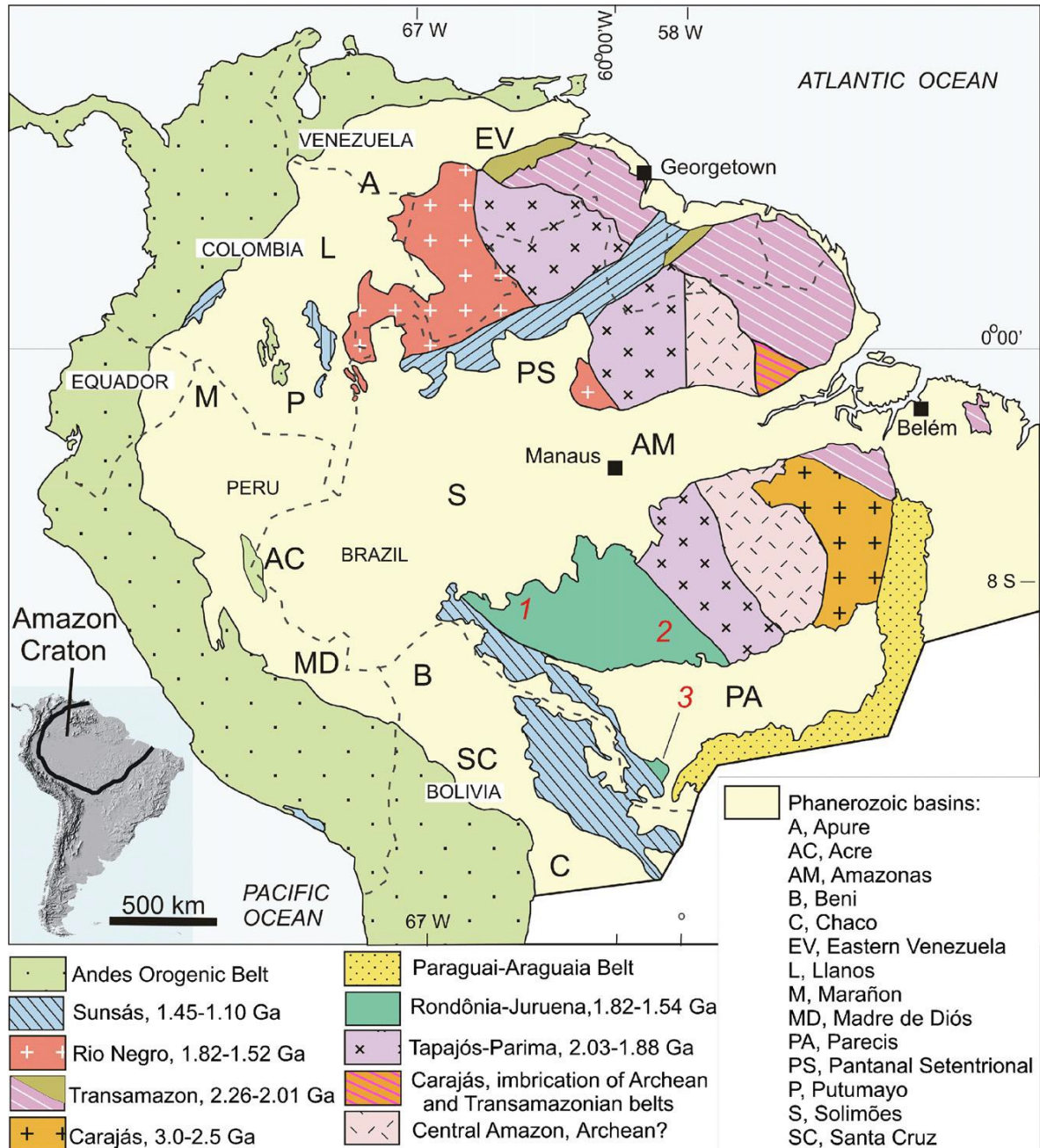


Figura 2.3. Províncias geocronológicas do Cráton Amazônico (Extraído de Santos *et al.*, 2008).

Ruiz (2005), baseado em Tassinari & Macambira (2004), resgata a concepção de Almeida (1967) e Amaral (1974), e, fundamentado em dados geológicos e geocronológicos, considera o Terreno Rio Apa, que aflora na Bacia do Pantanal, no Brasil (Mato Grosso do Sul) e Paraguai, como parte integrante do Cráton Amazônico (Figura 2.4). Nesse trabalho

adotou-se a proposta de compartimentação de Ruiz (2005), uma vez que inclui o Terreno Rio Apa como parte do Cráton.



Figura 2.4. Compartimentação geocronológica e tectônica do Cráton Amazônico, considerando o Maciço Rio Apa como seu extremo meridional (Extraído de Ruiz, 2005).

2.2 O SW DO CRÁTON AMAZÔNICO

Diversas propostas de divisão geológica e tectônica para o SW do Cráton Amazônico em Mato Grosso foram apresentadas, como as de Monteiro *et al.* (1986), Saes (1999), Geraldés (2000), Matos *et al.* (2004), Ruiz (2005), Ruiz (2009) e Bettencourt *et al.* (2010). Os dois últimos propõem a compartimentação em terrenos, os quais caracterizam um trato geológico particular, delimitado por zonas de cisalhamento de expressão regional, que apresenta um acervo de registros litológicos, estruturais e geocronológicos contrastantes com os segmentos imediatamente justapostos.

Segundo Tassinari & Macambira (2004), Ruiz (2009), Bettencourt *et al.* (2010) e Teixeira *et al.* (2010), o sudoeste do Cráton Amazônico em Mato Grosso é constituído pelas províncias Rondoniana-San Ignacio e Sunsás-Aguapeí.

2.2.1 Província Rondoniana-San Ignacio

Ruiz (2009) e Bettencourt *et al.* (2010) apresentam a Província Rondoniana-San Ignacio, no sudoeste do estado de Mato Grosso, como composta pelos seguintes terrenos: Jauru, Rio Alegre, Paraguá e Alto Guaporé (Figura 2.5).

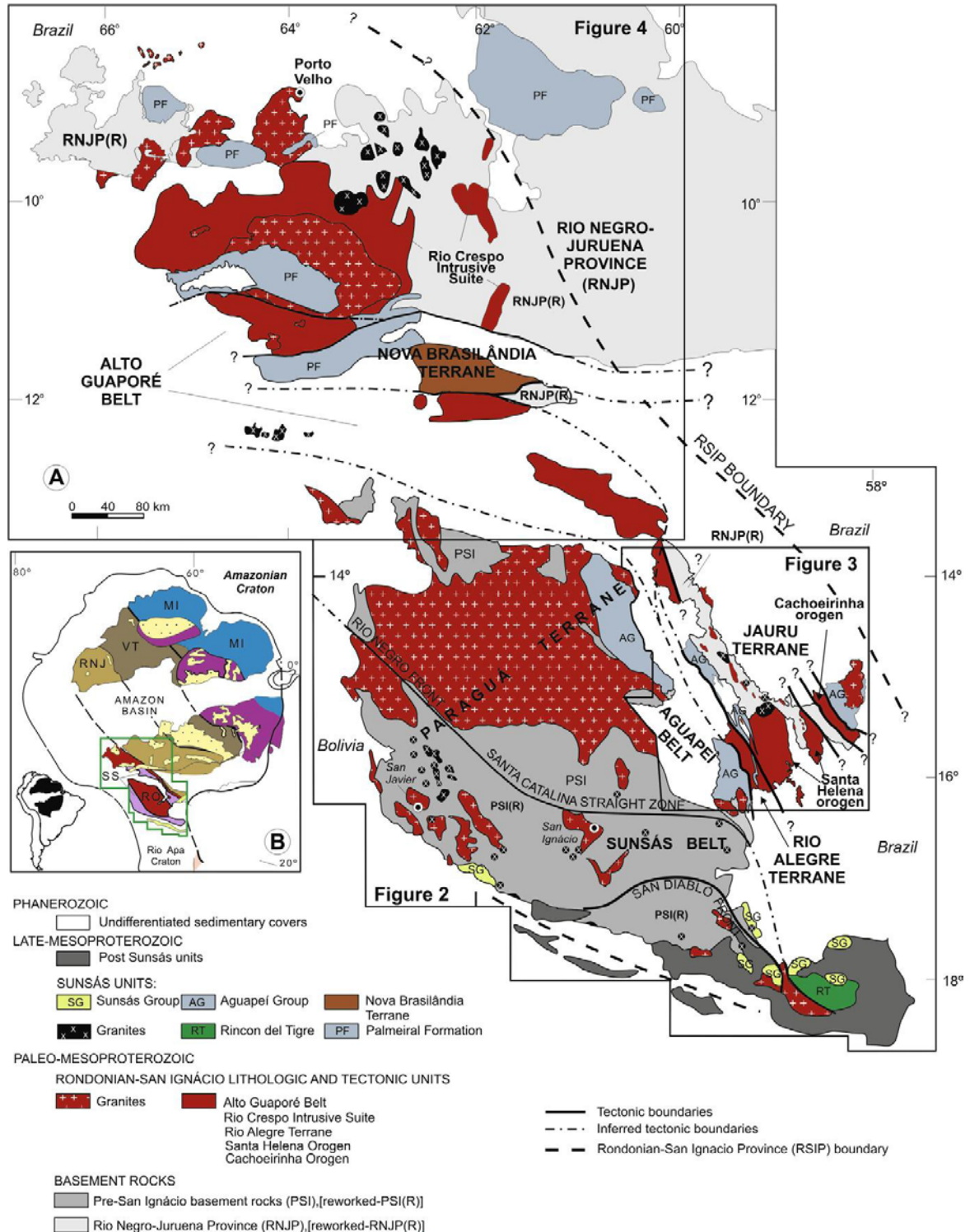


Figura 2.5. A. Mapa simplificado do SW de Mato Grosso ilustrando a distribuição dos terrenos; B. Províncias Geocronológicas do Cráton Amazônico (Extraído de Bettencourt *et al.*, 2010).

A tabela 2.1. ilustra a equivalência entre a compartimentação em terrenos sugerida por Ruiz (2009) e Bettencourt *et al.* (2010) e as propostas tectônicas anteriores para o SW do Cráton Amazônico em Mato Grosso.

Tabela 2.1. Equivalência entre a compartimentação em terrenos sugerida por Ruiz (2009) e Bettencourt *et al.* (2010) e as propostas tectônicas anteriores feitas para o SW do Cráton Amazônico em Mato Grosso.

Ruiz (2009) e Bettencourt <i>et al.</i> (2010)	TERRENO JAURU	TERRENO RIO ALEGRE	TERRENO PARAGUÁ
Saes & Fragoso César (1996)	Terreno Jauru	Zona de Sutura	Terrenos Paraguá e San Pablo
Saes (1999)	Terrenos Jauru e Santa Helena	Terreno Rio Alegre	Terreno Paraguá
Geraldes <i>et al.</i> (2001)	Terreno Alto Jauru e Batólito Santa Helena	Domínio Rio Alegre	Bloco Paraguá
Ruiz (2005)	Domínios Cachoeirinha e Jauru	Domínio Rio Alegre	Domínios Santa Bárbara, Sunsás e Paraguá

A seguir encontram-se descritas, de forma sucinta, as características dos terrenos Paraguá, Jauru e Rio Alegre.

2.2.1.1 Terreno Paraguá

Inicialmente, o termo Cráton Paraguá (Klinck & Litherland, 1982) foi utilizado para descrever o escudo pré-cambriano do oriente boliviano que foi poupado pela Orogenia Sunsás-Aguapeí. Saes & Fragoso Cesar (1996) subdividem esse escudo em dois terrenos, Paraguá e San Pablo, e Tohver *et al.* (2004) expandem o limite do Cráton para incluir a grande área de Mato Grosso, e propõem que o cinturão Nova Brasilândia (aproximadamente 2000 km de extensão), com direção E-W, marque o limite entre o Cráton Paraguá e o Cráton Amazônico.

Ruiz (2009) e Bettencourt *et al.* (2010) adotam o termo Terreno Paraguá para denotar um terreno composto por rochas do embasamento paleoproterozoico (Complexo Gnáissico Chiquitania, Grupo Xistos San Ignácio e Complexo Granulítico Lomas Manechis) e granitoides mesoproterozoicos (Complexo Granitoide Pensamiento), amalgamados ao proto-Cráton Amazônico durante a Orogenia Rondoniano-San Ignácio. O limite com o Terreno Rio Alegre, a leste, é marcado por uma zona de cisalhamento dúctil; a norte, o limite com o Cinturão Alto Guaporé é ocultado por sequências sedimentares cenozoicas. O limite sul é recoberto por rochas sedimentares plataformais, no Brasil, (unidades pós-Sunsás) e, a oeste, por sequências sedimentares cenozoicas.

Segundo Ruiz (2009), no Terreno Paraguá são reconhecidas duas orogêneses que precederam a Orogenia Sunsás: Orogenia Lomas Manechis (1,74 a 1,69 Ga) e Orogenia San Ignácio (1,35 a 1,3 Ga; Boger *et al.*, 2005; Ruiz, 2005; Santos *et al.*, 2008).

A Orogenia Lomas Manechis (1,74 a 1,69 Ga) é caracterizada pela formação e retrabalhamento termo-tectônico do Complexo Granulítico Lomas Manechis, Complexo Gnáissico Chiquitania e Grupo Xistos San Ignacio.

A Orogenia San Ignacio manifesta-se em todo o Terreno Paraguá, sendo caracterizada pela deformação penetrativa, com *trend* estrutural NNW, metamorfismo de fácies xisto-verde a anfíbolito e expressivo magmatismo félsico-intermediário, de caráter sin a tarde cinemático, representado, principalmente pelo Complexo Granitoide Pensamiento (Litherland *et al.*, 1986).

2.2.1.2 Terreno Jauru

O Terreno Jauru foi definido, inicialmente, por Saes & Frago Cesar (1996) para agrupar complexos metamórficos paleoproterozoicos resultantes de acreções de arcos intra-oceânicos na Província Amazônia Central.

Posteriormente, Ruiz (2009) e Bettencourt *et al.* (2010) admitem que o Terreno Jauru consiste de rochas do embasamento paleoproterozoico (Grupo Alto Jauru, Suíte Intrusiva Figueira Branca, Complexo Metamórfico Alto Guaporé e Tonalito Cabaçal) e rochas geradas nas orogêneses mesoproterozoicas (Cachoeirinha e Santa Helena). Esse terreno é limitado a oeste e norte pela bacia dos Parecis, a sul, pela bacia do Pantanal e a leste, por zona de cisalhamento normal, com o Terreno Rio Alegre. Esse bloco continental guarda registros geológicos do Estateriano ao Toniano que refletem pelo menos três orogênias proterozoicas (Santa Fé, Cachoeirinha e Santa Helena; Geraldès *et al.*, 2001; Matos *et al.*, 2004; Ruiz, 2005, 2009).

Segundo Ruiz (2009), o embasamento metamórfico do Terreno Jauru é constituído pelas seguintes unidades litoestratigráficas: sequências metavulcanossedimentares (Grupo Alto Jauru), suítes plutônicas máfica-ultramáficas (Suíte Intrusiva Figueira Branca), ortognaisses granodioríticos-tonalíticos (Complexo Metamórfico Alto Guaporé) e intrusões tonalíticas (Tonalito Cabaçal), todas submetidas a metamorfismo de médio a alto grau. Idades obtidas pelos métodos U-Pb e Pb-Pb indicam que o arcabouço geológico pré-orogênico do Sistema Rondoniano-San Ignacio formou-se no intervalo entre 1,8 a 1,75 Ga. Idades menores (1,55 Ga) podem ser atribuídas ao *resetting* do sistema isotópico durante as orogênias superimpostas (Pinho, 1996; Santos *et al.*, 2000; Geraldès *et al.*, 2001; Ruiz *et al.*, 2004; Ruiz, 2005).

A Orogenia Santa Fé (1,8 a 1,75 Ga; Ruiz, 2005) corresponde à formação de arcos insulares em regime orogênico acrescionário, dominado por processos de coalescência de arcos vulcânicos. As rochas meta-supracrustais representam os derrames e sedimentos clasto-químicos de arcos, enquanto os corpos plutônicos máfico-ultramáficos são interpretados como remanescentes da porção inferior da crosta oceânica (ofiolitos) e os ortognaisses, como intrusões cálcio-alcálicas do tipo TTG.

A Orogenia Cachoeirinha (1,56 a 1,45 Ga) é caracterizada por eventos magmáticos e metamórficos que afetaram o conjunto de unidades geológicas já descritas. Com base em Geraldès *et al.* (2001), Ruiz *et al.* (2004), Ruiz (2005) e Araújo (2008) distinguem-se dois estágios no magmatismo relacionado à Orogenia Cachoeirinha: magmatismo sin-cinemático (Suíte Intrusiva Santa Cruz) e magmatismo tarde-cinemático (Suíte Intrusiva Alvorada).

O ambiente geodinâmico sugerido para a Orogenia Cachoeirinha é caracterizado pela subducção do tipo B, geradora de arcos magmáticos continentais evoluídos sobre crosta estateriana edificada na Orogenia Santa Fé.

A Orogenia Santa Helena (1,48 a 1,42 Ga) retrata a implantação de um arco magmático continental (Arco Magmático Santa Helena, Geraldès 2000), caracterizado pela formação de intrusões sin-cinemáticas das Suítes Intrusivas Santa Helena e Água Clara (1,48 a 1,42 Ga) e Suíte Intrusiva Pindaituba (1,46 a 1,42 Ga) e pelo magmatismo rapakivi, pós-cinemático ou anorogênico da Suíte Rio Branco (1,42 Ga; Geraldès *et al.*, 2001; Geraldès *et al.*, 2004; Ruiz, 2005; Araújo, 2008).

O ambiente geodinâmico sugerido para a Orogenia Santa Helena é do tipo arco magmático continental implantado sobre crosta formada durante as orogenias Santa Fé e Cachoeirinha.

2.2.1.3 Terreno Rio Alegre

O Terreno Rio Alegre foi primeiramente definido como uma zona de sutura, por Saes & Fragoso Cesar (1996), e posteriormente denominado de Orogênese Rio Alegre por Matos *et al.* (2004).

Segundo Ruiz (2009), trata-se de um segmento crustal com cerca de 15 km de largura, com *trend* N40°W, limitado por zonas de cisalhamentos dúcteis a leste com o Terreno Jauru, a oeste com o Terreno Paraguá. A norte e sul sua extensão é desconhecida (Matos *et al.* 2004), estando recoberto por sequências sedimentares cenozoicas.

No Terreno Rio Alegre são reconhecidos dois estágios do Ciclo de Wilson. A fase de expansão do assoalho oceânico, entre 1,51 e 1,50 Ga, hipótese corroborada por dados litogeoquímicos e de isótopos de Nd (Geraldes, 2000; Matos *et al.*, 2004) da assembleia vulcanossedimentar; seguida pelos estágios de subducção e colisão continental, entre 1,44 e 1,38 Ga (Saes, 1999; Geraldes, 2000; Matos *et al.*, 2004; Ruiz, 2005).

O estágio *drift* (1,51 a 1,5 Ga) é caracterizado pela formação de crosta oceânica primitiva (Grupo Rio Alegre), constituída na base por derrames de lavas ultramáficas a máficas e, no topo, prevalecem derrames intermediários a félsicos, com sedimentação clastoquímica associada (Matos, 1994; Matos *et al.*, 2004). Plutons ultramáficos a máficos (Suíte Intrusiva Vale do Alegre) circulares a elípticos relacionam-se ao estágio extensional (Ruiz, 2005) do terreno.

O estágio orogênico - Orogenia Rio Alegre (1,44 a 1,38 Ga) - é caracterizado pelo consumo de crosta oceânica em provável arco vulcânico, com geração de *plutons* e batólitos (Suíte Intrusiva Santa Rita) constituídos por rochas toleíticas a cálcio-alcalinas, tipo I, metaluminosas a peraluminosas, com valores de $\epsilon_{Nd(t)}$ positivos, caracterizando a natureza juvenil do magma parental (Matos *et al.*, 2004; Ruiz, 2005).

2.2.2 Província Sunsás-Aguapeí

2.2.2.1 Faixa Móvel Aguapeí

A Faixa Móvel Aguapeí corresponde a um cinturão linear, orientado segundo a direção N20°-40°W, que se prolonga da região de Rincón del Tigre (BO) a sul, até a região de Rio Novo, próxima à divisa entre Mato Grosso e Rondônia, com cerca de 500 km de comprimento e largura variando entre 150 a 200 km (Figura 1.1).

O Grupo Aguapeí, que se assenta discordantemente sobre um amálgama de terrenos paleo a mesoproterozoicos, apresenta três estágios evolutivos bem demarcados (Saes, 1999): o estágio Rifte (Formação Fortuna), o estágio de Sinéclise (Formação Vale da Promissão) e o estágio de inversão tectônica (Formação Morro Cristalina).

A Faixa Móvel Aguapeí caracteriza-se por dois estágios tectônicos distintos: o primeiro, contracional, responsável pela formação de dobras e cavalgamentos regionais, com metamorfismo associado e, o segundo, extensional, provável colapso orogênico, assinalado por zonas de cisalhamentos dúcteis com cinemática normal ou transtracional (Ruiz, 2005).

Parte dos Terrenos Jauru e Paraguá foi poupado pela Orogenia Sunsás-Aguapeí, como demonstra a extensa cobertura siliciclástica, não deformada, do Grupo Aguapeí, que repousa horizontalmente sobre o substrato granítico-gnáissico em discordância angular e erosiva.

Nos terrenos Paraguá, Rio Alegre e Jauru são observadas estruturas tectônicas que demonstram o caráter polifásico da Faixa Móvel Aguapeí, sendo reconhecidas três fases deformacionais (F_1 , F_2 e F_3) no Grupo Aguapeí, relacionadas ao estágio contracional.

A principal fase de deformação (F_1) é caracterizada por dobras (D_1) suaves a cerradas, quilométricas, normais com caimento (Antiformal do Cágado e Sinformal do Caldeirão, p.ex.) A foliação plano-axial, xistosidade ou clivagem ardosiária, orienta-se segundo $250^\circ/80^\circ$, as charneiras caem entre 5° e 15° para 160° a 140° ou 340° a 310° .

A segunda fase de deformação (F_2) é responsável pela implantação de dobras assimétricas, centimétricas a métricas, com plano-axial mergulhando entre 20° e 40° para SW; enquanto as linhas de charneiras caem entre 5° e 10° para NNW. A foliação S_2 , típica clivagem de crenulação, dos metaruditos aos metapelitos exibem atitudes de $255^\circ/30^\circ$. A essa fase associam-se as principais zonas de cisalhamentos reversas ou de cavalgamento, Zona de Cisalhamento Morro Solteiro, por exemplo, exibem transporte de topo para NE e não afetam o embasamento (deformação pelicular ou epidérmica).

A terceira fase de deformação (F_3) é responsável formação de dobras suaves a abertas D_3 , em escala métrica a centimétrica, com plano-axial íngreme, entre 75° a 85° para SE e NW; enquanto foliação plano-axial (S_3) mostra atitude média de $160^\circ/80^\circ$ e $340^\circ/80^\circ$.

O grau metamórfico alcançado pelas rochas do Grupo Aguapeí situa-se na fácies xisto verde e a paragênese metamórfica desenvolveu-se durante a fase F_1 .

Dados Ar-Ar para rochas metassedimentares do Grupo Aguapeí indicam idades entre 908 a 925 Ma, e para o embasamento retrabalhado idades entre 1027 a 918 Ma, sugerindo um período de resfriamento regional relacionado ao estágio contracional e metamórfico do orógeno, entre 1030 e 910 Ma.

O estágio extensional é caracterizado pela formação de zonas de cisalhamento dúcteis, com cinemática normal (zonas de cisalhamento Indiavaí-Lucialva, Piratininga, Caramujo e Corredor), que afetam tanto as rochas metassedimentares Aguapeí como seu substrato metamórfico. Idades Ar-Ar em milonitos (Ruiz, 2005), indicam valores entre 915 ± 3 Ma (Zona de Cisalhamento Indiavaí-Lucialva) e 923 ± 3 Ma (Zona de Cisalhamento Piratininga).

2.3 A PARTE SUL DO CRÁTON AMAZÔNICO

Segundo Ruiz (2005), o extremo sul do Cráton Amazônico está representado pelo Terreno Rio Apa, que aflora na porção sudoeste do estado de Mato Grosso do Sul, fronteira com o Paraguai.

Esse terreno compreende um segmento crustal paleoproterozoico e constitui o embasamento da Faixa Paraguai, na região. Possui cerca de 220 km de comprimento segundo a direção N-S e 60 km de largura média. Limita-se, a leste, por rochas pelítico-carbonáticas do Grupo Corumbá (Serra da Bodoquena) e, a oeste, encontra-se coberto por sedimentos cenozoicos da Bacia do Pantanal (Lacerda Filho *et al.*, 2006).

Lacerda Filho *et al.* (2006) subdividem esse terreno em três compartimentos geotectônicos distintos, assim designados: Remanescente de Crosta Oceânica (2,2 a 1,95 Ga), representado por rochas metavulcanossedimentares do Grupo Alto Tererê; Arco Magmático Rio Apa (1,95 a 1,87 Ga), constituído por uma associação de rochas plutônicas; Arco Magmático Amoguijá (1,87 a 1,75 Ga), que inclui as rochas do Granito Alumiador e Vulcânicas Serra da Bocaina. Adicionalmente, esses autores apresentam um conjunto de rochas intrusivas máficas que corresponde à Suíte Gabro-Anortosítica Serra da Alegria, Gabro Morro do Triunfo e por enxame de diques e soleiras.

Cordani *et al.* (2010), considerando os aspectos deformacionais, as idades U-Pb e idades-modelo Sm-Nd, sugerem a divisão do Terreno Rio Apa em dois domínios distintos, Oriental e Ocidental. Esses domínios são limitados por uma zona de sutura de direção predominante N-S (Figura 2.6).

O Bloco Ocidental é representado pelo Complexo Porto Murtinho, Batólito Alumiador, Formação Serra da Bocaina, Complexo Triunfo, Suíte Gabro-Anortosito Serra da Alegria e as rochas metassedimentares do Grupo Campanário. O Bloco Oriental é constituído pelo Grupo Alto Tererê, Gnaisse Caracol e gnaisses, granitos e migmatitos da Província Paso Bravo.

O Terreno Rio Apa se estabilizou após a aglutinação desses dois domínios (Oriental e Ocidental) em torno de 1,3 Ga, conforme indicam os dados K-Ar e Ar-Ar (Araújo *et al.*, 1982; Cordani *et al.*, 2010).

Faleiros *et al.* (2016), utilizando dados geológicos e geocronológicos U-Pb (SHRIMP), sugerem que o Terreno Rio Apa foi formado pela acreção de arcos magmáticos como uma margem continental ativa entre 1950 a 1720 Ma, composto por 3 domínios

principais, sendo eles: sudeste, ocidental e oriental, estes dois últimos já indicados no trabalho de Cordani *et al.* (2010).

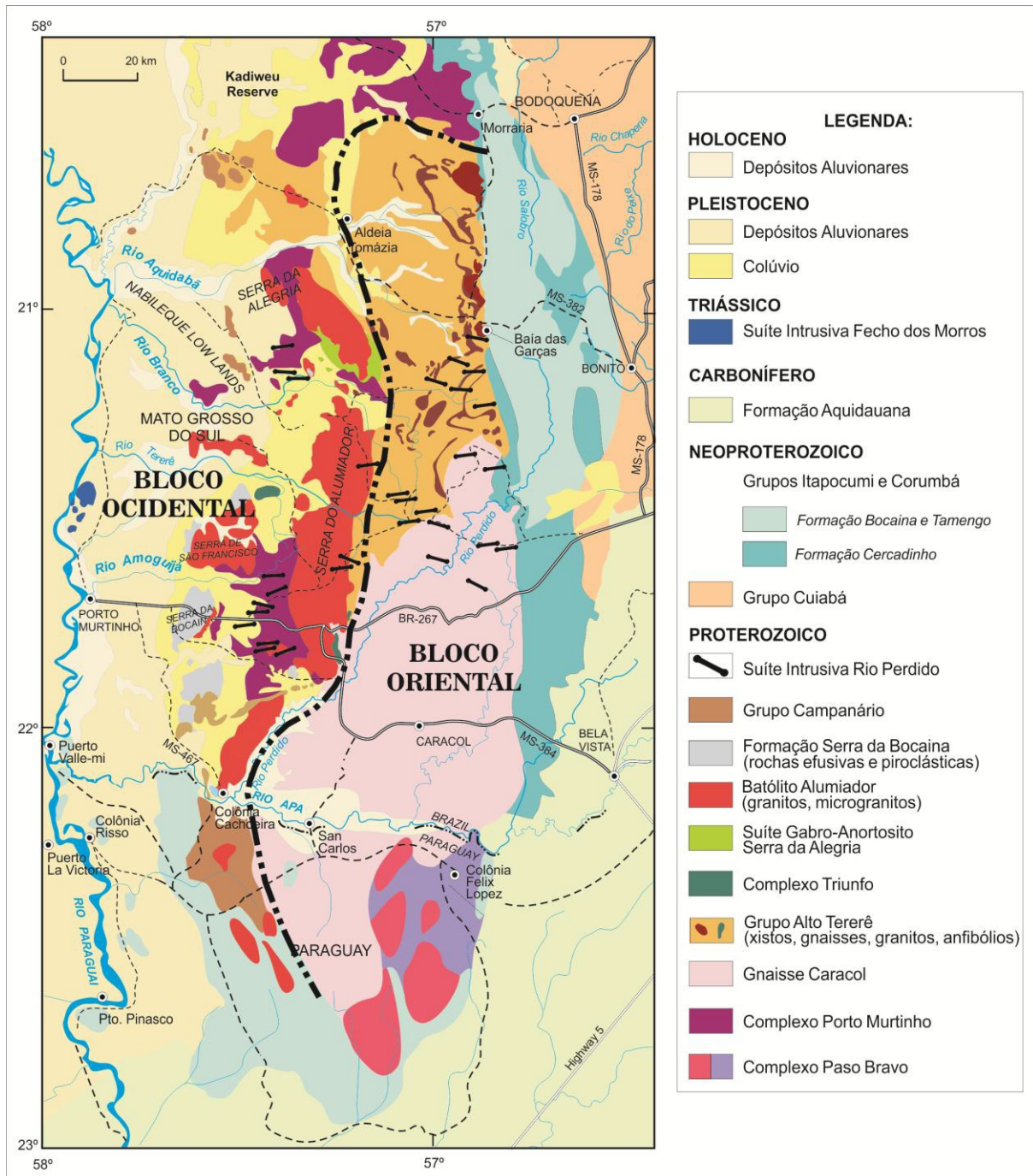


Figura 2.6. Esboço geológico do Terreno Rio Apa no sudoeste do estado de Mato Grosso do Sul (Brasil) e noroeste do Paraguai. Extraído e modificado de Cordani *et al.* (2010).

3 ARTIGOS SUBMETIDOS

3.1 SUÍTE INTRUSIVA RIO PERDIDO: MAGMATISMO INTRAPLACA NO SUL DO CRÁTON AMAZÔNICO – TERRENO RIO APA

Gabrielle Aparecida de Lima

Moacir José Buenano Macambira

Maria Zélia Aguiar de Sousa

Amarildo Salina Ruiz

Submetido: Geologia USP - Série Científica

[GUSPSC] Agradecimento pela submissão

Nanci Iurico Assakura <publigc@usp.br> 7 de julho de 2016 00:38

Responder a: Gabrielle Aparecida Lima <gabilimagel@gmail.com>

Para: Gabrielle Aparecida Lima <gabilimagel@gmail.com>

Gabrielle Aparecida Lima,

Agradecemos a submissão do trabalho "SUÍTE INTRUSIVA RIO PERDIDO: MAGMATISMO INTRAPLACA NO SUL DO CRÁTON AMAZÔNICO – TERRENO RIO APA" para a revista Geologia USP. Série Científica.

Acompanhe o progresso da sua submissão por meio da interface de administração do sistema, disponível em:

Em caso de dúvidas, entre em contato via e-mail.

Agradecemos mais uma vez considerar nossa revista como meio de compartilhar seu trabalho.

Nanci Iurico Assakura

Geologia USP. Série Científica

Geologia USP. Série Científica

<http://submission.ppegeo.igc.usp.br/index.php/guspssc>

**SUÍTE INTRUSIVA RIO PERDIDO: MAGMATISMO INTRAPLACA NO SUL DO
CRÁTON AMAZÔNICO – TERRENO RIO APA**

**RIO PERDIDO INTRUSIVE SUITE: INTRAPLATE MAGMATISM IN SOUTHERN
AMAZONIAN CRATON – RIO APA TERRANE**

Enxame de Diques Rio Perdido: uma LIP pré-Rodínia?

Gabrielle Aparecida de Lima^{1,4,5,6} (gabilimagel@gmail.com); Moacir José Buenano
Macambira^{2,5} (moamac@ufpa.br); Maria Zélia Aguiar de Sousa^{3,5,6}
(prof.mzaguiar@gmail.com); Amarildo Salina Ruiz^{3,5,6} (asruiz@gmail.com)

¹Programa de Pós-Graduação em Geologia e Geoquímica, IG/UFPA
(Rua Augusto Corrêa nº 1, Bairro Guamá, Cidade Universitária José da Silveira Netto
CEP: 66075-110, Belém, Pará, Brasil – 65-81134517)

²Laboratório de Geologia Isotópica – Pará-Iso, IG/UFPA

³Faculdade de Geociências, FAGEO/UFMT

⁴Instituto de Engenharia, IEng/UFMT

⁵Instituto Nacional de Ciência e Tecnologia de Geociências da Amazônia (GEOCIAM)

⁶Grupo de Pesquisa em Evolução Crustal e Tectônica – Guaporé

Número de palavras: 5.618

Total de figuras: 12

Total de tabelas: 1

RESUMO

O enxame de diques da Suíte Intrusiva Rio Perdido ocorre no sul do Cráton Amazônico, Terreno Rio Apa e representa importante evento magmático de natureza fissural, pré-aglutinação do Supercontinente Rodínia. Os diques são tabulares a lenticulares, com espessura variando entre 1 e 30 m, preferencialmente paralelos segundo as direções N70°-90°E e N70°-90°W, exibem contatos abruptos e discordantes ao *trend* regional NS. Os diques são homogêneos, compostos por diabásios de granulação muito fina a fina e microgabros finos a

médios, isotrópicos, sem quaisquer vestígios de deformação dúctil e metamorfismo. Ao microscópio estas rochas apresentam-se holocristalinas, com textura ofítica a subofítica, intergranular, por vezes porfirítica, e localmente *quenching*, com morfologia do tipo “cauda de andorinha”. Constituem-se essencialmente por plagioclásio, piroxênios e olivina. Apresenta *trend* toleítico, com enriquecimento em FeO_t em relação ao MgO para valores de álcalis relativamente constantes. As rochas dos diques classificam-se, quase que exclusivamente, como basaltos e basaltos andesíticos e quanto à ambiência tectônica os diagramas sugerem para essas rochas uma colocação semelhante a dos basaltos intraplaca fanerozoicos. O comportamento dos elementos terras raras (ETR), mostra forte fracionamento de ETR pesados em relação aos ETR leves, com razões La/Yb entre 2,8 e 6,2 e anomalia negativa pouco expressiva ou inexistente de Eu. Considerando a idade de cristalização em torno de 1100 Ma para as rochas das suítes Rio Perdido e Huanchaca e do Complexo Rincón del Tigre, sugere-se a existência de *Large Igneous Province* (LIP) esteniana, associada a tentativa de ruptura continental relacionada à evolução do Aulacógeno Aguapeí.

Palavras-chave: Cráton Amazônico, Terreno Rio Apa, Diques Máficos, Litoquímica

ABSTRACT

The dyke swarms of the Rio Perdido Intrusive Suite are located on the southern Amazonian Craton, Rio Apa Terrane, and they stand for an important fissural magmatic event that took place before the agglutination of the Rodinia Supercontinent. The dykes are 1 to 30 m-thick, with tabular to lenticular shape, and follow two preferential trends: N70°-90°E and N70°-90°W. They occur parallel to each other showing abrupt and discordant contacts relative to the regional NS trend. These rocks are compositionally homogeneous being composed of very fine- to fine-grained diabases, as well as fine- to medium-grained microgabbros that shows no evidence of ductile deformation or metamorphism. Under microscope, these rocks are holocrystalline, and display several types of textures such as ophitic to subophitic, intergranular, porphyritic in places, and locally, quench texture. The essential constituents are plagioclase, pyroxene, and olivine. Harker-type diagrams show a tholeiitic trend. They mostly plot as basalts and andesitic basalts. Diagrams suggest geological settings similar to that of Phanerozoic intraplate settings for the emplacement of these rocks. The geochemical signature of rare earth elements shows strong fractionation of heavy REE relative to light REE, with La/Yb ratios ranging from 2.8 to 6.2. Taking into account a crystallization age

around 1100 Ma for the rocks from the Rio Perdido and Huanchaca Intrusive Suites, and from the Rincón del Tigre Complex, here we suggest the existence of a Stenian Large Igneous Province (LIP) which may be associated with an attempted continental breakup related to the evolution of the Aguapeí Aulacogen.

Keywords: Amazonian Craton, Rio Apa Terrane, Mafic Dykes, Litochemistry

INTRODUÇÃO

Enxames de diques e soleiras máficas constituem importante ferramenta para o entendimento dos processos geodinâmicos, especialmente por marcarem o início de grandes eventos tectônicos extensionais, e serem indicadores significativos da natureza e evolução das fontes mantélicas (Halls, 1982). Adicionalmente, à história magmática e temporal das LIP's, pode fornecer informações importantes para a reconstrução paleogeográfica dos supercontinentes pré-cambrianos (Ernst *et al.*, 2013).

Na porção sul-sudoeste do Cráton Amazônico foram reconhecidos vários enxames de diques e soleiras máficas (Figura 1), cujas idades de formação foram recentemente definidas com emprego do método U-Pb (TIMS) em badeleíta (Teixeira *et al.*, 2015a, 2015b, 2016) e zircão (Faleiros *et al.*, 2016). Embora ainda ocorram debates sobre a petrogênese e ambientes tectônicos desse magmatismo máfico, atualmente há um consenso em relação às idades de formação, exceto para o enxame de diques da Suíte Rio Perdido, no Terreno Rio Apa.

Considerando que a Suíte Intrusiva Rio Perdido (SIRP) é a menos conhecida em seus aspectos geológicos, petrológicos e geocronológicos, o objetivo deste trabalho é, com base em dados de campo, petrográficos e litoquímicos, contribuir para a compreensão da evolução petrológica e tectônica desse evento magmático registrado na porção sul do Cráton Amazônico.

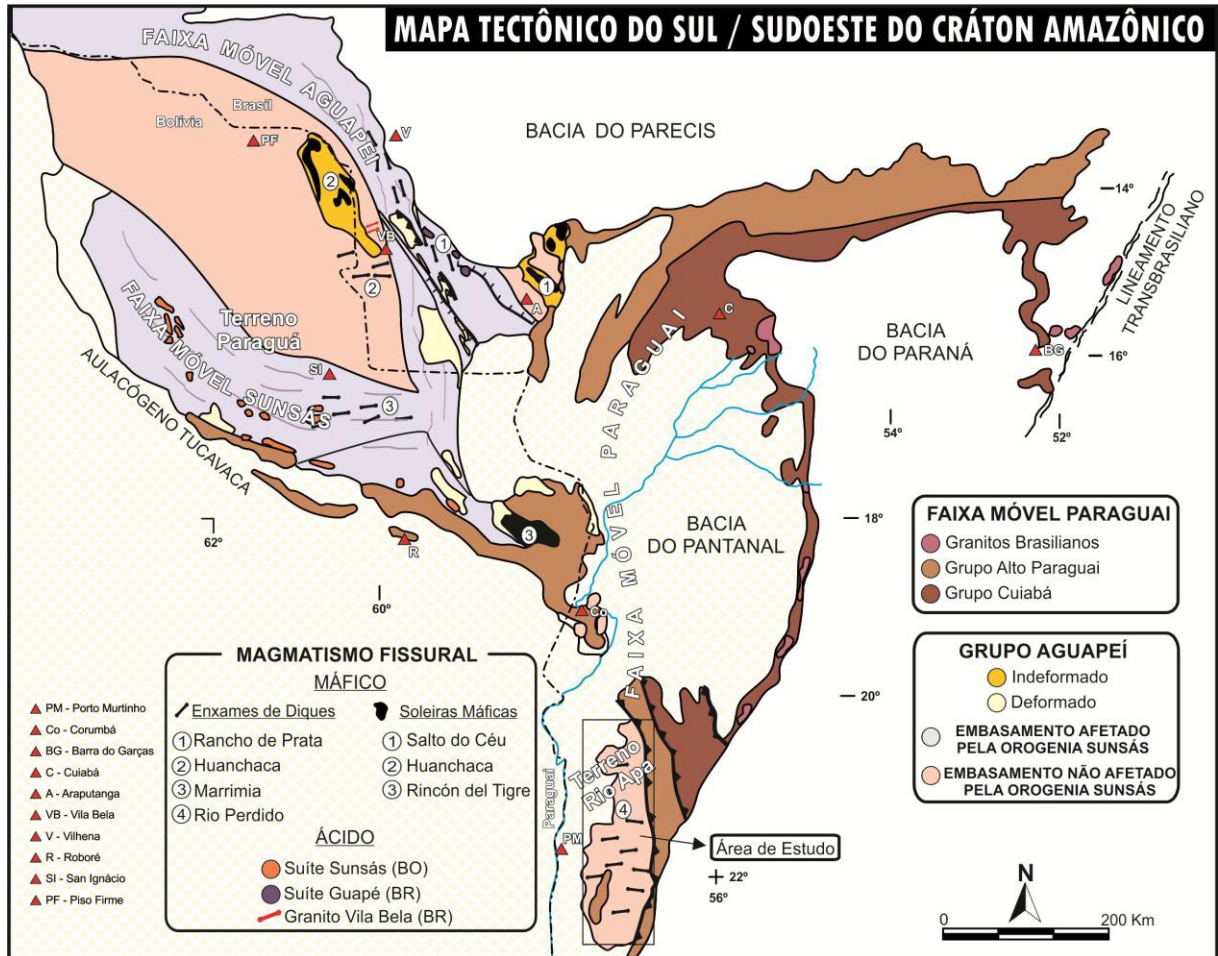


Figura 1. Mapa tectônico do Sul/Sudoeste do Cráton Amazônico (Extraído e modificado de Ruiz *et al.*, 2010a).

CONTEXTO GEOLÓGICO REGIONAL

Diques e soleiras máficas do sul e sudoeste do Cráton Amazônico

Os diques e soleiras máficas em Mato Grosso e Mato Grosso do Sul foram reconhecidos desde os levantamentos regionais do Projeto Radambrasil (Barros *et al.*, 1982; Araújo *et al.*, 1982; Santos *et al.*, 1979). No entanto, apenas a partir de 2005 esse magmatismo máfico passou a ser estudado em seus aspectos petrogenéticos e geocronológicos, com emprego de métodos isotópicos robustos, U-Pb em badeleíta e zircão. Na figura 1 estão representadas as áreas de ocorrência, das seguintes unidades, em território brasileiro: Suíte Intrusiva Huanchaca, Suíte Intrusiva Rancho de Prata, Suíte Intrusiva Salto do Céu e Suíte Intrusiva Rio Perdido.

A Suíte Intrusiva Huanchaca, inicialmente descrita por Litherland *et al.* (1986) como um conjunto de soleiras e diques máficos tonianos no oriente boliviano, foi também reconhecida no Brasil por Século *et al.* (2011) e Lima *et al.* (2012). O Complexo Estratiforme Rincón del

Tigre, contemporâneo a essa suíte, trata-se de uma soleira alojada no Grupo Sunsás/Aguapeí, deformado pela Orogenia Sunsás.

A Suíte Intrusiva Rancho de Prata, discriminada por Ruiz *et al.* (2005), corresponde a um enxame de diques máficos, com direção N-S, bem expostos na região de Nova Lacerda, com idade Rb-Sr em rocha total de, aproximadamente, 1380 Ma (Corrêa da Costa *et al.*, 2009).

A Suíte Intrusiva Salto do Céu (Araújo *et al.*, 2005) está representada por um conjunto de soleiras máficas tonianas alojadas em rochas descritas como Grupo Aguapeí, na região de Rio Branco e Salto do Céu, no estado de Mato Grosso. Foi interpretada por Araújo *et al.* (2005) como parte basal do Complexo Estratiforme de Rio Branco (Leite *et al.*, 1985).

Os diques máficos do Bloco Rio Apa foram descritos, inicialmente, por Araújo *et al.* (1982) que apresentaram uma idade K/Ar, em plagioclásio, de 914 ± 9 Ma, admitida como a idade de sua formação. Ruiz *et al.* (2010b) denominam esse enxame de diques como Suíte Intrusiva Rio Perdido (SIRP) e, com base na idade acima citada, o relacionam ao magmatismo intraplaca responsável pela ruptura do supercontinente Rodínia.

Godoi *et al.* (2001) posicionam os diques mapeados na região de Porto Murtinho e Corumbá como pertencentes ao Complexo Rio Apa, na Formação Serra Geral (Grupo São Bento).

Lacerda Filho *et al.* (2006) descrevem a ocorrência de diques e soleiras máficas, indeformados, que cortam a maioria das unidades paleoproterozoicas do Bloco Rio Apa.

Faleiros *et al.* (2015) apresentam um resultado U-Pb (LA-ICP-MS) em zircões de um dique de gabronorito, maciço, cujo intercepto superior em 1589 ± 44 Ma foi interpretado como a idade de sua formação.

Teixeira *et al.* (2016) obtiveram idade U-Pb (ID-TIMS) de 1110 Ma, em badeleíta, a partir da mesma amostra utilizada por Faleiros *et al.* (2016). Estes autores correlacionam esta idade à LIP Rincón del Tigre-Huanchaca.

Geologia do Terreno Rio Apa

Segundo Ruiz *et al.* (2005), Lacerda Filho *et al.* (2006) e Cordani *et al.* (2010), o extremo sul do Cráton Amazônico está representado pelo Terreno Rio Apa, que aflora na porção sudoeste do estado de Mato Grosso do Sul, fronteira com o Paraguai. As rochas paleoproterozoicas deste terreno serviram de encaixantes para o enxame de diques Rio Perdido, objeto deste trabalho.

Este terreno compreende um segmento crustal paleoproterozoico, e constitui o embasamento da Faixa Paraguai na região. Possui cerca de 220 km de comprimento segundo a direção N-S e 60 km de largura média. Limita-se a leste por rochas pelítico-carbonáticas do Grupo Corumbá (Serra da Bodoquena) e a oeste encontra-se coberto por sedimentos cenozoicos da Bacia do Pantanal (Lacerda *et al.*, 2006).

Cordani *et al.* (2010), considerando os aspectos deformacionais, as idades U-Pb e idades-modelo Sm-Nd, sugerem a divisão do Terreno Rio Apa em dois domínios distintos, Oriental e Ocidental. Esses domínios são limitados por uma zona de sutura de direção predominante N-S (Figura 2).

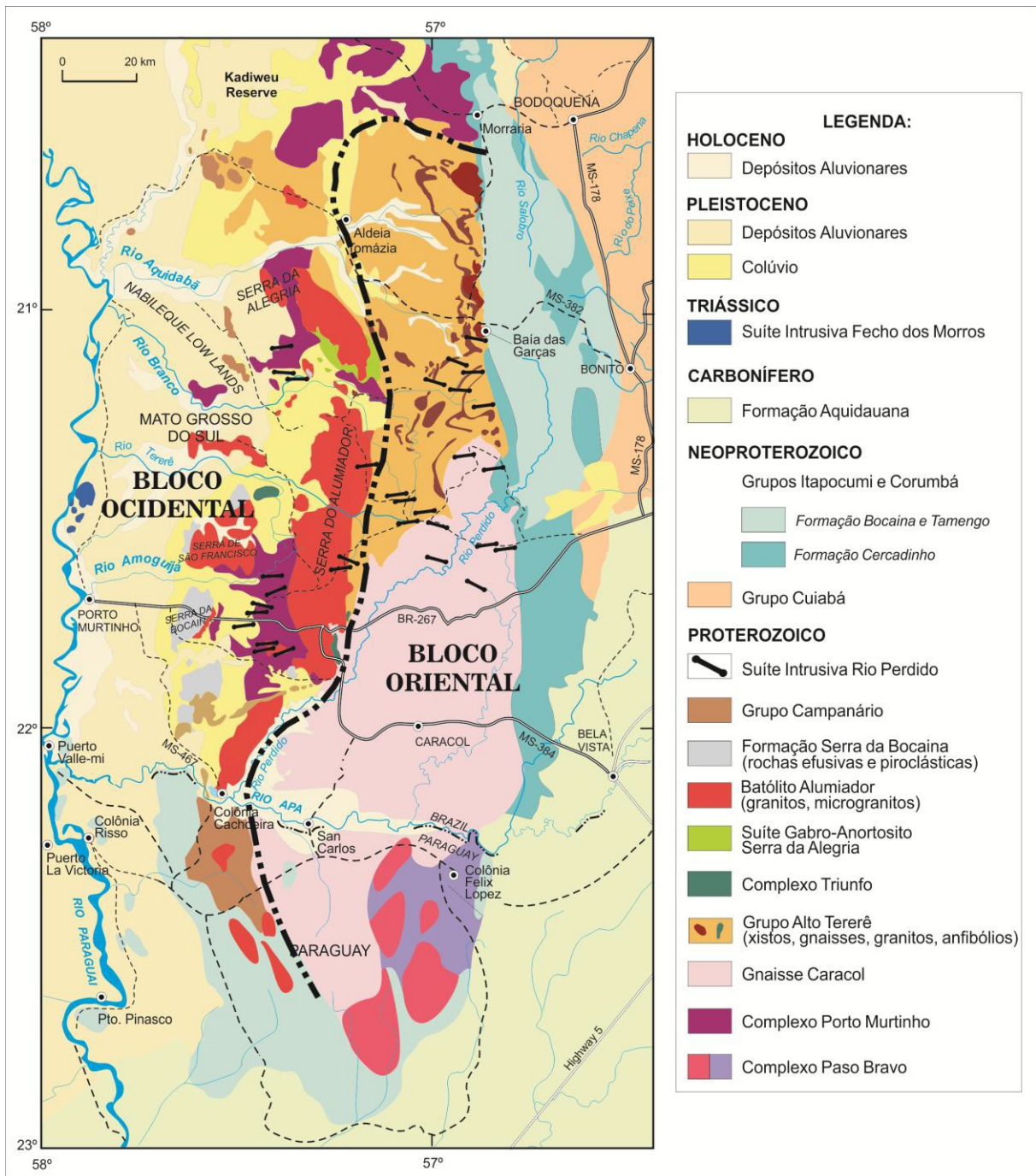


Figura 2. Esboço geológico do Terreno Rio Apa e a localização aproximada dos principais diques identificados. (Extraído e modificado de Cordani *et al.* 2010).

O Bloco Ocidental é representado pelo Complexo Porto Murtinho, Batólito Alumiador, Formação Serra da Bocaina, Complexo Triunfo, Suíte Gabro-Anortosito Serra da Alegria e as rochas metassedimentares do Grupo Campanário.

O Bloco Oriental é constituído pelo Grupo Alto Tererê, Gnaisse Caracol e gnaisses, granitos e migmatitos da Província Paso Bravo.

Segundo Cordani *et al.* (2010) o Terreno Rio Apa se estabilizou após a aglutinação desses dois domínios (Oriental e Ocidental) em torno de 1,3 Ga, conforme indicam os dados K-Ar e Ar-Ar.

ASPECTOS DE CAMPO DA SIRP

O enxame de diques que corresponde à SIRP ocorre na porção sul do Cráton Amazônico, encaixado em rochas paleoproterozoicas, em toda a extensão do Terreno Rio Apa no Brasil (sudeste do estado de Mato Grosso do Sul) e no Paraguai.

Constitui-se por diabásios de granulação muito fina a fina e microgabros finos a médios, maciços, de cor cinza-esverdeado a cinza-escuro (Figura 3), com direção preferencial entre N70°-90°E e N70°-90°W (Figura 4), e mergulhos íngremes entre 80° e 90° para os quadrantes SE e NW. Foram identificadas dezenas de diques cujas espessuras variam entre 1 e 30 m, com contatos abruptos e discordantes ao *trend* regional das encaixantes, sem registros de deformação e metamorfismo.

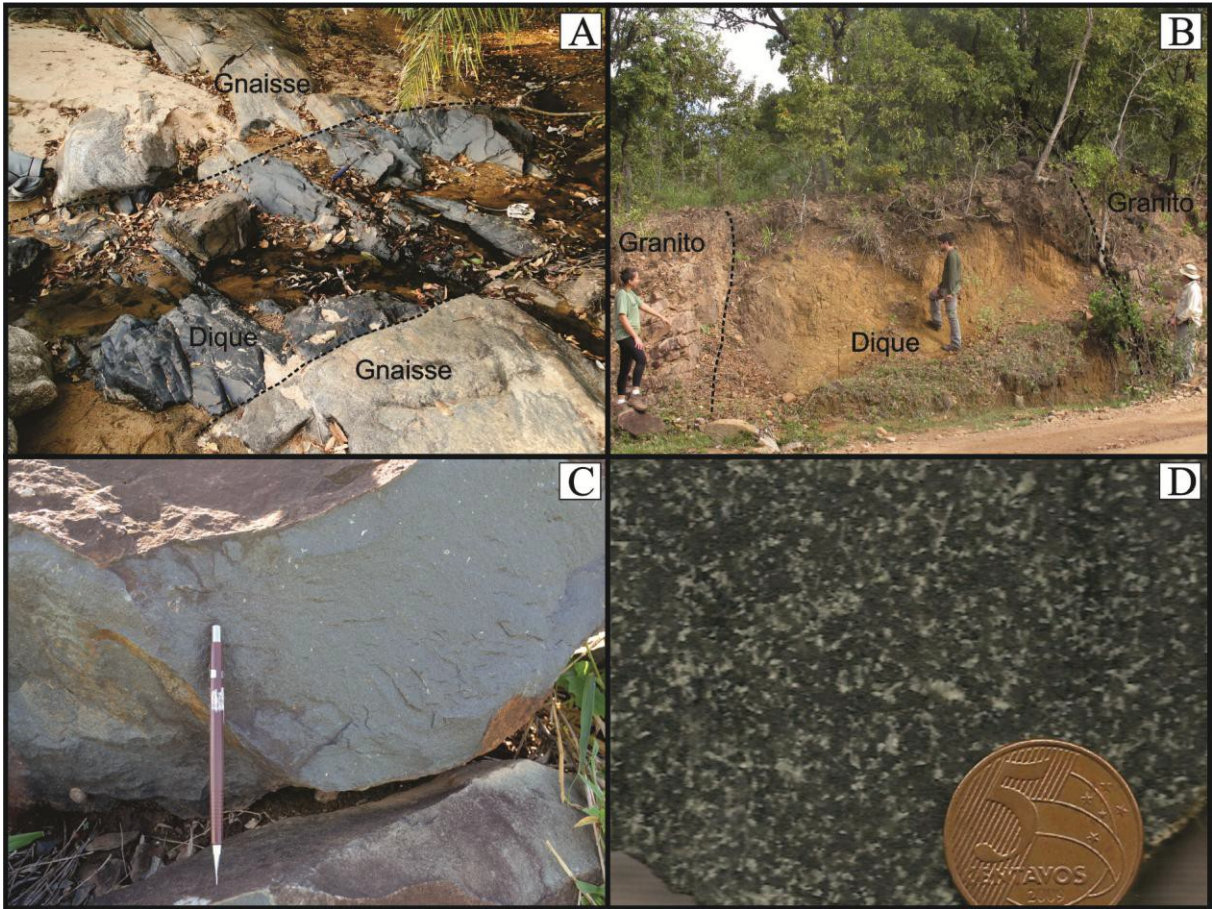


Figura 3. A e B) Diques da SIRP alojados em gnaiss do Complexo Rio Apa; C) dique de diabásio da SIRP de cor cinza-claro e granulação muito fina; D) detalhe de amostra de dique de microgabro da SIRP de textura intergranular a sub-ofítica.

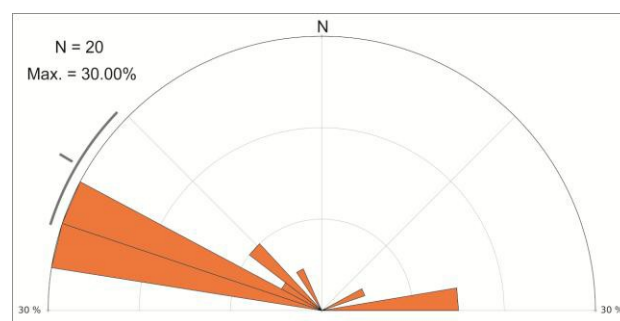


Figura 4. Diagrama de rosetas obtido para os diques da SIRP (20 medidas).

PETROGRAFIA

Macroscopicamente, as rochas da SIRP são maciças, com granulação muita fina a média, equi a inequigranulares, mesocráticas e de composição gabronorítica (Streckeisen, 1976). Ao microscópio, classificam-se como holocristalinas, com textura ofítica a subofítica (Figuras 5A e 5B), intergranular, por vezes porfirítica, e localmente *quenching*, com morfologia do tipo

“cauda de andorinha”, relacionada a resfriamento rápido (Figura 5A). Constituem-se essencialmente por plagioclásio, piroxênios e olivina; os minerais de alteração e acessórios são anfibólio, opacos, clorita, biotita, titanita, apatita, epídoto, serpentina, talco, calcita, sericita, argilominerais, iddingsita e boulingita.

Os plagioclásios, identificados como labradorita e andesina, constituem a principal fase, ocorrendo em ripas e cristais tabulares euédricos a subédricos, em geral, embricados ou radiados ou, raramente, em fenocristais tabulares, comumente zonados, saussuritizados/argilizados. Exibem geminações polissintéticas do tipo albita ou periclina e simples do tipo Carlsbad, por vezes combinadas. Frequentemente, as ripas encontram-se inclusas nos cristais de piroxênio ou entre eles caracterizando texturas, respectivamente, ofítica e subofítica.

Os piroxênios (Figuras 6A e 6B), monoclinicos (augita e pigeonita) e ortorrômnicos (hiperstênio), exibem-se em cristais prismáticos ou grãos anédricos, podendo apresentar geminação setorial, zonação, uralitização principalmente nas bordas e pseudomorfismo parcial a total para agregado de anfibólio (hornblenda), clorita, biotita e serpentina.

A olivina ocorre em grãos anédricos, por vezes, com bordas de reação para piroxênio, caracterizando textura coronítica (Figuras 7A, 7B e 7C). Altera-se também para cristais fibrosos de serpentina e/ou talco ou misturas caracterizadas como iddingsita e boulingita, restando apenas em grãos reliquiares, podendo também estar totalmente pseudomorfizada quando se observa apenas a sua forma primária. Minerais de alteração magnesianos, tais como serpentina e talco, indicam para olivina composição rica em molécula de forsterita.

O anfibólio, representado pela hornblenda ocorre, como produto de substituição do piroxênio, em raros grãos anédricos, apresentando pleocroísmo verde-escuro a verde-claro, estando parcialmente alterado para clorita.

Os minerais opacos apresentam-se normalmente cúbicos, triangulares ou com hábito esqueletal por vezes alterados para biotita/clorita. Muitas vezes, é encontrado associado a alteração dos máficos, principalmente da olivina.

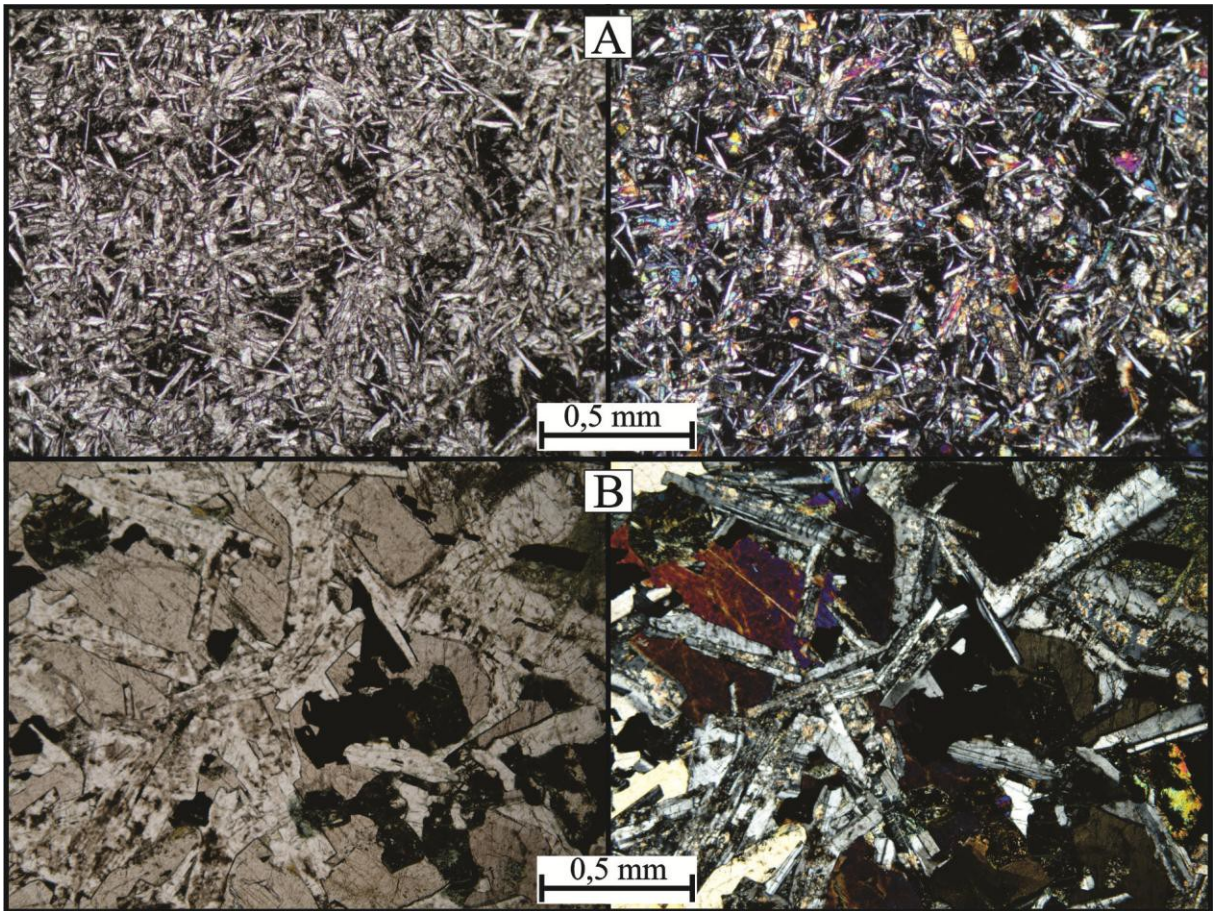


Figura 5. Fotomicrografias de amostras da SIRP, ilustrando: A) textura ofítica a subofítica, plagioclásio com morfologia do tipo “cauda de andorinha” indicando textura *quenching*; B) textura predominantemente ofítica formada por augita incluindo cristais tabulares de plagioclásio, pseudomorfos de olivina envolvidos por augita. Polarizadores paralelos à esquerda e cruzados à direita.

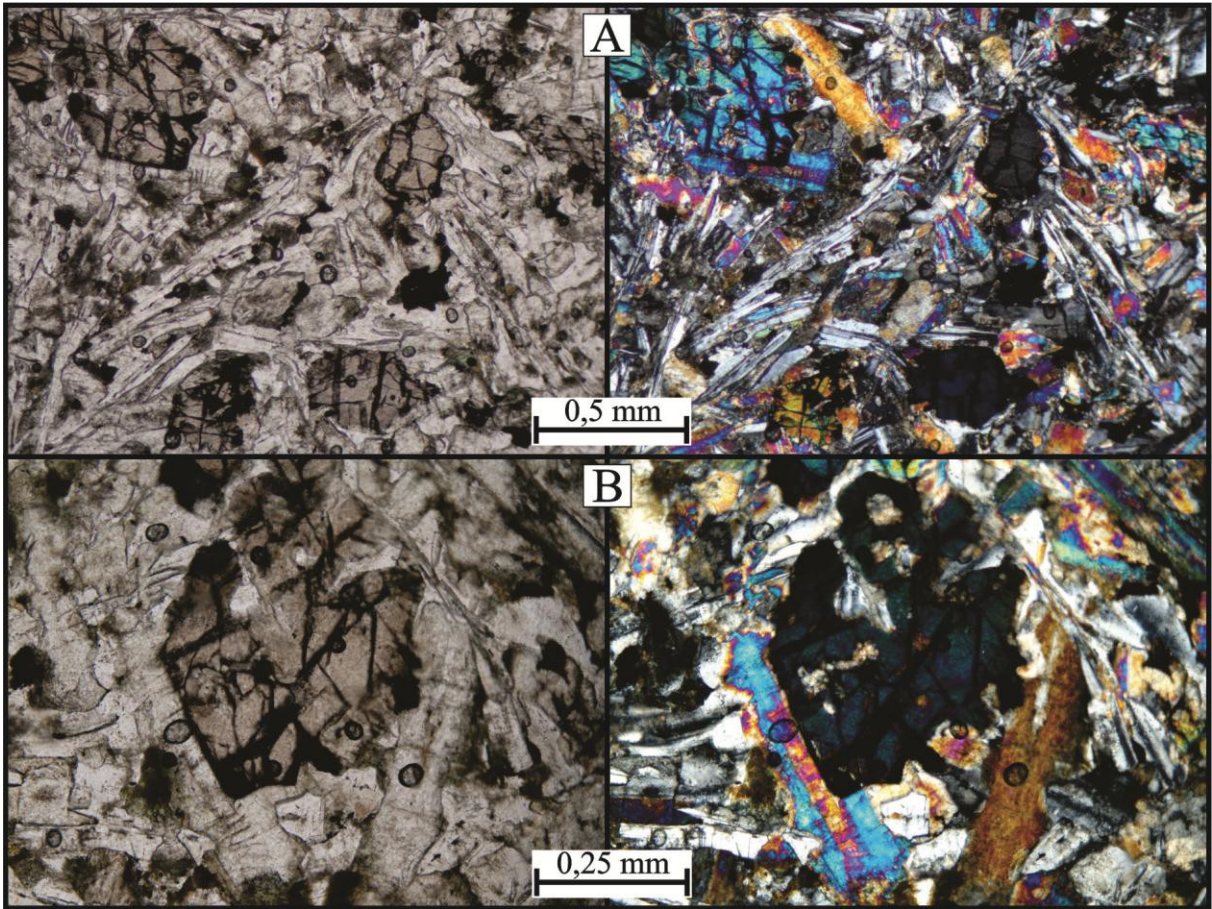


Figura 6. Fotomicrografias de amostras da SIRP, ilustrando: A) textura intergranular, presença de orto e clinopiroxênio; B) detalhe de ortopiroxênio rosa com inclusão de ripas de plagioclásio (textura ofítica) e clinopiroxênio branco prismático. Polarizadores paralelos à esquerda e cruzados à direita.

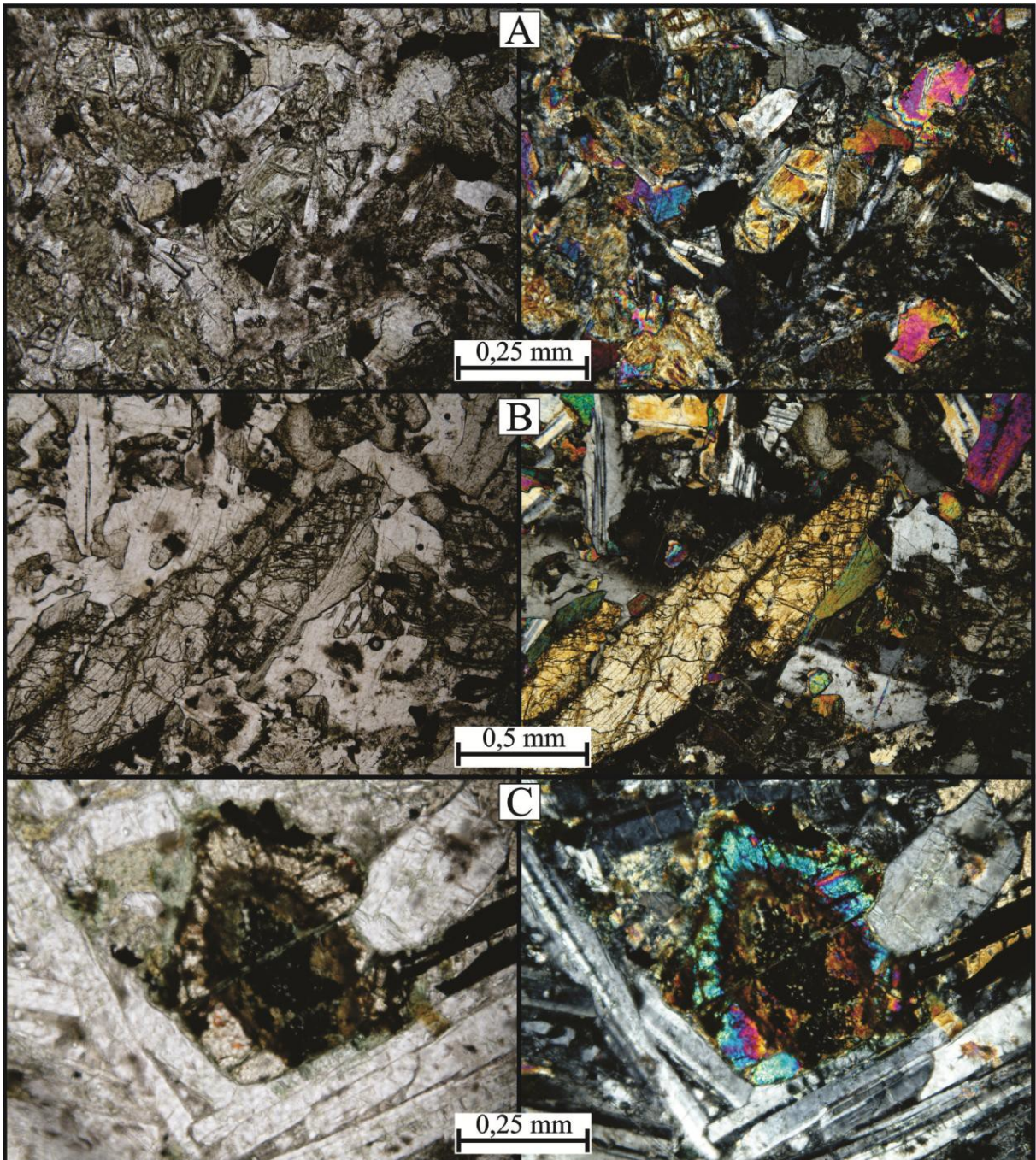


Figura 7. Fotomicrografias de amostras da SIRP ilustrando: A) textura subofítica, cristais hexagonais de olivina com fraturas serpentinizadas e coroa de reação para piroxênio; B) cristais de olivina com bordas de reação para piroxênio; C) textura intergranular com plagioclásio tabular e cristal pseudo-hexagonal zonado de olivina com núcleo substituído por opaco, anfibólio, iddingsita e boulingita, com coroa de reação de piroxênio. Polarizadores paralelos à esquerda e cruzados à direita.

ANÁLISES LITOQUÍMICAS

Após a descrição microscópica, foi feita a seleção de dezoito amostras de rocha, tidas como as mais representativas da SIRP, considerando sua distribuição na área de estudo, bem como sua diversidade textural e mineralógica, para realização das análises litoquímicas de elementos maiores (%), traço, incluindo terras raras (ppm). As amostras foram lavadas, cominuídas com marreta e britadores de mandíbula e pulverizadas em moinho de panelas, sendo todos esses procedimentos realizados no Laboratório de Preparação de Amostras da Universidade Federal de Mato Grosso.

Após a preparação, as amostras foram encaminhadas para o Laboratório Acme Analytical Laboratories (Vancouver - Canadá), onde foi empregada a técnica de ICP-ES (Inductively Coupled Plasma Emission Spectrometry) para análises dos elementos maiores [SiO_2 , Al_2O_3 , MgO , CaO , TiO_2 , MnO , Na_2O , K_2O , P_2O_5 , $\text{Fe}_2\text{O}_3(\text{t})$] e espectrometria de emissão atômica com plasma acoplado induzido (ICP-MS - Inductively Coupled Plasma-Mass Spectrometry) para os elementos traço e terras raras (Rb, Ba, Nb, Sr, Zr, Y, La, Ce, Pr, Nd, Sm, Eu, Gd, Tb, Dy, Ho, Er, Tm, Yb, Lu). Os dados de elementos maiores e traço encontram-se listados na tabela 1.

Tabela 1. Dados litoquímicos das rochas da SIRP [elementos maiores (% em peso), traço e terras raras (ppm)].

	RC-03	RC-06B	RC-09C	RC-15	RC-22	RC-27	FS78	FS32	FS72A
SiO ₂	51,70	54,50	52,87	53,75	51,79	51,21	50,54	48,71	54,26
TiO ₂	0,73	0,93	0,76	0,74	1,16	0,75	1,28	1,76	0,70
Al ₂ O ₃	12,14	13,05	12,71	13,72	14,68	12,72	13,64	14,24	14,18
Fe ₂ O ₃	10,58	10,58	11,48	10,30	10,98	11,52	13,91	14,42	9,91
MnO	0,16	0,15	0,17	0,16	0,15	0,17	0,20	0,19	0,15
MgO	11,35	6,69	8,66	7,86	5,76	10,20	6,31	6,19	7,75
CaO	8,29	7,30	8,69	8,10	8,68	8,84	9,59	8,89	8,80
Na ₂ O	1,73	2,05	1,71	1,88	2,73	1,63	2,20	1,66	1,78
K ₂ O	1,04	1,91	1,27	1,49	1,85	1,12	0,89	0,73	1,49
P ₂ O ₅	0,08	0,12	0,09	0,10	0,15	0,09	0,13	0,38	0,10
LOI	1,70	2,30	1,20	1,50	1,70	1,30	1,00	2,50	0,60
Total	99,50	99,58	99,61	99,60	99,63	99,55	99,69	99,67	99,72
Ba	207	343	216	393	473	208	175	183	267
Rb	60,0	116,9	71,3	60,0	110,3	64,3	49,3	35,1	52,8
Sr	156,6	189,1	133,1	237,0	220,3	117,7	150,3	366,6	147,5

Zr	79,9	128,0	86,4	98,6	133,1	77,6	93,5	139,9	88,5
Nb	4,6	9,1	6,1	4,9	7,9	4,5	5,2	4,6	4,7
La	11,4	20,7	13,4	17,3	19,9	9,9	11,9	19,8	14,0
Ce	25,7	46,7	29,6	38,3	43,4	22,5	25,2	39,9	27,6
Pr	3,03	5,50	3,48	4,40	5,17	2,65	3,44	5,20	3,27
Nd	12,1	20,8	13,6	16,8	21,2	11,2	13,8	24,7	13,4
Sm	2,69	4,52	3,04	3,42	4,54	2,58	3,74	5,23	2,91
Eu	0,81	1,08	0,86	0,94	1,25	0,77	1,14	1,61	0,84
Gd	3,01	4,63	3,35	3,46	4,81	2,80	4,24	5,60	3,33
Tb	0,52	0,79	0,58	0,59	0,86	0,52	0,74	0,90	0,53
Dy	2,90	4,45	3,42	3,32	4,89	3,22	4,34	5,43	3,66
Ho	0,62	0,90	0,73	0,69	0,95	0,65	0,95	1,01	0,71
Er	1,80	2,65	2,13	2,18	2,97	1,99	2,85	2,94	1,97
Tm	0,28	0,39	0,31	0,32	0,43	0,30	0,40	0,45	0,30
Yb	1,61	2,47	1,96	2,00	2,70	1,74	2,97	2,78	1,84
Lu	0,25	0,38	0,31	0,31	0,41	0,28	0,42	0,44	0,31
Y	17,3	25,6	20,4	20,7	28,4	17,3	24,2	28,5	17,9

Tabela 1. Continuação.

	FS80A	FS106	FS100	FS90	FS06	FS80	FS72	GZ47	RC11
SiO ₂	50,81	50,87	53,74	46,34	53,91	50,15	54,19	53,15	50,03
TiO ₂	1,31	1,29	0,75	2,67	0,74	1,32	0,74	1,04	0,66
Al ₂ O ₃	13,69	13,91	14,25	14,04	14,23	13,93	14,03	14,56	10,88
Fe ₂ O ₃	13,87	13,78	10,06	16,88	9,99	14,35	9,87	11,74	12,34
MnO	0,20	0,20	0,15	0,22	0,15	0,21	0,15	0,17	0,18
MgO	6,31	6,39	7,40	5,79	7,30	6,27	7,22	5,66	14,44
CaO	10,07	9,56	8,34	9,36	8,69	9,80	8,16	8,79	8,49
Na ₂ O	2,13	2,25	2,14	2,12	2,01	2,21	2,11	2,18	1,41
K ₂ O	0,71	0,84	1,45	0,88	1,33	0,86	1,72	1,30	0,69
P ₂ O ₅	0,14	0,13	0,11	0,29	0,11	0,14	0,10	0,16	0,07
LOI	0,50	0,50	1,30	1,10	1,20	0,50	1,40	1,00	0,30
Total	99,74	99,72	99,69	99,69	99,66	99,74	99,69	99,75	99,49
Ba	165	155	313	171	304	181	313	393	126
Rb	27,3	49,6	62,4	40,9	50,7	40,4	84,9	46,0	32,0
Sr	151,8	162,5	181,9	176,0	160,5	154,7	162,3	175,1	85,7
Zr	91,8	91,7	90,2	174,0	90,0	98,0	95,8	124,6	64,4
Nb	5,2	5,0	4,3	11,0	4,6	5,1	4,8	5,9	3,5
La	11,7	10,2	14,7	16,4	15,2	12,0	14,8	21,2	8,7

Ce	24,3	23,9	28,8	35,1	30,4	26,2	29,3	41,8	18,7
Pr	3,37	3,13	3,57	4,98	3,53	3,46	3,52	5,22	2,18
Nd	13,6	11,7	15,8	21,6	16,6	14,4	12,0	22,4	9,8
Sm	3,26	3,39	3,20	5,84	3,00	3,66	3,03	4,78	2,24
Eu	1,20	1,20	0,95	1,94	0,90	1,25	0,87	1,20	0,64
Gd	4,41	4,00	3,39	6,79	3,61	4,60	3,44	5,07	2,64
Tb	0,72	0,71	0,56	1,11	0,58	0,76	0,56	0,78	0,46
Dy	4,31	4,46	3,39	6,89	3,53	4,80	3,28	4,92	2,89
Ho	0,94	0,93	0,63	1,41	0,73	1,05	0,72	1,00	0,58
Er	2,82	2,82	1,83	3,90	2,09	2,93	1,93	2,84	1,72
Tm	0,38	0,37	0,32	0,57	0,33	0,43	0,32	0,44	0,23
Yb	2,66	2,57	1,85	3,74	2,22	3,04	2,17	2,70	1,41
Lu	0,44	0,38	0,32	0,57	0,29	0,44	0,32	0,42	0,23
Y	24,1	23,8	18,5	34,6	18,3	26,0	18,6	27,2	15,4

O tratamento dos dados e confecção dos diagramas foram feitos utilizando o *software* GCDkit (versão 3.0, Geochemical Data Toolkit for Windows; Janoušek *et al.*, 2006).

Os valores de MgO variam entre 5,66 e 14,44% e o índice de diferenciação mg# [$\text{mg\#} = \text{Mg}^{+2}/(\text{Mg}^{+2} + \text{Fe}^{+2})$] em porcentagem de peso, calculado assumindo a razão $\text{Fe}_2\text{O}_3/\text{FeO}$ igual a 0,15, para as rochas estudadas, apresentaram variações entre 0,23 e 0,51, valor comum para magmas basálticos evoluídos. Quanto ao teor de TiO_2 , as rochas classificam-se como baixo titânio (BTi; $\text{TiO}_2 \leq 2\%$), com concentrações variando entre 0,70 e 1,76%, com exceção de uma amostra com teor superior a 2 (2,67%).

De modo geral, as rochas apresentam nítidas variações composicionais dos elementos maiores com a evolução magmática, mostrando que com o decréscimo de MgO há um aumento dos teores de SiO_2 , Al_2O_3 , Fe_2O_3 , CaO, Na_2O , P_2O_5 , TiO_2 , K_2O , MnO (Figura 8).

Os diagramas de variação, MgO *versus* elementos traço, mostram que com aumento de MgO, Zr aumenta, enquanto os elementos Ba, Y, Sr, Nd, Ce, Nb, La, Sm, Ni, Yb e Eu têm seus teores decrescidos (Figura 9).

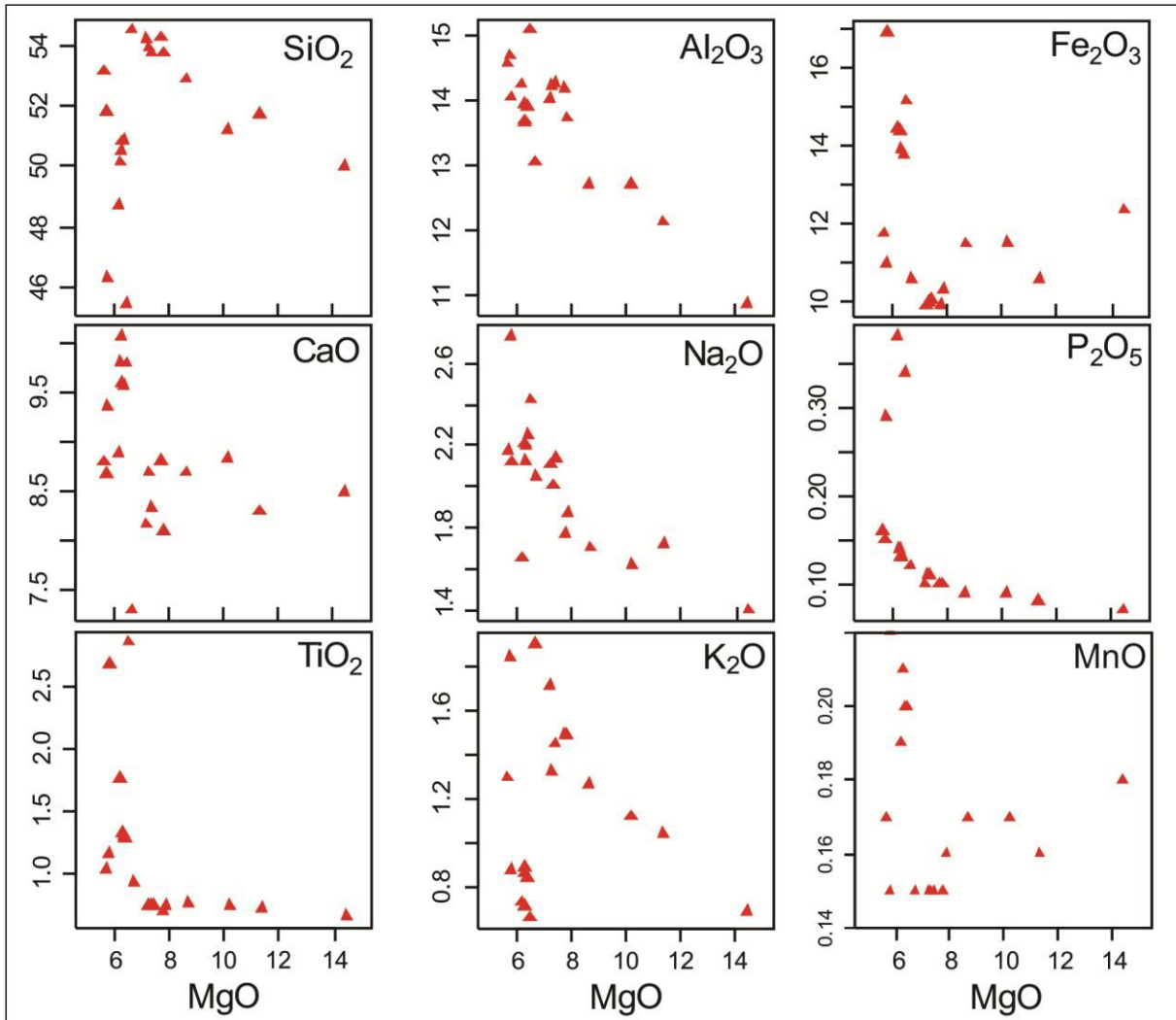


Figura 8. Diagramas de variação MgO *versus* óxidos de elementos maiores (% em peso) para as rochas da SIRP.

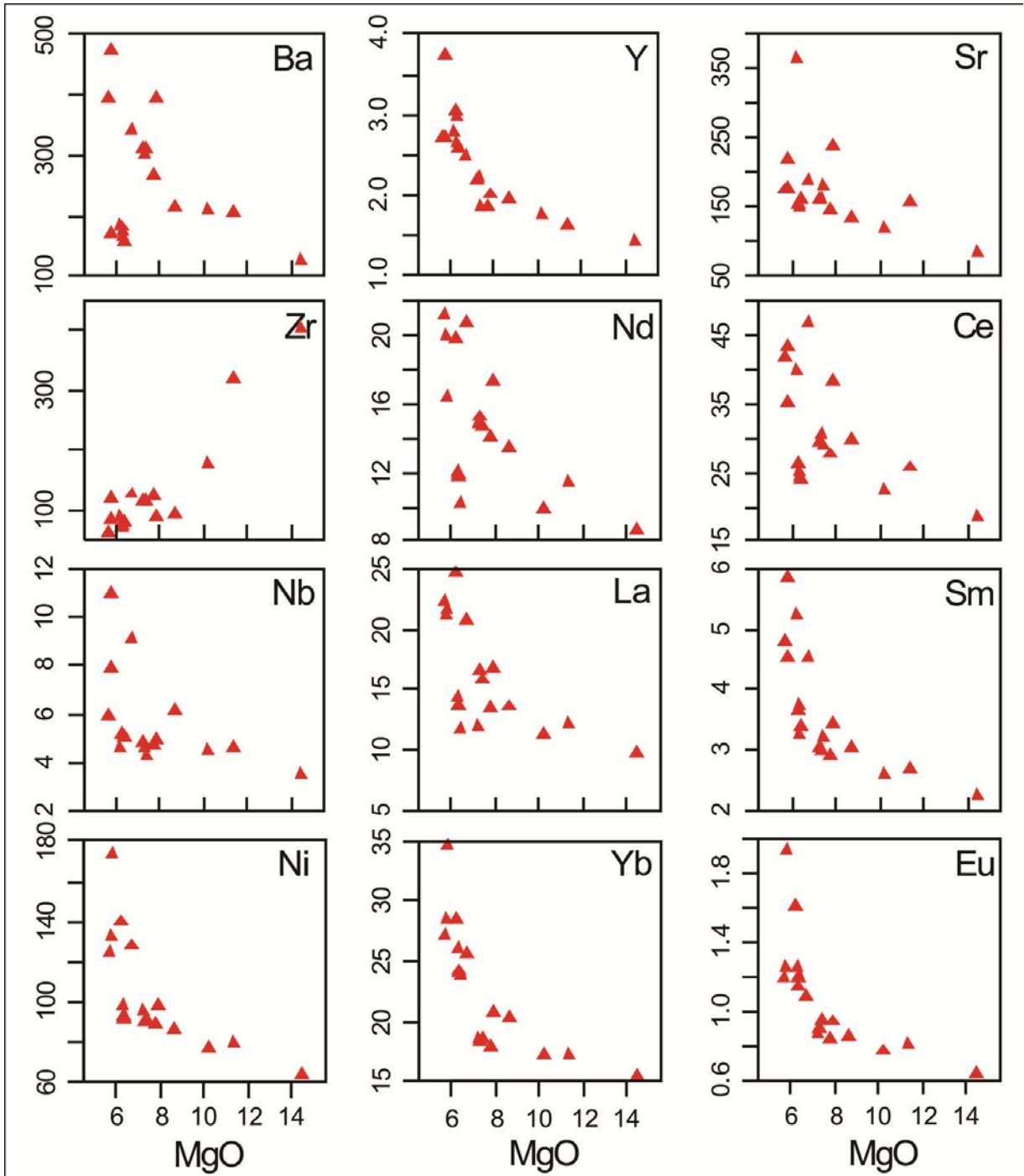


Figura 9. Diagramas de variação MgO *versus* elementos traço (% em peso) para as rochas da SIRP.

Quando plotadas no diagrama AFM (Irvine & Baragar, 1971; Figura 10A) observa-se que as amostras seguem um *trend* toleítico, com enriquecimento em FeOt em relação ao MgO para valores de álcalis relativamente constantes. Nos diagramas baseados no conteúdo de sílica total *versus* álcalis (Le Bas *et al.*, 1986; Figura 10B), R1-R2 (De La Roche *et al.*, 1980;

Figura 10C) e Nb/Y versus Zr/Ti (Winchester & Floyd, 1977; Figura 10D), as rochas classificam-se, quase que exclusivamente, como basaltos e basaltos andesíticos.

Quanto à ambiência tectônica, os diagramas Zr/4-2*Nb-Y, proposto por Meschede (1986; Figura 11A), e Zr versus Zr/Y de Pearce & Norry (1979; Figura 11B) sugerem para essas rochas uma colocação semelhante a dos basaltos intraplaca fanerozóicos.

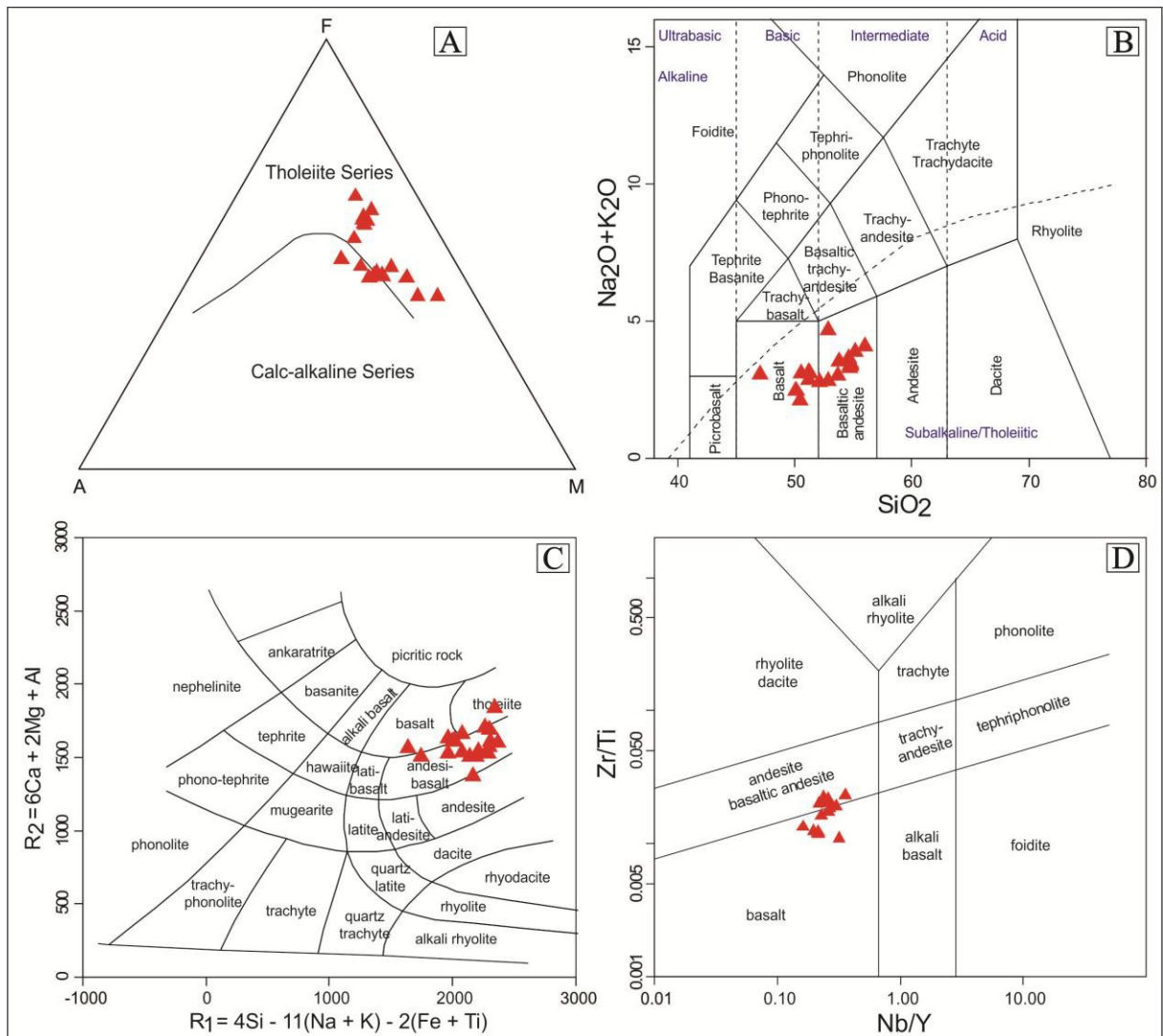


Figura 10. Diagramas classificatórios para as rochas da SIRP: A) AFM de Irvine & Baragar (1971); B) TAS de Le Bas *et al.* (1986); C) R1-R2 (De La Roche *et al.*, 1980) e D) Nb/Y versus Zr/Ti (Winchester & Floyd, 1977).

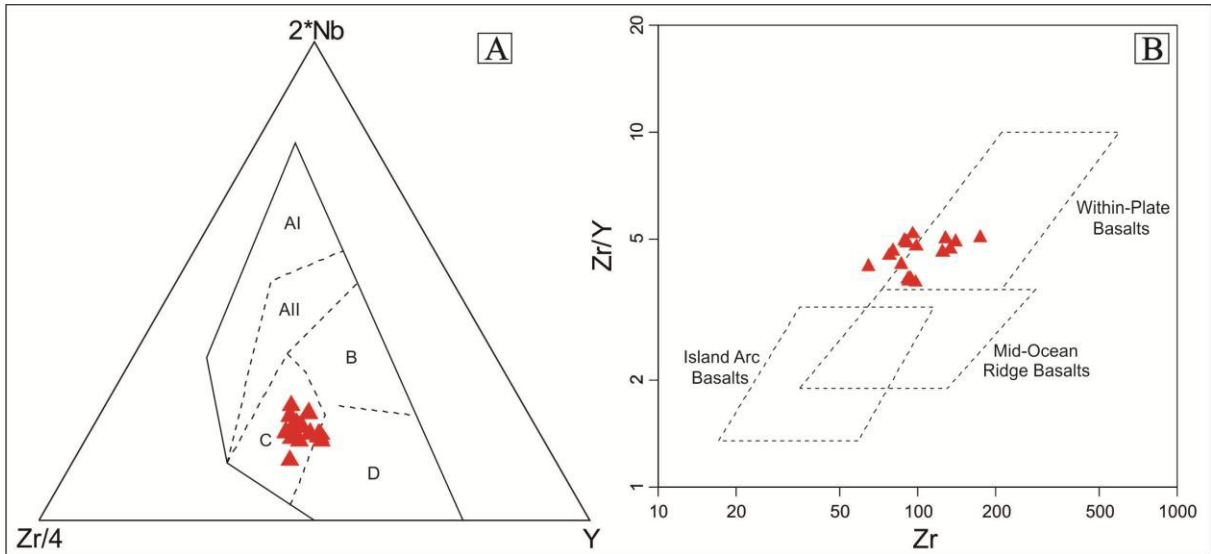


Figura 11. Diagramas classificatórios de ambiência tectônica. A) $Zr/4-2^*Nb-Y$ (Meschede, 1986) e B) Zr versus Zr/Y (Pearce & Norry, 1979).

No diagrama da figura 12A, o comportamento dos elementos terras raras (ETR), normalizados pelos valores condríticos de Boynton (1984), mostra forte fracionamento de ETR pesados em relação aos ETR leves, com razões La/Yb entre 2,8 e 6,2, com anomalia pouco expressiva ou inexistente de Eu.

No diagrama multi-elementar da figura 12B, normalizado pelo manto primitivo (McDonough & Sun, 1995), é possível identificar anomalias negativas de Rb, K e Nb. Para efeito de comparação foram utilizados os padrões médios de Basaltos de Ilha Oceânica (OIB), Basaltos de Cordilheira Meso-Oceânica Normal (N-MORB) e Basaltos de Cordilheira Meso-Oceânica Enriquecido (E-MORB; McDonough & Sun, 1995). Nota-se que o padrão das amostras estudadas assemelha-se ao dos OIB, diferenciando-se apenas por apresentar anomalia negativa de Nb.

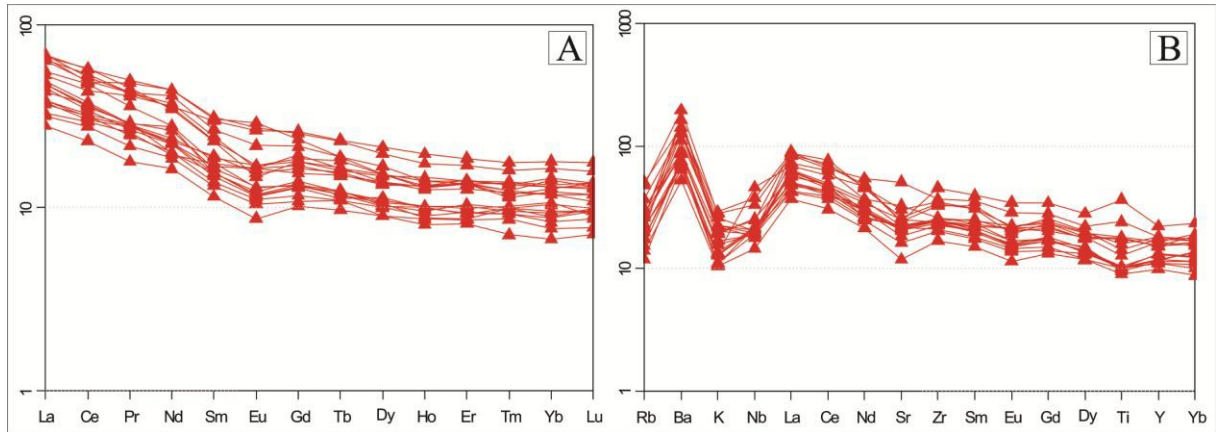


Figura 12. A) Diagrama de distribuição dos ETR para as rochas da SIRP, normalizados pelo condrito segundo Boynton (1984). B) Diagrama multi-elementar para as rochas da SIRP, normalizadas pelo manto primitivo (McDonough & Sun, 1995).

DISCUSSÃO E CONCLUSÕES

O enxame de diques da Suíte Rio Perdido aloja-se em unidades paleoproterozoicas polideformadas dos blocos Ocidental e Oriental do Terreno Rio Apa. Os diques cortam as foliações regionais dos gnaisses, anfibolitos, metavulcânicas e granitos e não exibem evidências de metamorfismo e deformação, como atestam as texturas ígneas preservadas e os contatos retos e não deformados com as encaixantes. Adicionalmente, não se observa os diques estudados cortando as unidades neoproterozoicas da Faixa Paraguai, situada a leste e sul do Terreno Rio Apa.

Os diques máficos Rio Perdido apresentam formato tabular a lenticular, com comprimento variando entre 5 e 300 m e espessura entre 1 e 30 m. Exibem contatos retos e seccionam oblíqua a ortogonalmente as foliações e contatos das encaixantes. Os diques são subverticais com direção preferencial E-W, com valores preferencialmente entre N70°-90°W, sendo raros os diques com direção N-S. Em termos de orientação, são paralelos ao enxame de diques Huanchaca que recortam o Terreno Paraguá (Litherland *et al.*, 1986; Século *et al.*, 2011; Lima *et al.*, 2012), no sudoeste do Cráton Amazônico.

Petrograficamente, as rochas que constituem os diques da SIRP são classificadas como gabronorito (Streckeisen, 1976), por conterem orto e clinopiroxênio. Apresentam granulação de muito fina a média, comumente com textura ofítica a subofítica, e compõem-se, essencialmente, por plagioclásio, piroxênios e olivina.

Do ponto de vista litoquímico, esta unidade apresenta nítida variação composicional dos elementos maiores com a evolução magmática, bem como dos elementos traço, sendo que o

comportamento desse último evidencia fracionamento predominante de clinopiroxênio, plagioclásio e olivina, típico de rochas gabróicas. Nos diagramas classificatórios, o comportamento é semelhante e as rochas são representadas, em sua grande maioria, por basaltos e basaltos andesíticos, com afinidade toleítica, geradas em ambiente tectônico intraplaca continental. A anomalia negativa de Nb, observada no diagrama multi-elementar, é característica de ambiente continental, ou ainda indicativa de processos de contaminação.

A idade de 1589 ± 44 Ma obtida através do método U-Pb em zircão, atribuída à formação do enxame de diques por Faleiros *et al.* (2016), deve ser vista com cautela, uma vez que metamorfismo regional de fácies xistos verdes, acompanhado de intensa deformação marcada pela implantação de foliação tectônica de baixo ângulo e zonas de cisalhamento de cavalgamento afeta indistintamente todas as unidades do Terreno Rio Apa, exceto os diques da Suíte Rio Perdido. Cordani *et al.* (2010) e Ruiz *et al.* (2014) apresentam dados Ar-Ar e K-Ar que indicam uma idade de 1300 Ma para esse evento deformacional-metamórfico regional, temporalmente correlato a Orogenia San Ignacio (Litherland *et al.*, 1986; Bettencourt *et al.*, 2010) no Terreno Paraguá. Considerando que as rochas dos diques Rio Perdido não exibem registros de deformação e metamórficos, é possível que a sua colocação tenha sido após o evento metamórfico e deformacional regional mencionado. Provavelmente os zircões analisados sejam herdados das rochas encaixantes, frequente para este tipo de intrusão.

Em termos de correlação regional, considerando-se que o enxame de diques Rio Perdido tenha se formado em 1110 Ma, conforme resultado U-Pb em badaleíta de Teixeira *et al.* (2016), há correlação temporal com os diques e soleiras da Suíte Huanchaca e o Complexo Rincón del Tigre na Província Sunsás, no SW do Craton Amazônico.

Quanto à correlação global, magmatismo básico em torno de 1100 Ma, estão presentes em diversas áreas cratônicas do planeta, por exemplo, os diques Kulgera e Stuart na Austrália, diques Ilhéus e Olivença no Cráton São Francisco, no Brasil, Província Ígnea Umkondo na África, Formações Malgina, Milkon e Nelkan, na Sibéria, Formação Tieling no Norte da China, e diversas soleiras e diques na Báltica e Laurentia (Li *et al.*, 2008). No Cráton Amazônico os diques de Nova Floresta apresenta idade próxima ao enxame Rio Perdido.

Tendo em vista a correlação temporal e tectônica entre os enxames Rio Perdido com as suítes Huanchaca e Rincón del Tigre no sudoeste do Cráton Amazônico, conclui-se que o Terreno/Bloco Rio Apa estaria aglutinado ao continente Amazônia, antes da Orogenia Sunsás desenvolver as faixas Aguapeí e Sunsás, um marco da formação do supercontinente Rodínia.

A provável LIP descrita reflete um episódio ígneo fissural vinculado à formação do Aulacógeno Aguapeí, numa tentativa de fragmentar o continente Amazônia.

AGRADECIMENTOS

Os autores agradecem à CAPES (PROCAD 096/2007), ao CNPq (479779/2011-2), à FAPEMAT (222473/2015) e ao GEOCIAM (Instituto Nacional de Ciência e Tecnologia de Geociências da Amazônia) pelo suporte financeiro ao desenvolvimento da pesquisa. A primeira autora agradece ao CNPq pela concessão de bolsa de doutorado.

REFERÊNCIAS

- Araújo H. J. T., Santos Neto A., Trindade C. A. H., Pinto J. C. A., Montalvão R. M. G., Dourado T. D. C.; Palmeira R. C. B., Tassinari C. C. G. (1982). *Folha SF.21 – Campo Grande*. Escala: 1:1.000.000. Rio de Janeiro: Ministério das Minas e Energia-Secretaria Geral, Projeto RADAMBRASIL – Geologia, 28,23-124.
- Araújo, L. M. B., Ruiz, A. S., Godoy, A. M., Sousa, M. Z. A. (2005). Soleiras Máficas Tonianas (Suíte Intrusiva Salto do Céu) no SW do Cráton Amazônico: Regime Extensional Relacionado à Orogenia Sunsás? *IX Simpósio de Geologia do Centro Oeste*, v. 1, 155-156. Goiânia: SBG.
- Barros, A. M., Silva, R. H., Cardoso, O. R. F. A., Freire, F. A., Souza Jr., J. J., Rivetti, M., Luz, D. S., Palmeira, R. C., Tassinari, C. C. G. (1982). *Folha SD.21.- Cuiabá*. Escala: 1:1.000.000. Rio de Janeiro, Ministério das Minas e Energia-Secretaria Geral, Projeto RADAMBRASIL – Geologia, 26, 25-192.
- Bettencourt, J. S., Leite Jr., W. B., Ruiz, A. S., Matos, R., Payolla, B. L., Tosdal, R. M. (2010). The Rondonian-San Ignacio Province in the SW Amazonian Craton: An Overview. *Journal of South American Earth Sciences*, 29, 28-46.
- Boynton, W. V. (1984). Cosmochemistry of Rare Earth Elements: Meteorite Studies. In: Henderson P. (Eds.), *Rare Earth Element Geochemistry* (v.1, 63-114). Amsterdam: Elsevier.
- Cordani, U, G., Teixeira, W., Tassinari, C. C. G., Ruiz, A. S. (2010). The Rio Apa Craton in Mato Grosso do Sul (Brazil) and Northern Paraguay: Geochronological Evolution, Correlations and Tectonic Implications for Rodinia and Gondwana. *American Journal of Science*, 310, 1-43.
- Corrêa da Costa, P. C., Girardi, V. A. V., Matos, J. B., Ruiz, A. S. (2009). Geocronologia Rb-Sr e Características Geoquímicas dos Diques Máficos da Região de Nova Lacerda e Conquista D'Oeste (MT), Porção Sudoeste do Cráton Amazônico. *Geologia USP - Série Científica*, 9, 115-132.

- De La Roche H., Leterrier J., Grandclaude P., & Marchal M. (1980). A classification of volcanic and plutonic rocks using R1R2- diagram and major element analyses - its relationships with current nomenclature. *Chemical Geology*, 29, 183-210.
- Ernst, R. E., Bleeker, W., Söderlund, U., Kerr, A. C., (2013). Large Igneous Provinces and supercontinents: toward completing the plate tectonic revolution. *Lithos*, 174, 1-14, DOI: 10.1016/j.lithos.2013.02.017.
- Faleiros, F. M., Pavan, M., Remédio, M. J., Rodrigues, J. B., Almeida, V. V., Caltabeloti, F. P., Pinto, L. G. R., Oliveira, A. A., Pinto de Azevedo, E. J., Costa, V. S. (2016). Zircon U–Pb ages of rocks from the Rio Apa Cratonic Terrane (Mato Grosso do Sul, Brazil): New insights for its connection with the Amazonian Craton in pre-Gondwana times. *Gondwana Research*. (In Press).
- Godoi H. O., Martins E. G., Mello C. R., Scislewski G. (2001). *Folhas Corumbá (SE. 21-Y-D), Aldeia Tomázia, (SF. 21-V-B) e Porto Murtinho (SF. 21-V-D)*. Escala 1:250.000. MME/SG. Programa Levantamentos Geológicos Básicos do Brasil.
- Halls, H. (1982). The Importance and Potencial of Mafic Dikes Swarms in Studies of Geodynamic Process. *Geoscience Canada*, 9, 145-154.
- Irvine, I. N., Baragar, W. R. A. (1971). A Guide To The Chemical Classification Of The Common Volcanics Rocks. *Canadian Journal Earth Science*, 8, 523-548.
- Janoušek, V., Farrow, C. M., Erban, V. (2006). Interpretation of whole-rock geochemical data in igneous geochemistry: introducing Geochemical Data Toolkit (GCDkit). *Journal of Petrology*, 47(6), 1255-1259.
- Lacerda Filho, J. V., Brito, R. S. C., Silva, M. G., Oliveira, C. C., Moreton, L. C., Martins, E.G., Lopes, R. C., Lima, T. M., Larizzatti, J. H. Valente, C. R. (2006). Geologia e Recursos Minerais do Estado de Mato Grosso do Sul. Programa Integração, Atualização e Difusão de Dados de Geologia do Brasil. Convênio CPRM/SICME - MS, MME, 10.
- Le Bas, M. J., Le Maitre, R. W., Streckeisen, A., Zanettin, B. A. (1986). Chemical Classification Of Volcanic Rocks Based On Total Alkali-Silica Diagram. *Journal of Petrology*, 27, 745-750.
- Leite, J. A. D., Saes, G. S., Weska, R. K. (1985). A Suíte Intrusiva Rio Branco e o Grupo Aguapeí na serra de Rio Branco, Mato Grosso. Simpósio de Geologia do Centro-Oeste, v.1, 247-255. Goiânia: SBG.
- Lima, G. A., Sousa, M. Z. A., Ruiz, A. S., D'agrella Filho, M. S., Vasconcelos, P. (2012). Sills máficos da Suíte Intrusiva Huanchaca - SW do Cráton Amazônico: registro de magmatismo fissural relacionado à ruptura do Supercontinente Rodínia. *Revista Brasileira de Geociências*, 42, 111-129.

Litherland, M., Annells, R. N., Appleton, J. D., Berrangé, J. P., Bloomfield, K., Burton, C. C. J., Darbyshire, D. P. F., Fletcher, C. J. N., Hawkins, M. P., Klinck, B. A., Llanos, A., Mithcell, W. I., O'Connor, E. A., Pitfield, P. E. J., Power, G. E., Webb, B. C. (1986). *The Geology and Mineral Resources of the Bolivian Precambrian Shield*. London: Her Majesty's Stationery Office.

McDonough, W. F., Sun, S. S. (1995). The composition of the earth. *Chemical Geology*, 120, 223-253.

Meschede, M. (1986). A method of discriminating between different types of mid-ocean ridge basalts and continental tholeiites with the Nb-Zr-Y diagram. *Chemical Geology*, 56, 207-218.

Pearce, J. A., Norry, M. J. (1979). Petrogenetic implications of Ti, Zr, Y and Nb variations Volcanic Rocks. *Contributions to Mineralogy and Petrology*, 69, 33-47.

Ruiz, A. S. (2005). *Evolução Geológica do Sudoeste do Cráton Amazônico Região Limítrofe Brasil-Bolívia – Mato Grosso*. Tese (Doutorado). Rio Claro: Instituto de Geociências e Ciências Exatas - Universidade Estadual Paulista.

Ruiz, A.S., Matos, J. B., Sousa, M. Z. A., Lima, G. A., Batata, M. E. F. (2010a). *Mapeamento Geológico e Levantamento de Recursos Minerais da Folha Santa Bárbara (SD.21-Y-C-V)*. Cuiabá: Convênio CPRM-UFMT. Programa Geologia do Brasil, Relatório Etapa de Mobilização.

Ruiz, A. S., D'agrella Filho, M. S., Sousa, M. Z. A., Lima, G. A. (2010b). Tonian sills and mafic dike swarms of S-SW Amazonian Cráton: records of Rodinia Supercontinent break-up? *The Meeting of the Americas*, v.1. Foz do Iguaçu: AGU.

Ruiz, A. S.,; Sousa, M. Z. A., Lima, G. A., D'agrella Filho, M. S. (2014). Ar-Ar step heating ages for milonitic low angle shear zones rocks in the Rio Apa Terrane, South of the Amazonian Craton. *9th South American Symposium on Isotope Geology*. São Paulo: CPGEO.

Santos, R. O. B., Pitthan, J. H. L., Barbosa, E. S., Fernandes, C. A. C., Tassinari, C. C.G., Campos, D. A. (1979). *Folha SD.20 - Guaporé*. Escala: 1:1.000.000. Rio de Janeiro, Ministério das Minas e Energia-Secretaria Geral, Projeto RADAMBRASIL – Geologia, 19, 21-123.

Sécolo, D. B., Ruiz, A. S., Sousa, M. Z. A., Lima, G. A. (2011). Geologia, Petrografia e Geoquímica do Enxame de Diques Máficos da região de Vila Bela da Santíssima Trindade (MT) Suíte Intrusiva Huanchaca - SW do Cráton Amazônico. *Geociências*, 30, 561-573.

Streckeisen, A. (1976). To each plutonic rocks its proper name. *Earth Science Review*. 12, 1-33.

Teixeira, W., Hamilton, M. A., Lima, G. A., Ruiz, A. S., Matos, R., Ernst, R. (2015a). Precise ID-TIMS U–Pb baddeleyite ages (1110–1112 Ma) for the Rincón del Tigre–Huanchaca Large

Igneous province (LIP) of the Amazonian Craton: Implications for the Rodinia supercontinent. *Precambrian Research*, 265, 273-285.

Teixeira, W., Ernst, R., Hamilton, M. A., Lima, G. A., Ruiz, A. S., Geraldés, M. C. (2015b). Widespread ca. 1.4 Ga intraplate magmatism and tectonics in a growing Amazonia. *GFF*, 00(Pt. 1), 1-14, DOI: 10.1080/11035897.2015.1042033.

Teixeira, W., Hamilton, M. A., Girardi, V. A. V., Faleiros, F. M. (2016). Key dolerite dyke swarms of Amazonia: U-Pb constraints on supercontinent cycles and geodynamic connections with global LIP events through time. *Seventh International Dyke Conference*. Pequim.

Winchester, J. A., Floyd, P. A. (1977). Geochemical discrimination of different magma series and their differentiation products using immobile elements. *Chemical Geology*, 20, 325-343.

3.2 GEOLOGY AND PETROLOGY OF THE SALTO DO CÉU SUITE: TECTONIC AND STRATIGRAPHIC IMPLICATIONS ON THE SW AMAZONIAN CRATON

Gabrielle Aparecida de Lima

Moacir José Buenano Macambira

Maria Zélia Aguiar de Sousa

Amarildo Salina Ruiz

Maria Elisa Fróes Batata

Ronaldo Pierosan

Submetido: *Brazilian Journal of Geology*

19-Jul-2016

Dear Ms. Lima:

Your manuscript entitled "GEOLOGY AND PETROLOGY OF THE SALTO DO CÉU SUITE: TECTONIC AND STRATIGRAPHIC IMPLICATIONS ON THE SW AMAZONIAN CRATON" has been successfully submitted online and is presently being given full consideration for publication in the Brazilian Journal of Geology.

Your manuscript ID is BJGEO-2016-0088.

Please mention the above manuscript ID in all future correspondence or when calling the office for questions. If there are any changes in your street address or e-mail address, please log in to ScholarOne Manuscripts at <https://mc04.manuscriptcentral.com/bjgeo-scielo> and edit your user information as appropriate.

You can also view the status of your manuscript at any time by checking your Author Center after logging in to <https://mc04.manuscriptcentral.com/bjgeo-scielo>.

Thank you for submitting your manuscript to the Brazilian Journal of Geology.

Sincerely,

Brazilian Journal of Geology Editorial Office

GEOLOGY AND PETROLOGY OF THE SALTO DO CÉU SUITE: TECTONIC AND STRATIGRAPHIC IMPLICATIONS ON THE SW AMAZONIAN CRATON

SALTO DO CÉU SUITE: GEOLOGY AND PETROLOGY

Gabrielle Aparecida de Lima^{1,5,6,7}; Moacir José Buenano Macambira^{2,6}; Maria Zélia Aguiar de Sousa^{3,6,7}; Amarildo Salina Ruiz^{3,6,7}; Maria Elisa Fróes Batata^{4,7}; Ronaldo Pierosan^{3,6}

¹Postgraduate Program in Geology and Geochemistry, Geosciences Institute (IG)/Federal University of Pará (UFPA) – Av. Perimetral, N° 1 – Bairro Guamá, Belém - PA, Brazil, CEP:66075-750

²Laboratory of Isotope Geology (PARÁ-ISO), IG/UFPA

³Geosciences Faculty (FAGEO)/Federal University of Mato Grosso (UFMT)

⁴Postgraduate Program in Geosciences (Mineralogy and Petrology), Geosciences Institute (IGc), University of São Paulo (USP)

⁵Engineering Institute (IEng)/UFMT

⁶National Institute of Sciences and Geoscience Technology of the Amazon (GEOCIAM)

⁷Crustal and Tectonic Evolution Research Group “Guaporé”

ABSTRACT

The basic rocks composing the Salto do Céu Suite outcrop as sills and flows in the area surrounding the municipalities of Salto do Céu and Rio Branco (MT), southwestern Amazon Craton, and are emplaced into the Jauru Terrane, Rondonian-San Ignacio Province, with an age of about 1.44 Ga. Sills are 2 to 30 m thick being hosted by pelites of the Vale da Promissão Formation (Aguapei Group). These flows cover this same unit and are up to 5 m thick. The rocks of this suite are mesocratic to melanocratic, equigranular, and very fine- to medium-grained. The sills are composed of diabases and massif gabbros displaying ophitic, subophitic, hyalophitic, porphyritic or amygdaloidal textures in a pseudo-trachytic and vitrophyric groundmass. Typical textures of magma mixing are observed near the contact with the Rio Branco Suite. They have chemical affinity to tholeiites being classified as subalkaline and iron-rich tholeiitic basalts, with mg# values between 0.30 and 0.51. There is a clear difference between two rock groups, one which is richer in ETR with LaN greater than 100 and discrete Eu negative anomaly, and another without this signature, with LaN less than 100.

Sills and flows of the Salto do Céu Suite, and the rocks of the Rio Branco Suite are interpreted as a bimodal suite showing magma mixing features developed in continental intraplate settings, extensive tectonic regime, anorogenic, and tectonic compatibility with the breakup of the Columbia/Nuna Supercontinent.

Keywords: bimodal suíte; flows and mafic sills; petrogenesis; extensional tectonics.

RESUMO

As rochas básicas, que compõem a Suíte Salto do Céu, afloram como soleiras e derrames nas proximidades dos municípios de Salto do Céu e Rio Branco (MT), sudoeste do Cráton Amazônico, inseridas no Terreno Jauru, Província Rondoniana-San Ignácio, com idade em torno de 1,44 Ga. As soleiras, com espessuras entre 2 e 30 m, alojam-se nos pelitos da Formação Vale da Promissão (Grupo Aguapeí). Os derrames recobrem essa mesma unidade, com espessuras em torno de 5 m. As rochas desta suíte são mesocráticas a melanocráticas, equigranulares variando de muito finas até médias. As soleiras compõem-se por diabásios e gabros maciços com texturas ofítica, subofítica, intergranular e coronítica. Os derrames constituem-se de basaltos e diabásios com texturas ofítica, subofítica, hialofítica, porfírica ou amigdaloidal em matriz pseudo-traquítica e vitrofírica. Texturas típicas de mistura de magmas são observadas próximas ao contato com a Suíte Rio Branco. Litoquimicamente, os litotipos apresentam afinidade toleítica, sendo classificados como basaltos subalcalinos e basaltos toleíticos de alto Fe, com valores de mg# entre 0,30 e 0,51. Há uma nítida separação em dois grupos de rochas, um mais rico em ETR, com LaN maior que 100 e discreta anomalia negativa de Eu, e outro sem essa assinatura, com LaN menor do que 100. As soleiras e derrames da Suíte Salto do Céu e as rochas da Suíte Rio Branco são interpretados como uma suíte bimodal com evidências de mistura de magmas, gerados em ambiente continental intraplaca, em regime tectônico distensivo, anorogênico, tectonicamente correlacionável à ruptura do Supercontinente Columbia/Nuna.

Palavras-chave: suíte bimodal; derrames e soleiras máficas; petrogênese; tectônica extensional.

INTRODUCTION

The mafic sills found in the region of Salto do Céu municipality (MT) belonging to the Salto do Céu Suite (SCS) are interpreted to record the breakup of the Rodinia Supercontinent (Ruiz *et al.*, 2010a e Lima *et al.*, 2012) with basis on K-Ar analyses that yields a cooling age around 0.9 Ga (Barros *et al.*, 1982). Recent U-Pb (TIMS) analyses on baddeleyite show crystallisation ages around 1.44 Ga (Teixeira *et al.*, 2015a). This new geochronological result challenges the widely accepted geological history of the SW Amazonian Craton both in terms of this magmatic event of basic nature as well as the age of its country rock, that is, the Aguapeí Group. Distensive magmatic events, with ages similar to those obtained for the Salto do Céu Suite, have been associated with the evolution of the Columbia Supercontinent by many authors (Ernst *et al.*, 2008, 2013; Rogers & Santosh, 2002).

Based on field work and new geochronological data available in the literature, as well as relying on unpublished petrographic and geochemical results of rocks from the Salto do Céu Suite (SCS), here we discuss the petrogenetic evolution of this mafic magmatism, its relationship to felsic rocks of the Rio Branco Intrusive Suite (RBIS), and its tectonic implication on the evolution of the southwestern Amazonian Craton.

REGIONAL GEOLOGICAL SETTINGS

The south-southwest portion of the Amazonian Craton records a widespread occurrence of mafic sills and dyke swarms (Figure 1) which have been interpreted as petro-tectonic evidence for breakup of the Rodinia Supercontinent (Ruiz *et al.*, 2010a; Século *et al.*, 2011; Lima, 2011 and Lima *et al.*, 2012).

Gabbros and diabases found in the regions of Salto do Céu and Rio Branco, southwest of the Brazilian state of Mato Grosso, were first reported by Oliva (1979), and later attributed to the Rio Branco Group by Barros *et al.* (1982). Leite *et al.* (1985) have attributed these exposure of mesocratic and melanocratic rocks of the Rio Branco Intrusive Suite to windows in the Vale da Promissao Formation cut by erosion. Therefore, these rocks are described as a differentiated stratiform igneous complex with typical bimodal character which may be an indicative of anorogenic magmatism likely developed in rift settings.

According to Geraldès (2000) and Geraldès *et al.* (2001, 2004), the basal portion of the Rio Branco Intrusive Suite is composed of basic rocks while its upper portion comprises a plutonic-volcanic association chiefly composed of acid to intermediate rocks. These authors

presented a U-Pb age of 1471 ± 8 Ma for the basic rocks, and an age of 1427 ± 10 Ma for the acid rocks that are interpreted as an extensional intracratonic magmatism, a reflection of the Santa Helena magmatic arc (1.47–1.42 Ga).

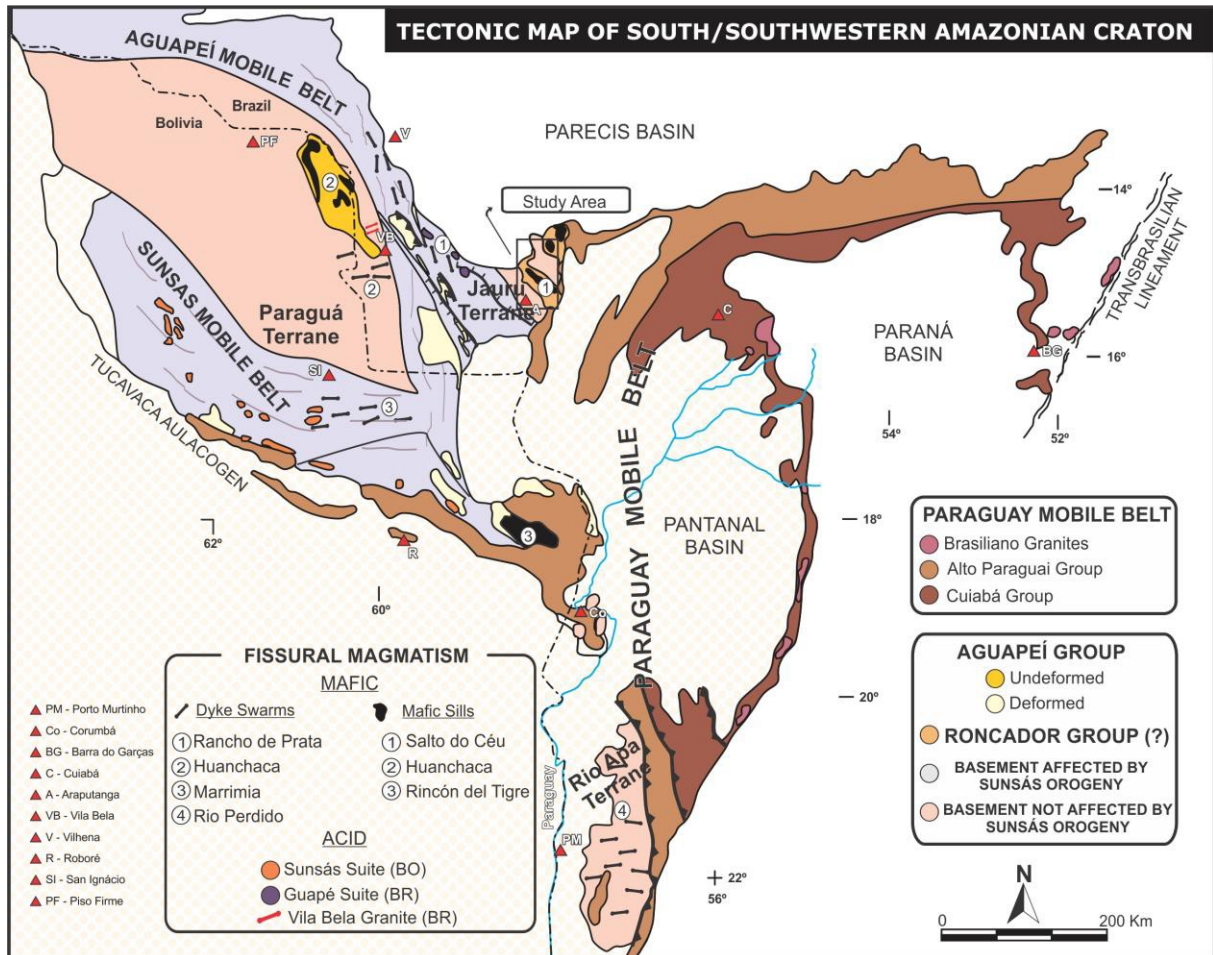


Figure 1. Tectonic Map of the South/Southwestern Amazonian Craton highlighting the fissural mafic magmatism (dykes of the intrusive suites Rio Perdido, Rancho de Prata and Huanchaca; and sills of the intrusive suites Salto do Céu and Huanchaca), and felsic magmatism (plutons of the Guapé Intrusive Suite and granitic dykes of the Vila Bela Granite). Extracted and modified from Ruiz *et al.*, 2010b.

Araújo *et al.* (2005) name as Salto do Céu Intrusive Suite the assemblage of intrusions occurring parallel to the bedding of pelites and psammites of the Vale da Promissão Formation (Aguapeí Group), and composed of mafic sills 1 to 5 m thick. Araújo *et al.* (2007) recognized two main plutonic series in the Rio Branco Batholith, one of basic nature with discontinuous distribution located in the intrusion borders, and another one of acid/intermediate nature that is composed of three petrographic facies. It was concluded that

the occurrence of gabbroic rocks represent two separate magmatic events: the basic plutonic rocks (gabbros and diorites) belonging to the Rio Branco Intrusive Suite, and the hypoabissal rocks (diabases, microgabbros) belonging to the Salto do Céu Intrusive Suite.

Araújo (2008) showed that the bimodal magmatism of the Rio Branco batholith is clearly represented by two types of magmas, one of basic nature, mantle-derived, and another type of acid/intermediate composition formed by crustal melting and magmatic differentiation processes that gave rise to the intermediate/acid lithotypes. The same author also obtained U-Pb (TIMS) ages of 1403 ± 0.6 Ma and 1382 ± 49 Ma for the intermediate to acid rocks, interpreted as the time of igneous crystallization for felsic magmas that gave rise to the Rio Branco Acid Intrusive Suite.

The Rio Branco batholith, as reported by Araújo *et al.* (2009) and Araújo & Godoy (2011), comprises two main plutonic suites: the Rio Branco Basic Intrusive Suite that is composed of basic to intermediate rocks, and the Rio Branco Acid Intrusive Suite which is intermediate to acid in composition. Also, according to these authors, the gabbroic association comprises two temporally distinct magmatic events: the first one is composed of basic to intermediate plutonic rocks, such as microgabbros to diabases, monzogabbros, and quartz-monzonites to quartz-diorites that are grouped into the Rio Branco Basic Intrusive Suite; the latter is associated with hypoabissal lithotypes, such as diabases and microgabbros, occurring as sills hosted by the Aguapeí Group, and grouped together under the name of Salto do Céu Basic Intrusive Suite.

Based on more detailed geological mapping, Sousa *et al.* (2011) assigned the term Rio Branco Intrusive Suite only to the acid to intermediate rocks, thus assigning all the gabbroic rocks to the Salto do Céu Intrusive Suite.

Teixeira *et al.* (2015a) obtained U-Pb baddeleyite ages of 1439 ± 4 Ma for the Salto do Céu sills, and of 1387 ± 17 Ma for the Nova Lacerda mafic dyke swarms. These ages reflect a single magmatic event for these units associated with the evolution of the Columbia Supercontinent.

Sedimentary and metasedimentary covers occurring in the southwest of Mato Grosso, and in Eastern Bolivia were first reported in the LASA report (1968). These rocks were latter named Aguapeí Unit by Figueiredo & Olivatti (1974). Souza & Hildred (1980) used the term Aguapeí Group in order to group the formations Fortuna, Vale da Promissão and Morro Cristalina which was then described as a marine transgressive-regressive platform cover sequence.

According to Saes (1999), Fortuna Formation is composed of sandstones and orthoquartzitic conglomerates. These rocks with widespread cross-bedding indicates deposition in braided fluvial systems in the areas of Huanchaca and Sao Vicente Hills which eventually prograded into a shallow-marine platform influenced by tidal currents, fan deltas and tempestites in the region of Pontes and Lacerda, and Rio Branco. The Vale da Promissao Formation represents a progradational wedge of marine sediments thickening towards the SE. In the regions of Rio Branco, and Pontes and Lacerda, this unit consists of pelitic rocks intercalated with sand that were deposited by storms on shallow marine platform. The Morro Cristalina Formation is chiefly composed of quartz-arenites, and rarely composed of conglomerates whose main characteristics are the high level of maturity and the exclusive continental character (fluvial and eolian) of its deposits.

Geraldes *et al.* (2014) obtained U-Pb (LA-ICP-MS) ages on detrital zircons for samples from the Aguapeí Group collected in three hills: Rio Branco, Ricardo Franco and Santa Bárbara. The results from the Rio Branco Hill, same region where the target rocks crop out, yield four main age peaks at 1544 Ma, 1655 Ma, 1812 Ma and 2515 Ma. According to these authors, the first peak is likely related to the rocks of the Cachoeirinha orogeny, the second peak represents the rocks of the Lomas Manechis Complex (Bolivia) and, in their turn, the last two peaks may represent the older units not mapped yet.

Table 1 shows geochronological data available so far for the acid to intermediate rocks and basic rocks, respectively, from the suites Rio Branco and Salto do Céu.

Table 1. Geochronological and isotopic database for the acid to intermediate rocks (Rio Branco Suite) and basic rocks (Salto do Céu Suite). (Z) zircon; (S) sphene; (B) baddeleyite; (WR) whole-rock; (P) plagioclase.

	References	U-Pb	Rb-Sr		Sm-Nd		K-Ar
		Age (Ma)	Age (Ma)	$(^{87}\text{Sr}/^{86}\text{Sr})_0$	T_{DM} (Ga)	$\epsilon\text{Nd}(t)$	Age (Ma)
Acid to intermediate rocks	Barros <i>et al.</i> (1982)		(WR) 1130 ± 72	0,708			
	Ruiz (1992)		(WR) 1126 ± 39	0,7165			
	Geraldes <i>et al.</i> (2001)	(Z) 1427 ± 10			1,89 a 1,79	-0,2	
	Geraldes <i>et al.</i> (2004)	(Z) 1423 ± 0,2			1,89 a 1,81	-0,96 a +0,16	
	Araújo (2008)	(Z) 1423 ± 06 (Z) 1380 ± 49			1,91 a 1,65	-1,78 a +1,24	
	Sousa <i>et al.</i> (2011)				2,08	-3,39	
rock	Hama (1976) in Ruiz (2005)						(P) 1006 ± 16

Barros <i>et al.</i> (1982)						(WR) 875 ± 21 (P) 878 ± 10 (P) 930 ± 14 (P) 960 ± 21
Leite <i>et al.</i> (1985)						(P) 1015 ± 17
Geraldes <i>et al.</i> (2001)	(Z) 1471 ± 08			1,86 a 1,73	-2,3	
Geraldes <i>et al.</i> (2004)	(Z) 1471 ± 31			1,86 a 1,73	-2,33 a +1,91	
Araújo (2008)	(S) 808 ± 620			1,74	+2,61	
Teixeira <i>et al.</i> (2015a)	(B) 1439 ± 4					

GEOLOGICAL AND PETROGRAPHIC CHARACTERIZATION

The basic rocks crop out in the study area as sills and lava flows, blocks or as large low-lying outcrops along drainages. The main outcrops are exposed on the road joining the town of Salto do Céu to the Progresso Village, on the upper reaches of the Bracinho Stream in the municipality of Rio Branco, and on the slopes of the homonymous hill (Figure 2).

Locally, typical features of magma mixing near the outcrops of the Rio Branco Suite are observed, such as mafic enclaves within felsic rocks (Figure 3A), and phenocrysts of alkali feldspar in the basic rocks, as well as hybridized zones derived from the interaction between felsic and mafic magmas (Figure 3B).

Sills are 2 to 30 m thick, and show well-defined intrusive contacts with pelites of Vale da Promissão Formation (Figure 3C) as well as are observed in tectonic contacts with the sandstones of Morro Cristalina Formation as a result of normal faulting. They are gently dipping between 10° and 15° WSW in general, but in places their dip is 5° towards both SW and ENE. The shape-rounded outcrops display typical spheroidal exfoliation.

Lava flows are about 6 m thick and show vertical internal structures as well as flow-top structures typical of thin basaltic lava flows (<10 m) as highlighted by Aubele *et al.* (1988) and Cashman & Kauahikaua (1997). Their internal structure is marked by zoning consisting of an upper vesicular portion (~1.7 m), and another intermediate portion without vesicular texture (~4.0 m); no vesicular lower portion was recognized as usual in the basaltic lava flows. The abundance and size of vesicles increase towards the top (Figures 4A and 4B). Flow folds (Figures 4C and 4D) deformed during lava flow motion result in surfaces of pahoehoe flows observed at the top of flows (30 to 40 cm below the top). The deformation caused by lava flow motion also led to fragmentation of ropy lava in the upper crusts resulting in its brecciated aspect (Figures 4E and 4F), formation of alkali feldspar phenocrysts partially resorbed (Figure 4H) in places showing rapakivi texture (Figure 4G). Internal structures and

flow-top aspects are characteristics similar to those pointed out by Chitwood (1994), Hon *et al.* (1994) and Self *et al.* (1998) for pahoehoe inflated flows deposited in subaerial settings. Vesicles are mostly filled with fibrous to fibro-radiated material consisting of zeolites chlorite, fluorite and opaque minerals.

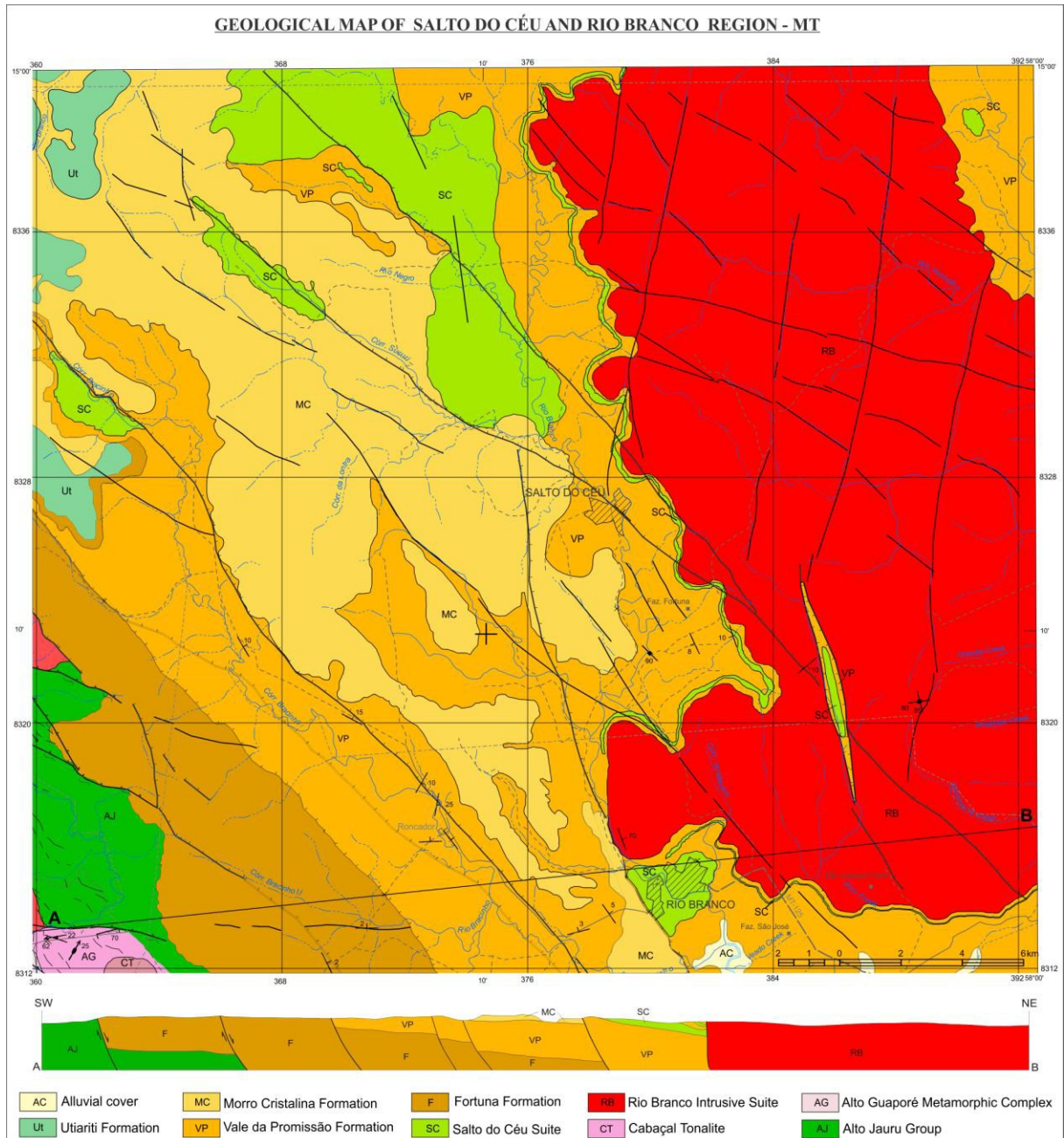


Figure 2. Location of the study area in the geological map of Salto do Céu and Rio Branco region – MT (Modified from Sousa *et al.*, 2011).

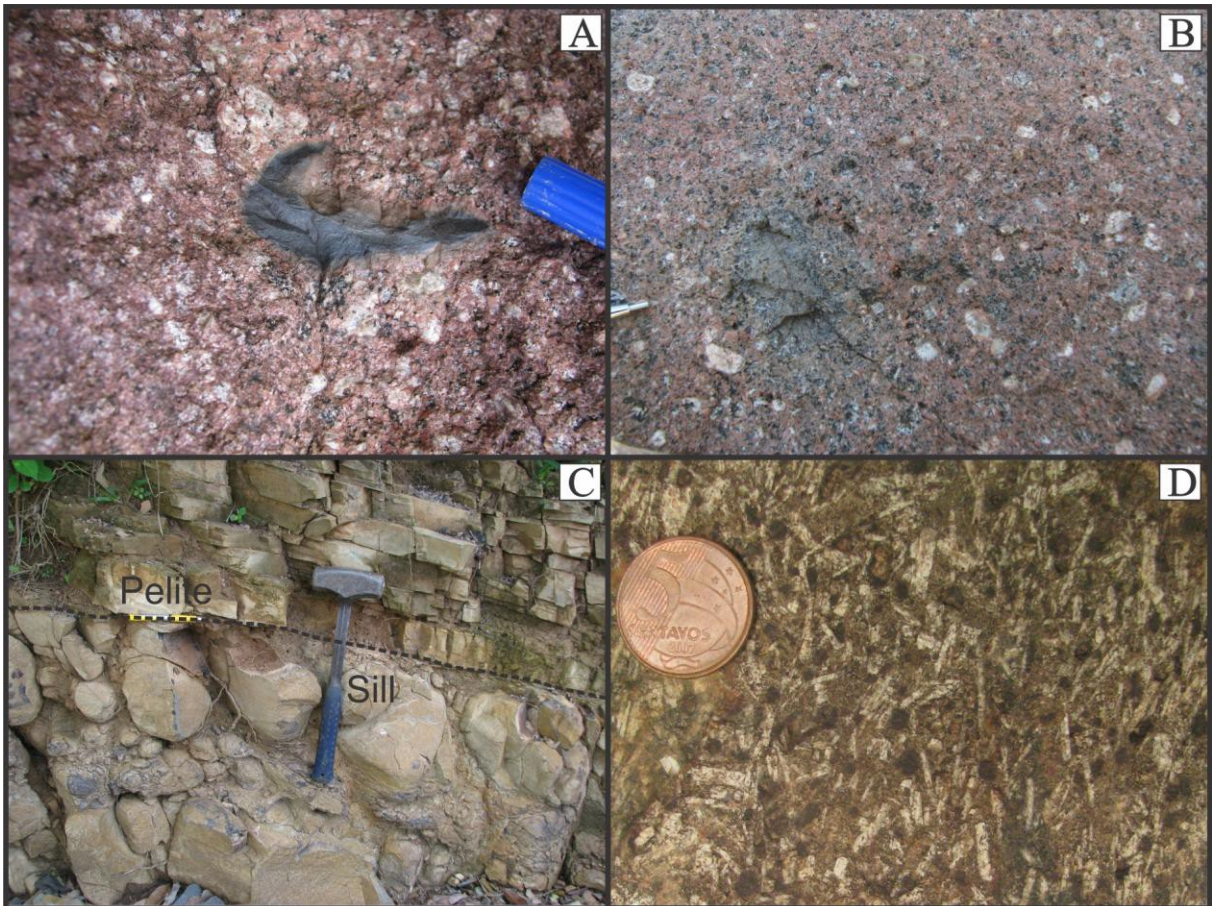


Figure 3. Field aspects of sills from SCS: A) mafic enclave likely from the SCS enclosed in rocks of the RBIS; B) hybridized areas resulting from interaction between felsic (RBIS) and mafic (SCS) magmas; C) concordant contact between sills of SCS and laminated pelites of Vale da Promissao Formation; D) macroscopic aspect of sills, with emphasis on subophitic texture marked by interstitial plagioclase laths between pyroxene crystals.

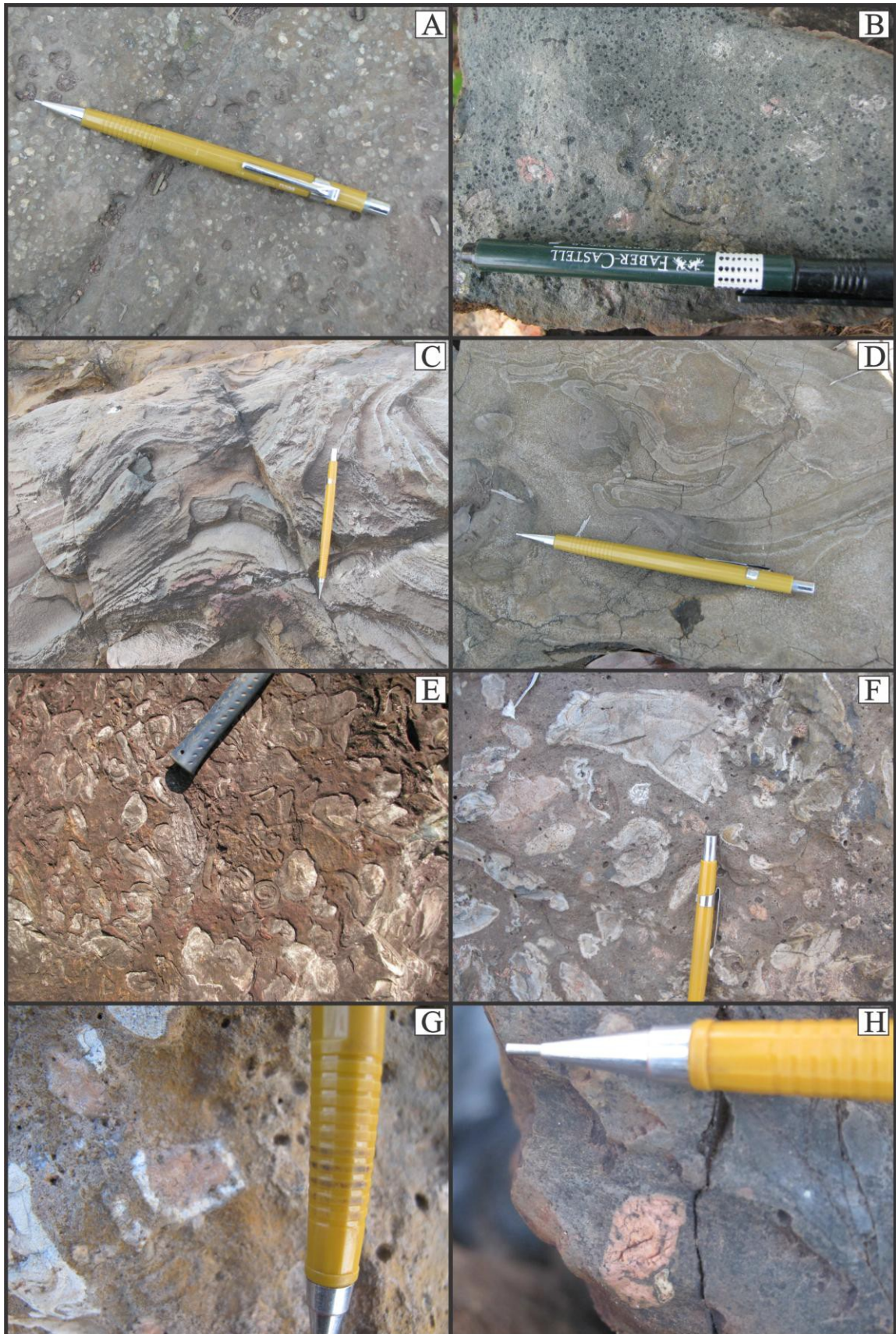


Figure 4. Field aspects of lava flows from SCS: A) e B) large amount of round vesicles in the flow top; C) and D) flow folds; E) and F) brecciated aspect resulting from flow lava

fragmentation as deformation occurs during its motion; G) and H) alkali feldspar phenocryst displaying rapakivi texture and partially resorbed, respectively.

Both sills and lava flows are mesocratic to melanocratic, greenish-gray to black in colour, and equigranular varying from very fine- to medium-grained.

The sills consist of diabases and massif gabbros that under the microscope display ophitic, subophitic, intergranular, and coronitic textures (Figures 5A, 5B and 5C). They are essentially composed of plagioclase and pyroxene having as accessory mineral assemblage opaque minerals, acicular apatite crystals, and subhedral brown sphene crystals. Alteration paragenesis is represented by amphibole, biotite, epidote/clinozoisite, sericite, calcite, clay minerals, and chlorite. Rare grains of alkali feldspar and quartz exhibiting graphic intergrowth are found as late-forming minerals.

The plagioclase, identified as labradorite occurs as subhedral to tabular euhedral crystals showing albite, pericline and Carlsbad twinning; in places, albite and Carlsbad twinning are combined. It is intensely argilized and saussuritized resulting in the formation of epidote/clinozoisite, sericite/muscovite and calcite.

The monoclinic pyroxene is identified as augite-titanoaugite and pigeonite being euhedral, prismatic, well-preserved, and mostly pink to dark pink in colour which indicates a Ti-rich composition, and exhibits sectorial twinning in places. Green amphibole occurs in reaction borders characterizing uralitization processes (Figures 6A, 6B and 6C). Occasionally, pyroxene shows complete pseudomorphism by amphibole, chlorite and biotite, but it may also occur as relict mineral.

The types of amphibole here observed are actinolite-tremolite and hornblende. Light green actinolite-tremolite occurs as acicular subhedral crystals, single crystals or fibrous aggregates that fills microvenules and microfractures following a fibrorradiated arrangement. They are mainly associated to the borders of pyroxene featuring coronitic texture, and may completely replace the pyroxene. Brown hornblende is observed as anhedral grains or pseudomorphs of pyroxene. It is usually altered to biotite and chlorite that may replace it completely.

Opaque minerals (Figures 7A and 7B) are common in these rocks as well-developed, subhedral, skeletal and symplectite crystals, and may be partially replaced by biotite, chlorite, rutile and sphene.

Biotite is a common product from the alteration of amphibole, pyroxene or opaque minerals. These minerals are in places surrounded by a biotite fringe consisting of tiny fibrous crystals. Biotite seldom occur as well-developed blades with reddish brown to brownish pleochroism. Chlorite is observed in thin microscopic greenish blades displaying a fibrous to fibro-radiated habit. Chlorite also occurs associated with amphibole in pseudomorphs of pyroxene and opaques, or in a pervasive way occurs as fracture filling in plagioclase.



Figure 5. Photomicrographs of sills from SCS displaying: A) ophitic texture featured by pseudomorph augite (titanoaugite) crystal consisting of opaque minerals and actinolite, including intensely altered plagioclase laths; B) Tabular plagioclase between prisms and grains of pyroxene characterizing subophitic texture; C) intergranular texture consisting of saussuritized tabular plagioclase crystals and partially uralitized interstitial pyroxene. Parallel polarizers to the left and crossed polarizers to the right. Abbreviations are as in Fettes & Desmons (2008).

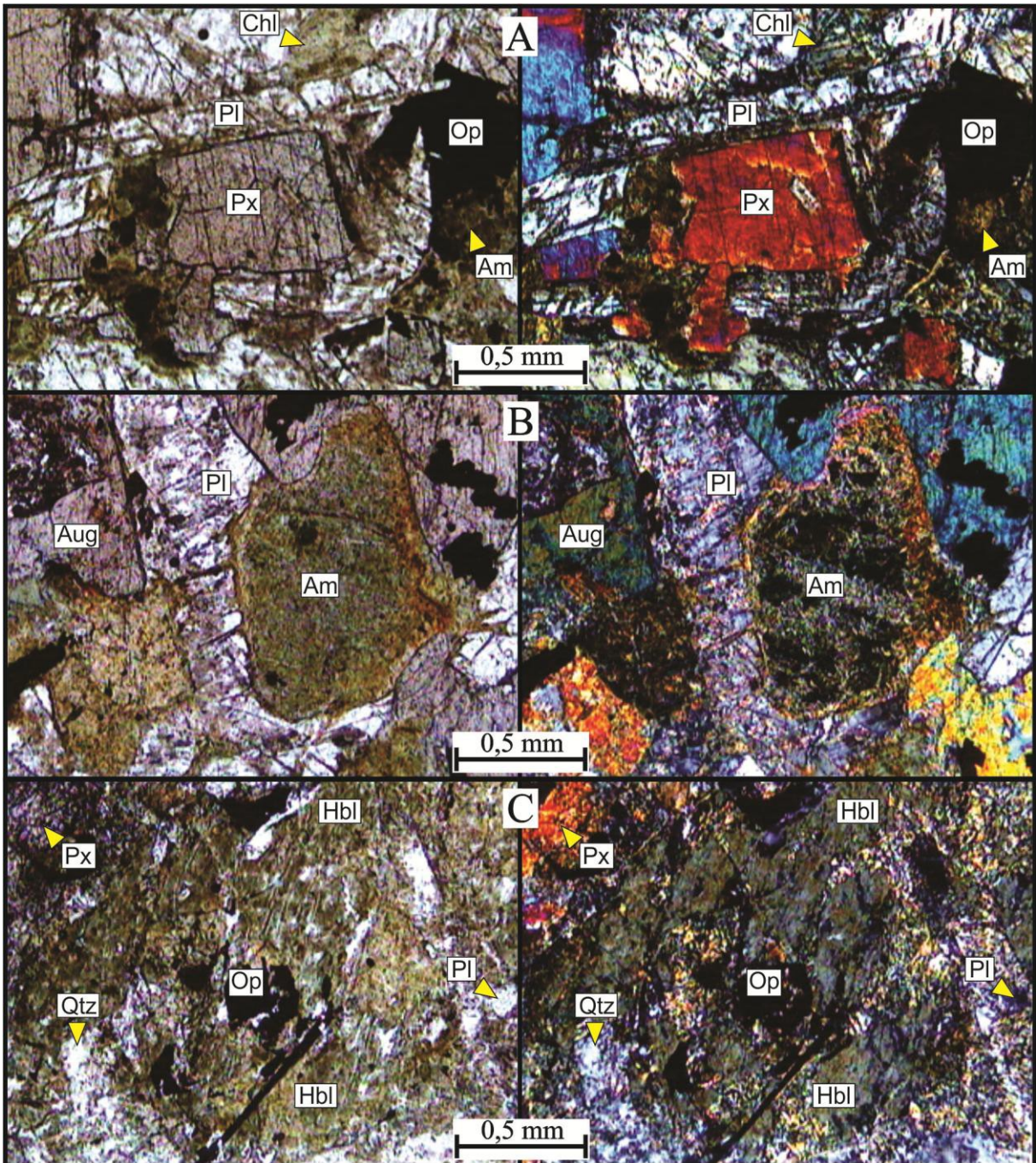


Figure 6. Photomicrographs of sills from the SCS showing: A) fractured plagioclase crystals, pyroxene and opaque minerals partially altered to amphibole, biotite and chlorite; B) subophitic texture consisting of tabular plagioclase and augite crystals, some pseudomorphized by amphibole; C) Pseudomorph of amphibole (hornblende) after pyroxene associated with plagioclase, quartz and opaques. Parallel polarizers to the left and crossed polarizers to the right. Abbreviations are as in Fettes & Desmons (2008).

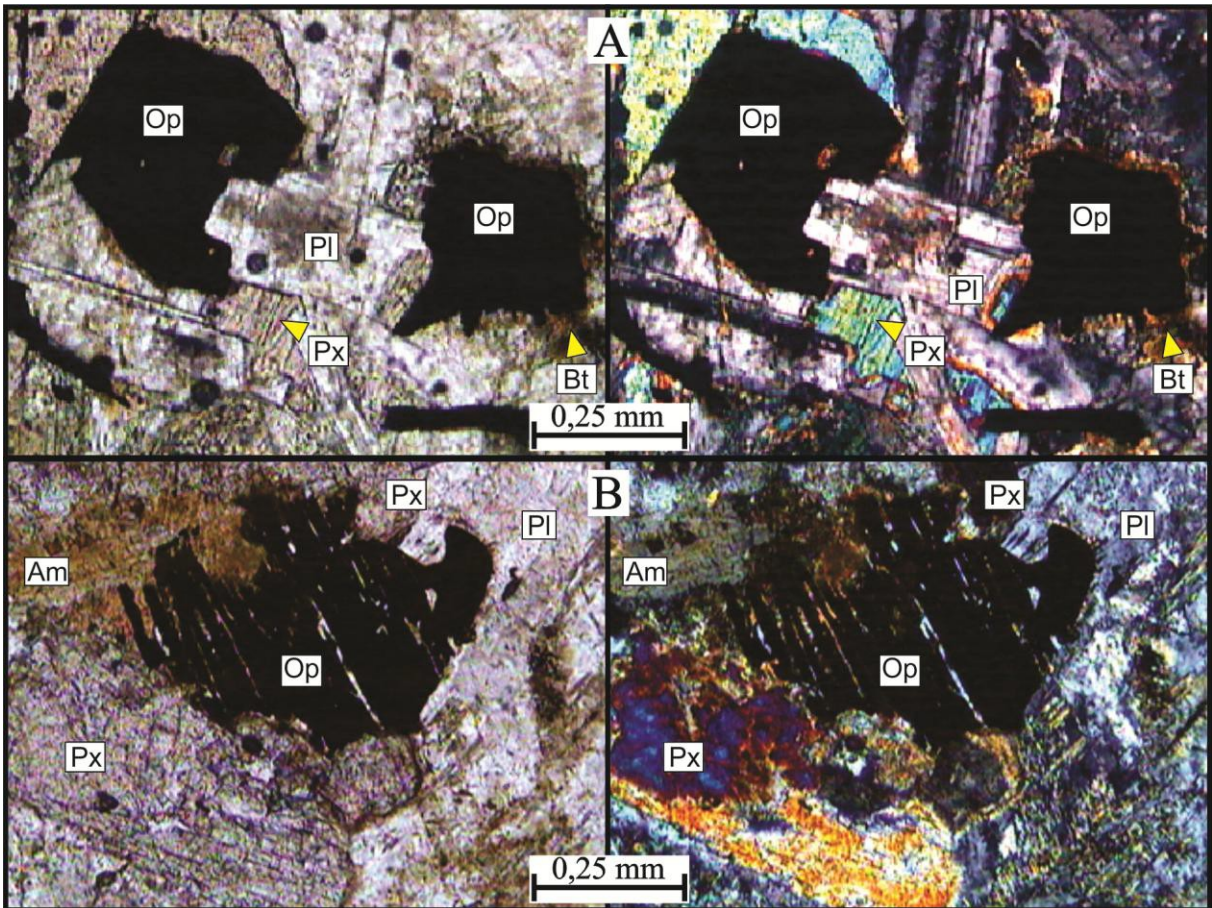


Figure 7. Photomicrographs of sills from SCS illustrating: A) detail of opaque minerals with biotite corona and plagioclase showing normal zoning; B) opaque mineral with symplectite texture associated with pyroxene, amphibole and plagioclase. Parallel polarizers to the left and crossed polarizers to the right. Abbreviations are as in Fettes & Desmons (2008).

The lava flows consist of basalts and diabases exhibiting the following textures: ophitic, subophitic, hyalophitic, porphyritic or amygdaloidal in pseudo-trachytic groundmass (Figures 8A, 8B and 8C); vitrophyric texture is also observed in some samples.

Their main components are plagioclase, pyroxene, and relict glass having as accessory and alteration paragenesis: amphibole, biotite, chlorite, opaque, rutile, sphalerite, apatite, sericite, epidote/clinozoisite, calcite and clay minerals.

The amygdales are round to ellipsoidal in shape, with diameter up to 3 mm, filled by fibrous to fibro-radiated material (Figures 9A, 9B, 9C, 9D, 9E and 9F) consisting of zeolites, chlorite, fluorite (Figures 10A and 10B) and opaque minerals. They may present reaction rims composed of a red-coloured mixture of iron oxides/hydroxides, biotite and rutile.

Labradorite/andesine occurs as euhedral to subhedral tabular phenocrysts and submillimetre-sized laths displaying albite, pericline and Carlsbad twinning. Alteration

processes such as argilization, *sericitization*, and mostly *saussuritization* are observed. Some crystals delineate a *pseudotrachytic flow texture* and may show normal, oscillatory and reverse zoning that are recognized by its higher degree of *saussuritization* in the more calcium-rich portions of plagioclase.

Clinopyroxene is identified as augite and pigeonite, white to pink in colour, in places exhibiting zoning and twinning, partially to completely uralitized or pseudomorphized by a mixture of amphibole, chlorite and biotite; some lithotypes contain orthopyroxene recognized as colourless to beige enstatite, partially altered to tremolite-actinolite and chlorite.

The amphibole types are products of pyroxene transformation occurring as hornblende prismatic crystals and grains, dark-green to brown in colour, and show drop-like quartz texture as well as acicular, fibrous and fibro-radiated, and white to greenish in colour tremolite-actinolite is seen. Both of them alters to biotite, chlorite and opaques.

Opaque minerals occur mostly as primary minerals or result from alteration of mafic minerals. They are more developed crystals showing dendritic habit and symplectitic texture, in places partially altered to biotite, chlorite, rutile, and sphene. Biotite occurs as tiny blades, brown to brownish, sparsely distributed in the rock or in association with amphibole. Rare biotite crystals are found well-preserved and often result from the alteration of opaque minerals.

Euhedral sphalerite phenocrysts displaying magmatic corrosion (Figures 10D and 10E) and reaction border consisting of calcite in very fine-grained fluidal groundmass (Figure 10C).

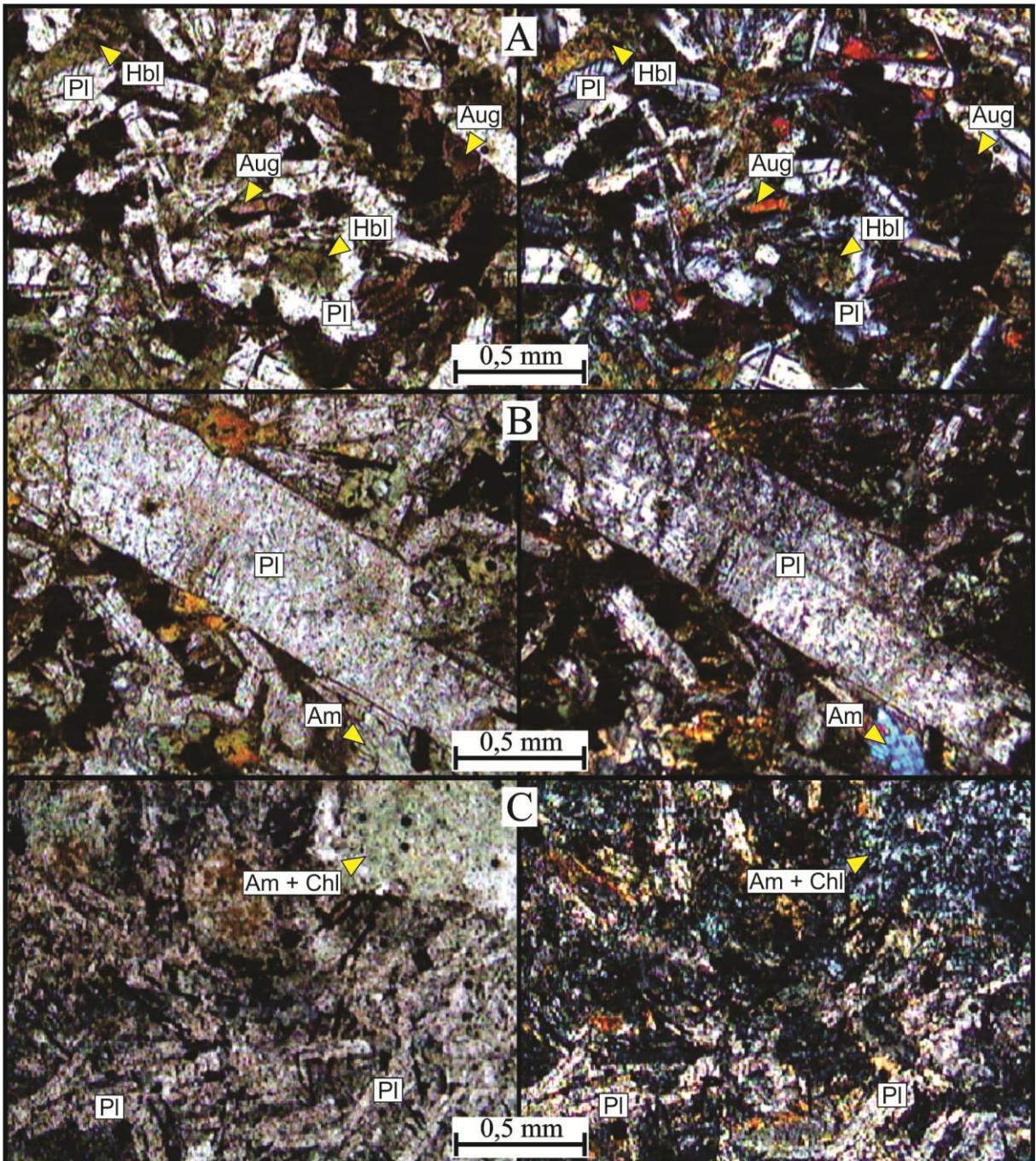


Figure 8. Photomicrographs of lava flows from SCS displaying: A) ophitic to intergranular texture featured by plagioclase laths and dark-pink titanite with partial to complete replacement by green-coloured hornblende; B) porphyritic texture formed by tabular plagioclase enclosed into a subophitic to intergranular groundmass; C) fluidal groundmass showing pseudo-trachytic texture delineated by the arrangement of deformed plagioclase laths intercalated with mafic minerals, and amphibole pseudomorphs of original pyroxene. Parallel polarizers to the left and crossed polarizers to the right. Abbreviations are as in Fettes & Desmons (2008).

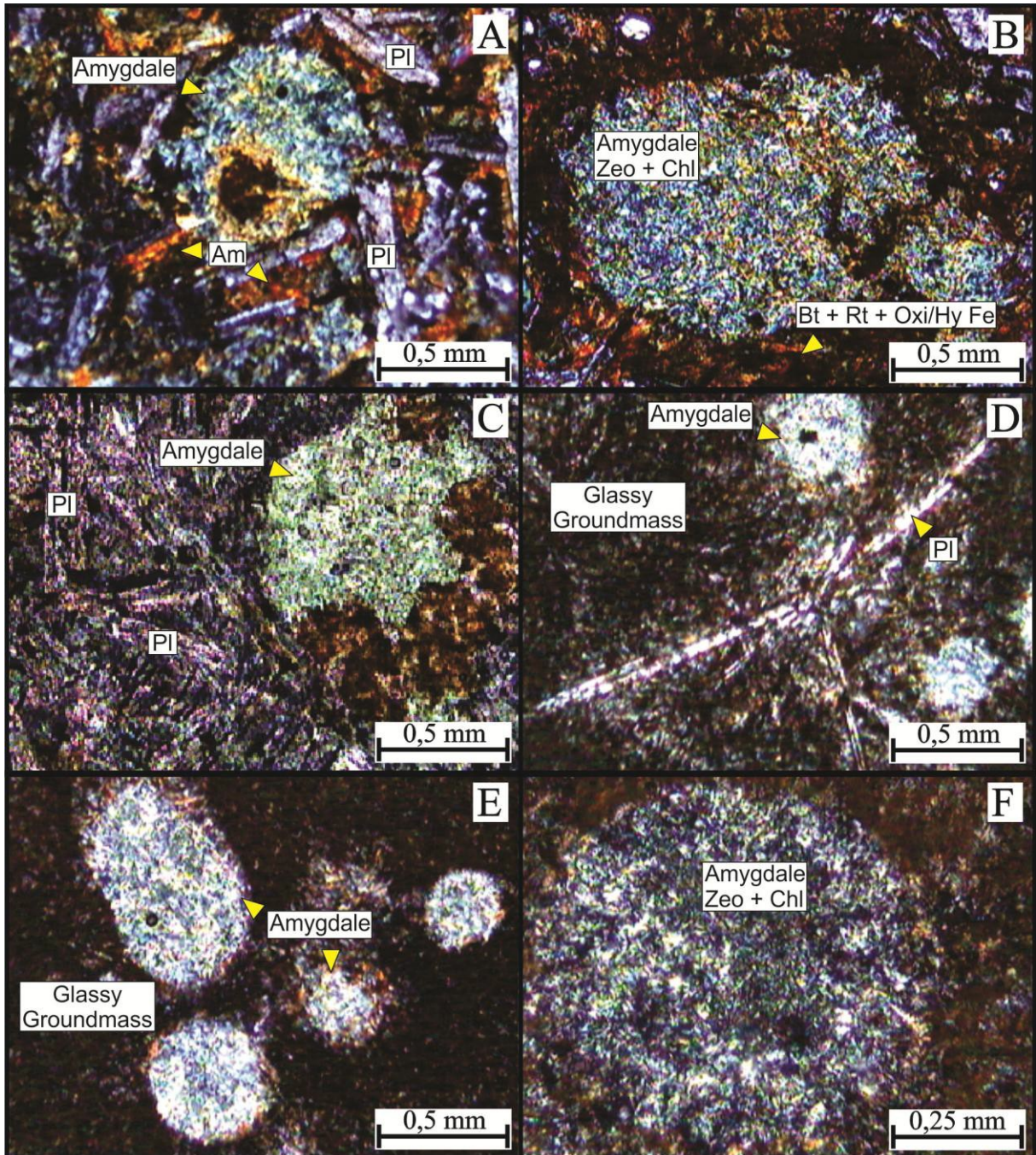


Figure 9. Photomicrographs of lava flows from SCS showing: A) amygdale enclosed in subophitic groundmass with plagioclase laths and amphibole; B) amygdale filled with zeolite and chlorite surrounded by a halo consisting of a mixture of biotite, rutile, and iron oxides/hydroxides; C) amygdale filled with zeolite, chlorite, biotite, and iron oxides/hydroxides in fluidal groundmass; D) vitrophyric texture formed by elongate laths of plagioclase phenocrysts and amygdale enclosed in glassy groundmass; E) round and ellipsoidal amygdale in glassy groundmass; F) Detail of rounded amygdale filled with zeolite and chlorite. Parallel polarizers in (C) and crossed polarizers in (A), (B), (D), (E) and (F). Abbreviations are as in Fettes & Desmons (2008).

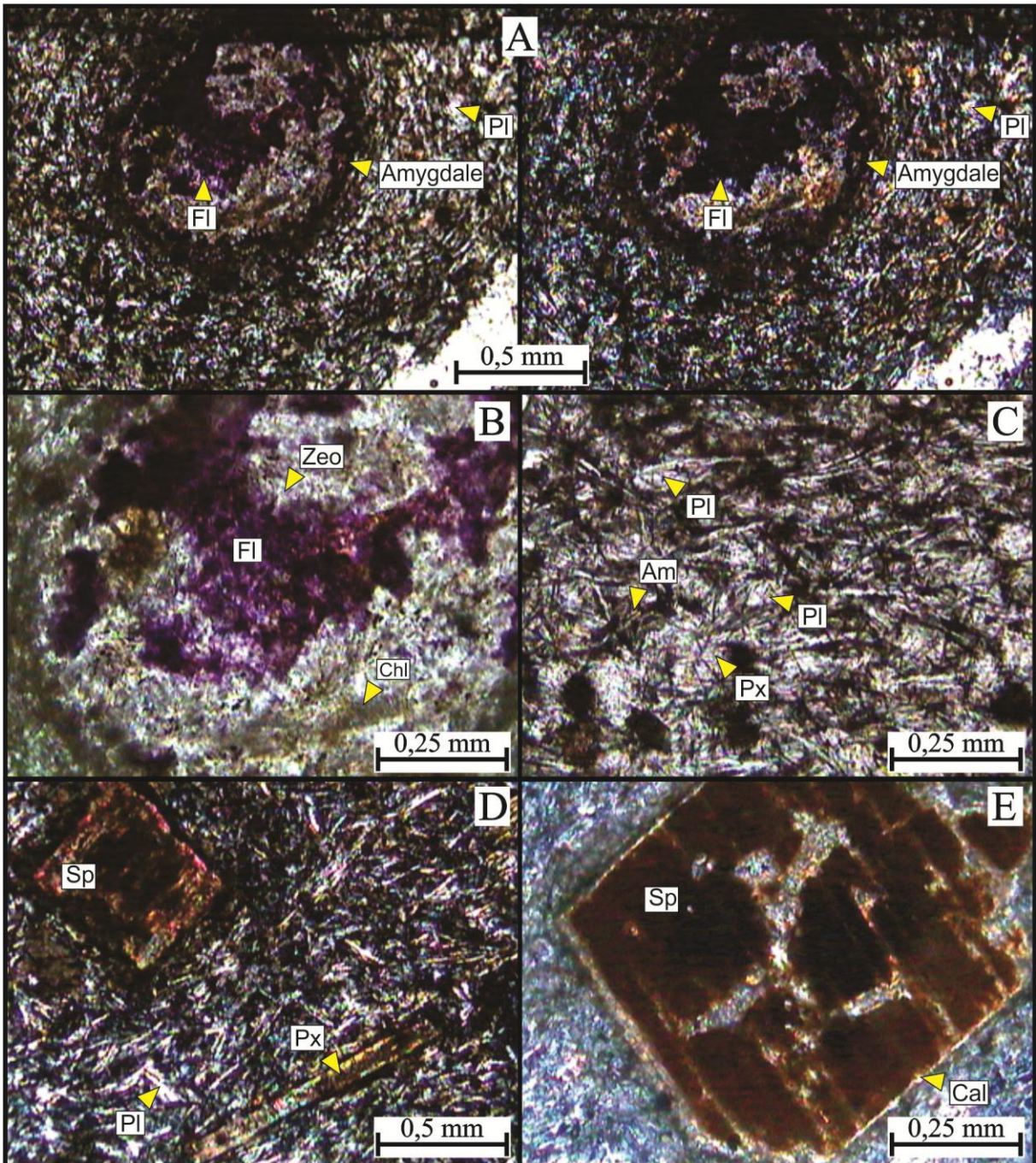


Figure 10. Photomicrographs of lava flows from SCS showing: A) fine-grained groundmass with pseudo-trachytic texture marked by alignment of plagioclase laths and mafic minerals, and amygdale filled with secondary phases, such as fluorite, opaques, chlorite and zeolite; B) details of previous image highlighting the purple colour of fluorite; C) detail of groundmass composed of plagioclase laths, pyroxene grains and amphibole; D) sphalerite and pyroxene phenocrysts in a trachytoid groundmass consisting of submillimetre-sized laths of plagioclase and mafic minerals; E) detail of euhedral sphalerite crystal with magmatic corrosion and

reaction rim of calcite. Parallel polarizers to the left and crossed polarizers to the right in (A), parallel in (B) and (C), and crossed polarizers in (D) and (E).

LITHOCHEMICAL CHARACTERIZATION

The lithochemical study of sills and lava flows from SCS was carried out on fourteen samples; also, sills and lava flows were studied together due to their chemical affinity. These samples were previously crushed and pulverized in the Sample Preparation Laboratory of the Geosciences Faculty at the Federal University of Mato Grosso and forwarded to the Acme Analytical Laboratories (Vancouver – Canada) in order to measure major and minor elements using the ICP-MS, and measure trace-elements including rare earth elements using the ICP-ES. Analytical data are shown on table 2. Data processing was performed using GCDkit software (version 3.0, Geochemical Data Toolkit for Windows; Janoušek *et al.* 2006).

MgO contents vary between 3.75 and 6.86 %, and SiO₂ contents vary between 44.03 and 49.32 %. Calculated mg# values [Mg/(Mg+Fe⁺²)] vary from 0.30 to 0.51 taking into account Fe₂O₃/FeO equals 0.15. These values suggest an evolved basaltic magma source for these rocks once higher values between 0.74 and 0.80 refers to primitive magma (Jaques & Green, 1979, 1980; Takahari & Kushiro, 1983).

Table 2. Lithochemical data of rocks from Salto do Céu Suite [major elements (% weight), trace-elements (ppm)]. # Sills e * Lava flows.

	#RB	#RB	#RB	#RB	#RB	#RB	#RB	#RB	#RB	#RB	#RB	*PG	*PG	*PG
	533A	42D2	22B	22C2	317	46B	344	532	531	320	317A	120 5	120 6	120 3
SiO ₂	44.03	45.06	45.09	45.22	45.56	45.80	45.86	46.11	46.90	47.25	48.9	49.02	49.15	49.32
TiO ₂	2.23	3.48	2.03	2.74	2.15	2.59	2.65	2.88	4.38	3.92	3.67	3.65	3.25	3.30
Al ₂ O ₃	15.76	14.78	16.53	14.45	15.83	16.10	16.23	16.09	11.73	12.41	13.04	13.68	13.90	13.63
Fe ₂ O ₃	14.70	15.10	13.05	15.56	13.61	13.96	14.40	14.03	17.60	17.36	16.19	14.94	14.85	14.67
FeOt	13.22	13.58	11.74	14.00	12.24	12.56	12.95	12.62	15.83	15.62	14.56	13.44	13.36	13.20
MnO	0.19	0.19	0.16	0.20	0.17	0.19	0.19	0.19	0.23	0.22	0.15	0.23	0.21	0.22
MgO	6.80	5.14	6.86	5.77	6.66	6.01	5.67	5.11	4.31	3.75	3.97	3.92	4.56	4.66
CaO	8.57	8.88	7.98	8.52	8.5	8.65	8.93	8.48	8.98	8.25	5.81	6.22	5.05	6.89
Na ₂ O	2.58	2.9	2.98	3.41	2.75	2.77	2.82	2.95	2.64	2.93	3.54	3.28	3.72	2.69
K ₂ O	1.06	0.45	1.06	0.55	0.78	0.65	0.39	0.83	1.38	1.69	0.40	1.74	1.34	1.19
P ₂ O ₅	0.35	0.66	0.34	0.45	0.38	0.49	0.49	0.54	0.59	0.67	0.70	0.61	0.58	0.57
LOI	3.4	3	3.6	2.8	3.3	2.5	2.1	2.5	1	1.3	3.3	2.4	3.0	2.5
Ba	437	312	455	326	562	390	350	491	516	631	562	826	1183	772

Rb	27.5	12.1	31.3	12.2	22.3	19.3	9.1	17.3	32.7	39.8	22.3	53.9	40.0	32.4
Sr	537.7	338.4	515.4	499.8	611.1	352.8	345.2	345.7	291.6	293.7	611.1	295.1	333.2	293.3
Zr	150.3	244.1	134.1	173.1	153.1	205.6	205.5	215.8	255	313	329.1	283.2	261.3	251.1
Nb	12.6	21.4	11.3	15.5	12.9	13.5	13.9	14.8	19.9	22.2	12.9	19.5	18.2	16.7
Zn	70	88	58	81	84	89	91	91	97	119	196	86	107	72
La	17.5	30.3	16.5	21.6	18.6	18.6	20.2	20.4	28.7	35.6	42.7	34.2	35.0	29.4
Ce	40.7	69.2	38.2	51.8	43.5	44.2	46.5	50	68.3	79.9	98.7	75.0	74.8	65.3
Pr	5.71	9.55	5.35	7.18	6.16	6.34	6.66	6.82	9.51	11	13.12	10.19	9.91	8.90
Nd	26.5	41.7	24.3	32	26.1	27.8	29.1	30.7	43.6	50.1	56.9	42.8	42.2	39.3
Sm	5.56	8.92	5.02	6.8	5.6	6.2	6.61	6.9	9.62	10.76	12.15	9.27	9.32	8.73
Eu	1.94	2.71	1.81	2.28	2.01	2.15	2.22	2.26	2.74	3.08	3.31	2.71	2.63	2.39
Gd	5.84	9.29	5.14	6.87	5.71	6.53	7.04	7.35	10.09	11.45	12.93	10.06	9.63	8.94
Tb	0.91	1.49	0.82	1.11	0.92	1.14	1.17	1.19	1.61	1.71	2.07	1.61	1.51	1.40
Dy	5.06	8.05	4.53	6.14	5.12	6.41	6.35	6.79	9.53	10.25	11.75	9.46	9.46	8.26
Ho	1	1.62	0.89	1.19	1.01	1.25	1.31	1.31	1.82	2.02	2.31	1.67	1.62	1.61
Er	2.79	4.39	2.38	3.35	2.83	3.61	3.75	3.7	4.94	5.39	6.58	4.59	4.72	4.56
Tm	0.4	0.65	0.36	0.49	0.39	0.52	0.54	0.55	0.76	0.81	0.94	0.74	0.65	0.65
Yb	2.37	4.15	2.3	3.04	2.5	3.09	3.41	3.46	4.44	5.02	5.92	4.58	4.08	3.83
Lu	0.36	0.57	0.31	0.43	0.36	0.46	0.5	0.52	0.65	0.73	0.84	0.71	0.64	0.63
Y	33.4	43	23.3	32.9	27.1	33.5	35.6	36.5	49.8	52.5	66	46.7	43.4	42.0
Ga	19.5	24.9	20.2	21.7	22.1	23.3	22.3	21.6	23.1	24.4	22.1	21.2	21.2	20.0
mg#	0.48	0.40	0.51	0.42	0.49	0.46	0.44	0.42	0.33	0.30	0.33	0.34	0.38	0.39

Major and trace-elements variation diagrams using MgO as differentiation index (Fenner's diagrams; Figures 11 and 12) define relative linear trends, mostly well-defined, therefore suggesting magma mixing. A negative relationship is observed in the major-elements diagrams between MgO and contents of SiO₂, TiO₂, P₂O₅, Fe₂O₃ and MnO while CaO and Na₂O are randomly distributed which suggests they were largely mobilized during post-magmatic events. K₂O yields a divergent pattern in which its content decreases and then increases again as the MgO content decreases. Trace-elements show that concentrations of Ba, Nb, Zr, La, Ce and Y decreases as the MgO content increases.

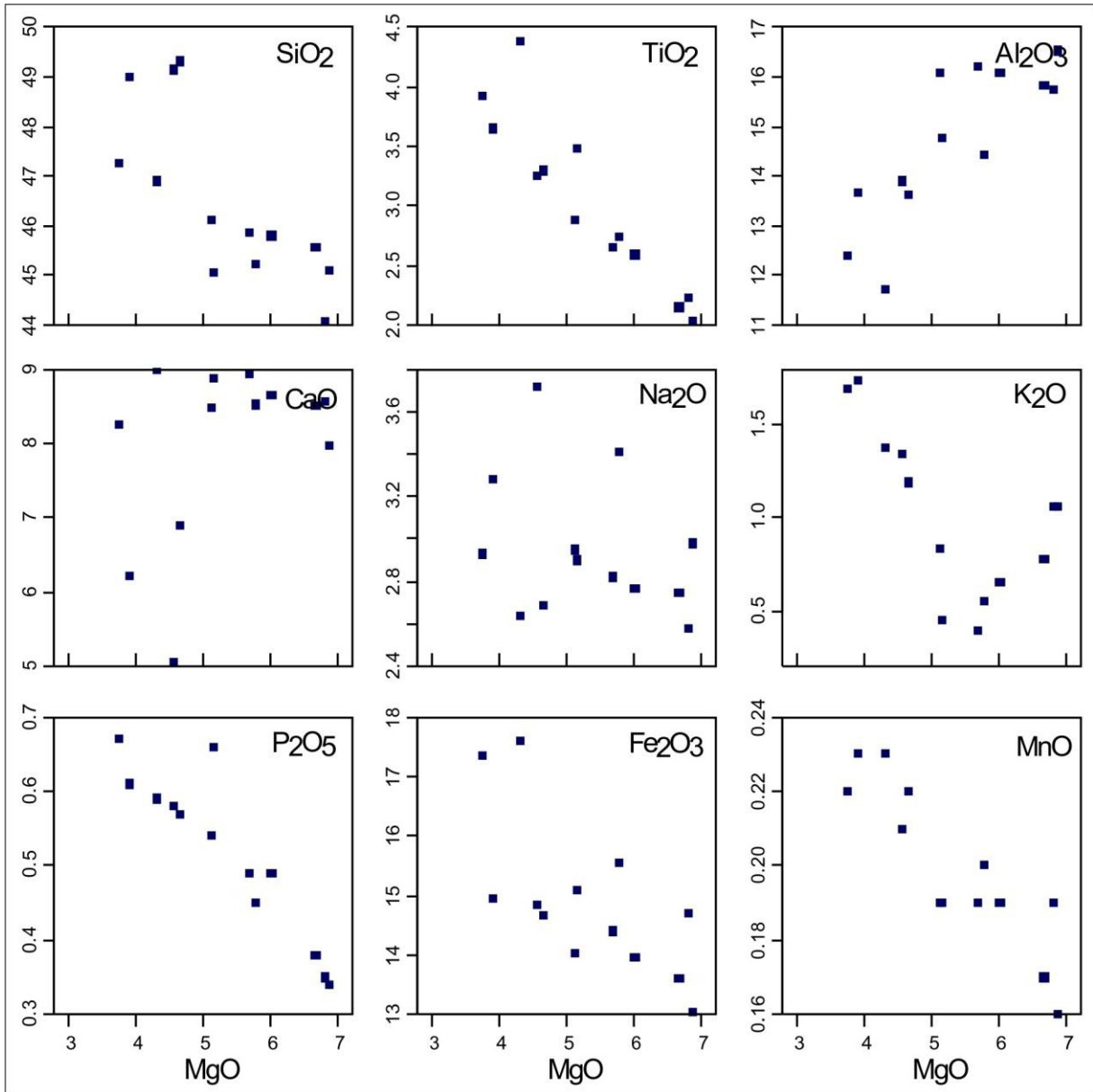


Figure 11. MgO variation diagrams versus major-elements (% weight) for rocks from SCS.

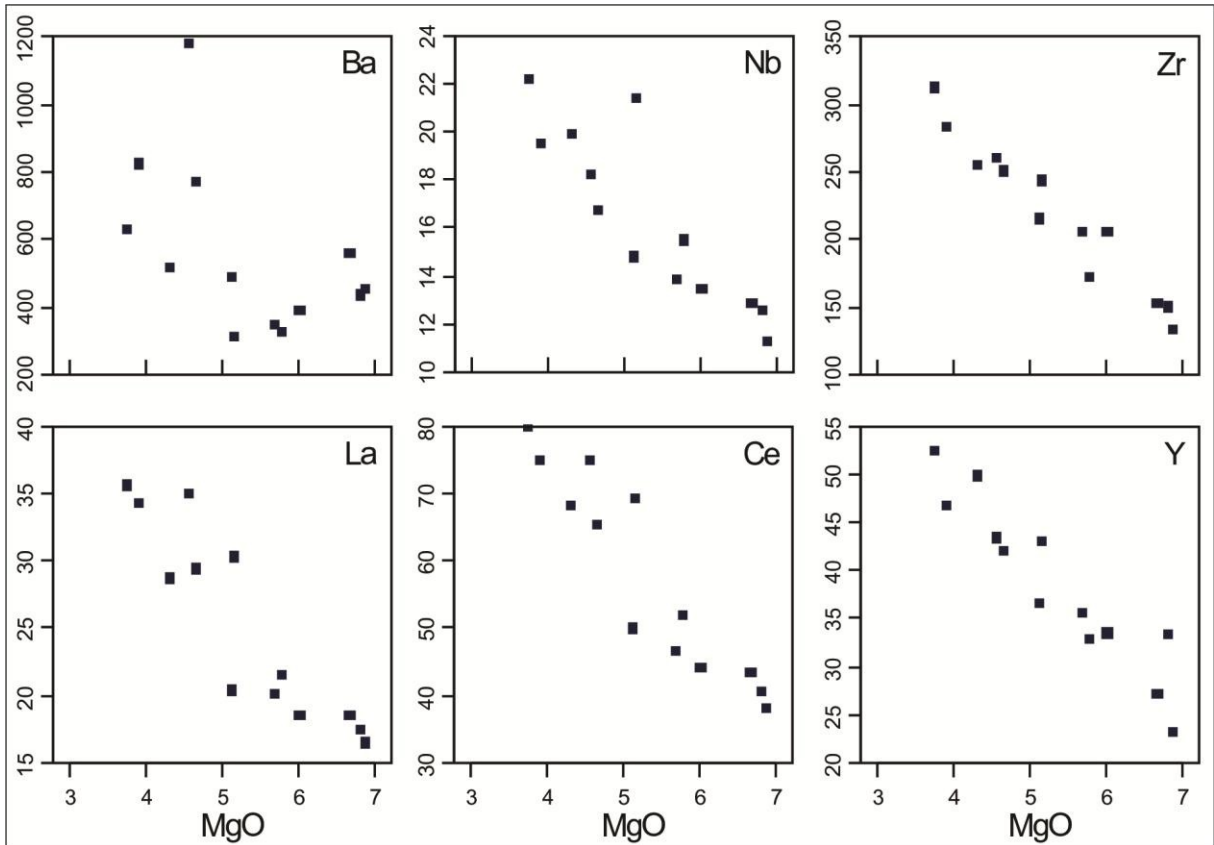


Figure 12. MgO variation diagrams (% weight) versus trace-elements (ppm) for rocks from SCS.

The rocks from Salto do Céu Suite have tholeiitic affinity with typical FeO_t enrichment relative to MgO taking into account alkali values nearly constant, as seen in the AFM diagram (Irvine & Baragar, 1971; Figure 13A), and are classified as sub-alkaline basalts and iron-rich tholeiitic basalts following the classification of Winchester & Floyd (1977; Figure 13B) and Jensen (1976; Figure 13C), respectively.

In order to unravel their tectonic settings, diagrams Zr/Y versus Zr (Pearce & Norry, 1979; Figure 13D), Zr – Nb – Y (Meschede, 1986; Figure 13E) and MgO – FeO_t – Al_2O_3 (Pearce *et al.*, 1977; Figure 13F) were elaborated in which the rocks from SCS overlap the domains proposed by these authors for continental intraplate basalts

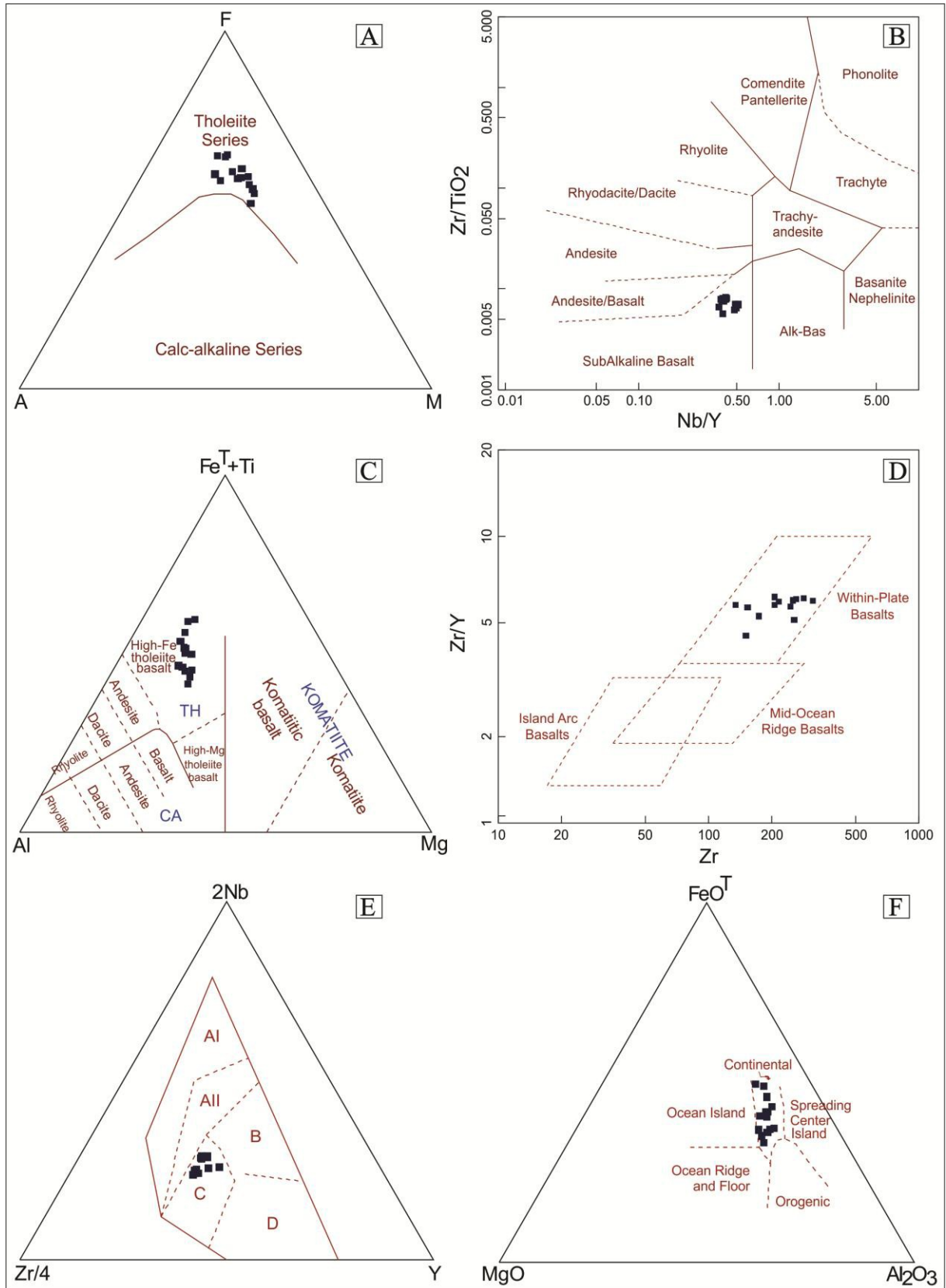


Figure 13. Classification diagrams for rocks from SCS: (A) Irvine & Baragar (1971); (B) Winchester & Floyd (1977); (C) Jensen (1976); (D) Pearce & Norry, (1979); (E) Meschede (1986; AI-AII = Within-Plate Alkaline Basalts; AII-C = Within-Plate Tholeiites; B = P-type

Mid-Ocean Ridge Basalts; D = N-type Mid-Ocean Ridge Basalts; C-D = Volcanic Arc Basalts); (F) Pearce *et al.* (1977).

Patterns distribution of rare earth elements (RRE) normalized to primitive mantle values of McDonough & Sun (1995) are illustrated in Figure 14A. Heavy REE (HREE) fractionation relative to light REE (LREE) is observed. There is a clear distinction between the two rock groups in which one of them is richer in REE, with La_N greater than 100 and a discrete negative Eu anomaly (group 1), corresponding to the rocks with lower MgO contents; the second group does not show this pattern having La_N less than 100 (group 2).

Figure 14B shows a primitive-mantle normalized multi-element spidergram according to values of McDonough & Sun (1995). Here rocks also show a separation into two groups, where the main difference is the negative Sr anomalies for the group with La_N greater than 100, and positive Sr anomalies for the group with La_N less than 100 which corresponds to the group with discrete Eu anomaly. For the other elements, both groups follow a very similar pattern with negative Rb, K, and Nb anomalies, and positive Ti anomaly likely reflecting no fractionation of Fe-Ti oxides. The negative Nb anomaly, in its turn, may be attributable to crustal assimilation processes.

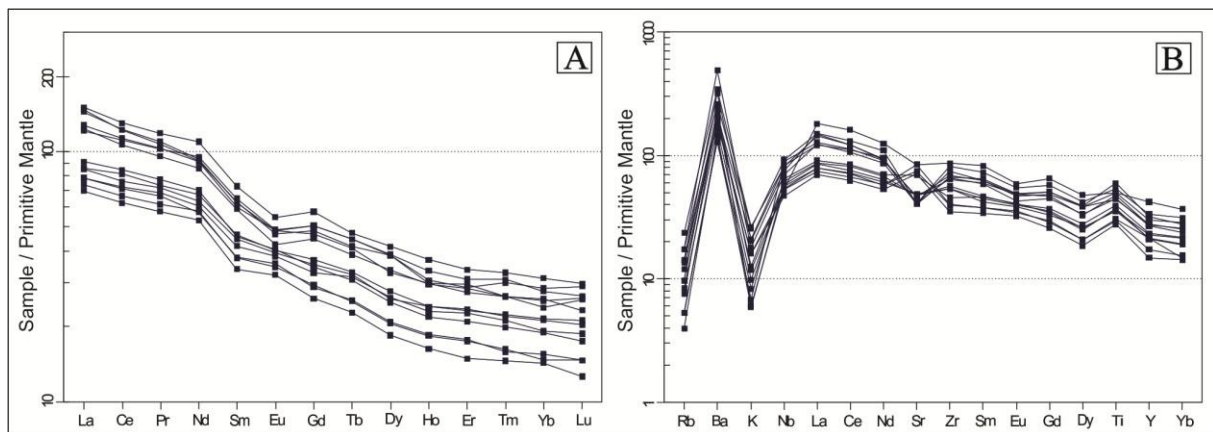


Figure 14. REE (A) and multi-element spidergrams (B) normalized to primitive values of McDonough & Sun (1995) for rocks from SCS.

DISCUSSION AND FINAL CONSIDERATIONS

Based on data from semi-detailed geological mapping as well as petrographic and lithochemical characterization, here we conclude the basic rocks from the region of Salto do Céu (MT) occurring as sills and lava flows belong to the same magmatic event that gave rise

to the Salto do Céu Suite. Moreover, the U-Pb baddeleyite age of 1439 ± 4 Ma (Teixeira *et al.* 2015a), and geochronological dataset available for rocks from Rio Branco Intrusive Suite (1427 ± 10 Ma, 1423 ± 0.2 Ma and 1423 ± 6 Ma obtained by Geraldès *et al.*, 2001; Geraldès *et al.*, 2004 and Araújo, 2008; respectively) indicates that both the suites are derived from a bimodal *chrono-correlated* magmatism.

The temporal correlation of Salto do Céu suite (basic rocks) to the Rio Branco Suite (acid rocks) is corroborated given the presence of diagnostic features from magma mixing, such as mafic enclaves enclosed into felsic rocks, alkali feldspar phenocrysts in basic rocks, oscillatory or reverse zoning in plagioclase, and hybridized zones resulting from the interaction of felsic and mafic magmas.

The TIMS U-Pb baddeleyite ages of 1110 ± 2 Ma and 1112 ± 2 Ma measured by Teixeira *et al.* (2015b) for the mafic sills from Rincon del Tigre, respectively, in Bolivia and Huanchaca as well as that U-Pb baddeleyite age of 1439 ± 4 Ma obtained by Teixeira *et al.* (2015a) for the basic magmatism of the Salto do Céu Suite in Brazil show that they are not related to a single igneous-tectonic event attributable to an older crustal extension episode that resulted in mantellic magma ascent, opposing previous proposals of Ruiz *et al.* (2010a), Lima *et al.* (2012) among others.

Geochronological data made available by Leite & Saes (2003), Santos *et al.* (2005) and Geraldès *et al.* (2014) point out that the sedimentary cover hosting sills and lava flows of the SCS is not attributable to the defined Aguapeí Group of the type-area in Santa Barbara Hill (Sousa e Hildred, 1980)

The diagenesis of Fortuna Formation, basal unit of Aguapeí Group, occurred between 1165 ± 27 Ma and 1149 ± 7 Ma based on SHRIMP U-Pb dating of diagenetic xenotime from Santa Barbara Hill (Santos *et al.*, 2005). A maximum deposition age of 1.3 Ga on detrital zircons is attributed to it according to Leite & Saes (2003; bottom of Aguapeí Group in São Vicente and Lavrinha hills) and Geraldès *et al.* (2014; Fortuna Formation in Ricardo Franco and Santa Barbara hills). The younger basement rocks of this group in the surrounding region are the post-kinematic granites of the Pensamiento Suite dated at 1290 Ma by U-Pb (LA-IPC-MS) (Jesus *et al.*, 2010).

Geraldès *et al.* (2014) report a maximum deposition age around 1540 Ma (U-Pb, LA-ICP-MS) for this group in the Rio Branco Hill, which supports the notion that is a different sedimentary cover, likely another stratigraphic unit deposited in the Calymmian once the

younger rocks of the underlying basement consist of post-kinematic granites of the Alvorada Suite dated around 1440 Ma by U-Pb (TIMS) on zircon (Geraldés *et al.*, 2001; Ruiz, 2005).

The mafic-ultramafic suites named Figueira Branca and Indiavaí (1.42 a 1.41 Ga; Teixeira *et al.*, 2011) are part of the Jauru Terrane and are chrono-correlated to the Salto do Céu and Rio Branco suites as well as may be derived from a single magmatic event.

The mafic sills and lava flows from Salto do Céu Suite and the rocks from Rio Branco Suite are here interpreted as an anorogenic bimodal suite formed in intraplate settings, in extensive tectonic regime, which may reflect an important tectonic milestone associated with the breakup of the Columbia (Nuna) Supercontinent.

Acknowledgements

Authors gratefully acknowledge the financial support from CAPES (PROCAD 096/2007, National Program of Academic Cooperation), CNPq (process number 479779/2011-2, National Council for Scientific and Technological Development), FAPEMAT (process number 222473/2015, *Foundation for Research Support of Mato Grosso*), and GEOCIAM (*National Institute of Sciences and Geoscience Technology of the Amazon*). The first author acknowledges CNPq for granting the PhD scholarship.

References

- Araújo L.M.B., Godoy A.M., Ruiz A.S., Souza M.Z.A. 2005. Soleiras Máficas Tonianas (Suíte Intrusiva Salto do Céu) no SW do Cráton Amazônico: regime extensional relacionado à Orogenia Sunsás? *In: Simpósio de Geologia do Centro Oeste. Goiânia, Short Papers*, p. 155-156.
- Araújo L.M.B., Godoy A.M., Ruiz A.S., Manzano J.C., Souza M. Z. A. 2007. Geologia e Geoquímica do Batólito Rapakivi Rio Branco, SW do Cráton Amazônico - MT. *Geologia USP - Série Científica*, **7**:57-72.
- Araújo L.M.B. 2008. *Evolução do magmatismo pós-cinemático do Domínio Cachoeirinha: Suítes Intrusivas Santa Cruz, Alvorada e Rio Branco—SW do Cráton Amazônico—MT*. PhD Thesis, Universidade Estadual Paulista, Rio Claro, 158 p.
- Araújo L.M.B., Godoy A.M., Zanardo A. 2009. As Rochas Básicas Intrusivas das Suítes Rio Branco e Salto Do Céu, na região de Rio Branco (MT) Sudoeste do Cráton Amazônico. *Revista Brasileira de Geociências*, **39**:289-303.
- Araújo L.M.B., Godoy A.M. 2011. Magmatismo o Batólito Rapakivi Rio Branco, SW do Cráton Amazônico (MT). *Geociências*, **30**:173-195.

- Aubele J.C., Crumpler L.S., Elston W.E. 1988. Vesicle zonation and vertical structure of basalt flows. *Journal of Volcanology and Geothermal Research*, **35**:349-374.
- Barros A.M., Silva R.H., Cardoso O.R.F.A., Freire F.A., Souza Jr. J.J., Rivetti M., Luz D.S., Palmeira R.C., Tassinari C.C.G. 1982. *Folha SD.21. - Cuiabá*. Rio de Janeiro, Ministério das Minas e Energia-Secretaria Geral, Projeto RADAMBRASIL.
- Cashman K.V., & Kauaikaia J.P. 1997. Reevaluation of vesicle distributions in basaltic lava flows. *Geology*, **25**(5):419-422.
- Chitwood L.A. 1994. Inflated basaltic lava – examples of processes and landform from central and southeast Oregon. *Oregon Geology*, **56**(1):11-21.
- Ernst R.E., Wingate M.T.D., Buchan K.L., Li, Z.X. 2008. Global record of 1600–700 Ma Large Igneous Provinces (LIPs): implications for the reconstruction of the pro-posed Nuna (Columbia) and Rodinia supercontinents. *Precambrian Research*, **160**:159-178.
- Ernst R.E., Pereira E., Hamilton M.A., Pisavevsky S.A., Rodrigues J., Tassinari C.C.G., Teixeira W., Van-Dunem V. 2013. Mesoproterozoic intraplate magmatic „barcode“ record of the Angola portion of the Congo Craton: newlydated magmatic events at 1505 and 1110 Ma and implications for Nuna (Columbia) supercontinent reconstructions. *Precambrian Research*, **230**:103-118.
- Fettes D. & Desmons. J. (eds.). 2008. *Metamorphic rocks: a classification and glossary of terms*. Cambridge, Cambridge University Press, 243 p.
- Geraldes M.C. 2000. *Geocronologia e geoquímica do plutonismo mesoproterozoico do SW do Estado de Mato Grosso (SW do Cráton Amazônico)*. PhD Thesis, Universidade de São Paulo, São Paulo, 193 p.
- Geraldes M.C., Van Schmus W.R., Condie K.C., Bell S., Teixeira W., Babinski M. 2001. Proterozoic geologic evolution of the SW part of the Amazonian Craton in Mato Grosso state, Brazil. *Precambrian Research*, **111**:91-128.
- Geraldes M.C., Bettencourt J.S., Teixeira W, Matos J.M. 2004. Geochemistry and isotopic constraints on the origin of the mesoproterozoic Rio Branco „anorogenic“ plutonic suite, SW of Amazonian craton, Brazil: high heat flow and crustal extension behind the Santa Helena arc? *Journal of South American Earth Sciences*, **17**:195-208.
- Geraldes M.C., Nogueira C., Vargas-Mattos G., Matos R., Teixeira W., Valencia V., Ruiz J. 2014. U-Pb detrital zircon ages from the Aguapeí Group (Brazil): Implications for the geological evolution of the SW border of the Amazonian Craton. *Precambrian Research*, **244**:306-316.
- Hon K., Kauahikaua J., Denlinger R., Mackay K. 1994. Emplacement and inflation of pahoehoe sheet flows: observations and measurements of active lava flows on Kilauea Volcano, Hawaii. *Geological Society America Bulletin*, **106**:351-370.

- Irvine I.N. & Baragar W.R. A. 1971. A Guide To The Chemical Classification Of The Common Volcanics Rocks. *Canadian Journal Earth Science*, **8**:523-548.
- Janoušek V., Farrow C.M., Erban V. 2006. Interpretation of whole-rock geochemical data in igneous geochemistry: introducing Geochemical Data Toolkit (GCDkit). *Journal of Petrology*, **47**(6):1255-1259.
- Jacques A.L. & Green D.H. 1979. Determination of liquid compositions in high pressure melting of peridotite. *American Mineralogist*, **64**:1312-1321.
- Jaques A.L. & Green D.H. 1980. Anhydrous melting of peridotite at 0-15 kb pressure and the genesis of tholeiitic basalts. *Contributions to Mineralogy and Petrology*, **73**:287-310.
- Jensen L.S. 1976. A new cation plot for classifying subalkalic volcanic rocks. Ontario Division of Mines, Miscellaneous Paper 66, 22 p.
- Jesus G.C., Sousa M.Z.A., Ruiz A.S., Matos J.B. 2010. Petrologia e geocronologia (U-Pb/Sm-Nd) do Granito Passagem, Complexo Granitoide Pensamiento, SW do Cráton Amazônico (MT). *Revista Brasileira de Geociências*, **40**(3):392-408.
- Leite J.A.D., Saes, G.S., Weska R.K. 1985. A Suíte Intrusiva Rio Branco e o Grupo Aguapeí na serra de Rio Branco, Mato Grosso. In: Simpósio de Geologia do Centro Oeste. Goiânia, *Short Papers*, p. 247-255.
- Leite J.A.D. & Saes G.S. 2003. Geocronologia Pb-Pb de zircões detríticos e análise estratigráfica das coberturas sedimentares proterozoicas do sudoeste do Cráton Amazônico. *Geologia USP - Série Científica*, **3**(2):113-127.
- Lima G.A. 2011. *Geologia, Geoquímica e Geocronologia dos sills máficos da Suíte Intrusiva Huanchaca na porção nordeste da Serra Ricardo Franco (MT) – SW do Cráton Amazônico*. MS Dissertation, Instituto de Ciências Exatas e da Terra, Universidade Federal de Mato Grosso, Cuiabá, 62 p.
- Lima G.A., Sousa M.Z.A., Ruiz A.S., D'agrella Filho M.S., Vasconcelos P. 2012. Sills máficos da Suíte Intrusiva Huanchaca - SW do Cráton Amazônico: registro de magmatismo fissural relacionado à ruptura do Supercontinente Rodínia. *Revista Brasileira de Geociências*, **42**:111-129.
- Meschede M. 1986. A method of discriminating between different types of mid-ocean ridge basalts and continental tholeiites with the Nb-Zr-Y diagram. *Chemical Geology*, **56**:207-218.
- McDonough W.F. & Sun S.S. 1995. The composition of the earth. *Chemical Geology*, **120**: 223-253.
- Oliva L.A. 1979. Ocorrências Minerais na Folha Cuiabá (SD.21). Relatório de Viagem Goiânia, DNPM, p. 18.

- Pearce T.H., Gorman B.E., Birkett T.C. 1977. The relationship between major element chemistry and tectonic environment of basic and intermediate volcanic rocks. *Earth and Planetary Science Letters*, **36**:121-132.
- Pearce J.A. & Norry M.J. 1979. Petrogenetic implications of Ti, Zr, Y and Nb variations Volcanic Rocks. *Contributions to Mineralogy and Petrology*, **69**:33-47.
- Rogers J.J.W. & Santosh M. 2002. Configuration of Columbia, a mesoproterozoic supercontinent. *Gondwana Research*, **5**:5-22.
- Ruiz A.S. 1992. *Contribuição a Geologia do Distrito de Cachoeirinha, MT*. São Paulo. MS Dissertation, Instituto de Geociências, Universidade de São Paulo, São Paulo, 98 p.
- Ruiz A.S. 2005. *Evolução Geológica do Sudoeste do Cráton Amazônico Região Limítrofe Brasil-Bolívia – Mato Grosso*. PhD Thesis, Universidade Estadual Paulista, Rio Claro, 250 p.
- Ruiz A.S., D'agrella Filho M.S., Sousa M.Z.A., Lima G.A. 2010a. Tonian sills and mafic dike swarms of S-SW Amazonian Cráton: records of Rodinia Supercontinent break-up? *In: The Meeting of the Americas*. Foz do Iguaçu, *Short Papers*, 1.
- Ruiz A.S., Matos J.B., Sousa M.Z.A., Lima G.A., Batata M.E.F. 2010b. Mapeamento Geológico e Levantamento de Recursos Minerais da Folha Santa Bárbara (SD.21-Y-C-V). Convênio CPRM-UFMT. Programa Geologia do Brasil, Relatório Etapa de Mobilização, 35p.
- Santos J.O.S., McNaughton N.J., Hartmann L.A., Fletcher I.R., Salinas R.M. 2005. The age of deposition of the Aguapeí Group, Western Amazon Craton, based on U–Pb study of diagenetic xenotime and detrital zircon. *In: Latin American Geological Congress*. Quito, *Short Papers*, p. 1-4.
- Século D.B., Ruiz A.S., Sousa M.Z.A., Lima G.A. 2011. Geologia, Petrografia e Geoquímica do Enxame de Diques Máficos da região de Vila Bela da Santíssima Trindade (MT) Suíte Intrusiva Huanchaca SW do Cráton Amazônico. *Geociências*, **30**:561-573.
- Self S., Keszthelyi L., Thordason T. 1998. The importance of pahoehoe. *Annual Review Earth Planetary Science*, **26**:81-110.
- Sousa M.Z.A., Batata M.E.F., Ruiz A.S., Lima G.A., Matos J.B., Paz J.D.S., Costa A.C.D., Silva C.H., Corrêa da Costa P.C. 2011. *Geologia da Folha Rio Branco (SD21-Y-D-I)*. Ministério das Minas e Energia. Programa Nacional de Geologia (PRONAGEO). CPRM/UFMT. 178 p.
- Souza E.P. & Hildred P.R. 1980. Contribuição ao estudo da geologia do Grupo Aguapeí, Oeste de Mato Grosso. *In: Congresso Brasileiro de Geologia*. Camboriú, *Short Papers*, p. 813-825.
- Takahashi E. & Kushiro I. 1983. Melting of dry peridotite at high pressures and basalt magma genesis. *American Mineralogist*, **68**:859-879.

Teixeira W., Geraldes M.C., D'Agrella-Filho M.S., Santos J.O.S., Sant'Ana Barros M.A., Ruiz A.S., Corrêa da Costa P.C. 2011. Mesoproterozoic juvenile mafic-ultramafic magmatism in the SW Amazonian Craton (Rio Negro-Juruena province): SHRIMP U–Pb geochronology and Nd–Sr constraints of the Figueira Branca Suite. *Journal of South American Earth Sciences*, **32**:309-323.

Teixeira W., Ernst R., Hamilton M.A., Lima G., Ruiz A.S., Geraldes M.C. 2015a. Widespread ca. 1.4 Ga intraplate magmatism and tectonics in a growing Amazonia. *GFF (Uppsala)*, **1**:1-14.

Teixeira W., Hamilton M.A., Lima G.A., Ruiz A.S., Matos R., Erns, R.E. 2015b. Precise ID-TIMS U-Pb baddeleyite ages (1110-1112Ma) for the Rincón del Tigre-Huanchaca large igneous province (LIP) of the Amazonian Craton: Implications for the Rodinia supercontinent. *Precambrian Research*, **265**:273-285.

Winchester J.A. & Floyd P.A. 1977. Geochemical discrimination of different magma series and their differentiation products using immobile elements. *Chemical Geology*, **20**:325-343.

3.3 FISSURAL MAFIC MAGMATISM ON SOUTHWESTERN AMAZONIAN CRATON: PETROGENESIS AND ^{40}Ar - ^{39}Ar GEOCHRONOLOGY

Gabrielle Aparecida de Lima

Moacir José Buenano Macambira

Maria Zélia Aguiar de Sousa

Amarildo Salina Ruiz

Manoel Souza D'Agrella-Filho

Submetido: *Journal of South American Earth Sciences*

Ref: SAMES_2016_3

Title: Fissural mafic magmatism on southwestern Amazonian Craton: petrogenesis and ^{40}Ar - ^{39}Ar geochronology

Journal: *Journal of South American Earth Sciences*

Dear Prof. Aparecida Lima,

Thank you for submitting your manuscript for consideration for publication in *Journal of South American Earth Sciences*. Your submission was received in good order.

To track the status of your manuscript, please log into EVISE® at: http://www.evise.com/evise/faces/pages/navigation/NavController.jspx?JRNL_ACR=SAMES and locate your submission under the header 'My Submissions with Journal' on your 'My Author Tasks' view.

Thank you for submitting your work to this journal.

Kind regards,

Journal of South American Earth Sciences

Have questions or need assistance?

For further assistance, please visit our Customer Support site. Here you can search for solutions on a range of topics, find answers to frequently asked questions, and learn more about EVISE® via interactive tutorials. You can also talk 24/5 to our customer support team by phone and 24/7 by live chat and email.

Copyright © 2016 Elsevier B.V. | Privacy Policy

Elsevier B.V., Radarweg 29, 1043 NX Amsterdam, The Netherlands, Reg. No. 33156677.

Fissural mafic magmatism on southwestern Amazonian Craton: petrogenesis and ^{40}Ar - ^{39}Ar geochronology

Gabrielle Aparecida de Lima ^{a, d, e, g, *}, Moacir José Buenano Macambira ^{b, f}, Maria Zélia Aguiar de Sousa ^{c, f, g}, Amarildo Salina Ruiz ^{c, f, g}; Manoel Souza D'Agrella-Filho ^e

^a *Postgraduate Program in Geology and Geochemistry, IG/UFPA*

^b *Laboratory of Isotope Geology – Pará-Iso, IG/UFPA*

^c *Geosciences Faculty, FAGEO/UFMT*

^d *Engineering Institute, IEng/UFMT*

^e *Institute of Astronomy, Geophysics and Atmospheric Sciences, IAG/USP*

^f *National Institute of Science and Technology for Geosciences of the Amazon (GEOCIAM)*

^g *Research Group of Crustal Evolution and Tectonics – Guaporé*

* Corresponding author: gabilimigel@gmail.com

ABSTRACT

Expressive occurrences of sills and mafic dyke swarms as a result of tectonogenetic processes that led to break-up or attempted break-up of continental crust are found on the south and southwestern Amazonian Craton. This work focuses on the magmatic-tectonic processes that formed the Salto do Céu, Huanchaca, and Rancho de Prata suites. The Salto do Céu Suite, with a U-Pb (TIMS) baddeleyite age of 1439 ± 4 Ma, occurs as sills and lava flows emplacing and, in places, overlaying the Vale da Promissão Formation (Aguapeí Group). Plagioclase and amphibole Ar-Ar geochronological data provided a plateau age of 1021 ± 5 Ma, and an integrated age of 1385 ± 9 Ma, respectively. The Rancho de Prata Suite consists of mafic dyke swarms intruded into the basement rocks of the Jauru Terrane, with a U-Pb (TIMS) baddeleyite age of 1387 ± 17 Ma. Plagioclase Ar-Ar data yielded a plateau age of 967 ± 5 Ma, while amphibole Ar-Ar data provided an integrated age of 1495 ± 8 Ma. Sills and mafic dykes of the Huanchaca Intrusive Suite are sited in the portion of the Paraguá Terrane which is not affected by the Sunsás Orogeny (1.1 to 0.9 Ga). Dykes occur emplaced into the basement rocks underlying the Aguapeí Group, whereas sills are intruded into pelites and sandstones of the Vale da Promissão Formation (Aguapeí Group). Ar-Ar ages obtained for the sills provided both a plateau age of 1041 ± 6 Ma (plagioclase) and an integrated age of 1113 ± 11 Ma (amphibole). A U-Pb (TIMS) baddeleyite age of 1111.5 ± 1.9 Ma was obtained for the sills as

well. The units studied here are composed of gabbros, diabases, and basalts. Regardless their distinct crystallization ages, all of them are tholeiitic with high iron enrichment which indicates accentuated mantle melting in distensive tectonic regimes. Their chemical characteristics mainly suggest affinity to intraplate basalts. Significant variations in the patterns of rare earth elements (REE) are observed among these suites, yet all of them show enrichment of light REE relative to the heavy. The main difference among ratios (Zr versus incompatible element) obtained for each unit combined with interpretations from variation and classification diagrams, as well as geochronological data available, allow us to suggest that these rocks derived from a heterogeneous mantle source. The integration of results from this research allowed us to recognize two distinct magmatic events on the south-southwestern Amazonian Craton: an older one with age between 1387 e 1439 Ma, and a younger one around 1110 Ma old. The former event, which gave rise to the Salto do Céu and Rancho de Prata suites, would be associated with post-orogenic stages of the Santa Helena Magmatic Arc in the Jauru Terrane, while the younger event, which is represented by the Huanchaca and Rio Perdido suites, and Rincón del Tigre Complex, forms a Stenian Large Igneous Province (LIP) evolved during an attempted break-up of continental crust that resulted in the set-up of the Aguapeí Aulacogen.

Keywords: Mafic magmatism; Distensive tectonics; Stenian LIP; Ar-Ar Geochronology; Petrology

1. Introduction

Sills and mafic dyke swarms, present in all continents, have been formed since the Archean in extensional tectonic settings (Halls, 1982). Magmatic events derived from extension and continental crust break-up are often associated with the formation of Large Igneous Provinces (LIPs) and deep-mantle source magmatism (Morgan, 1971, 1972; Anderson, 2005; Ernst et al., 2013; Ernst, 2014; Santosh et al., 2009; Nance et al., 2014).

Sills and mafic dyke swarms were partially recognized on southwestern Amazonian Craton in the 80s (Santos et al., 1979; Barros et al., 1982; Leite et al. 1985; Litherland et al. 1986). Petrogenetic, geochronological (U-Pb ID-TIMS baddeleyite) and paleomagnetic studies have contributed to temporally delimit these mafic intrusions, and geodynamic processes involved in their formation (Araújo et al., 2005; Corrêa da Costa al., 2009; Ruiz et

al., 2010a; Século et al., 2011; Lima et al., 2012; Teixeira et al., 2015a, 2015b, 2016; D'Agrella-Filho et al., 2016).

Ruiz et al. (2010a), with basis on K-Ar data available, grouped all the occurrences of sills and mafic dykes sited in the southwestern Amazonian Craton into a LIP related to the break-up of Rodinia. Girardi et al. (2012) assign these mafic dyke swarms in Nova Lacerda (Rancho de Prata Intrusive Suite) to the Santa Helena magmatic arc, with age close to 1380 Ma (Corrêa da Costa et al., 2009), supported by Nd and Sr isotope data. Teixeira et al. (2015a, 2015b), based on U-Pb baddeleyite ID-TIMS ages attribute an interval from 1110 and 1112 Ma for the emplacement of the Huanchaca and Rincón del Tigre sills, and an emplacement age of 1387 Ma for the dyke swarms of Rancho de Prata suite.

This work aims to review and compare the sills and mafic dyke swarms, intruded into the Salto do Céu, Huanchaca and Rancho de Prata suites with basis on new field, petrographic and lithochemical data, as well as to provide new Ar-Ar geochronological data in order to improve our knowledge on the tectonic and magmatic evolution of mafic igneous events that affected the southwest of the Amazonian Craton.

2. Regional Geological Settings

Geological, lithochemical and geochronological data collected along the last three decades for the southwestern Amazonian Craton point out to repeated extensional magmatic events that are associated with break-up or attempted break-up of supercontinents. The following is a geological review of units approached in this work.

2.1. Salto do Céu Suite

The rocks that occur in the region of Salto do Céu and Rio Branco, southwestern Amazonian Craton, were initially reported by Oliva (1979). Later, Barros *et al.* (1982) described gabbros and diabases that outcrop in those regions as part of the Rio Branco Group, whereas Leite *et al.* (1985) interpreted these occurrences as exposures of a meso-melanocratic portion of the Rio Branco Intrusive Suite describing them as a differentiated and bimodal igneous complex that may be an indicative of an anorogenic magmatism likely formed in rift settings.

According to Geraldés (2000), and Geraldés *et al.* (2001, 2004), the base of the Rio Branco Intrusive Suite is composed of basic rocks that comprises a volcano-plutonic association mostly composed of acid and intermediate rocks at the top. These authors provide

U-Pb age of 1471 ± 8 Ma for the basic rocks, and an age of 1427 ± 10 Ma for the acid rocks. These are attributed to an extensional intracratonic magmatism as a reflection of Santa Helena magmatic arc (1.47–1.42 Ga).

Araújo *et al.* (2005) first individualized the set of intrusions parallel to the layering of rocks of Vale da Promissão Formation that consist of mafic sills ranging from 1 to 5 m thick called Salto do Céu Intrusive Suite. Araújo *et al.* (2007) describe two plutonic series for the Rio Branco Batholith, one of basic composition and discontinuous distribution in the borders of these intrusions, and another one of acid/intermediate composition that shows three petrographic facies. They conclude that these exposures of gabbroic rocks represent two distinct magmatic events: the plutonic basic rocks (gabbros and diorites) that are grouped into the Rio Branco Intrusive Suite, and the hypoabissal rocks (diabases, microgabbros) that are grouped into the Salto do Céu Intrusive Suite.

According to Araújo (2008), the bimodal magmatism of the Rio Branco Batholith is well represented by two magma types, one of basic nature derived from a mantle source, and another one of acid/intermediate nature derived from crustal melting and magmatic differentiation processes. This author defines crystallization ages of 1403 ± 0.6 Ma and 1382 ± 49 Ma for the intermediate to acid rocks that gave rise to the Rio Branco Acid Intrusive Suite.

Araújo *et al.* (2009), and Araújo and Godoy (2011) argue that the Rio Branco Batholith comprises two main plutonic suites: the Rio Branco Basic Intrusive Suite, which is composed of basic/intermediate rocks, and the Rio Branco Acid Intrusive Suite which is composed of intermediate/acid rocks. These authors also attribute the gabbroic association to two temporally independent magmatic events: basic/intermediate plutonic rocks are represented by microgabbros to diabases, monzogabbros, and quartz monzonites to quartz diorites grouped under the name of Salto do Céu Basic Intrusive Suite that intrudes the sedimentary Aguapeí Group parallel to their rock layering.

Sousa *et al.* (2011) based on detailed field work restricted the name Rio Branco Intrusive Suite only to the acid to intermediate rocks, while the gabbroic rocks were assigned to the Salto do Céu Intrusive Suite.

Geraldes *et al.* (2014) provided U-Pb ages (*laser ablation*) on detrital zircons for the Aguapeí Group in the three hills: Rio Branco, Ricardo Franco and Santa Bárbara. The results obtained for the Rio Branco Hill yielded an age interval between 1.9 and 1.5 Ga from which four zircon age populations are identified: 1544 Ma, 1655 Ma, 1812 Ma, and 2515 Ma.

Teixeira *et al.* (2015a) show a U-Pb baddeleyite age of 1439 ± 4 Ma for sills of Salto do Céu suite which they interpret as a magmatic event associated with the evolution of the Supercontinent Columbia.

Lima *et al.* (submitted), based on field relationships and new geochronological data, recognize not only sills for this unit, but also mafic flows which characterizes it as a bimodal suite where the acid portion is the Rio Branco Intrusive Suite. According to these authors, this unit was formed in intraplate settings, distensional tectonic regime with anorogenic magmatism, which likely reflects a tectonic milestone with respect to the evolution of the Supercontinent Columbia/Nuna.

2.2. Rancho de Prata Intrusive Suite

The mafic dykes in Nova Lacerda (MT) were first described by Ruiz *et al.* (2005) and Ruiz (2005), then named as Rancho de Prata Intrusive Suite. This unit is composed of tabular dyke swarms that intrudes into the basement rocks of the Jauru Terrane. They were first observed in the homonymous farm.

Corrêa da Costa *et al.* (2009) identify NNW-trending mafic dyke swarms emplaced into the Nova Lacerda Granite sited in the region of Nova Lacerda, and Conquista D'Oeste. These authors describe three rock types: diabases, metadiabases and amphibolites with Rb-Sr ages of 1380 ± 32 Ma for the diabases, and of 1330 ± 120 Ma for the metadiabases.

Girardi *et al.* (2012) attribute their genesis to fractional crystallization of evolved melts derived from a heterogeneous mantle source. Based on geochemical and isotope data, these authors suggest these dykes were emplaced in continental arc settings.

Ruiz *et al.* (in press) describe a parallel mafic dyke swarms emplaced into gnaissic, granitic and metavolcanosedimentary rocks belonging to the regional basement (Jauru Terrane); therefore, attributing them to the Rancho de Prata Intrusive Suite.

Baddeleyite gave a U-Pb age of 1387 ± 17 Ma for the mafic dyke swarms in Nova Lacerda which is interpreted to be a magmatic event associated with the evolution of the Supercontinent Columbia (Teixeira *et al.*, 2015a).

2.3. Huanchaca Intrusive Suite

Mafic dykes and sills occurring in eastern Huanchaca Hill in the border between Bolivia and Brasil are intruded into rocks of the Sunsás Group and its basement; they were previously called Huanchaca Dolerite Suite by Litherland *et al.* (1986).

Lima (2008, 2011) and Lima *et al.* (2012) describe for the first time the occurrences of sills emplaced into the Aguapeí Group on the northern of Ricardo Franco/Huanchaca Hill in the SW of the Brazilian State of Mato Grosso. Similarly, Sécolo *et al.* (2008, 2012), and Sécolo (2011) performed studies on mafic dyke swarms emplaced into the basement rocks in the region of Vila Bela da Santíssima Trindade – MT.

Both sills and dykes identified in Brazil were correlated with those described by Litherland *et al.* (1986) in Bolivia and grouped under the name of Huanchaca Intrusive Suite (Lima 2008, 2011; Lima *et al.* 2012; Sécolo *et al.* 2008, 2012; Sécolo 2011; Ruiz *et al.* 2010a).

Teixeira *et al.* (2015b) present a U-Pb baddeleyite age of $1,111.5 \pm 1.9$ Ma for sills of this unit, and suggest that these rocks along with rocks of the Rincón del Tigre Igneous Complex characterize a LIP in the Amazonian Craton.

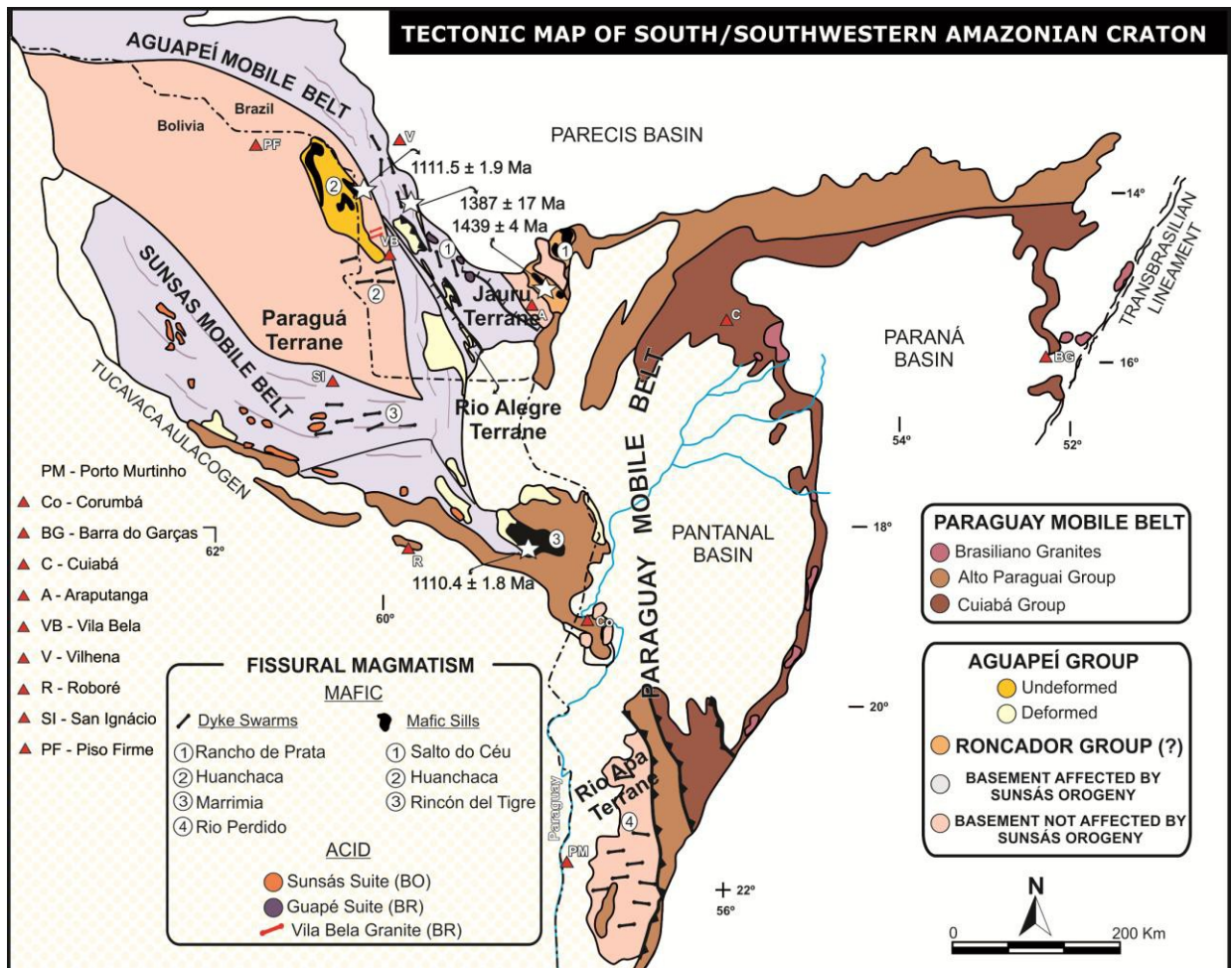


Fig. 1. South/Southwest Tectonic Map of Amazonian Craton highlighting U-Pb (ID-TIMS) baddeleyite ages obtained by Teixeira et al. (2015a, 2015b) for the suites Santo do Céu, Rancho de Prata and Huanchaca, and the Rincón del Tigre Complex. Extracted and modified from Ruiz et al. (2010b).

3. Geology and Petrography of Dykes and Sills

The main field and petrographic characteristics shown below raised accentuated differences between the studied samples that will be subsequently backed by geochemical analysis.

3.1 Salto do Céu Suite

Their basic rocks occur in the surrounding region of Salto do Céu and Rio Branco (MT), and outcrop as sills and lava flows. Sills are found emplaced into pelitic rocks (Fig. 2A) previously attributed to the Vale da Promissão Formation (Aguapeí Group) which generally

dip with a low angle towards the WSW. Lava flows cover the same sedimentary unit showing vertical internal structures as well as flow-top structures typical of thin basaltic flows. Vesicles and amygdalas, as well as flow-folds (Fig. 2B) and breccia are commonly observed.

These rocks are mesocratic to melanocratic, greenish-gray to black in colour, equigranular, very fine- to medium-grained.

Sills are composed of diabases and massif gabbros that under the microscope show ophitic (Fig. 3A), subophitic, intergranular and coronitic textures. They essentially consist of plagioclase (labradorite) and clinopyroxene (augite/titanoaugite/pigeonite) having opaques, acicular apatite, and subhedral brown sphene as accessory minerals. The alteration paragenesis is represented by amphiboles (actinolite-tremolite and hornblende), biotite, epidote/clinozoisite, sericite, calcite, clay minerals, and chlorite. Rare alkali feldspar and quartz are also found as late-forming minerals, generally displaying graphic intergrowth.

Lava flows consist of basalts and diabases with ophitic, subophitic, hyalophitic, and porphyritic textures or amygdaloidal texture in pseudo-trachytic groundmass, and subordinate vitrophyric texture (Fig. 3B). The main components are plagioclase (labradorite and andesine), as well as clinopyroxene (augite-pigeonite) and relict glass, but may have accessory and alteration minerals, such as amphiboles (hornblende and tremolite-actinolite), biotite, chlorite, opaques, rutile, sphalerite, apatite, sericite, epidote/clinozoisite, calcite and clay minerals. Amygdales are round to ellipsoid in shape filled with fibrous to fibro-radiated material composed of zeolites, chlorite, fluorite, and opaques.

3.2. Rancho de Prata Intrusive Suite

The mafic dykes of this suite are observed in many locations around Nova Lacerda and Conquista D'Oeste (MT) along a NNW-trending belt approximately 30 km thick and 150 km long, where both single dykes and dyke swarms occur striking N30°–40°W and dipping steeply. They show no evidence of deformation or metamorphism and are in intrusive contact with gneissic, granitic, and metavolcanosedimentary rocks of the basement (Fig. 2C and D).

The rocks of Rancho de Prata Intrusive Suite are described as gabbros, diabases and basalts, phaneritic, aphanitic to porphyritic, very fine- to medium-grained. They are melanocratic, dark-gray to black in colour, showing massif structure in places with subtle foliation parallel to the dyke walls. Under the microscope, these rocks are holo to hypocrySTALLINE, and have porphyritic, intergranular, subophitic to ophitic textures (Fig. 3C and D) being essentially composed of plagioclase (labradorite), clino (augite/pigeonite) and

orthopyroxene (hypersthene, bronzite), olivine and amphiboles (hornblende and actinolite-tremolite). Accessory minerals are opaques, sphene, and apatite; alteration minerals are represented by biotite, chlorite, talc, iddingsite, serpentine, sericite, epidote, calcite, clay minerals and very seldom quartz. Basalts show sporadic dark-brown intergranular glass.

3.3. Huanchaca Intrusive Suite

Sills and mafic dykes of the Huanchaca Intrusive Suite are included in the non-affected portion of Paraguá Terrane caused by the Sunsás Orogeny (1.1 to 0.9 Ga). Dykes are emplaced into the basement rocks overlaid by the Aguapeí Group which consist of the Mesoproterozoic Guaporeí Granites and Pensamiento Granitoid Complex, as well as the Paleoproterozoic Shangri-lá and Turvo orthogneisses belonging to the Chiquitania Metamorphic Complex; while sills are hosted by pelites and sandstones of the Vale da Promissão Fomation, Aguapeí Group.

Sills outcrop as blocks, and low-lying outcrops usually in abrupt contact and parallel to rock layering (Fig. 2E). Dykes occur as single, rounded to angular blocks (Fig. 2F) in the granitic-gnaissic terrane, or as small and discontinuous crests whose main orientation varies between N70°-90°E with steep dips towards NW or SE.

The sills, which consist of gabbros and diabases, are greenish-gray to black in colour, fine- to medium-grained. Optically, they are holocrystalline showing subophitic to ophitic texture, and rarely intergranular texture. Cumulate rocks are of restricted occurrence and have similar paragenesis and textures to that of sills differing only by the presence of olivine, and high content of mafic minerals.

Sills are essentially composed of plagioclase (andesine), pyroxene (augite/pigeonite, and hypersthene), amphiboles (hornblende and actinolite), opaques, and some of them contain alkali feldspar and quartz with graphic intergrowth. Their post-magmatic, and accessory assemblage is composed of biotite, chlorite, talc, sphene, apatite, clay minerals, epidote/clinozoisite, sericite, calcite, and serpentine. Olivine is only only in a few samples, which are cumulates, making up to 40% of the rock volume.

Dykes are dark-gray to greenish-gray with grain size decreasing from the rock wall towards the center of the body from very fine-grained or glassy to medium-grained. The dykes are classified into diabases and basalts, respectively holo- and hypocrySTALLINE, composed mostly of plagioclase (andesine and labradorite), pyroxenes (augite/pigeonite, hypersthene and bronzite), and olivine. Their accessory paragenesis consist of amphiboles

(hornblende and actinolite-tremolite), sphene, opaques, apatite, and in places diabases display very fine-grained intergrowth of alkali feldspar and quartz as a result of devitrification. Alteration minerals derived from plagioclase are sericite, epidote/clinozoisite, calcite and/or clay minerals, while the alteration of mafic minerals results in amphiboles, biotite, chlorite, serpentine, talc, iddingsite/boulingite and opaques.

Optically, diabases are fine- to medium-grained showing inequigranular, sub-ophitic textures, and subordinate ophitic texture, while basalts display mostly porphyritic, glomeroporphyritic, vitrophyric, and rarely intersertal and hyalophitic textures. Partially to totally pseudomorphized microphenocrysts of pyroxene and olivine occur embayed and/or corroded in a very fine-grained to glassy groundmass, in places trachytic groundmass, usually showing fibro-radiated habit caused by intercalation of laths of pyroxene and plagioclase. Dark-brown to black glassy material is commonly found in basalt samples in places making up only a small percentage of the total rock volume, but in places making up to 60% of the rock volume in other samples.

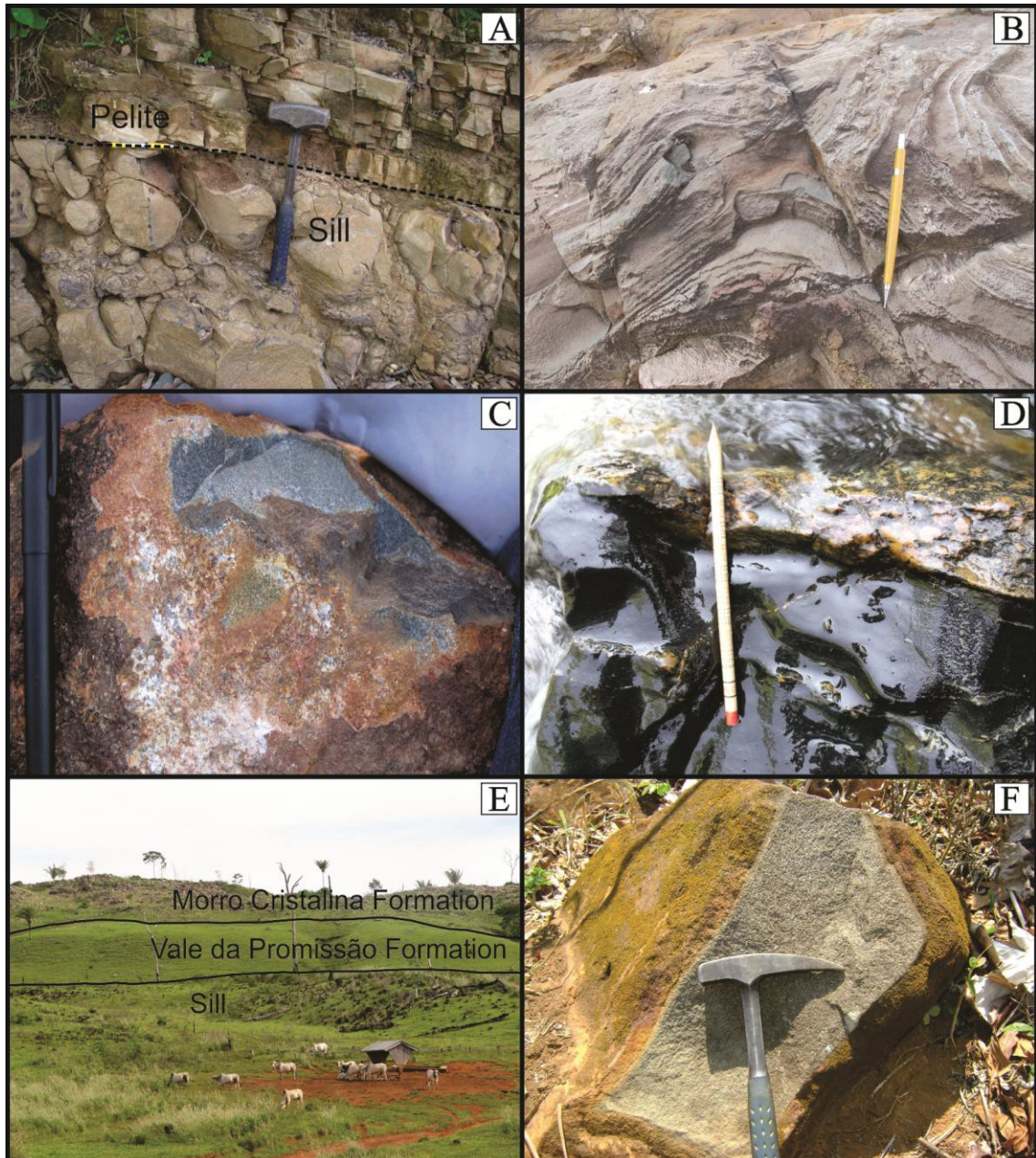


Fig. 2. Field aspects. A – Concordant contact between sill of the Salto do Céu Suite and pelitic rocks of the Vale da Promissão Formation. B – Magmatic flow-folds in lava flows of the Salto do Céu Suite. C – Massif structure in sample of the Rancho de Prata Intrusive Suite. D – Contact between dyke of the Rancho de Prata Intrusive Suite and granitic rocks. E – Contact between sill of the Huanchaca Intrusive Suite, and pelites of the Vale da Promissão Formation. F – Angular block of dyke of the Huanchaca Intrusive Suite emplaced into rocks of the Guaporeí Granite.

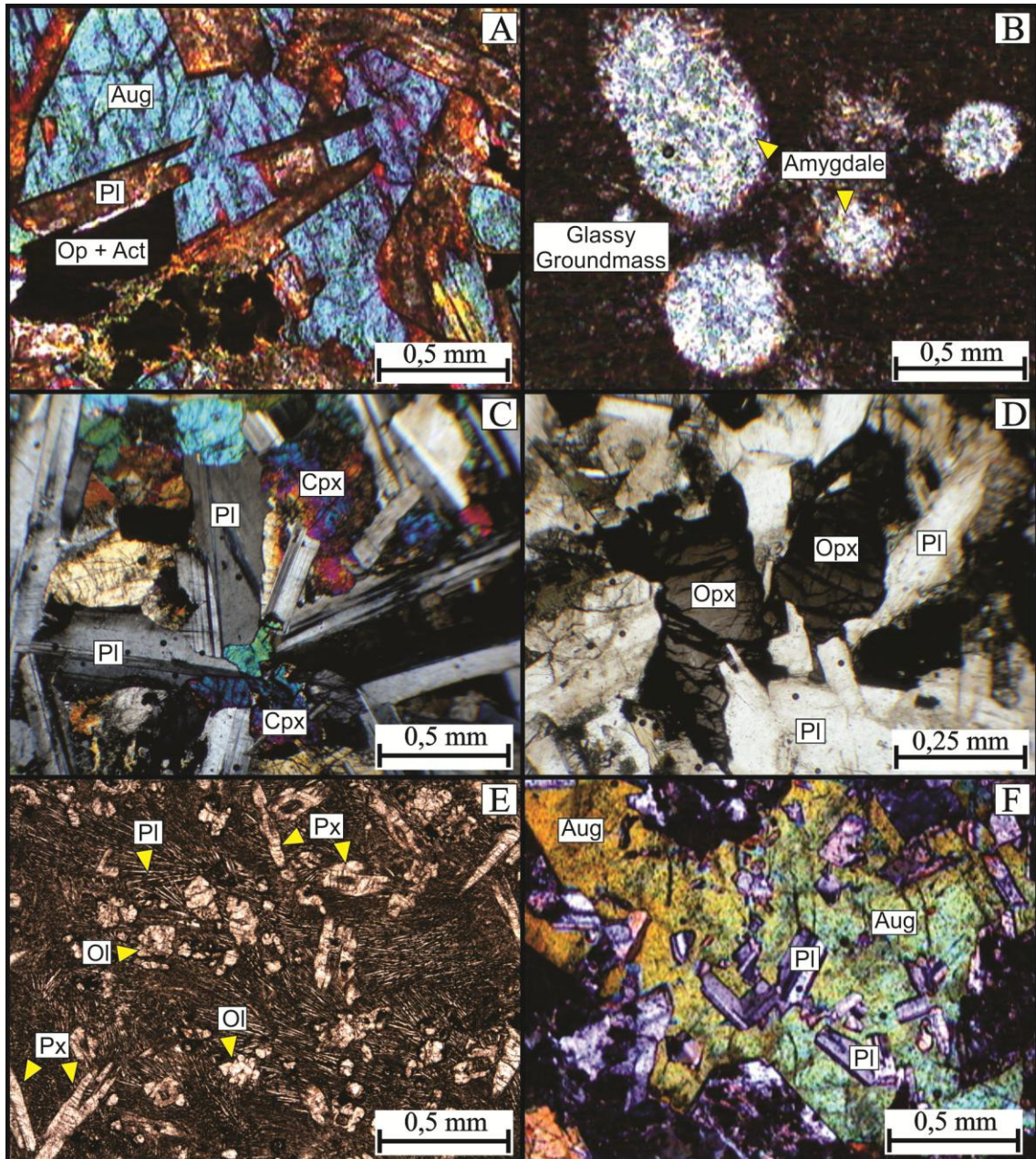


Fig. 3. Photomicrography of samples of the Salto do Ceú (A and B), Rancho de Prata (C and D), and Huanchaca suites (E and F) illustrating: A – Sill: ophitic texture formed by titanite with lath-shaped plagioclase intensely altered, pseudomorphized by opaque minerals and actinolite. B – Lava flow: rounded and ellipsoidal amygdales in glassy groundmass. C – Intergranular texture formed by tabular plagioclase and interstitial pyroxene. D – Subophitic texture highlighting orthopyroxene crystals. E – Dyke: microphenocrysts of pyroxene showing coronitic texture, relict olivine, and swallow-tail plagioclase. F – Sill: ophitic texture formed by augite crystal enclosing tiny euhedral to subhedral laths of plagioclase. Parallel polarizers in (D) and (E), and crossed polarizers in (A), (B), (C) e (F).

4. Lithochemistry

A set of 54 samples of mafic rocks from SW Amazonian Craton was used for geochemical characterisation. Among them, 14 samples are from the Salto do Céu Suite (sills and lava flows), 30 from the Huanchaca Intrusive Suite (sills and dykes), and 10 from the Rancho de Prata Intrusive Suite (dykes). Analytical data was compiled from Lima *et al.* (submitted) for the Salto do Céu Suite, and from Lima *et al.* (2012) and Sécolo *et al.* (2011) for the Huanchaca Intrusive Suite. Unpublished data for rocks of the Rancho de Prata Intrusive Suite was also compiled.

Samples were analysed at the Acme Analytical Laboratories, Vancouver (Canadá) by the ICP-ES technique (Inductively Coupled Plasma Emission Spectrometry) for measuring major elements, and by the ICP-MS technique (Inductively Coupled Plasma Mass Spectrometry) for trace-elements, including rare earth elements. Analytical data are shown in tables 1, 2, and 3.

In order to evaluate the effects of hydrothermal alteration and/or metamorphism, which could mobilize chemical elements of rocks from the studied units, molecular proportion ratio (MPR) diagrams developed by Pearce (1968) and adapted by Beswick & Soucie (1978) and Beswick (1982) were used. Linear correlation trends show rare dispersions in diagrams (Fig. 4), and the fact that these lines do not intersect the origin of diagrams reveals the immobility of such oxides indicating that these data reflect the original igneous composition of the samples.

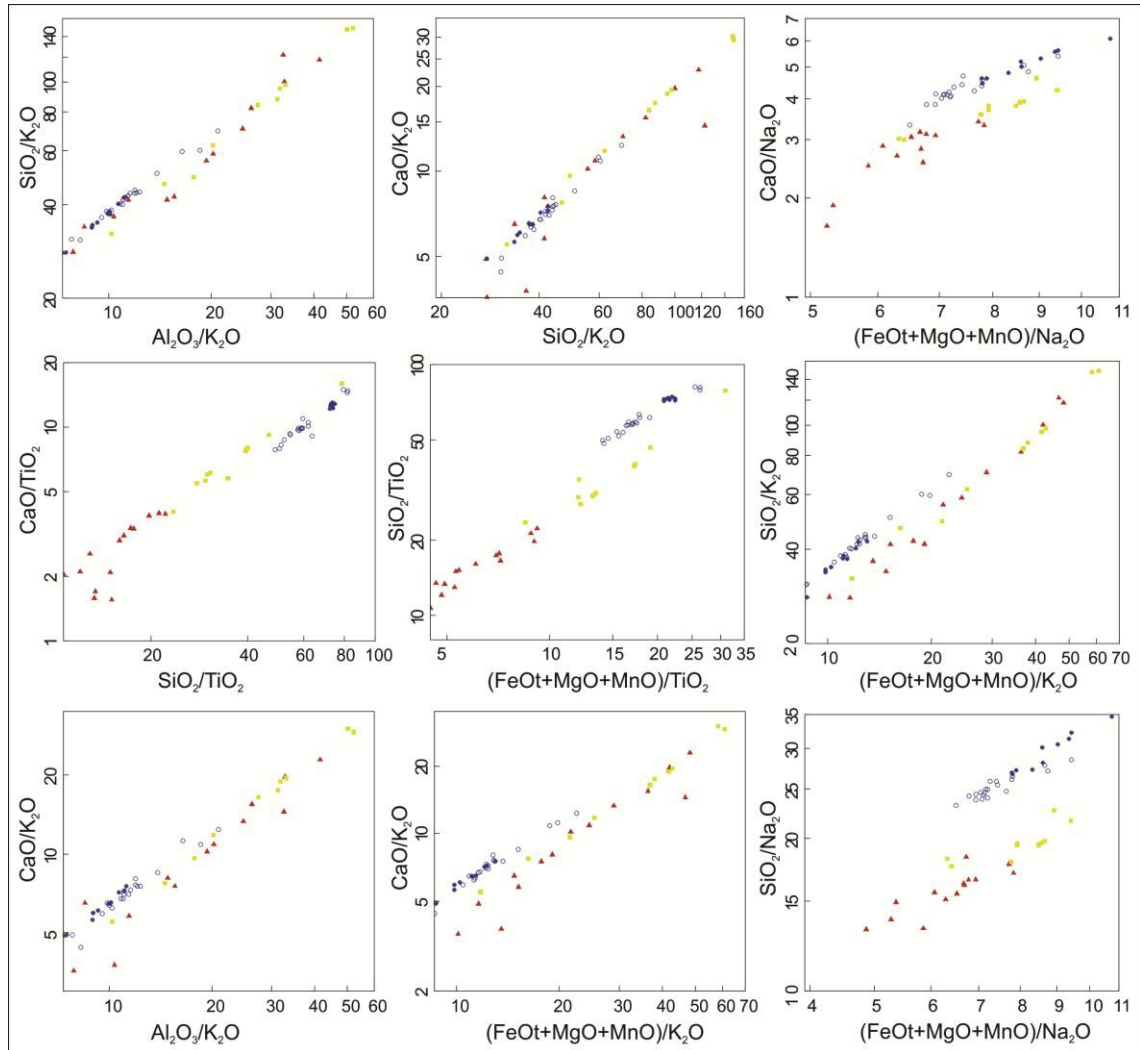


Fig. 4. Molecular proportion ratio diagrams for the studied units (logarithmic scale). ▲ Salto do Céu Suite, ■ Rancho de Prata Intrusive Suite, ● Huanchaca Intrusive Suite (dykes), ○ Huanchaca Intrusive Suite (sills).

As for the TiO_2 content, according to the classification used for basalts of Serra Geral Formation (Paraná Magmatic Province; Bellieni *et al.*, 1983, 1984; among others), in general, the Rancho de Prata and Huanchaca suites are classified as low titanium rocks (LTi; $\text{TiO}_2 \leq 2\%$) meanwhile the Salto do Céu Suite is classified as high titanium rocks (HTi; $\text{TiO}_2 > 2\%$).

The confection of major and trace-element variation diagrams (Fig. 5 and Fig. 6) required a differentiation index which in this case was the magnesium number - $\text{mg}\# = [\text{Mg}^{+2}/(\text{Mg}^{+2} + \text{Fe}^{+2})]$ in weight percent values. This index values ($\text{mg}\#$) vary between 0.30 and 0.51; 0.44 and 0.55; 0.43 and 0.65, respectively, for the Salto do Céu Suite, Rancho de Prata Suite and Huanchaca Suite therefore indicating that these units formed from evolved basaltic magma. Jaques & Green (1979, 1980), and Takahashi & Kushiro (1983) show that

primitive basaltic magma derived from mantle peridotite have mg# values varying between 0.74 and 0.80.

Binary diagrams in Fig. 5 for the units above show well-defined trends for most oxides, except for K_2O that shows obvious data dispersion. CaO and Al_2O_3 show a positive correlation while SiO_2 , TiO_2 , Fe_2O_3 , Na_2O , K_2O , P_2O_5 and MnO exhibits negative correlation with decrease of mg#. The correlations observed, mainly those related to CaO and Al_2O_3 , may be assigned to fractional crystallization of pyroxene and plagioclase during rock evolution. The negative correlation between P_2O_5 and mg# may be explained through concentration of apatite in the initial stages of magmatic differentiation.

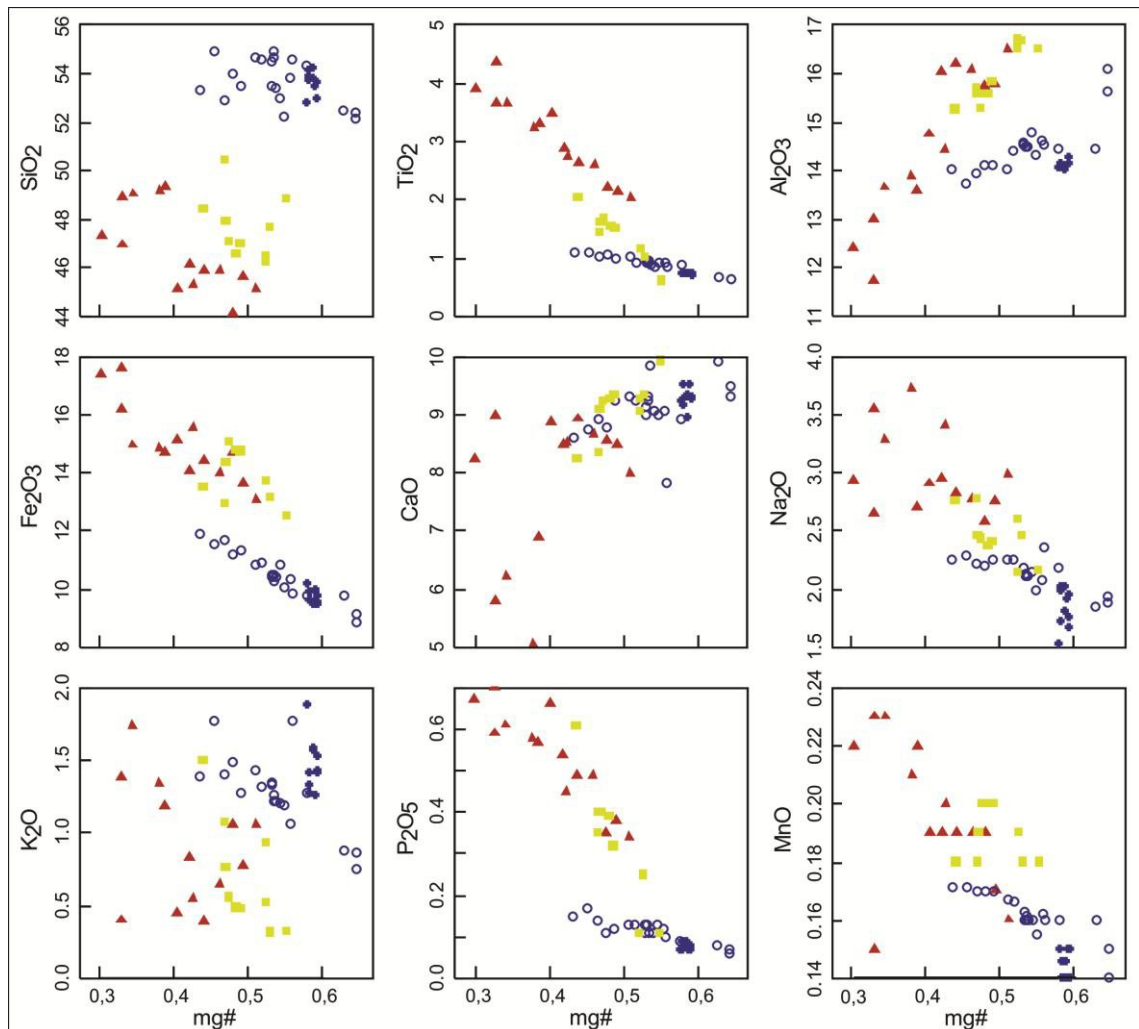


Fig. 5. Variation diagrams mg# versus major elements (% weight) for rocks of the Salto do Ceu, Rancho de Prata, and Huanchaca suites. \blacktriangle Salto do Céu Suite, \blacksquare Rancho de Prata Intrusive Suite, \bullet Huanchaca Intrusive Suite (dykes), \circ Huanchaca Intrusive Suite (sills).

As for trace elements (Ba, Rb, Zr, La, Ce, Y, Nb, Zn, and Nd; Fig. 6), all of them exhibits clear trends in which their contents decrease with magmatic evolution except for dispersion of Rb that likely reflects mobilization of this element. The relationships shown in Fig. 5 and Fig. 6 for major and trace elements are typical of gabbro differentiation/fractionation.

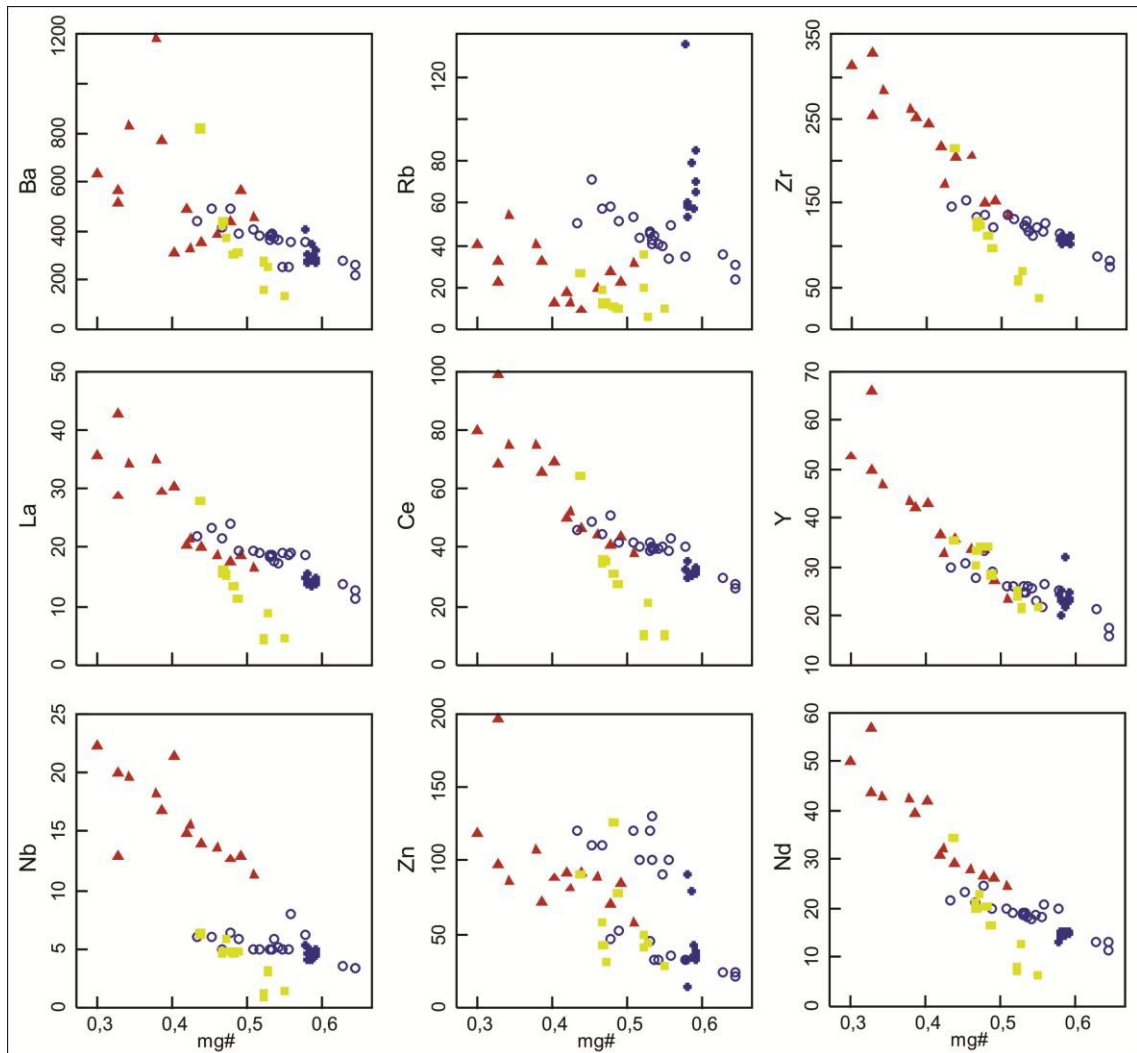


Fig. 6. Variation diagrams mg# versus trace elements (ppm) for rocks of Salto do Céu, Rancho de Prata and Huanchaca suites. ▲ Salto do Céu Suite, ■ Rancho de Prata Intrusive Suite, ● Huanchaca Intrusive Suite (dykes), ○ Huanchaca Intrusive Suite (sills).

Rock classification for the Salto do Céu, Rancho de Prata and Huanchaca suites was based on the TAS diagram (total alkali-silica - $\text{Na}_2\text{O} + \text{K}_2\text{O}$ versus SiO_2 ; Fig. 7A) as proposed by Cox *et al.* (1979) in which elements are recalculated on an anhydrous basis total 100%. The rocks of the two first suites are characterized as basic, and plot mostly in the field of

basalts, while rocks of the Huanchaca Intrusive Suite are classified as andesite basalts, therefore they have greater silica contents and plot in the field of intermediate rocks. In the Zr/TiO_2 versus Nb/Y diagram (Winchester & Floyd, 1977; Fig. 7B), rocks of the Salto do Céu Suite plot as sub-alkaline basalts; on the other hand, rocks of the Rancho de Prata Suite plot as andesites/basalts and, finally, rocks of the Huanchaca Suite plot as andesites/basalts, and andesites.

In the AFM diagram ($Na_2O+K_2O-FeO-MgO$; Irvine & Baragar, 1971; Fig. 7C), samples show iron enrichment and have a similar trend to that of Hawaiian tholeiitic suites. In the Jensen cationic diagram (1976; Fig. 7D), rocks of the Salto do Céu Suite plot in the field of high-Fe tholeiitic basalts, while rocks of the Rancho de Prata and Huanchaca suites plot between the fields of high-Fe and high-Mg tholeiitic basalts.

Diagrams proposed by Meschede (1986; Fig. 7E) and Pearce & Norry (1979; Fig. 7F) were used in order to unveil the tectonic environment where these units formed. In general, rocks from Salto do Céu and Huanchaca suites plot in the field of intraplate basalts in both diagrams, while rocks of the Rancho de Prata Intrusive Suite plot in the field of island arc basalts as illustrated in Fig. 7E, as well as they plot between the fields of mid-ocean ridge basalts, and continental intraplate basalts (Fig. 7F).

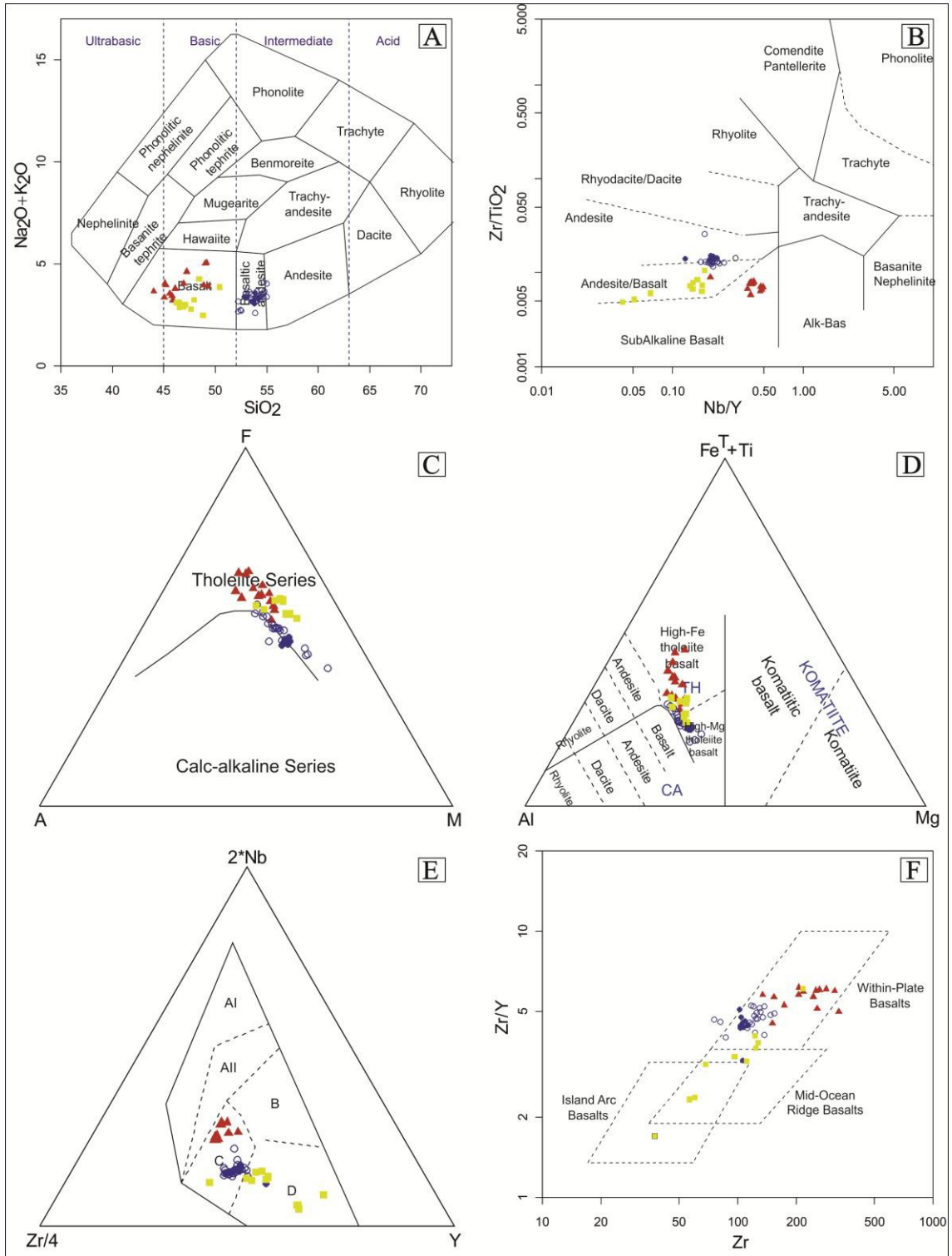


Fig. 7. Classification diagrams for rocks of the Salto do Céu, Rancho de Prata and Huanchaca suites: A – Cox et al. (1979). B – Winchester & Floyd (1977). C – Irvine & Baragar (1971). D – Jensen (1976). E – Meschede (1986). F – Pearce & Norry (1979). \blacktriangle Salto do Céu Suite, \blacksquare Rancho de Prata Intrusive Suite, \bullet Huanchaca Intrusive Suite (dykes), \circ Huanchaca Intrusive Suite (sills).

Rare Earth Elements diagrams (ETR) normalized to CI Chondrite values (McDonough & Sun, 1995; Fig. 8) show accentuated differences amongst patterns observed, although all of them show enrichment of light ETR relative to the heavy. The Salto do Céu and Huanchaca suites show similar patterns for their samples, while the Rancho de Prata Intrusive suite show wide dispersion for its samples. This is clearly observed in figure 8 through ratios variation in $(La/Yb)_N$ from 4.01 to 5.83; 1.17 to 6.00; 3.87 to 5.06; respectively, for the Salto do Céu, Rancho de Prata, and Huanchaca suites. Sample of the Salto do Céu suite may be divided into two groups, one richer in ETR with La_N values higher than 100, and another group with La_N values lower than 100. The former have Eu negative anomaly, which is also observed in the Huanchaca Intrusive Suite, suggesting though that plagioclase fractionation may be an important variable during magmatic evolution. A comparison to OIB, E-MORB and N-MORB patterns (Sun & McDonough, 1989) allow us to observe that patterns of the Salto do Céu and Huanchaca suites best resemble OIB patterns; on the other hand, the Rancho de Prata Intrusive Suite sits between OIB and E-MORB patterns.

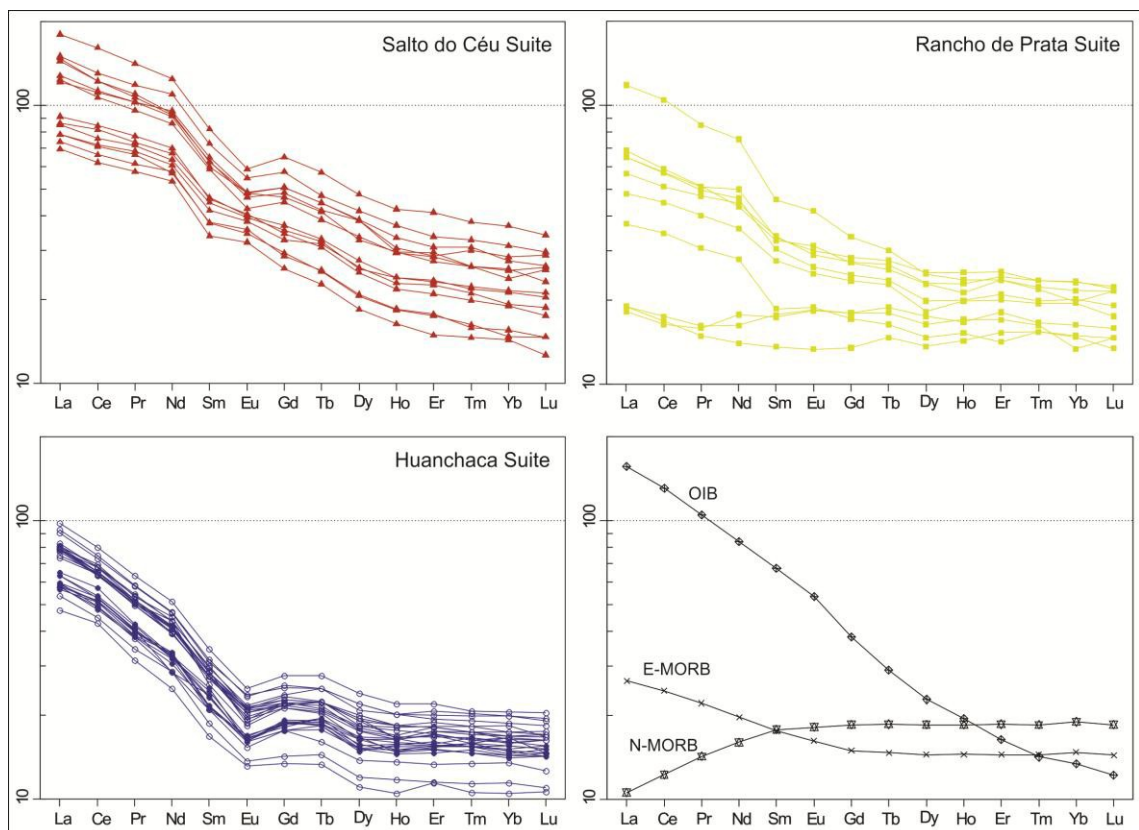


Fig. 8. Rare Earth Elements (REE) diagrams normalized to CI Chondrite values from McDonough & Sun (1995) for Salto do Céu, Rancho de Prata and Huanchaca suites \blacktriangle Salto do Céu Suite, \blacksquare Rancho de Prata Intrusive Suite, \bullet Huanchaca Intrusive Suite (dykes), \circ Huanchaca Intrusive Suite (sills).

In primitive mantle normalized (Sun & McDonough, 1989) multi-element diagrams (Fig. 9) are observed Nb negative anomalies common to all units with better representativeness in the Rancho de Prata and Huanchaca suites. That is typical of continental basalts or related to crustal assimilation processes. Sr positive anomalies observed in the Rancho de Prata intrusive Suite, as well as in samples of the Salto do Céu Suite, which are enriched in REE, are likely related to plagioclase fractionation. In turn, the less enriched group of Salto do Céu Suite, and Huanchaca Intrusive Suite show negative Sr anomalies. The Salto do Céu suite exhibits positive Ti anomaly as opposed to the Huanchaca Intrusive Suite that shows negative Ti anomaly.

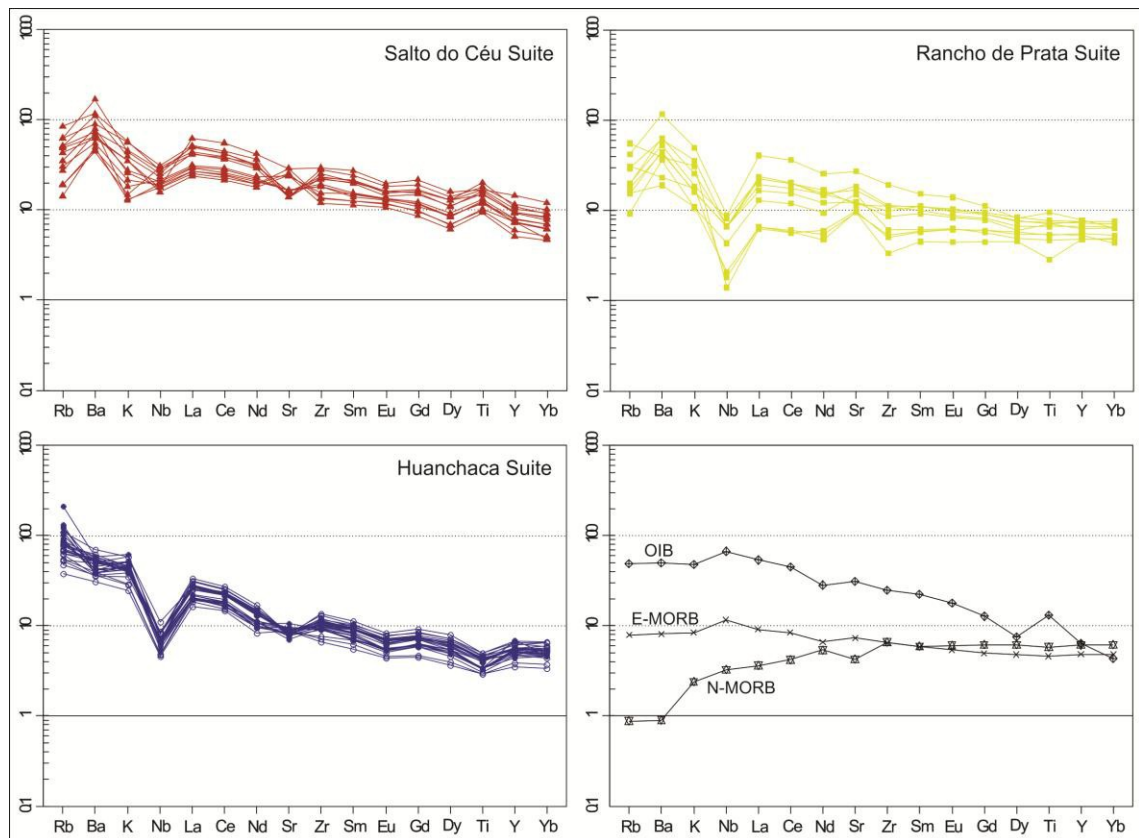


Fig. 9. Primitive mantle normalized (Sun e McDonough, 1989) multi-element diagrams for the Salto do Céu, Rancho de Prata and Huanchaca suites. OIB, E- and N-MORB patterns (Sun e McDonough, 1989) are presented for comparison issues. ▲ Salto do Céu Suite, ■ Rancho de Prata Intrusive Suite, ● Huanchaca Intrusive Suite (dykes), ○ Huanchaca Intrusive Suite (sills).

Zr ratios and incompatible elements have been used for investigate source and mantle heterogeneity of basaltic rocks owing to their low mobility during magmatic processes. The studied rocks show Zr/Y ratios varying between 4.50 and 6.14; 1.70 and 6.07; 3.28 and 5.72; Zr/Nb – 11.20 and 25.50; 20 and 56.2; 15.6 and 26.6; Zr/Ti – 0.010 and 0.015; 0.008 and

0.017; 0.020 and 0.026, respectively, for the Salto do Céu, Rancho de Prata and Huanchaca suites.

The main difference between ratios obtained for each suite, supported by diagrams in Fig. 5, Fig. 6, Fig. 8 and Fig. 9 as well as available geochronological data, confirm the participation of a heterogeneous mantle source in the formation of these units.

5. ^{40}Ar - ^{39}Ar Geochronology

The samples chosen for ^{40}Ar - ^{39}Ar isotope analysis were grinded until 2 mm, then fully washed in ultrasonic machine followed by a 15-minute washing in distilled water and absolute ethanol, and then air-dried. After that, plagioclase and amphibole with a grain size of 0.5-2 mm were hand-picked using a binocular microscope. Minerals were placed into aluminium irradiation disks along with Fish Canyon Sanidine - age 28.201 ± 0.046 Ma; Kuiper *et al.*, 2008) to monitor neutron flux, following the geometry illustrated in Vasconcelos *et al.* (2002). The irradiation disks were closed with aluminium covers, wrapped in aluminium foil, sealed in quartz tubes, and inserted into a cadmium column. Finally, they were irradiated for 42 hours in the TRIGA reactor at Oregon University (USA).

Each sample was heated incrementally in a continuous way with a laser beam 2 mm in diameter in order to release Ar from the irradiated samples using the step-heating technique. This procedure results in the release of gas fractions with increasing temperature that are then individually measured with a MAP-215-50 mass spectrometer using the software MassSpec Versão 7.527, which was developed by the Berkeley Geochronology Center (USA). Analytical procedures are described by Deino & Potts (1990), and Vasconcelos *et al.* (2002). Analytical data were obtained at Queensland University, Australia, and are shown in tables 4, 5, and 6.

5.1. Salto do Céu Suite

The Salto do Céu Suite shows an integrated age of 1385 ± 9 Ma (Fig. 10A) for amphiboles, which is interpreted to be the cooling age of its sills and lava flows; however, a plateau age (Fig. 10B) yielded from plagioclase crystals indicates an opening of the Ar-Ar system at 1021 ± 5 Ma below the 200°C isotherm, likely as a response to the installation of the Aguapeí Mobile Belt, Jauru Terrane.

The age obtained from amphibole crystals (1385 ± 9 Ma) is similar to that baddeleyite age of 1439 ± 4 Ma (U-Pb ID-TIMS) presented by Teixeira *et al.* (2015a), which is interpreted to be the crystallization age of this unit.

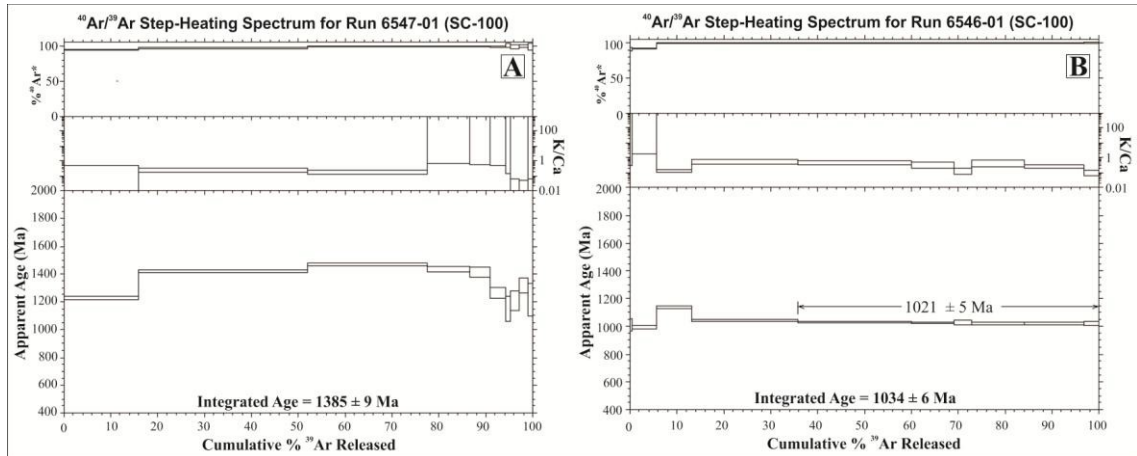


Fig. 10. $^{40}\text{Ar}/^{39}\text{Ar}$ (mineral) diagrams for the Salto do Céu Suite. A – Amphibole (hornblende). B – Plagioclase.

5.2. Rancho de Prata Intrusive Suite

Ar-Ar data yields a plateau age of 967 ± 5 Ma from plagioclase (Fig. 11A); while data obtained from amphibole yields a discordant age spectra with an integrated age of 1495 ± 8 Ma (Fig. 11B). Such results may indicate that the amphibole age stands for the cooling age of this mafic intrusion; however, the plagioclase age may indicate the opening of the Ar-Ar system as a result of thermal effects caused by the Sunsás-Aguapeí Orogeny.

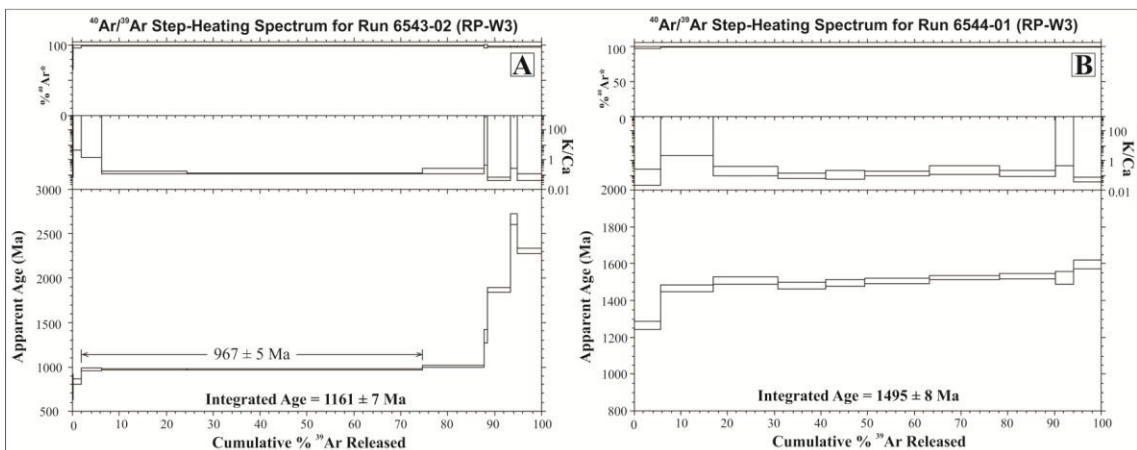


Fig. 11. $^{40}\text{Ar}/^{39}\text{Ar}$ (mineral) diagrams of the Rancho de Prata Intrusive Suite. A – Plagioclase. B – Amphibole (hornblende).

5.3. Huanchaca Intrusive Suite

Ar-Ar ages obtained for sills of the Huanchaca Intrusive Suite are of 1041 ± 6 Ma (plagioclase, integrated age; Fig. 12A), and 1113 ± 11 Ma (amphibole, plateau age; Fig. 12B). This latter age points out that the Ar-Ar system of these minerals remained closed. All the ages obtained at different temperatures were the same resulting in a homogeneous age spectra that represent the best age estimate for emplacement of these rocks.

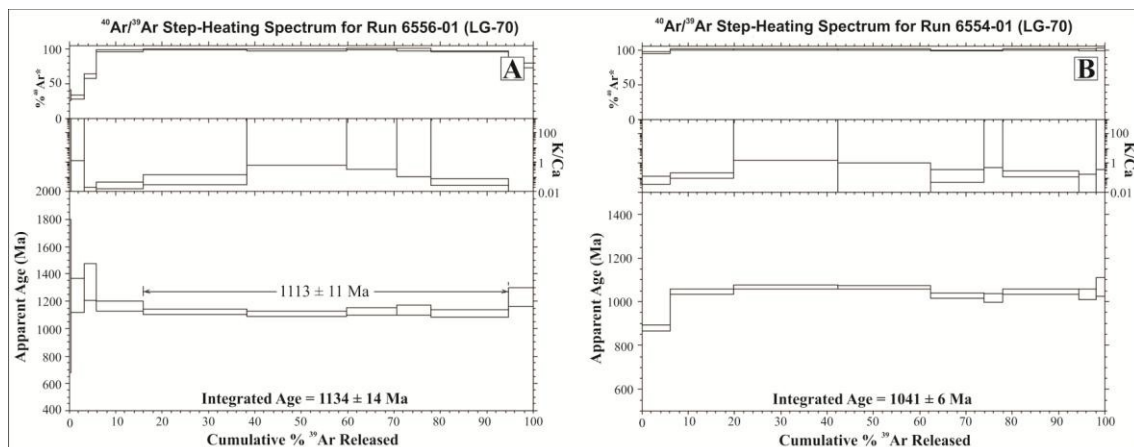


Fig. 12. $^{40}\text{Ar}/^{39}\text{Ar}$ (mineral) diagrams for the Huanchaca Intrusive Suite. A – Plagioclase. B – Amphibole (hornblende).

6. FINAL CONSIDERATIONS AND CONCLUSIONS

Based on K-Ar data available in the literature (Barros *et al.*, 1982; Santos *et al.*, 1979; Leite *et al.*, 1985), with ages between 845 and 1006 Ma, the units described were assigned to a single magmatic event responsible for generation of LIP associated with the attempted break-up of Rodinia (Ruiz *et al.*, 2010a; Séclo *et al.*, 2011; Lima *et al.*, 2012).

The interpretation of precision geochronologic data (U-Pb TIMS on baddeleyite, and Ar-Ar on amphibole and plagioclase) as well as field and petrological data allowed us to conclude that these igneous records are not linked to geodynamic processes involved in the attempted break-up of Rodinia, but related to tectonic events that preceded the agglutination of this supercontinent.

Two fissural magmatic events on regional scale are distinguished: and older one between 1387 and 1439 Ma restricted to the Jauru Terrane, and a younger one at 1110 Ma, which is observed in the Paraguá and Rio Apa Terranes. By taking into account the evolution of the Amazonian Craton, the older event, which is marked by dyke swarms of the Rancho de Prata

and lava flows and sills of the Salto do Céu, is likely related to post-orogenic stages of the Santa Helena Magmatic Arc in the Jauru Terrane; the younger event, which is restricted to the Paraguá and Rio Apa Terranes, is represented by the Huanchaca, Rio Perdido, and Rincón del Tigre suites that together characterize a Stenian LIP sited in the south-southwestern Amazonian Craton. This LIP results of a continental attempted break-up likely associated with the setting-up of the Aguapeí Aulacogen. The Sunsás and Aguapeí belts mark the final agglutination of Rodinia and partially metamorphose and deform the Stenian LIP (Litherland *et al.*, 1986; Teixeira *et al.*, 2010).

In this way, respective plateau Ar-Ar ages of 1021 ± 6 Ma and 967 ± 5 Ma obtained for the Salto do Céu and Rancho de Prata suites indicate an opening of the Ar-Ar system as a result of regional heating caused by evolution of the Aguapeí Group.

Tafrogenetic events to which are related these dyke swarms and sills sited in the south and southwestern Amazonian Craton are schematically illustrated in the tectonic evolution sequence shown in [Fig. 13](#).

The Ectasian-Calymmian event, with records only in the Jauru Terrane, have bimodal nature, and is post-kinematic with respect to the Santa Helena Orogeny. Despite the opening of the Ar-Ar system around 1000 Ma, both sedimentary country rocks and mafic rocks (Rancho de Prata and Salto do Céu suites), and acid rocks (Rio Branco suite) show no record of deformation related to the Aguapeí Belt ([Fig. 13A](#)).

The Stenian event, in turn, have unimodal nature, and covers a vast area in the Paraguá and Rio Apa terranes being related to a crustal extension stage responsible for the establishment of the Aguapeí aborted rift, and deposition of the siliciclastic Aguapeí Group. Mafic dyke swarms were not deformed by the Sunsás Orogeny in the Rio Apa Terrane as well as in the region of Huanchaca Sierra, however they were deformed and metamorphosed in the region of Rincón del Tigre as a result of the Sunsás Belt ([Fig. 13B and C](#)).

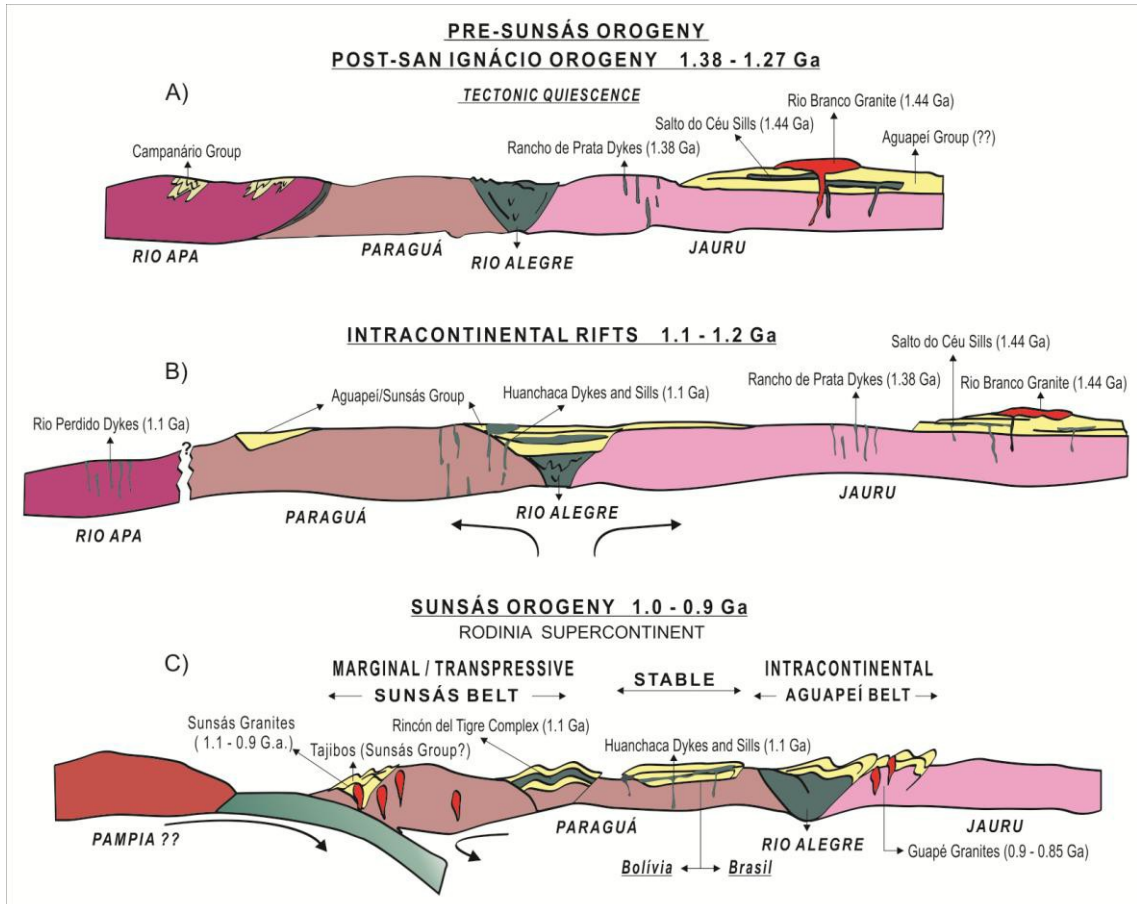


Fig. 13. Tectonic evolution scheme for the mafic dyke swarms, and mafic and acid sills sited in the south and southwestern Amazonian Craton.

ACKNOWLEDGEMENTS

Authors acknowledge CAPES (PROCAD 096/2007), CNPq (Process No. 479779/2011-2), FAPEMAT (Process No. 222473/2015), FAPESP (Proc. 2011/50887-6), and INCT-GEOCIAM for providing the financial support for this research. The first author thanks CNPq for the PhD scholarship grant.

References

- Anderson, D.L., 2005. Large Igneous Provinces, Delamination, and Fertile Mantle. *Elements*, 1 (5), 271-275.
- Araújo, L.M.B., Godoy, A.M., Ruiz, A.S., Souza, M.Z.A., 2005. Soleiras Máficas Tonianas (Suíte Intrusiva Salto do Céu) no SW do Cráton Amazônico: regime extensional relacionado à Orogenia Sunsás? In: IX Simpósio de Geologia do Centro Oeste, Goiânia, v. 1, 155-156.
- Araújo, L.M.B., Godoy, A.M., Ruiz, A.S., Manzano, J.C., Souza, M.Z.A., 2007. Geologia e Geoquímica do Batólito Rapakivi Rio Branco, SW do Cráton Amazônico - MT. *Geologia USP - Série Científica*, 7, 57-72.
- Araújo, L.M.B., 2008. Evolução do Magmatismo do Domínio Cachoeirinha: Suítes Intrusivas Santa Cruz, Alvorada, Rio Branco e Salto do Céu, SW do Cráton Amazônico MT. Doctoral Thesis. Instituto de Geociências e Ciências Exatas, State University of São Paulo, Rio Claro, Brazil, p. 165.
- Araújo, L.M.B., Godoy, A.M., Zanardo, A., 2009. As Rochas Básicas Intrusivas das Suítes Rio Branco e Salto do Céu, na região de Rio Branco (MT) Sudoeste do Cráton Amazônico. *Revista Brasileira de Geociências*, 39, 289-303.

- Araújo, L.M.B., Godoy, A.M., 2011. Magmatismo o Batólito Rapakivi Rio Branco, SW do Cráton Amazônico (MT). *Geociências* (UNESP. Impresso), 30, 173-195.
- Barros, A.M., Silva, R.H. da, Cardoso, O.R.F.A., Freire, F.A., Souza Jr., J.J., Rivetti, M., Luz, D.S., Palmeira, R.C., Tassinari, C.C.G., 1982. Geologia. In: Ministério das Minas e Energia. Projecto RADAMBRASIL, Folha SD. 21, Cuiabá, p. 544.
- Bellieni, G., Brotzu, P., Comin-Chiaramonti, P., Ernesto, M., Melfi, A.J., Pacca, I.G., Piccirilo, E.M., Stolva, D., 1983. Petrological and Paleomagnetic Data on the Plateau Basalts to Rhyolite sequences of the Southern Paraná Basin (Brazil). *Anais da Academia Brasileira de Ciências*, 55, 355-383.
- Bellieni, G., Comin-Chiaramonti, P., Marques, L.S., Melfi, A.J., Piccirilo, E.M., Nardy, A.J.R., Roisenberg, A. 1984. High- and low-Ti flood basalts from the Paraná plateau (Brazil): petrology and geochemical aspects bearing on their mantle origin. *Neues Jahrbuch für Mineralogie Abhandlungen*, 150, 272-306.
- Beswick, A.E., Soucie, G., 1978. A correction procedure for metasomatism in an Archean greenstone belt. *Precambrian Research*, 6 (2), 235-248.
- Beswick, A.E., 1982. Some geochemical aspects of alteration and genetic relations in Komatiitic suites. In: Arndt, N.T. & Nesbit, E.G. (Eds.), *Komatiites*. Allen, London, 283-308.
- Corrêa da Costa, P.C., Girardi, V.A.V., Matos, J.B., Ruiz, A.S., 2009. Geocronologia Rb-Sr e Características Geoquímicas dos Diques Máficos da Região de Nova Lacerda e Conquista D'Oeste (MT), Porção Sudoeste do Cráton Amazônico. *Geologia USP - Série Científica*, 9, 115-132.
- Cox, K.G., Bell, J., Pankhurst, R.J., 1979. *The interpretation of igneous rocks*. Allen & Unwin, London, pp. 450.
- D'Agrella-Filho, M.S., Trindade, R.I.F., Queiroz, M.V.B., Meira, V.T., Janikian, L., Ruiz, A.S., Bispo-Santos, F., 2016. Reassessment of Aguapeí (Salto do Céu) paleomagnetic pole, Amazonian Craton and implications for Proterozoic supercontinents. *Precambrian Research*, 272, 1-17.
- Deino, A., Potts, R. 1990. Single-crystal $^{40}\text{Ar}/^{39}\text{Ar}$ dating of the Ologesailie Formation, southern Kenya rift: *Journal of Geophysical Research*, 95, 8453-8470.
- Ernst, R.E., Bleeker, W., Söderlund, U., Kerr, A.C., 2013. Large igneous provinces and supercontinents: toward completing the plate tectonic revolution. *Lithos*, 174, 1-14.
- Ernst, R.E., 2014. *Large Igneous Provinces*. Cambridge University Press, Cambridge, pp. 1-653.
- Geraldes, M.C., 2000. Geocronologia e geoquímica do plutonismo mesoproterozoico do SW do Estado de Mato Grosso (SW do Cráton Amazônico). Doctoral Thesis. Instituto de Geociências, Universidade de São Paulo, São Paulo, Brazil, p. 193.
- Geraldes, M.C. Van Schmus, W.R. Condie, K.C. Bell, S., Teixeira, W., Babinski, M., 2001. Proterozoic geologic evolution of the SW part of the Amazonian Cráton in Mato Grosso state, Brazil. *Precambrian Research*, 111, 91-128.
- Geraldes, M.C., Bettencourt, J.S., Teixeira, W., Matos, J.M., 2004. Geochemistry and isotopic constraints on the origin of the mesoproterozoic Rio Branco „anorogenic“ plutonic suite, SW of Amazonian craton, Brazil: high heat flow and crustal extension behind the Santa Helena arc? *Journal of South American Earth Sciences*, 17, 195-208.
- Geraldes, M.C., Nogueira, C., Vargas-Mattos, G., Matos, R., Teixeira, W., Valencia, V., Ruiz, J., 2014. U-Pb detrital zircon ages from the Aguapeí Group (Brazil): Implications for the geological evolution of the SW border of the Amazonian Craton. *Precambrian Research*, 244, 306-316.
- Girardi, V.A.V., Corrêa da Costa, P.C., Teixeira, W., 2012. Petrology and Sr e Nd characteristics of the Nova Lacerda dike swarm, SW Amazonian craton: new insights regarding its subcontinental mantle source and Mesoproterozoic geodynamics. *International Geology Review*, 54, 165-182.
- Halls, H., 1982. The Importance and Potencial of Mafic Dikes Swarms in Studies of Geodynamic Process. *Geoscience Canada*, 9, 145-154.
- Irvine, I.N. & Baragar, W.R.A., 1971. A Guide To The Chemical Classification Of The Common Volcanics Rocks. *Canadian Journal Earth Science*, 8, 523-548.

- Kuiper, K.F., Deino, A., Hilgen, F.J., Krijgsman, W., Renne, P.R., Wijbrans, J.B., 2008. Synchronizing Rock Clocks of Earth History: *Science*, 320, 500-504.
- Jacques, A.L. & Green, D.H., 1979. Determination of liquid compositions in high pressure melting of peridotite. *American Mineralogist*, 64, 1312-1321.
- Jacques, A.L. & Green, D.H., 1980. Anhydrous melting of peridotite at 0-15 kb pressure and the genesis of tholeiitic basalts. *Contributions to Mineralogy and Petrology*, 73, 287-310.
- Jensen, L.S., 1976. A new cation plot for classifying subalkalic volcanic rocks. *Ontario Geological Survey Miscellaneous Paper* 66, 22 pp.
- Le Bas, M.J., Le Maitre, R.W., Streckeisen, A., Zanettin, B.A., 1986. Chemical Classification Of Volcanic Rocks Based On Total Alkali-Silica Diagram. *Journal Of Petrology*, 27, 745-750.
- Leite, J.A.D., Saes, G.S., Weska, R.K., 1985. A Suíte Intrusiva Rio Branco e o Grupo Aguapeí na serra de Rio Branco, Mato Grosso. In: *Simpósio de Geologia do Centro-Oeste, Goiânia*, v. 1, 247-255.
- Lima, G.A., 2008. Geologia da Porção Nordeste da Serra Ricardo Franco (MT) - Região da Fazenda Paredão: ênfase nas Soleiras Máficas-Ultramáficas da Suíte Intrusiva Huanchaca. Trabalho de Conclusão de Curso, Instituto de Ciências Exatas e da Terra, Universidade Federal de Mato Grosso, p. 64.
- Lima, G.A., 2011. Geologia, Geoquímica e Geocronologia dos sills máficos da Suíte Intrusiva Huanchaca na porção nordeste da Serra Ricardo Franco (MT) – SW do Cráton Amazônico. Masters dissertation. Instituto de Ciências Exatas e da Terra, Universidade Federal de Mato Grosso, Cuiabá, Brazil, 62 p.
- Lima, G.A., Sousa, M.Z.A., Ruiz, A.S., D'agrella Filho, M.S., Vasconcelos, P., 2012. Sills máficos da Suíte Intrusiva Huanchaca - SW do Cráton Amazônico: registro de magmatismo fissural relacionado à ruptura do Supercontinente Rodínia. *Revista Brasileira de Geociências*, 42, 111-129.
- Lima, G.A., Macambira, M.J.B., Sousa, M.Z.A., Ruiz, A.S., Batata, M.E.F., Pierosan, R. (subm.). Geologia e Petrologia da Suíte Salto do Céu (MT): Implicações Tectônicas e Estratigráficas para o SW do Cráton Amazônico. *Brazilian Journal of Geology*.
- Litherland, M., Annels, R.N., Appleton, J.D., Berrange, J.P., Boomfield, K., Darbyshire, D.P.F., Fletcher, C.J.N., Hawkins, M.P., Klinck, B.A., Mitchell, W.I., O'Connor, E.A., Pitfield, P.E.J., Power, G., Webb, B.C., 1986. The geology and mineral resources of the Bolivian Precambrian Shield. *Overseas Memoir. British Geological Survey*, v. 9, p. 153.
- McDonough, W.F. & Sun, S.S., 1995. The composition of the earth. *Chemical Geology*, 120, 223-253.
- Meschede, M., 1986. A method of discriminating between different types of mid-ocean ridge basalts and continental tholeiites with the Nb-Zr-Y diagram. *Chemical Geology*, 56, 207-218.
- Morgan, W.J., 1971. Convection plumes in the lower mantle. *Nature*, 230, 42-43.
- Morgan, W.J., 1972. Plate motions and deep mantle convection. *Mem. Geol. Soc. Am.* 132, 7-22.
- Nance, R.D., Murphy, J.B., Santosh, M., 2014. The supercontinent cycle: a retrospective essay. *Gondwana Research*, 25, 4-29.
- Pearce, J.A., Norry, M. J., 1979. Petrogenetic implications of Ti, Zr, Y and Nb variations in Volcanic Rocks. *Contrib. Mineral. Petrol*, 69, 33-47.
- Ruiz, A. S. 2005. Evolução Geológica do Sudoeste do Cráton Amazônico Região Limítrofe Brasil-Bolívia – Mato Grosso. Doctoral Thesis. Instituto de Geociências e Ciências Exatas, State University of São Paulo, Rio Claro, Brazil, p. 250.
- Ruiz, A.S., Simões, L.S.A., Costa, P.C.C., Matos, J.B., Araújo, L.M.B., Godoy, A.M., Souza, M.Z.A., 2005. Enxame de Diques Máficos (Suíte Intrusiva Rancho de Prata) no SW do Cráton Amazônico: Índícios de Colapso Extensional no Orógeno Sunsás? III Simpósio de Vulcanismo e Ambientes Associados, Cabo Frio, vol. 1, 1-5.
- Ruiz, A.S., D'Agrella-Filho, M.S., Sousa, M.Z.A., Lima, G.A., 2010a. Tonian sills and mafic dike swarms of the S-SW Amazonian craton, records of Rodinia Supercontinent break-up?, vol. 91, no. 26. Meeting of the Americas, EOS Transactions American Geophysical Union, pp. 3.

- Ruiz, A.S., Matos, J.B., Sousa, M.Z.A., Lima, G.A., Batata, M.E.F. 2010b. Mapeamento Geológico e Levantamento de Recursos Minerais da Folha Santa Bárbara (SD.21-Y-C-V). Convênio CPRM-UFMT. Programa Geologia do Brasil, Relatório Etapa de Mobilização, p. 35.
- Ruiz, A.S., Sousa, M.Z.A., Lima, G.A., Matos, J.B., Batata, M.E.F., Corrêa da Costa, P. C., Campos, F.A.P. (no prelo). Geologia da Folha Rio Pindaituba (SD.21-Y-A-V). Programa Nacional de Geologia (PRONAGEO). CPRM/UFMT. p. 100.
- Santos, R.O.B., Pitthan, J.H.L., Barbosa, E.S., Fernandes, C.A.C., Tassinari, C.C.G., Campos, D.A., 1979. Folha SD.20 - Guaporé. Geologia. Rio De Janeiro, Ministério das Minas e Energia-Secretaria Geral, Projeto RADAMBRASIL - Geologia, 19, 21-123.
- Santosh, M., Maruyama, S., Yamamoto, S., 2009. The making and breaking of super-continent: some speculations based on superplumes, super downwelling and the role of tectosphere. *Gondwana Research*. 15, 324-341.
- Século, D.B., Ruiz, A.S., Sousa, M.Z.A., Lima, G.A., Batata, M.E.F., 2008. Caracterização Geológica e Petrográfica do Enxame de Diques Máficos (Suíte Intrusiva Huanchaca) no Domínio Tectônico Paraguá - SW do Cráton Amazônico - MT. In: Congresso Brasileiro de Geologia, 44, p. 545.
- Século, D.B., 2011. Geologia, Petrografia e Geoquímica do enxame de diques máficos (Suíte Intrusiva Huanchaca) na região de Vila Bela da Santíssima Trindade (MT) – SW do Cráton Amazônico. Masters dissertation. Instituto de Ciências Exatas e da Terra, Universidade Federal de Mato Grosso, Cuiabá, Brazil, 57 p.
- Século, D.B., Ruiz, A.S., Sousa, M.Z.A., Lima, G.A., 2011. Geologia, Petrografia e Geoquímica do Enxame de Diques Máficos da região de Vila Bela da Santíssima Trindade (MT) Suíte Intrusiva Huanchaca SW do Cráton Amazônico. *Geociências*, 30, 561-573.
- Sousa, M.Z.A., Batata, M.E.F., Ruiz, A.S., Lima, G.A., Matos, J.B., Paz, J.D.S., Costa, A.C.D., Silva, C.H., Corrêa da Costa, P.C., 2011. Geologia da Folha Rio Branco (SD21-Y-D-I). Programa Nacional de Geologia (PRONAGEO). CPRM/UFMT. p. 178.
- Sun, S.S. & McDonough, W.F., 1989. Chemical and isotopic systematic of oceanic basalts: implications for mantle composition and processes. In: A.D. Saunders e M.J. Norry (Eds.) *Magmatism in the Ocean Basins*. Geological Society. London, 313-345.
- Takahashi, E., Kushiro, I., 1983. Melting of dry peridotite at high pressures and basalt magma genesis. *American Mineralogist*, 68, 859-879.
- Teixeira, W., Geraldés, M.C., Matos, R., Ruiz, A.S., Saes, G., Vargas-Mattos, G.L., 2010. A review of the tectonic evolution of the Sunsas belt, SW Amazonian Craton. *J.S. Am. Earth Sci.*, 29, 47-60.
- Teixeira, W., Hamilton, M.A., Lima, G.A., Ruiz, A.S., Matos, R., Ernst, R., 2015a. Precise ID-TIMS U–Pb baddeleyite ages (1110–1112 Ma) for the Rincón del Tigre–Huanchaca large igneous province (LIP) of the Amazonian Craton: Implications for the Rodinia supercontinent. *Precambrian Research*, 265, 273-285.
- Teixeira, W., Ernst, R., Hamilton, M. A., Lima, G.A., Ruiz, A.S., Geraldés, M.C., 2015b. Widespread ca. 1.4 Ga intraplate magmatism and tectonics in a growing Amazonia. *GFF*, 1-14.
- Teixeira, W., Hamilton, M.A., Girardi, V.A.V., Faleiros, F.M., 2016. Key dolerite dyke swarms of Amazonia: U-Pb constraints on supercontinent cycles and geodynamic connections with global LIP events through time. *Seventh International Dyke Conference*. Pequim.
- Vasconcelos P.M., Onoe A.T., Kawashita K., Soares A.J., and Teixeira W., 2002. ⁴⁰Ar/³⁹Ar geochronology at the Instituto de Geociências, USP: instrumentation, analytical procedures, and calibration: *Annals of the Brazilian Academy of Sciences*, 74, 297-342.
- Oliva, L.A., 1979. Ocorrências Minerais na Folha Cuiabá (SD.21). Relatório de Viagem Goiânia, DNPM, p.18.

Table 1. Lithochemical data of rocks from Salto do Céu Suite [major elements (% weight), trace-elements (ppm)].

	RB 317A	RB 320	RB 531	RB 532	RB 344	RB 46B	RB 317	RB 22C2	RB 22B	RB 42D2	RB 533A	PG 120 5	PG 120 6	PG 120 3
SiO ₂	48,9	47,25	46,9	46,11	45,86	45,8	45,56	45,22	45,09	45,06	44,03	49,02	49,15	49,32
TiO ₂	3,67	3,92	4,38	2,88	2,65	2,59	2,15	2,74	2,03	3,48	2,23	3,65	3,25	3,30
Al ₂ O ₃	13,04	12,41	11,73	16,09	16,23	16,1	15,83	14,45	16,53	14,78	15,76	13,68	13,90	13,63
Fe ₂ O ₃	16,19	17,36	17,6	14,03	14,4	13,96	13,61	15,56	13,05	15,1	14,7	14,94	14,85	14,67
FeO _t	14,56	15,62	15,83	12,62	12,95	12,56	12,24	14,00	11,74	13,58	13,22	13,44	13,36	13,20
MnO	0,15	0,22	0,23	0,19	0,19	0,19	0,17	0,2	0,16	0,19	0,19	0,23	0,21	0,22
MgO	3,97	3,75	4,31	5,11	5,67	6,01	6,66	5,77	6,86	5,14	6,80	3,92	4,56	4,66
CaO	5,81	8,25	8,98	8,48	8,93	8,65	8,5	8,52	7,98	8,88	8,57	6,22	5,05	6,89
Na ₂ O	3,54	2,93	2,64	2,95	2,82	2,77	2,75	3,41	2,98	2,9	2,58	3,28	3,72	2,69
K ₂ O	0,4	1,69	1,38	0,83	0,39	0,65	0,78	0,55	1,06	0,45	1,06	1,74	1,34	1,19
P ₂ O ₅	0,7	0,67	0,59	0,54	0,49	0,49	0,38	0,45	0,34	0,66	0,35	0,61	0,58	0,57
LOI	3,3	1,3	1	2,5	2,1	2,5	3,3	2,8	3,6	3	3,4	2,4	3,0	2,5
Ba	562	631	516	491	350	390	562	326	455	312	437	826	1183	772
Rb	22,3	39,8	32,7	17,3	9,1	19,3	22,3	12,2	31,3	12,1	27,5	53,9	40,0	32,4
Sr	611,1	293,7	291,6	345,7	345,2	352,8	611,1	499,8	515,4	338,4	537,7	295,1	333,2	293,3
Zr	329,1	313	255	215,8	205,5	205,6	153,1	173,1	134,1	244,1	150,3	283,2	261,3	251,1
Nb	12,9	22,2	19,9	14,8	13,9	13,5	12,9	15,5	11,3	21,4	12,6	19,5	18,2	16,7
Zn	196	119	97	91	91	89	84	81	58	88	70	86	107	72
La	42,7	35,6	28,7	20,4	20,2	18,6	18,6	21,6	16,5	30,3	17,5	34,2	35,0	29,4
Ce	98,7	79,9	68,3	50	46,5	44,2	43,5	51,8	38,2	69,2	40,7	75,0	74,8	65,3
Pr	13,12	11	9,51	6,82	6,66	6,34	6,16	7,18	5,35	9,55	5,71	10,19	9,91	8,90
Nd	56,9	50,1	43,6	30,7	29,1	27,8	26,1	32	24,3	41,7	26,5	42,8	42,2	39,3
Sm	12,15	10,76	9,62	6,9	6,61	6,2	5,6	6,8	5,02	8,92	5,56	9,27	9,32	8,73
Eu	3,31	3,08	2,74	2,26	2,22	2,15	2,01	2,28	1,81	2,71	1,94	2,71	2,63	2,39
Gd	12,93	11,45	10,09	7,35	7,04	6,53	5,71	6,87	5,14	9,29	5,84	10,06	9,63	8,94
Tb	2,07	1,71	1,61	1,19	1,17	1,14	0,92	1,11	0,82	1,49	0,91	1,61	1,51	1,40
Dy	11,75	10,25	9,53	6,79	6,35	6,41	5,12	6,14	4,53	8,05	5,06	9,46	9,46	8,26
Ho	2,31	2,02	1,82	1,31	1,31	1,25	1,01	1,19	0,89	1,62	1	1,67	1,62	1,61
Er	6,58	5,39	4,94	3,7	3,75	3,61	2,83	3,35	2,38	4,39	2,79	4,59	4,72	4,56
Tm	0,94	0,81	0,76	0,55	0,54	0,52	0,39	0,49	0,36	0,65	0,4	0,74	0,65	0,65
Yb	5,92	5,02	4,44	3,46	3,41	3,09	2,5	3,04	2,3	4,15	2,37	4,58	4,08	3,83
Lu	0,84	0,73	0,65	0,52	0,5	0,46	0,36	0,43	0,31	0,57	0,36	0,71	0,64	0,63
Y	66	52,5	49,8	36,5	35,6	33,5	27,1	32,9	23,3	43	33,4	46,7	43,4	42,0
mg#	0,33	0,30	0,33	0,42	0,44	0,46	0,49	0,42	0,51	0,40	0,48	0,34	0,38	0,39
K	3321	14029	11456	6890	3238	5396	6475	4566	8799	3736	8799	14444	11124	9879
Ti	22002	23501	26259	17266	15887	15527	12889	16427	12170	20863	13369	21882	19484	19784

Table 2. Lithochemical data of rocks from Rancho de Prata Intrusive Suite [major elements (% weight), trace-elements (ppm)].

	RP	RP 01	RP 02	RP 1A	RP 1B	RP 462	RP-II30	RP W1A	RP W2	RP W3
SiO ₂	50,43	47,65	46,94	47,07	46,51	46,48	46,25	48,81	48,42	47,91
TiO ₂	1,45	1,02	1,53	1,69	1,55	1,16	1,17	0,62	2,06	1,62
Al ₂ O ₃	15,75	16,72	15,87	15,34	15,62	16,58	16,76	16,55	15,3	15,61
Fe ₂ O ₃	12,93	13,16	14,75	15,09	14,77	13,71	13,73	12,5	13,5	14,37
FeO _t	11,63	11,84	13,27	13,57	13,29	12,33	12,35	11,24	12,14	12,93
MnO	0,18	0,18	0,2	0,2	0,2	0,19	0,19	0,18	0,18	0,19
MgO	5,71	7,46	7,09	6,85	6,94	7,6	7,6	7,77	5,3	6,38
CaO	8,37	9,36	9,36	9,24	9,27	9,29	9,07	9,93	8,26	9,1
Na ₂ O	2,77	2,46	2,4	2,43	2,36	2,59	2,14	2,15	2,75	2,46
K ₂ O	1,08	0,32	0,48	0,56	0,49	0,53	0,94	0,33	1,5	0,77
P ₂ O ₅	0,35	0,25	0,32	0,4	0,39	0,11	0,11	0,11	0,61	0,4
LOI	0,7	1,1	0,8	0,8	1,6	1,5	1,8	0,8	1,7	0,9
Ba	428	254	315	372	305	162	276	133	818	444
Rb	18,5	5,9	9,7	12,6	11,1	19,7	35,2	9,9	26,5	12,4
Sr	354,6	319,7	263,4	245,7	258,9	201,9	209,5	202,1	572,2	390,3
Zr	122,5	68,5	96,2	124	111,2	60,1	56,4	37,4	216	127,1
Nb	4,7	3,1	4,8	5,8	4,7	1,3	1	1,5	6,3	4,8
Ni	50	82	84	54	63	80	98	95	40	49
Zn	58	44	78	31	126	41	50	28	91	43
La	15,5	8,9	11,4	15,4	13,5	4,5	4,3	4,5	28	16,3
Ce	35	21,3	27,4	35,2	31,3	10,7	10	10,3	64,1	36,2
Pr	4,6	2,85	3,73	4,71	4,38	1,5	1,47	1,38	7,88	4,75
Nd	21,2	12,8	16,5	22,8	20,4	7,4	8,1	6,4	34,5	19,8
Sm	4,51	2,75	4,09	4,94	5,01	2,62	2,57	2,01	6,78	4,85
Eu	1,48	1,06	1,4	1,69	1,63	1,04	1,03	0,75	2,35	1,76
Gd	4,89	3,4	4,67	5,66	5,46	3,58	3,57	2,68	6,71	5,42
Tb	0,85	0,59	0,82	1	0,97	0,68	0,65	0,53	1,09	0,93
Dy	4,88	3,61	4,47	6,18	5,65	4,29	4,02	3,35	6,1	5,61
Ho	1,09	0,83	1,08	1,37	1,25	0,91	0,93	0,78	1,29	1,16
Er	3,35	2,26	3,2	4,05	3,88	2,89	2,72	2,44	3,78	3,78
Tm	0,49	0,38	0,48	0,58	0,58	0,41	0,4	0,38	0,54	0,55
Yb	3,24	2,37	3,14	3,76	3,72	2,62	2,15	2,4	3,17	3,48
Lu	0,47	0,33	0,43	0,54	0,55	0,39	0,36	0,36	0,53	0,53
Y	30,3	21,7	28,5	34,1	34,3	25,4	24,2	22	35,6	33,3
mg#	0,47	0,53	0,49	0,47	0,48	0,52	0,52	0,55	0,44	0,47
K	8965,40	2656,42	3984,62	4648,73	4067,64	4399,69	7803,22	2739,43	12451,95	6392,00
Ti	8692,90	6115,00	9172,50	10131,72	9292,41	6954,32	7014,27	3716,96	12349,91	9712,06

Table 3. Lithochemical data of rocks from Huanchaca Intrusive Suite [major elements (% weight), trace-elements (ppm)].

	DS-01	DS-02	DS-03	DS-04	DS-05	DS-06	DS-07	DS-08	DS-09	DS-10	HU-1	HU-2	HU-3	HU-4	HU-5
SiO ₂	53,68	53,83	53,94	53,65	52,99	53,48	53,77	52,81	54,29	54,17	54,95	52,91	53,31	53,83	54,49
TiO ₂	0,73	0,73	0,75	0,72	0,72	0,73	0,74	0,73	0,742	0,737	1,095	1,018	1,097	0,917	0,943
Al ₂ O ₃	14,17	14,15	14,2	14,18	14,32	14,14	14,16	14,09	14,05	14,15	13,77	13,96	14,06	14,65	14,57
Fe ₂ O ₃	9,48	9,58	9,64	9,57	9,76	9,95	9,9	10,17	9,47	9,66	11,53	11,65	11,92	10,36	10,49
FeO _t	8,53	8,62	8,67	8,61	8,78	8,95	8,91	9,15	8,52	8,69	10,37	10,48	10,72	9,32	9,44
MnO	0,14	0,14	0,14	0,15	0,14	0,15	0,14	0,15	0,146	0,146	0,171	0,17	0,171	0,162	0,163
MgO	6,98	6,9	6,8	7,04	7,21	7,24	6,95	7,03	6,79	6,81	4,83	5,17	4,62	6,56	6,01
CaO	9,32	8,96	9,16	9,28	9,31	9,52	9,51	9,25	9,35	9,29	8,73	8,92	8,62	9,05	9,14
Na ₂ O	1,66	2,01	1,98	1,75	1,94	1,9	1,71	1,52	1,8	2,01	2,27	2,2	2,24	2,06	2,18
K ₂ O	1,53	1,59	1,41	1,43	1,42	1,26	1,33	1,88	1,57	1,28	1,77	1,4	1,38	1,06	1,35
P ₂ O ₅	0,07	0,08	0,09	0,08	0,08	0,07	0,07	0,07	0,09	0,09	0,17	0,14	0,15	0,12	0,13
LOI	1,9	1,7	1,6	1,8	1,8	1,3	1,4	1,9	2,16	1,55	1,21	0,97	0,86	0,78	1,11
Ba	324	289	276	270	292	296	302	411	345	272	493	414	439	250	384
Rb	65,7	79,4	58,1	84,8	70,4	56,9	53,3	135,8	79	60	71	57	50	34	46
Sr	202,7	194,9	150	170,2	193,3	165,7	162,7	203,5	225	167	171	179	177	176	184
Zr	102,3	103,6	105,9	107,9	110,9	102,7	112,1	106,3	105	102	153	133	146	116	124
Nb	4,5	4,3	4,7	4,8	4,9	4,8	5,1	5,3	4	4	6	5	6	5	5
Ni	66	50	45,2	45,5	142	140	1,2	150	120	130	40	50	40	60	60
Zn	38	34	33	35	32	43	14	33	80	90	110	110	120	100	120
La	13,8	13,4	13,8	14,2	15	14	15,4	15	14,2	13,8	23,3	21,4	22	18,6	18,4
Ce	31,4	31,2	31,7	32,4	33	31,5	35,2	32,3	30,2	29,4	49,1	44,8	46,1	39,2	39
Pr	3,71	3,6	3,7	3,78	3,89	3,74	3,95	3,76	3,57	3,54	5,9	5,4	5,45	4,59	4,67
Nd	15,4	15,3	15,1	14,7	14,7	14,9	15	13	14,6	14	23,5	21,3	21,5	18,2	18,7
Sm	3,2	3,2	3,16	3,42	3,62	3,47	3,71	3,5	3,1	3,2	5,1	4,6	4,7	4	4,1
Eu	0,9	0,9	0,92	0,92	0,94	0,91	0,9	0,91	0,95	0,93	1,4	1,33	1,31	1,15	1,19
Gd	3,51	3,51	3,69	3,74	3,78	3,66	3,81	3,74	3,7	3,6	5,5	5	5,1	4,4	4,4
Tb	0,64	0,66	0,67	0,67	0,68	0,7	0,69	0,66	0,7	0,7	1	0,9	0,9	0,8	0,8
Dy	3,7	3,72	3,87	4,03	3,73	3,82	4,04	3,63	4,1	4,1	5,9	5,4	5,4	4,7	4,7
Ho	0,79	0,82	0,81	0,82	0,84	0,86	0,87	0,85	0,9	0,8	1,2	1,1	1,1	0,9	1
Er	2,33	2,41	2,44	2,48	2,46	2,48	2,51	2,57	2,5	2,4	3,5	3,2	3,3	2,8	2,9
Tm	0,37	0,36	0,39	0,39	0,38	0,38	0,41	0,38	0,38	0,36	0,51	0,49	0,5	0,43	0,43
Yb	2,3	2,26	2,38	2,49	2,49	2,43	2,58	2,33	2,4	2,3	3,3	3,2	3,2	2,7	2,7
Lu	0,35	0,35	0,35	0,37	0,37	0,38	0,38	0,37	0,36	0,36	0,5	0,48	0,47	0,41	0,42
Y	23,1	21,8	23,3	23,4	25	23,7	25,2	24,4	32	20	31	28	30	22	25
mg#	0,59	0,59	0,58	0,59	0,59	0,59	0,58	0,58	0,59	0,58	0,45	0,47	0,43	0,56	0,53
K	1270 1	1319 9	1170 5	1187 1	1178 8	1046 0	1104 1	1560 6	1303 3	1062 6	1469 3	1162 2	1145 6	8799	1120 7
Ti	4376	4376	4496	4316	4316	4376	4436	4376	4448	4418	6565	6103	6577	5498	5653

Table 3. Continuation.

	HU-6	HU-7	HU-9	HU-10	HU-11	HU-12	HU-13	HU-14	HU-15	HU-16	HU-17	HU-18	HU-19	HU-20	HU-21
SiO ₂	54,63	54,98	54,71	52,21	54,65	53,46	52,52	53,99	53	54,63	52,42	54,37	53,47	52,17	53,42
TiO ₂	0,935	0,928	1,009	0,906	0,956	0,99	0,66	1,06	0,86	0,86	0,64	0,88	0,91	0,64	0,9
Al ₂ O ₃	14,45	14,54	14,07	14,37	14,54	14,13	14,47	14,12	14,8	14,56	16,13	14,48	14,61	15,68	14,54
Fe ₂ O ₃	10,89	10,28	10,82	10,06	10,46	11,32	9,76	11,17	10,81	9,83	8,85	9,76	10,44	9,15	10,39
FeO _t	9,80	9,25	9,73	9,05	9,41	10,18	8,78	10,05	9,72	8,84	7,96	8,78	9,39	8,23	9,35
MnO	0,166	0,161	0,167	0,155	0,16	0,17	0,16	0,17	0,16	0,16	0,14	0,16	0,16	0,15	0,16
MgO	5,92	5,98	5,63	6,14	6,04	5,48	8,4	5,19	6,46	6,26	8,16	6,74	5,99	8,41	6,09
CaO	9,23	9,23	9,3	8,99	9,33	9,25	9,92	8,79	9,08	7,83	9,5	8,93	9,01	9,31	9,85
Na ₂ O	2,24	2,12	2,24	1,97	2,11	2,24	1,84	2,19	2,14	2,35	1,88	2,18	2,18	1,92	2,1
K ₂ O	1,31	1,26	1,43	1,19	1,22	1,28	0,88	1,48	1,2	1,77	0,87	1,27	1,33	0,75	1,22
P ₂ O ₅	0,13	0,13	0,13	0,13	0,13	0,12	0,08	0,11	0,11	0,1	0,07	0,09	0,11	0,06	0,11
LOI	0,93	1,1	1,12	3,58	1,08	1,3	1	1,4	1,1	1,3	1	0,8	1,5	1,4	0,9
Ba	384	392	408	256	380	391	280	489	361	360	259	353	361	220	369
Rb	44	41	53	40	43	51,6	35,3	58,4	41	49,8	30,3	34,2	45,2	24,2	44,6
Sr	171	172	169	175	173	185,3	175,6	185,9	194,8	171,7	188,8	171,7	186,8	189,3	176,2
Zr	130	121	136	120	129	121,9	85,9	136,5	111,6	125	81,2	114,4	122,9	75,2	117,3
Nb	5	5	5	5	5	5,8	3,5	6,3	5,2	8	3,4	6,2	5	3,3	5,8
Ni	60	40	50	60	50	51	99	53	72	53	99	59	70	101	64
Zn	100	130	120	90	100	52	24	47	33	36	22	32	46	24	33
La	19,1	18,7	19,6	19,1	18,9	19,3	13,7	24,1	17,4	19	12,7	18,6	18,6	11,3	17,8
Ce	40,3	39,4	41,7	40,3	40,2	41,8	30	51,1	39,3	42,8	27,5	40,1	41,5	26,3	39,9
Pr	4,81	4,74	4,98	4,75	4,81	5,04	3,5	6,83	4,61	4,94	3,2	4,69	4,83	2,93	4,77
Nd	19,1	18,9	20	18,7	18,8	19,8	13,1	24,7	17,9	20,6	13,1	19,9	19,2	11,4	18,1
Sm	4,2	4,1	4,4	4,1	4,2	4,45	3,09	5,97	4,08	4,26	2,77	3,82	4,23	2,49	4,07
Eu	1,2	1,17	1,22	1,15	1,18	1,19	0,86	2,11	1,09	1,05	0,77	1,03	1,08	0,74	1,11
Gd	4,5	4,3	4,7	4,3	4,5	4,64	3,5	6,19	4,23	4,38	2,83	4,22	4,42	2,67	4,32
Tb	0,8	0,8	0,9	0,8	0,8	0,81	0,58	1,89	0,74	0,78	0,52	0,73	0,76	0,48	0,75
Dy	4,9	4,8	5,1	4,8	4,9	4,52	3,39	6,19	4,31	4,33	2,94	4,01	4,49	2,72	4,42
Ho	1	1	1,1	0,9	1	0,99	0,74	2,02	0,89	0,91	0,64	0,89	0,96	0,57	0,92
Er	3	2,9	3,1	2,8	2,9	2,92	2,12	4,16	2,73	2,67	1,83	2,71	2,74	1,82	2,89
Tm	0,45	0,43	0,47	0,42	0,43	0,45	0,33	1,37	0,4	0,41	0,28	0,39	0,4	0,26	0,43
Yb	2,8	2,7	3	2,7	2,8	2,94	2,17	4,04	2,57	2,55	1,84	2,66	2,67	1,68	2,63
Lu	0,43	0,41	0,45	0,41	0,42	0,41	0,31	1,35	0,4	0,4	0,27	0,36	0,4	0,26	0,4
Y	26	25	26	23	25	29,2	21,5	33,5	25,8	26,6	17,7	25,2	26,1	16,1	26,1
mg#	0,52	0,54	0,51	0,55	0,53	0,49	0,63	0,48	0,54	0,56	0,65	0,58	0,53	0,65	0,54
K	10875	10460	11871	9879	10128	10626	7305	12286	9962	14693	7222	10543	11041	6226	10128
Ti	5605	5563	6049	5432	5731	5935	3957	6355	5156	5156	3837	5276	5456	3837	5396

Table 4. $^{39}\text{Ar}/^{40}\text{Ar}$ analytical data obtained from plagioclase and amphibole of the Salto do Céu Suite (SC-100).

SAMPLE/ MATERIAL	Lab #	40Ar/ 39Ar	38Ar/ 39Ar	37Ar/ 39Ar	36Ar/ 39Ar	40*Ar/ 39Ar	%40*Ar	40Ar (Mols)	Age (Ma)	± Ma
SC-100/ Amphibole	6547-01A	94.39	0.01727	2.1	0.02025	88.63	93.76	2.04E-13	1224.1	6.6
	6547-01B	112.65	0.01633	2.12	0.01444	108.66	96.32	5.45E-13	1414.5	5.4
	6547-01C	115.08	0.01287	2.87	0.00331	114.53	99.33	3.96E-13	1466.7	6
	6547-01D	111.3	0.0115	2.1	0.00388	110.5	99.11	1.35E-13	1431	11
	6547-01E	109	0.0116	2.9	0.0055	107.8	98.69	6.61E-14	1.407	17
	6547-01F	94.5	0.0171	3.6	0.0081	92.6	97.75	4.09E-14	1.264	20
	6547-01G	80.3	0.0103	12	0.0034	80.8	99.9	1.17E-14	1144	47
	6547-01H	87.7	0.0197	17.8	0.0116	86.7	97.6	2.11E-14	1205	35
	6547-01I	98.2	0.0169	19.9	0.0108	97.8	98.26	2.78E-14	1.314	27
	6547-01J	88.1	0.0183	22	0.0129	87.2	97.5	9.63E-15	1.210	58
SC-100/ Plagioclase	6546-01A	75.4	0.0222	6.3	0.0259	68.4	90.4	1.92E-14	1009	23
	6546-01B	72.93	0.01686	0.82	0.02137	66.65	91.34	2.06E-13	989	6.1
	6546-01C	80.47	0.01409	3.96	0.00403	79.78	98.88	3.32E-13	1133.1	4.7
	6546-01D	71.91	0.01237	0.97	0.00207	71.41	99.24	8.91E-13	1042.6	3.8
	6546-01E	70.59	0.01257	1.2	0.00191	70.18	99.32	9.36E-13	1028.8	4
	6546-01F	70.17	0.01286	1.56	0.00299	69.47	98.9	3.46E-13	1021	4.5
	6546-01G	70.46	0.01302	4.03	0.00388	69.81	98.79	1.47E-13	1024.7	7.1
	6546-01H	69.79	0.01384	1.16	0.00248	69.19	99.07	4.27E-13	1017.8	3.5
	6546-01I	69.66	0.01321	2.14	0.0026	69.15	99.12	4.85E-13	1017.3	3.7
	6546-01J	69.54	0.01537	5.07	0.00332	69.18	99.13	1.22E-13	1017.7	6.8
	6556-01B	299	0.155	4	0.702	89.9	30	4.03E-14	1237	63
	6556-01C	159.6	0.0706	49	0.223	100.2	60.7	1.94E-14	1337	67
	6556-01D	84.3	0.0391	18.1	0.0149	82.3	96.39	4.04E-14	1160	18
	6556-01E	78.9	0.0407	6.3	0.00488	78.27	98.77	8.29E-14	1117.1	9.8
	6556-01F	78.53	0.0383	2.4	0.00594	77.07	97.98	7.95E-14	1104.3	8.8
	6556-01G	79	0.0438	4.6	0.0032	78.7	99.26	3.96E-14	1122	15
	6556-01H	79.9	0.0412	11.1	0.0057	79.6	98.94	2.72E-14	1132	21
	6556-01I	79.8	0.0385	11.9	0.01324	77.4	96.19	6.37E-14	1108	13
6556-01J	107.7	0.0543	117	0.1178	88.6	75.6	2.85E-14	1224	35	

Table 5. $^{39}\text{Ar}/^{40}\text{Ar}$ analytical data obtained from plagioclase and amphibole of the Rancho de Prata Intrusive Suite (RP-W3).

SAMPLE/ MATERIAL	Lab #	$^{40}\text{Ar}/$ ^{39}Ar	$^{38}\text{Ar}/$ ^{39}Ar	$^{37}\text{Ar}/$ ^{39}Ar	$^{36}\text{Ar}/$ ^{39}Ar	$^{40}^*\text{Ar}/$ ^{39}Ar	% $^{40}^*\text{Ar}$	^{40}Ar (Mols)	Age (Ma)	\pm Ma
RP-W3/ Amphibole	6544-01A	94.1	0.0137	4.1	0.00727	92.5	98.03	1.00E-13	1262	11
	6544-01B	115.81	0.01379	0.84	0.0068	113.91	98.3	2.35E-13	1461.3	8.5
	6544-01C	120.7	0.01486	2.3	0.00657	119.1	98.52	3.05E-13	1506.3	9.5
	6544-01D	116.99	0.01603	5.43	0.007	115.75	98.57	2.18E-13	1477.4	8.2
	6544-01E	118.9	0.01465	3.8	0.00724	117.4	98.43	1.84E-13	1491.3	9
	6544-01F	120.22	0.01733	3.68	0.0061	118.99	98.72	3.06E-13	1505.4	7
	6544-01G	122.81	0.01486	1.9	0.00695	121.04	98.43	3.38E-13	1522.9	6.2
	6544-01H	123.05	0.01692	3.77	0.00633	121.76	98.7	2.67E-13	1529	8.4
	6544-01I	122.6	0.0194	3.3	0.0081	120.7	98.23	8.41E-14	1520	17
	6544-01J	130.9	0.0195	10.2	0.01062	129.4	98.18	1.42E-13	1593	12
RP-W3/ Plagioclase	6543-02A	64.9	0.0112	24	0.0631	48.7	73.8	4.28E-15	771	73
	6543-02B	54.94	0.0094	1.1	0.0059	53.3	96.92	2.46E-14	829	13
	6543-02C	66.2	0.01391	1.4	0.00412	65.14	98.31	7.01E-14	971.7	7.3
	6543-02D	64.94	0.01215	4.05	0.00283	64.58	99.18	2.93E-13	965.3	3.9
	6543-02E	65.02	0.01221	4.76	0.00257	64.83	99.38	8.10E-13	968.1	3.4
	6543-02F	68.38	0.01226	3.02	0.00274	67.93	99.14	2.20E-13	1003.6	5
	6543-02G	103.1	0.0138	-4.4	0.0047	101.1	98.3	1.85E-14	1345	39
	6543-02H	167.8	0.0132	9.5	0.01603	164.8	97.58	2.06E-13	1861	12
	6543-02I	313.7	0.0151	6.1	0.0278	307.1	97.5	1.14E-13	2658	32
	6543-02J	239.4	0.0164	7.5	0.01948	235.4	97.81	3.06E-13	2300	15

Table 6. $^{39}\text{Ar}/^{40}\text{Ar}$ analytical data obtained from plagioclase and amphibole of the Huanchaca Intrusive Suite (LG-70).

SAMPLE/ MATERIAL	Lab #	$^{40}\text{Ar}/$ ^{39}Ar	$^{38}\text{Ar}/$ ^{39}Ar	$^{37}\text{Ar}/$ ^{39}Ar	$^{36}\text{Ar}/$ ^{39}Ar	$^{40}^*\text{Ar}/$ ^{39}Ar	% $^{40}^*\text{Ar}$	^{40}Ar (Mols)	Age (Ma)	\pm Ma
LG-70/ Amphibole	6554-01A	103	0.072	38	0.058	91	86.1	3.32E-15	1250	200
	6554-01B	59.64	0.0149	6.9	0.0108	57.21	95.48	6.98E-14	877.9	6.9
	6554-01C	71.7	0.01201	3.44	0.0024	71.41	99.37	1.90E-13	1042.6	5.3
	6554-01D	73.9	0.01331	0.8	0.0014	73.58	99.52	3.20E-13	1066.5	5.1
	6554-01E	73.62	0.01374	1.05	0.00143	73.32	99.53	2.86E-13	1063.7	4.3
	6554-01F	70.59	0.01375	2.45	0.00271	70.09	99.12	1.57E-13	1027.9	5.9
	6554-01G	69.81	0.016	3	0.00432	68.89	98.48	5.50E-14	1014	10
	6554-01H	71.55	0.01336	2.64	0.00158	71.41	99.63	2.29E-13	1042.6	5.4
	6554-01I	70.6	0.012	6.5	0.00328	70.4	99.32	5.00E-14	1032	12
	6554-01J	73.4	0.0172	5	0.0015	73.5	99.9	2.56E-14	1066	21
	LG-70/ Plagioclase	6556-01A	240	0.141	184	0.59	90	32.7	6.88E-15	1240
6556-01B		299	0.155	4	0.702	89.9	30	4.03E-14	1237	63
6556-01C		159.6	0.0706	49	0.223	100.2	60.7	1.94E-14	1337	67
6556-01D		84.3	0.0391	18.1	0.0149	82.3	96.39	4.04E-14	1160	18
6556-01E		78.9	0.0407	6.3	0.00488	78.27	98.77	8.29E-14	1117.1	9.8
6556-01F		78.53	0.0383	2.4	0.00594	77.07	97.98	7.95E-14	1104.3	8.8
6556-01G		79	0.0438	4.6	0.0032	78.7	99.26	3.96E-14	1122	15
6556-01H		79.9	0.0412	11.1	0.0057	79.6	98.94	2.72E-14	1132	21
6556-01I		79.8	0.0385	11.9	0.01324	77.4	96.19	6.37E-14	1108	13
6556-01J		107.7	0.0543	117	0.1178	88.6	75.6	2.85E-14	1224	35

4 CONCLUSÕES E CONSIDERAÇÕES FINAIS

A partir da abordagem multidisciplinar, que envolveu mapeamento geológico, análises petrográfica, litoquímica e geocronológica (U-Pb ID-TIMS e Ar-Ar) foi possível caracterizar os enxames de diques das suítes intrusivas Huanchaca, Rancho de Prata e Rio Perdido, bem como as soleiras máficas Huanchaca, Salto do Céu e Rincón del Tigre.

A Suíte Salto do Céu aflora na região dos municípios de Salto do Céu e Rio Branco (MT) como soleiras e derrames. As soleiras encontram-se alojadas em rochas pelíticas, até então inseridas como parte do Grupo Aguapeí, com baixos valores de mergulho, quase sempre para WSW. Os derrames recobrem a mesma unidade sedimentar e apresentam estruturas verticais internas e de topo, típicas de fluxos basálticos de pequena espessura. Vesículas e amígdalas, além de feições como dobras de fluxo e brechas são comumente observadas. Petrograficamente, essas rochas são mesocráticas a melanocráticas, cinza-esverdeadas a pretas, equigranulares variando, em geral, de muito finas até médias. As soleiras são compostas por diabásios e gabros maciços que ao microscópio apresentam texturas ofítica, subofítica, intergranular e coronítica. Constituem-se, essencialmente, por plagioclásio e piroxênio, tendo como minerais acessórios: opacos, cristais aciculares de apatita e subédricos de titanita. Os derrames constituem-se de basaltos e diabásios com texturas ofítica, subofítica, hialofítica, porfirítica ou amigdaloidal em matriz pseudo-traquítica e, em alguns exemplares, vitrofítica. Os componentes principais correspondem a cristais de plagioclásio e piroxênio, além de vidro reliquiar. As amígdalas são arredondadas a elipsoidais, preenchidas por material fibroso a fibro-radiado, composto por zeólitas, clorita, fluorita e opacos. As soleiras e derrames têm afinidade toleítica, sendo classificadas como basaltos gerados em ambiente intraplaca continental. Essa unidade apresenta idade U-Pb (ID-TIMS), obtida em badeleíta, de 1439 ± 4 Ma (Teixeira *et al.*, 2015a). Dados geocronológicos Ar-Ar em plagioclásio e anfibólio, forneceram idades plateau de 1021 ± 5 Ma e integrada de 1385 ± 9 Ma, respectivamente.

O enxame de diques máficos da Suíte Intrusiva Rancho de Prata foi identificado em diversos sítios nas regiões de Nova Lacerda e Conquista D'Oeste (MT), ao longo de uma faixa com direção NNW, de aproximadamente 30 km de largura e 150 km de extensão, se apresentando como um enxame de intrusões paralelas, orientadas segundo a direção N30°–40°W com mergulhos íngremes. Exibem-se isentos de deformação e metamorfismo e mantêm contato intrusivo com as rochas gnáissicas, graníticas e metavulcanossedimentares do

embasamento. As rochas dessa unidade caracterizam-se como gabros, diabásios e basaltos, faneríticos, afaníticos a porfiríticos, de granulação muito fina a média. Apresentam-se melanocráticas de cor cinza-escuro a preta, exibindo estrutura maciça, por vezes com foliação discreta paralela às paredes do dique. Microscopicamente, essas rochas são holo a hipocristalinas, e apresentam textura porfirítica, intergranular, sub-ofítica a ofítica, sendo constituídas, predominantemente, por plagioclásio, clino e ortopiroxênio, olivina e anfibólio. Nos basaltos encontra-se esporadicamente vidro intergranular de cor marrom-escuro. Litoquimicamente classificam-se como basaltos e andesi-basaltos. O magmatismo é do tipo subalcalino e toleítico que, pelas características químicas, se assemelham a basaltos continentais. Os padrões de distribuição dos elementos terras raras (ETR) estão em dois grupos: um fortemente fracionado e enriquecido em ETR leves e outro com pouco fracionamento, com razões médias La/Yb, respectivamente, iguais a 3,22 e 1,26. Idade U-Pb (ID-TIMS), em badeleíta, de 1387 ± 17 Ma (Teixeira *et al.*, 2015a) foi obtida para este enxame. Dados Ar-Ar em plagioclásio apresentam idades plateaus de 967 ± 5 Ma e 980 ± 7 Ma. Já os dados em anfibólio são heterogêneos, com idades integradas de 1495 ± 8 Ma e 1509 ± 7 Ma.

As soleiras e os diques máficos da Suíte Intrusiva Huanchaca estão inseridos no contexto geológico do Terreno Paraguá, em sua porção não afetada pelos efeitos da Orogenia Sunsás (1,1 a 0,9 Ga). Os diques têm como encaixantes rochas do embasamento do Grupo Aguapeí, representadas pelos granitos mesoproterozoicos Guaporeí e Passagem, ambos do Complexo Granitoide Pensamiento, e ortognaisses paleoproterozoicos Shangri-lá e Turvo, do Complexo Metamórfico Chiquitania; enquanto as soleiras encontram-se alojadas nos pelitos e arenitos da Formação Vale da Promissão, Grupo Aguapeí. As soleiras afloram como blocos e lajedos com contatos sempre abruptos e paralelos ao acamamento das rochas sedimentares. Os diques afloram em pequenas e descontínuas cristas orientadas segundo a direção ENE ou como blocos arredondados a angulosos, isolados no terreno granítico-gnáissico, cuja direção preferencial varia entre N70°-90°E. As soleiras, caracterizadas por gabros e diabásios, exibem cor cinza-esverdeado a preta e granulação fina a média. Opticamente, são rochas holocristalinas de textura sub-ofítica a ofítica e, mais raramente, intergranular. Rochas cumuláticas, de ocorrência restrita, foram identificadas com paragênese e texturas semelhantes diferenciando-se pela presença de olivina e grande quantidade de minerais máficos. As rochas das soleiras consistem, essencialmente, de plagioclásio, piroxênio, anfibólio, opacos, e em algumas delas, feldspato alcalino e quartzo com intercrescimento

gráfico. Os diques apresentam cor cinza-escuro a cinza-esverdeado, granulação variando da margem para a porção central do corpo de muito fina ou vítrea a média, respectivamente. Classificam-se como diabásios e basaltos, respectivamente holo e hipocristalinos, constituídos essencialmente por plagioclásios, piroxênios e olivina. Ao exame óptico, os diabásios apresentam texturas inequigranular, sub-ofítica e subordinadamente ofítica, granulação fina a média, enquanto nos basaltos domina textura porfirítica, glomeroporfirítica, vitrofírica e, mais raramente, intersertal e hialofítica. Litoquimicamente, os diques e soleiras classificam-se como basaltos andesíticos de magmatismo subalcalino do tipo toleítico, de ambiente intraplaca continental. Os ETR mostram que as rochas das soleiras são mais enriquecidas em ETRtotais do que as dos diques e apresentam uma considerável variação vertical ao envelope, no entanto a ele paralelizada. Idades plateaus Ar-Ar foram obtidas para as soleiras, tanto para o plagioclásio (948 ± 5 Ma) como para o anfibólio (1113 ± 11 Ma). Ainda para as soleiras, foi conseguida uma idade U-Pb (ID-TIMS), em badeleíta, de $1111,5 \pm 1,9$ Ma (Teixeira *et al.*, 2015b).

O enxame de diques da Suíte Intrusiva Rio Perdido ocorre encaixado em rochas paleoproterozoicas, ao longo do Terreno Rio Apa (SW do MS) e no Paraguai. Os diques são tabulares a lenticulares, com espessura entre 1 e 30 m, são preferencialmente paralelos segundo as direções N70°-90°E e N70°-90°W, exibem contatos abruptos e discordantes ao trend geral NS. São compostos por diabásios de granulação muito fina a fina e microgabros finos a médios, isotrópicos, sem quaisquer vestígios de deformação dúctil e metamorfismo. Ao microscópio, classificam-se como holocristalinos, com textura ofítica a subofítica, intergranular, por vezes porfirítica, e localmente quenching, com morfologia do tipo “cauda de andorinha”. Constituem-se essencialmente por plagioclásio, piroxênios e olivina. Apresentam trend toleítico, com enriquecimento em FeO_t em relação ao MgO para valores de álcalis relativamente constantes. Classificam-se como basaltos e basaltos andesíticos e quanto à ambiência tectônica, se assemelham à basaltos intraplaca fanerozoicos. O comportamento dos ETR, mostra forte fracionamento de ETR pesados em relação aos ETR leves, com razões La/Yb entre 2,8 e 6,2, com anomalia pouco expressiva ou inexistente de Eu. Dados recentes U-Pb (ID-TIMS), em badeleíta, forneceram idade de 1110 Ma (Teixeira *et al.*, 2016).

O Complexo Ígneo Rincón del Tigre corresponde a uma intrusão acamadada, espessa, alojada em rochas do Grupo Sunsás (abaixo) e Grupo Vibosi (acima). Foi denominado na região de Rincón del Tigre (Bolívia), e caracterizado como um registro ígneo relacionado à Orogenia Sunsás. As rochas que compõem esse complexo foram litoestratigraficamente

divididas em três unidades: Ultramáfica (basal), Máfica (intermediária) e Félsica (superior). A Unidade Ultramáfica constitui-se por dunito serpentinizado, harzburgito, olivina bronzitito, bronzita picrito e melanorito, enquanto a Unidade Máfica por norito e gabro. A Unidade Félsica está representada por granófiro. Idade U-Pb (ID-TIMS), em badeleíta, de $1110,4 \pm 1,8$ Ma (Teixeira *et al.*, 2015b), obtida a partir de amostra coletada da Unidade Félsica, demonstram similaridade cronológica com rochas de suítes graníticas sin e pós-orogênicas que ocorrem na província Sunsás-Aguapeí, na Bolívia e no Brasil.

Com base em dados K-Ar, disponíveis na literatura (Barros *et al.*, 1982; Santos *et al.*, 1979; Leite *et al.*, 1985), com valores entre 845 e 1006 Ma, as unidades descritas eram tectonicamente agrupadas a um evento magmático responsável pela geração de LIP associada à tentativa de ruptura do supercontinente Rodínia (Ruiz *et al.*, 2010a; Século *et al.*, 2011; Lima *et al.*, 2012).

A partir de novos resultados geocronológicos de precisão (U-Pb TIMS em badeleíta e Ar-Ar em anfibólio e plagioclásio) e dados de campo e petrológicos, constatou-se que os registros ígneos estudados não se vinculam aos processos geodinâmicos responsáveis pela ruptura do supercontinente Rodínia, mas a eventos tectônicos que antecederam a aglutinação desse supercontinente.

Foram distinguidos dois episódios magmáticos fissurais de expressão regional: o mais antigo entre 1439 e 1387 Ma, restrito ao Terreno Jauru, e o mais jovem em torno de 1110 Ma, verificado nos Terrenos Paraguá e Rio Apa.

O episódio ectasiano-calymmiano (1439 a 1387 Ma), marcado pelo enxame de diques Rancho de Prata e derrames e soleiras Salto do Céu, é de natureza bimodal e restringe-se geotectonicamente ao Terreno Jauru e temporalmente enquadra-se como pós-cinemático em relação à Orogenia Santa Helena. Apesar da abertura do sistema Ar-Ar em torno de 1000 Ma, em decorrência do aquecimento regional provocado pela evolução da Faixa Aguapeí, tanto as encaixantes sedimentares como as rochas máficas (Suítes Rancho de Prata e Salto do Céu) e ácidas (Suíte Rio Branco), mostram-se sem registro de deformação dúctil.

O episódio esteniano (~ 1100 Ma) é de natureza unimodal, abrange vasta área nos terrenos Paraguá e Rio Apa, representado pelas suítes Huanchaca, Rio Perdido e pelo Complexo Rincón del Tigre, integram uma LIP esteniana na porção sul-sudoeste do Cráton Amazônico, evoluída durante uma tentativa de ruptura continental provavelmente relacionada à implantação do Aulacógeno Aguapeí e deposição dos sedimentos siliciclásticos do Grupo Aguapeí. Os enxames de diques máficos foram poupados pela deformação Sunsás no Terreno

Rio Apa e na região da Serrania Huanchaca, enquanto na região de Rincón del Tigre, foi afetado pela deformação e metamorfismo provocados pela evolução da Faixa Sunsás (Litherland *et al.*, 1986; Teixeira *et al.*, 2010).

REFERÊNCIAS

- Almeida F.F.M. 1967. Origem e evolução da Plataforma Brasileira. Rio de Janeiro, DNPM/DGM, 36 p. (Boletim 241).
- Almeida F.F.M., Brito-Neves B.B., Carneiro C.D.R. 2000. The origin and evolution of the South American Platform. *Earth-Science Reviews*, **50**:77-111.
- Almeida F.F.M. 1974. Evolução Tectônica do Cráton do Guaporé comparada com a do Escudo Báltico. *Revista Brasileira de Geociências*, **4**(3):191-201.
- Almeida F.F.M., Hasui Y., Fuck R.A. 1981. Brazilian structural provinces: Na introduction. *Earth Sciences Reviews*, **17**:1-29.
- Amaral G. 1974. *Geologia Pré-Cambriana da Região Amazônica*. Tese de Doutorado, Universidade de São Paulo, São Paulo, 212 p.
- Araújo H.J.T., Santos Neto A., Trindade C.A.H., Pinto J.C.A., Montalvão R.M.G., Dourado T.D.C., Palmeira R.C.B., Tassinari C.C.G. 1982. *Folha SF. 21 – Campo Grande*. Rio De Janeiro, Ministério das Minas e Energia-Secretaria Geral, Projeto RADAMBRASIL – Geologia, 28:23-124.
- Araújo L.M.B., Godoy A.M., Ruiz A.S., Souza M.Z.A. 2005. Soleiras Máficas Tonianas (Suíte Intrusiva Salto do Céu) no SW do Cráton Amazônico: regime extensional relacionado à Orogenia Sunsás? *In: Simpósio de Geologia do Centro Oeste. Goiânia, Resumos*, p. 155-156.
- Araújo L.M.B., Godoy A.M., Ruiz A.S., Manzano J.C., Souza M. Z. A. 2007. Geologia e Geoquímica do Batólito Rapakivi Rio Branco, SW do Cráton Amazônico - MT. *Geologia USP - Série Científica*, **7**:57-72.
- Araújo L.M.B. 2008. *Evolução do magmatismo pós-cinemático do Domínio Cachoeirinha: Suítes Intrusivas Santa Cruz, Alvorada e Rio Branco–SW do Cráton Amazônico–MT*. Tese de Doutorado, Universidade Estadual Paulista, Rio Claro, 158 p.
- Araújo L.M.B., Godoy A.M., Zanardo A. 2009. As Rochas Básicas Intrusivas das Suítes Rio Branco e Salto Do Céu, na região de Rio Branco (MT) Sudoeste do Cráton Amazônico. *Revista Brasileira de Geociências*, **39**:289-303.
- Araújo L.M.B., Godoy A.M. 2011. Magmatismo o Batólito Rapakivi Rio Branco, SW do Cráton Amazônico (MT). *Geociências*, **30**:173-195.
- Barros A.M., Silva R.H., Cardoso O.R.F.A., Freire F.A., Souza Jr. J.J., Rivetti M., Luz D.S., Palmeira R.C., Tassinari C.C.G. 1982. *Folha SD.21. - Cuiabá*. Rio de Janeiro, Ministério das Minas e Energia-Secretaria Geral, Projeto RADAMBRASIL, 26:25-192.
- Bettencourt J.S., Leite Jr. W.B., Ruiz A.S., Matos R., Payolla B.L., Tosdal R.M. 2010. The Rondonian-San Ignacio Province in the SW Amazonian Cráton: An Overview. *Journal of South American Earth Sciences*, **29**:28-46.
- Boger S.D., Raetz M., Giles D., Etchart E., Fanning C.M. 2005. U-Pb Age data from the Sunsas Region of eastern Bolivia, evidence for the allochthonous origin of the Paragua Block. *Precambrian Research*, **139**:121-146.
- Cordani U.G., Tassinari C.C.G., Teixeira W., Basei M.A.S., Kawashita K. 1979. Evolução Tectônica da Amazônia com base nos dados geocronológicos. *In: Congresso Geológico Chileno, 2, Chile. Actas*, p.137-48.
- Cordani U.G., Sato K., Teixeira W., Tassinari C.C.G., Basei M.A.S. 2000. Crustal evolution of South America Platform. *In: Cordani U.G., Milani E.J., Thomaz Filho A., Campos D.A. (eds.) Tectonic Evolution of South America*, Rio de Janeiro p. 19-40.
- Cordani U.G., Teixeira W., Tassinari C.C.G., Ruiz, A.S. 2010. The Rio Apa Craton in Mato Grosso do Sul (Brazil) and Northern Paraguay: Geochronological Evolution, Correlations and Tectonic Implications for Rodinia and Gondwana. *American Journal of Science*, **310**:1-43.
- Corrêa da Costa P.C., Girardi V.A.V., Matos J.B., Ruiz A.S. 2009. Geocronologia Rb-Sr e Características Geoquímicas dos Diques Máficos da Região de Nova Lacerda e Conquista D'Oeste (MT), Porção Sudoeste do Cráton Amazônico. *Geologia USP - Série Científica*, **9**: 115-132.
- Deino A. & Potts R. 1990. Single-crystal $^{40}\text{Ar}/^{39}\text{Ar}$ dating of the Ologesailie Formation, southern Kenya rift. *Journal of Geophysical Research*, **95**:8453-8470.

- Faleiros F.M., Pavan M., Remédio M.J., Rodrigues J.B., Almeida V.V., Caltabeloti F.P., Pinto L.G.R., Oliveira A.A., Pinto de Azevedo E.J., Costa V.S. 2016. Zircon U–Pb ages of rocks from the Rio Apa Cratonic Terrane (Mato Grosso do Sul, Brazil): New insights for its connection with the Amazonian Craton in pre-Gondwana times. *Gondwana Research*, **34**:187–204.
- Geraldes M.C. 2000. *Geocronologia e geoquímica do plutonismo mesoproterozoico do SW do Estado de Mato Grosso (SW do Cráton Amazônico)*. Tese de Doutorado, Universidade de São Paulo, São Paulo, 193 p.
- Geraldes M.C., Van Schmus W.R., Condie K.C., Bell S., Teixeira W., Babinski M. 2001. Proterozoic geologic evolution of the SW part of the Amazonian Craton in Mato Grosso state, Brazil. *Precambrian Research*, **111**:91-128.
- Geraldes M.C., Bettencourt J.S., Teixeira W., Matos J.M. 2004. Geochemistry and isotopic constraints on the origin of the mesoproterozoic Rio Branco „anorogenic“ plutonic suite, SW of Amazonian craton, Brazil: high heat flow and crustal extension behind the Santa Helena arc? *Journal of South American Earth Sciences*, **17**:195-208.
- Girardi V.A.V., Corrêa da Costa P.C., Teixeira W. 2012. Petrology and Sr e Nd characteristics of the Nova Lacerda dike swarm, SW Amazonian craton: new insights regarding its subcontinental mantle source and Mesoproterozoic geodynamics. *International Geology Review*, **54**:165-182.
- Godoi H.O., Martins E.G., Mello C.R., Scislawski G. 2001. *Folhas Corumbá (SE. 21-Y-D), Aldeia Tomázia, (SF. 21-V-B) e Porto Murtinho (SF. 21-V-D). Escala 1:250.000*. Rio De Janeiro, Ministério das Minas e Energia-Secretaria Geral, Programa Levantamentos Geológicos Básicos do Brasil.
- Issler R.S. 1977. Esboço geológico-tectônico do Cráton do Guaporé. *Revista Brasileira de Geociências*, **7**(3):177-211.
- Janoušek V., Farrow C.M., Erban V. 2006. Interpretation of whole-rock geochemical data in igneous geochemistry: introducing Geochemical Data Toolkit (GCDkit). *Journal of Petrology*, **47**(6):1255-1259.
- Klinck B.A. & Litherland M. 1982. A model for the Proterozoic structural history of eastern Bolivia. *Rep. East. Bolivia Miner. Expl. Proj. Santa Cruz*, BAK/15.
- Kuiper K.F., Deino A., Hilgen F.J., Krijgsman W., Renne P.R., Wijbrans, J.B. 2008. Synchronizing Rock Clocks of Earth History. *Science*, **320**:500-504.
- Lacerda Filho J.W., Brito R.S.C., Silva M.G., Oliveira C.C, Moreton L.C., Martins E.G., Lopes R.C., Lima T.M., Larizzatti J.H., Valente C.R. 2006. *Geologia e Recursos Minerais do Estado de Mato Grosso do Sul*. Convênio CPRM/SICME - MS, MME, p. 10-28.
- Leite J.A.D., Saes, G.S., Weska R.K. 1985. A Suíte Intrusiva Rio Branco e o Grupo Aguapeí na serra de Rio Branco, Mato Grosso. *In: Simpósio de Geologia do Centro Oeste. Goiânia, Resumos*, p. 247-255.
- Leite J.A.D. & Saes, G.S. 2000. Geology of southern Amazon Craton, in southwestern Mato Grosso, Brazil: a review. *Revista Brasileira de Geociências*, **30**(1):91-94.
- Lima G.A. 2008. *Geologia da Porção Nordeste da Serra Ricardo Franco (MT) - Região da Fazenda Paredão: ênfase nas Soleiras Máficas-Ultramáficas da Suíte Intrusiva Huanchaca*. Trabalho de Conclusão de Curso, Instituto de Ciências Exatas e da Terra, Universidade Federal de Mato Grosso, Cuiabá, 64 p.
- Lima G.A. 2011. *Geologia, Geoquímica e Geocronologia dos sills máficos da Suíte Intrusiva Huanchaca na porção nordeste da Serra Ricardo Franco (MT) – SW do Cráton Amazônico*. Dissertação de Mestrado, Instituto de Ciências Exatas e da Terra, Universidade Federal de Mato Grosso, Cuiabá, 62 p.
- Lima G.A., Sousa M.Z.A., Ruiz A.S., D'agrella Filho M.S., Vasconcelos P. 2012. Sills máficos da Suíte Intrusiva Huanchaca - SW do Cráton Amazônico: registro de magmatismo fissural relacionado à ruptura do Supercontinente Rodínia. *Revista Brasileira de Geociências*, **42**:111-129.
- Lima G.A., Macambira M.J.B., Sousa M.Z.A., Ruiz A.S., Batata M.E.F., Pierosan R. (subm.). Geologia e Petrologia da Suíte Salto do Céu (MT): Implicações Tectônicas e Estratigráficas para o SW do Cráton Amazônico. *Brazilian Journal of Geology*.
- Litherland M., Annells R.N., Appleton J.D., Berrangé J.P., Bloomfield K., Burton C.C.J., Darbyshire D.P.F., Fletcher C.J.N., Hawkins M.P., Klinck B.A., Llanos A., Mitchell W.I., O'Connor E.A., Pitfield

- P.E.J., Powe, G., Webb B.C. (eds.). 1986. *The Geology and Mineral Resources of the Bolivian Precambrian Shield*. London, British Geological Survey Overseas Memoir, 9, 153 p.
- Ludwig K.R. 2003. Isoplot/EX 3. A Geochronological Toolkit for Microsoft Excel. Special Publication 4. Berkeley Geochronological Center.
- Matos J.B. 1994. *Contribuição à geologia de parte da porção meridional do Cráton Amazônico, região do Rio Alegre-MT*. Dissertação de Mestrado, Instituto de Geociências, Universidade de São Paulo, São Paulo, 133 p.
- Matos J.B., Schorscher J.H.D., Geraldtes M.C., Sousa M.Z.A., Ruiz A.S. 2004. Petrografia, geoquímica e geocronologia das rochas do Orógeno Rio Alegre, Mato Grosso: um registro de crosta oceânica Mesoproterozoica no SW do Cráton Amazônico. *Geologia USP – Série Científica*, **4**:75-90.
- Matos R., Teixeira W., Geraldtes M.C., Bettencourt J.S., 2009. Geochemistry and isotopic evidence of the Pensamiento Granitoid Complex, Rondonian–San Ignacio province, eastern Precambrian Shield of Bolivia: petrogenetic constraints for a Mesoproterozoic magmatic arc setting. *Geologia USP – Série Científica*, **9**(2):89-117.
- Montalvão R.M.G. 1976. Esboço geológico-tectônico do Cráton Guianês. *Revista Brasileira de Geociências*, **6**(4):230-255.
- Montalvão R.M.G., Silva G.H., Bezerra P.E.L., Pimenta O.N.S. 1979. Coberturas sedimentares e vulcanossedimentares pré-cambrianas das folhas SB-20 Purus, SC-20 Porto Velho e SC-21 Juruena (Plataforma Amazônica). *Revista Brasileira de Geociências*, **9**(1):27-32.
- Montalvão R.G.M. & Bezerra P.E.L. 1980. Geologia e tectônica da Plataforma (Cráton) Amazônica (parte da Amazônia Legal Brasileira). *Revista Brasileira de Geociências*, **10**(1):1-27.
- Monteiro H., Macedo P.M., Silva M.D., Moraes A.A., Marchetto C.M.L. 1986. O „Greenstone Belt“ do Alto Jauru. In: Congresso Brasileiro de Geologia, 34, *Resumos*, p. 630-647.
- Oliva L.A. 1979. Ocorrências Minerais na Folha Cuiabá (SD.21). Relatório de Viagem Goiânia, DNPM, p. 18.
- Pinho F.E.C. 1996. The origin of the Cabaçal Cu-Au deposit, Alto Jauru Greenstone Belt, Brazil. PhD Thesis. University of Western Ontário, Canadá, 211 p.
- Pinho F.E.C., Fyfe, W.S., Pinho, M.A.S.B. 1997. Early proterozoic evolution of the Alto Jauru greenstone belt, southern Amazonian Craton, Brazil. *International Geology Review*, **39**:220-229.
- Reis N.J., Teixeira W., Hamilton M.A., Bispo-Santos F., Almeida M.E., D’Agrella-Filho, M.S. 2013. Avanavero mafic magmatism, a late Paleoproterozoic LIP in the Guiana Shield, Amazonian Craton: U–Pb IDTIMS baddeleyite, geochemical and paleomagnetic evidence. *Lithos*, **174**:175–195.
- Ruiz A.S. 1992. *Contribuição a Geologia do Distrito de Cachoeirinha, MT*. São Paulo. Dissertação de Mestrado, Instituto de Geociências, Universidade de São Paulo, São Paulo, 98 p.
- Ruiz A.S., Geraldtes M.C., Matos J.B, Teixeira W., Van Schmus W.R., Schmitt R. 2004. The 1590-1520 Ma Cachoeirinha magmatic arc and its tectonic implications for the Mesoproterozoic. SW Amazonian Craton crustal evolution. *Anais da Academia Brasileira de Ciências*, **76**(4):807-824.
- Ruiz A.S. 2005. *Evolução Geológica do Sudoeste do Cráton Amazônico Região Limítrofe Brasil-Bolívia – Mato Grosso*. Tese de Doutorado, Universidade Estadual Paulista, Rio Claro, 250 p.
- Ruiz A.S., Simões L.S.A., Corrêa da Costa P.C., Matos J.B., Araújo L.M.B., Godoy A.M., Sousa M.Z.A. 2005. Enxames de diques máficos (Suíte Intrusiva Rancho de Prata) no SW do Cráton Amazônico: indícios de colapso extensional no Orógeno Sunsás? In: Simpósio de Vulcanismo e Ambientes Associados. Cabo Frio, *Resumos*, p. 297-302.
- Ruiz A.S. 2009. Compartimentação Tectônica (Pré-Sunsás) do SW do Cráton Amazônico: ênfase em Mato Grosso – Brasil. In: Congreso Geológico Boliviano, 18, *Actas*, p. 159-163.
- Ruiz A.S., Matos J.B., Sousa M.Z.A., Lima G.A., Batata M.E.F. 2010a. Mapeamento Geológico e Levantamento de Recursos Minerais da Folha Santa Bárbara (SD.21-Y-C-V). Convênio CPRM-UFMT. Programa Geologia do Brasil, Relatório Etapa de Mobilização, 35p.
- Ruiz A.S., D’agrella Filho M.S., Sousa M.Z.A., Lima G.A. 2010b. Tonian sills and mafic dike swarms of S-SW Amazonian Cráton: records of Rodinia Supercontinent break-up? In: The Meeting of the Americas. Foz do Iguaçu, *Short Papers*, p. 3.
- Sadowski G.R., Bettencourt J.S. 1996. Mesoproterozoic tectonic correlations between eastern Laurentia and the western border of the Amazon Craton. *Precambrian Research*, **76**:213–227.

- Saes G.S. 1999. *Evolução Tectônica e Paleogeográfica do Aulacógeno Aguapeí (1.2 – 1.0 Ga) e dos Terrenos do seu embasamento na porção sul do Cráton Amazônico*. Tese de Doutorado, Universidade de São Paulo, São Paulo, 135 p.
- Saes G.S. & Fragoso César A.R.S. 1996. Acresção de terrenos mesoproteróicos no SW da Amazônia. *In: Congresso Brasileiro de Geologia, 39, Resumos*, p. 348.
- Santos R.O.B., Pitthan J.H.L., Barbosa E.S., Fernandes C.A.C., Tassinari C.C.G., Campos D. A. 1979. *Folha SD.20 - Guaporé*. Geologia. Rio De Janeiro, Ministério das Minas e Energia-Secretaria Geral, Projeto RADAMBRASIL – Geologia, 19:21-123.
- Santos J.O.S., Hartmann L.A., Gaudette H.E., Groves D.I., Mcnaughton N.J., Fletcher I.R. 2000. A new understanding of the Amazon Cráton Provinces based on integration of field mapping and U-Pb and Sm-Nd Geochronology, *Gondwana Research*, **3**:453-488.
- Santos J.O.S., Rizzotto G.J., Potter P.E., Mcnaughton N.J., Matos R.S., Hartmann L.A., Chemale Jr F., Quadros M.E.S. 2008. Age and Autochthonous Evolution of The Sunsás Orogen in the West Amazon Cráton based on mapping and U-Pb Geochronology. *Precambrian Research*, **165**:120-152.
- Santos F. 2010. *Caracterização Geológica do Terreno Rio Apa, na região da Fazenda Santa Marta, Porto Murtinho (MS): enfoque no Complexo Metamórfico Rio Apa*. Monografia de Conclusão de Curso, Instituto de Ciências Exatas e da Terra, Universidade Federal de Mato Grosso, Cuiabá, 64 p.
- Século D.B., Ruiz A.S., Sousa M.Z.A., Lima G.A., Batata M.E.F. 2008. Caracterização Geológica e Petrográfica do Enxame de Diques Máficos (Suíte Intrusiva Huanchaca) no Domínio Tectônico Paraguá - SW do Cráton Amazônico - MT. *In: Congresso Brasileiro de Geologia, 44, Resumos*, p. 545.
- Século D.B. 2011. *Geologia, Petrografia e Geoquímica do enxame de diques máficos (Suíte Intrusiva Huanchaca) na região de Vila Bela da Santíssima Trindade (MT) – SW do Cráton Amazônico*. Dissertação de Mestrado, Instituto de Ciências Exatas e da Terra, Universidade Federal de Mato Grosso, Cuiabá, 57 p.
- Século D.B., Ruiz A.S., Sousa M.Z.A., Lima G.A. 2011. Geologia, Petrografia e Geoquímica do Enxame de Diques Máficos da região de Vila Bela da Santíssima Trindade (MT) Suíte Intrusiva Huanchaca SW do Cráton Amazônico. *Geociências*, **30**:561-573.
- Söderlund U. & Johanssen U. 2002. A simple way to extract baddeleyite (ZrO₂). *Geochemistry, Geophysics, and Geosystems*, **3**:1-7.
- Sousa M.Z.A., Batata M.E.F., Ruiz A.S., Lima G.A., Matos J.B., Paz J.D.S., Costa A.C.D., Silva C.H., Corrêa da Costa P.C. 2011. *Geologia da Folha Rio Branco (SD21-Y-D-I)*. Ministério das Minas e Energia. Programa Nacional de Geologia (PRONAGEO). CPRM/UFMT. 178 p.
- Tassinari C.C.G. 1996. *O Mapa Geocronológico do Cráton Amazônico no Brasil: revisão dos dados isotópicos*. Tese de Livre Docência, Universidade de São Paulo, São Paulo, 139 p.
- Tassinari C.C.G. & Macambira M.J.B. 1999. Geochronological Provinces of the Amazonian Craton. *Episodes*, **38**:174-182.
- Tassinari C.C.G., Bettencourt J.S., Geraldés M.C., Macambira M.J.B., Lafon, J.M. 2000. The Amazonian Craton. *In: Cordani U.G., Milani E.J., Thomaz Filho A., Campos D.A. (eds.) Tectonic Evolution of South America*, Rio de Janeiro p. 41-95.
- Tassinari C.G.C. & Macambira, M.J.B. 2004. A Evolução Tectônica do Cráton Amazônico. *In: Neto-Mantesso V., Bartorelli A, Carneiro C.D.R., Brito-Neves B.B. (eds). Geologia do Continente Sul-Americano: Evolução da Obra de Fernando Flávio Marques de Almeida*, São Paulo, p. 471-486.
- Teixeira W., Tassinari C.C.G., Cordani U.G., Kawashita, K. 1989. A review of the Geochronology of the Amazonian Cráton: Tectonic Implications. *Precambrian Research*, **42**: 213-227.
- Teixeira W., Geraldés M.C., Matos R., Ruiz A.S., Saes G., Vargas-Mattos G. 2010. A Review of the tectonic evolution of the Sunsás Belt, SW Amazonian Cráton. *Journal of South American Earth Sciences*, **29**:47-60.
- Teixeira W., D'Agrella-Filho M.S., Hamilton M.A., Ernst R.E., Girardi V.A.V., Mazzucchelli M., Bettencourt J.S. 2013. U-Pb (ID-TIMS) baddeleyite ages and paleomagnetism of 1.79 and 1.59 Ga tholeiitic dyke swarms, and position of the Rio de la Plata Craton within the Columbia supercontinent. *Lithos*, **174**:157-174.
- Teixeira W., Ernst R., Hamilton M.A., Lima G., Ruiz A.S., Geraldés M.C. 2015a. Widespread ca. 1.4 Ga intraplate magmatism and tectonics in a growing Amazonia. *GFF (Uppsala)*, **1**:1-14.

Teixeira W., Hamilton M.A., Lima G.A., Ruiz A.S., Matos R., Erns, R.E. 2015b. Precise ID-TIMS U-Pb baddeleyite ages (1110-1112Ma) for the Rincón del Tigre-Huanchaca large igneous province (LIP) of the Amazonian Craton: Implications for the Rodinia supercontinent. *Precambrian Research*, **265**:273-285.

Teixeira W., Hamilton M.A., Girardi V.A.V., Faleiros F.M. 2016. Key dolerite dyke swarms of Amazonia: U-Pb constraints on supercontinent cycles and geodynamic connections with global LIP events through time. *In: Seventh International Dyke Conference*. Pequim.

Tohver E., Van der Pluijm B., Mezger K., Essene E.J., Scandolaro J.E., Rizzotto G.R. 2004. Significance of the Nova Brasilândia metasedimentary belt in western Brazil: redefining the Mesoproterozoic boundary of the Amazon Craton. *Tectonics*, **23**(6):1-20.

Vasconcelos P.M., Onoe A.T., Kawashita K., Soares A.J., and Teixeira W. 2002. $^{40}\text{Ar}/^{39}\text{Ar}$ geochronology at the Instituto de Geociências, USP: instrumentation, analytical procedures, and calibration. *Anais da Academia Brasileira de Ciências*, **74**:297-342.

Zenardi G.C. 2011. *Geologia, Petrografia e Geoquímica do Complexo Metamórfico Rio Apa na Região de Porto Murtinho-MS*. Trabalho de Conclusão de Curso, Instituto de Ciências Exatas e da Terra, Universidade Federal de Mato Grosso, Cuiabá, 80 p.

ANEXOS – ARTIGOS PUBLICADOS

ANEXO A - PRECISE ID-TIMS U–PB BADDELEYITE AGES (1110–1112 MA) FOR THE INCÓN DEL TIGRE–HUANCHACA LARGE IGNEOUS PROVINCE (LIP) OF THE AMAZONIAN CRATON: IMPLICATIONS FOR THE RODINIA SUPERCONTINENT

ANEXO B - WIDESPREAD CA. 1.4 GA INTRAPLATE MAGMATISM AND TECTONICS IN A GROWING AMAZONIA



Precise ID-TIMS U–Pb baddeleyite ages (1110–1112 Ma) for the Rincón del Tigre–Huanchaca large igneous province (LIP) of the Amazonian Craton: Implications for the Rodinia supercontinent

Wilson Teixeira^{a,*}, Mike A. Hamilton^{b,1}, Gabrielle A. Lima^c, Amarildo S. Ruiz^d, Ramiro Matos^e, Richard E. Ernst^{f,g}

^a Instituto de Geociências, Universidade de São Paulo, São Paulo, SP 05508-080, Brazil

^b Jack Satterly Geochronology Laboratory, Department of Earth Sciences, University of Toronto, 22 Russell St., Toronto, ON M5S 3B1, Canada

^c Programa de Pós-Graduação em Geologia e Geoquímica, Universidade Federal do Pará, Belém, PA 66075-110, Brazil

^d Departamento de Geologia Geral, Universidade Federal de Mato Grosso, Cuiabá, MT 78060-900, Brazil

^e Instituto de Investigaciones Geológicas y del Medio Ambiente, Universidad Mayor de San Andrés, Calle 27, Pabellón Geología, Campus Universitario Cota Cota, La Paz, Bolivia

^f Department of Earth Sciences, Carleton University, Ottawa K1S 5B6, Canada

^g Faculty of Geology and Geography, Tomsk State University, Tomsk 634050, Russia

article info

Article history:

Received 5 February 2014

Received in revised form 26 May 2014

Accepted 14 July 2014

Available online 23 July 2014

Keywords:

Amazonian Craton U–Pb baddeleyite ages

Mafic–ultramafic intrusions

LIPs

Rodinia

abstract

High quality U–Pb (ID-TIMS) baddeleyite ages define the timing of crystallization of the Rincón del Tigre layered intrusion (1110 ± 2 Ma) and the Huanchaca mafic suite (1112 ± 2 Ma) in the Bolivian Precambrian shield – SW portion of the Amazonian Craton. The identical ca. 1110–1112 Ma ages obtained for each (about 500 km apart) suggest these belong to a previously unrecognized LIP. The large area of distribution and the intraplate geochemistry for the 1110 Ma Huanchaca–Rincón del Tigre rocks support a relationship with mantle plume activity pre-dating Rodinia breakup. Contemporary anorogenic magmatism in Amazonia is probably linked to crustal melting caused by the LIP. The newly identified 1110 Ma LIP has a tight age match with intraplate magmatism in the Congo, Kalahari and Indian cratons, and the Keweenaw event of central Laurentia among others. While a reconstruction history of Amazonia and Laurentia is still a matter of debate on paleomagnetic grounds, a reconstruction link with other crustal blocks remains possible.

© 2014 Elsevier B.V. All rights reserved.

1. Introduction

Current knowledge of the Precambrian geology of Eastern Bolivia, SW portion of the Amazonian Craton, is largely a consequence of systematic mapping of the so-called *Proyecto Precambrico* – a British-Bolivian cooperative program of the 1980s. This program established the general geologic relations, structural framework and tectonic significance of the major lithostratigraphic units with the support of reconnaissance geochronological and chemical data (Litherland and Bloomfield, 1981; Berrangé, 1982; Litherland et al.,

1986, 1989). Subsequent efforts have led to a better understanding of the timing and nature of the particular magmatic–tectonic events (e.g., Boger et al., 2005; Vargas-Mattos, 2006; Cordani and Teixeira, 2007; Santos et al., 2002, 2008; Cordani et al., 2009; Matos et al., 2009; Teixeira et al., 2010).

The geologic and tectonic history of Bolivia correlates well with that of the Brazilian portion of the SW Amazonian Craton where the magmatic, sedimentary, and metamorphic histories have revealed a polycyclic evolution of the continental crust, highlighted within the Mesoproterozoic Rondonian–San Ignacio and Sunsas–Aguapeí provinces (e.g., Sadowski and Bettencourt, 1996; Geraldés et al., 2001; Ruiz, 2005; Teixeira et al., 2010; Bettencourt et al., 2010; Rizzotto et al., 2014) – Fig. 1.

From a paleogeographic perspective, Amazonia is a key land-mass within supercontinent cycles and for large igneous provinces – LIPs (e.g., Ernst et al., 2013a, 2014; Reis et al., 2013; Nance et al., 2014). Nevertheless, the position of the proto-Amazonian Craton in plate tectonic reconstructions is a matter of debate, such as within

* Corresponding author. Tel.: +55 11 210 7844; fax: +55 11 210 4958.

E-mail addresses: wteixeir@usp.br (W. Teixeira), mahamilton@geology.utoronto.ca (M.A. Hamilton), gabilimagel@gmail.com (G.A. Lima), asruiz@gmail.com (A.S. Ruiz), rmatos@yahoo.com (R. Matos), Richard.Ernst@ErnstGeosciences.com (R.E. Ernst).

¹ Tel.: +1 416 946 7424.

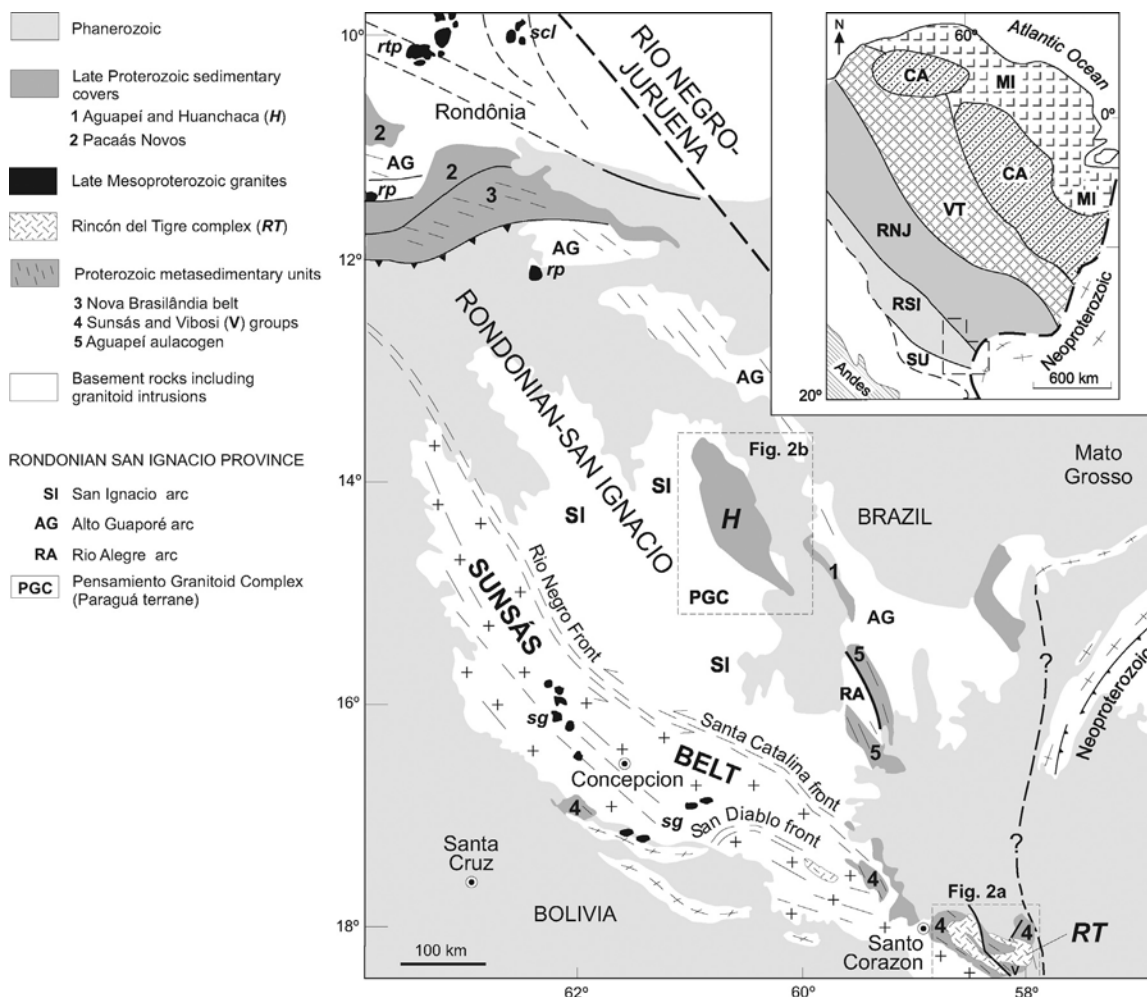


Fig. 1. Geologic–tectonic crustal architecture of the SW Amazonian Craton, showing the investigated areas (squares): the Rincón del Tigre layered intrusion and Huanchaca platform cover where mafic sills occur. The tectonic fronts that outline the northern limit between the Sunsás collisional belt (Sunsás-Aguapeí province) with the Rondonian-San Ignacio province (Pensamiento Granitoid Complex – PGC) are also shown. Geologic units assigned to the Sunsás-Aguapeí province: (a) the Vibosi and Sunsás metasedimentary sequences, the Nova Brasilândia supracrustal belt and Aguapeí aulacogen; (b) platform covers (e.g., Huanchaca, Aguapeí, Pacaás Novos); (c) granitic suites: scl = Santa Clara (1.08–1.07 Ga); sg = Sunsás granites (1.13–1.00 Ga); rp = Rio Pardo (1.05 Ga); rtp = Rondônia Tin Province (0.99–0.97 Ga); rp = Rio Pardo (1.05 Ga). Tectonic provinces (inset): CA = Central Amazonian (>2.6 Ga); MI = Maroni-Itaiciunas (2.25–2.05 Ga); VT = Ventuari-Tapajós (2.00–1.81 Ga); RNJ = Rio Negro-Juruena (1.80–1.60 Ga), RSI = Rondonian-San Ignacio (1.56–1.30 Ga), SA = Sunsás-Aguapeí (1.20–0.97 Ga).

Adapted from Teixeira et al. (2010), Bettencourt et al. (2010) and Rizzotto et al. (2014).

Nuna (also known as Columbia) and Rodinia supercontinents (e.g., Sadowski, 2002; Tohver et al., 2002, 2006; Li et al., 2008; Fuck et al., 2008; Bispo-Santos et al., 2008; Cordani et al., 2009; Johansson, 2009; Casquet et al., 2010; D'Agrella-Filho et al., 2012; Reis et al., 2013).

The Proterozoic growth of Amazonia occurred through a long-lived soft accretion/collision regime from ca. 2.25 to 1.00 Ga, developed outboard from one Archean nucleus (>2.6 Ga; Central Amazonian province) – see Cordani and Teixeira (2007) for a review. As a consequence of this accretionary history, lithostratigraphic units and metamorphic episodes are progressively younger in time and space toward the SW portion of Amazonia. Hence, the Proterozoic crustal architecture encompasses five sub-parallel, NW-trending tectonic provinces, namely: Maroni-Itaiciunas (2.25–2.00 Ga), Ventuari-Tapajós (1.98–1.81 Ga), Rio Negro-Juruena (1.78–1.60 Ga), Rondonian-San Ignacio (1.56–1.30 Ga), and Sunsás-Aguapeí (1.28–0.97 Ga) – see inset; Fig. 1. The youngest province – where the Rincón del Tigre–Huanchaca magmatism (the focus of this study) occurs – results from the 1.11–1.00 Ga Sunsás collisional orogeny (see Teixeira et al., 2010 for review). This orogeny marks the final amalgamation of the Amazonian

Craton during the assembly of Rodinia, and overlaps in time with the Grenville Orogen of Laurentia (e.g., Tohver et al., 2004, 2006; Cordani et al., 2009; Chew et al., 2011).

Alternative scenarios have been put forward for the Precambrian architecture of Amazonia on the basis of geologic correlations of country rocks, U–Pb data, and regional structures and metamorphic patterns. For instance, a few models argue the Sunsás belt is autochthonous, and evolved from 1.45 to 1.10 Ga (e.g., Santos, 2003; Santos et al., 2000, 2008). Nevertheless, this idea contrasts with the observed allochthonous features of the Sunsás orogen (Litherland et al., 1986, 1989), such as the coherent transport of the folded strata of the main belt against the structurally defined Paraguá Craton or terrane as described below (e.g., Litherland and Bloomfield, 1981). In our view, the Paraguá terrane played an important role in the consolidation of the Rondonian-San Ignacio province according to geologic and tectonic evidence (Bettencourt et al., 2010; see Fig. 1). The Santos model is also inconsistent with the observed decrease in U–Pb ages of granitoid rocks in time and spatially, in coherence with coeval geologic units that are ascribed to the evolution of Paleo- to Mesoproterozoic tectonic provinces (see above). These facts are consistent with a stepwise accretionary outgrowth

of the SW Amazonia, as considered in most models (e.g., Sadowski and Bettencourt, 1996; Geraldès et al., 2001; Boger et al., 2005; Ruiz, 2005; Tohver et al., 2006; Cordani and Teixeira, 2007). Consequently, we follow the tectonic model of Cordani and Teixeira (2007) with refinements by Teixeira et al. (2010) and Bettencourt et al. (2010) that consider an evolving accretionary scenario akin to modern arc settings worldwide (e.g., Condie, 2007; Cawood et al., 2009). In addition, an increasing number of paleomagnetic poles obtained from mafic rocks emplaced into the Proterozoic tectonic provinces support a plausible correlation in time and space with other crustal blocks in the world, such as Baltica and Laurentia (e.g., Tohver et al., 2006; D'Agrella-Filho et al., 2008, 2012; Bispo-Santos et al., 2012; Reis et al., 2013). However, systematic deep seismic data are needed to characterize better the internal crustal discontinuities of Amazonia and their potential relationship with Proterozoic global paleogeography.

This paper documents new, high quality U–Pb (ID-TIMS) baddeleyite ages from two widely separated late Proterozoic igneous complexes in the Precambrian shield of Bolivia, namely the Rincón del Tigre mafic–ultramafic layered intrusion and the Huanchaca mafic intrusive suite (e.g., Berrangé, 1982; Litherland et al., 1986; Litherland and Power, 1989; Ruiz, 2005; Lima et al., 2012). The tectonic significance of the ages is addressed in the context of the evolution of the Sunsas orogeny, and as a potential link of the mafic–ultramafic magmatism with a mantle plume event.

2. Geologic–tectonic framework of Eastern Bolivia and its Brazilian counterpart

For the purpose of this work, we summarize first the Precambrian framework of the Eastern Bolivian shield with special emphasis on the Late Mesoproterozoic Sunsas orogeny (Sunsas-Aguapeí province; after Teixeira et al., 2010) to which the Huanchaca and Rincón del Tigre igneous complexes are spatially associated.

The Huanchaca intrusive suite (see Fig. 1) crops out in the Paraguá terrane (or Paraguá Craton; after Litherland and Bloomfield, 1981). Much of the Paraguá terrane was formed during the San Ignacio orogeny (1.37–1.34 Ga) that developed on basement rocks older than 1.64 Ga (e.g., Litherland et al., 1986; Darbyshire, 2000; Santos et al., 2008; Matos et al., 2009). This orogeny produced large amounts of crustally-derived granitic plutons in the Paraguá terrane, collectively termed the Pensamiento Granitoid Complex (e.g., Litherland et al., 1986; Boger et al., 2005; Matos, 2010) – see Fig. 1.

On the Brazilian side (state of Rondônia), continental arc type plutonic rocks coeval with the Pensamiento Granitoid Complex, are also present (e.g., Ruiz, 2005; Santos et al., 2008; Matos et al., 2009; Jesus et al., 2010; Nalon et al., 2013). Collectively, these rocks have been ascribed to the Rondonian-San Ignacio belt, and are good indicators of the youngest arc-type plutonism of a composite orogeny that created the 1.56–1.30 Ga Rondonian-San Ignacio province (see Bettencourt et al., 2010 for review). Of note, older Mesoproterozoic plutons that also occur in portions of this province in Brazil were produced by various precedent arcs that resulted from convergence between the Paraguá terrane and the Rio Negro-Juruena province, such as the Rio Alegre (1.51–1.38 Ga) and the Alto Guaporé (ca. 1.47–1.43 Ga) – see Fig. 1. For instance, both belts contain remnants of mafic–ultramafic rocks, as well as chemical and clastic sedimentary assemblages (e.g., Bettencourt et al., 2010 and references therein). The Alto Guaporé rocks, in particular, were overprinted by high-grade metamorphism and deformation, accompanying the emplacement of gabbros and granites at 1.35–1.34 Ga (Rizzotto and Hartmann, 2012; Rizzotto et al., 2014). Therefore the Alto Guaporé belt is coeval with the Pensamiento Granitoid Complex.

From a geodynamic point of view, the propagation and stacking of magmatic arcs during the Mesoproterozoic (see above) has led to progressive consumption of the intervening oceanic lithosphere and eventual final docking of the Paraguá terrane onto the SW portion of the Rio Negro-Juruena province at ca. 1.30 Ga (e.g., Bettencourt et al., 2010 and references therein). However, Santos et al. (2008) mention a discrete granitic episode in Bolivia (attributed by them to the so-called Candeias orogeny) such as the weakly foliated 1275 ± 7 Ma San Andres pluton (not shown). In any case this suggests that the juxtaposition of the Paraguá terrane might be slightly younger than previously thought. Eventually, the Sunsas collisional orogeny, characterized by an allochthonous-type belt (1130–1000 Ma), developed along the southern margin of the Paraguá continental crust, consolidating the Precambrian crustal evolution of Amazonia.

2.1. Sunsas belt

This belt comprises supracrustal rocks (the Sunsas and Vibosi Groups) intruded by syn- to late tectonic granitic suites, mafic dykes, as well as the Rincón del Tigre layered complex. Post-tectonic to anorogenic plutons are also present, expressed as a suite of A-type granites (see Fig. 1). All these rocks are attributed to the Sunsas-Aguapeí province (after Teixeira et al., 2010). A basement paragneiss yields a zircon U–Pb recrystallization age of 1118 Ma (Santos et al., 2008), approximating the timing of peak metamorphism within the Sunsas belt.

The Sunsas granites yield U–Pb crystallization ages between 1105 and 1004 Ma, and are related to lower crustal anatexis according to isotopic evidence (e.g., Litherland et al., 1986; Boger et al., 2005; Santos et al., 2008; Vargas-Mattos, 2006; Vargas-Mattos et al., 2009). This age range allows correlation with potential Brazilian counterparts, such as the A-type Santa Clara suite (1082–1074 Ma) and AMCG (anorthosite, mangerite, charnockite, granite) plutons that crosscut both the Rondonian-San Ignacio and Rio Negro-Juruena provinces, and have crystallization ages from 995 to 974 Ma. The youngest intrusions, of anorogenic tectonic affinity, are commonly associated with metal deposits (e.g., Sn, Mo, W) and collectively termed the Rondônia Tin Province (Bettencourt et al., 1999; Sparrenberger et al., 2002) – see Fig. 1.

Prominent shear zones with mylonite belts (ca. 1080–1050 Ma) have a horizontal sense of movement, are collectively named Rio Negro and Santa Catalina, and define the northern front of the Sunsas belt against the Paraguá terrane in Bolivia (Litherland et al., 1986, 1989). These fronts are always directed toward the Paraguá terrane (i.e., NW–SE shortening direction), and likewise the southward San Diablo front, together with an associated large-scale transcurrent motion (see Fig. 1) are good indications of the allochthonous character of the Sunsas collisional belt (Landivar and Gonzalez, 1997; Litherland et al., 1986; Boger et al., 2005; Matos, 2010).

Low-grade equivalents of the Sunsas and Vibosi groups overlie the country rocks with a marked unconformity (Litherland et al., 1986), and have been interpreted as typical sedimentary units of the Sunsas-Aguapeí province (Teixeira et al., 2010 and references therein). Both groups consist of alluvial to deltaic lithologies that originated in an initial passive margin environment, and represent a period of quiescence and erosion of an older continental landmass that was subsequently inverted and folded during the Sunsas collision. Notably, at the southeast tip of the Sunsas belt, metamorphosed Vibosi strata locally unconformably overlie Sunsas Group strata, in the neighborhood of the Rincón del Tigre layered intrusion (e.g., Litherland et al., 1986, 1989). The Sunsas and Vibosi groups are thought to be contemporary with the Huanchaca Group that occurs further north (see Figs. 1 and 2). The latter is a shallow-water, rift type sedimentary sequence

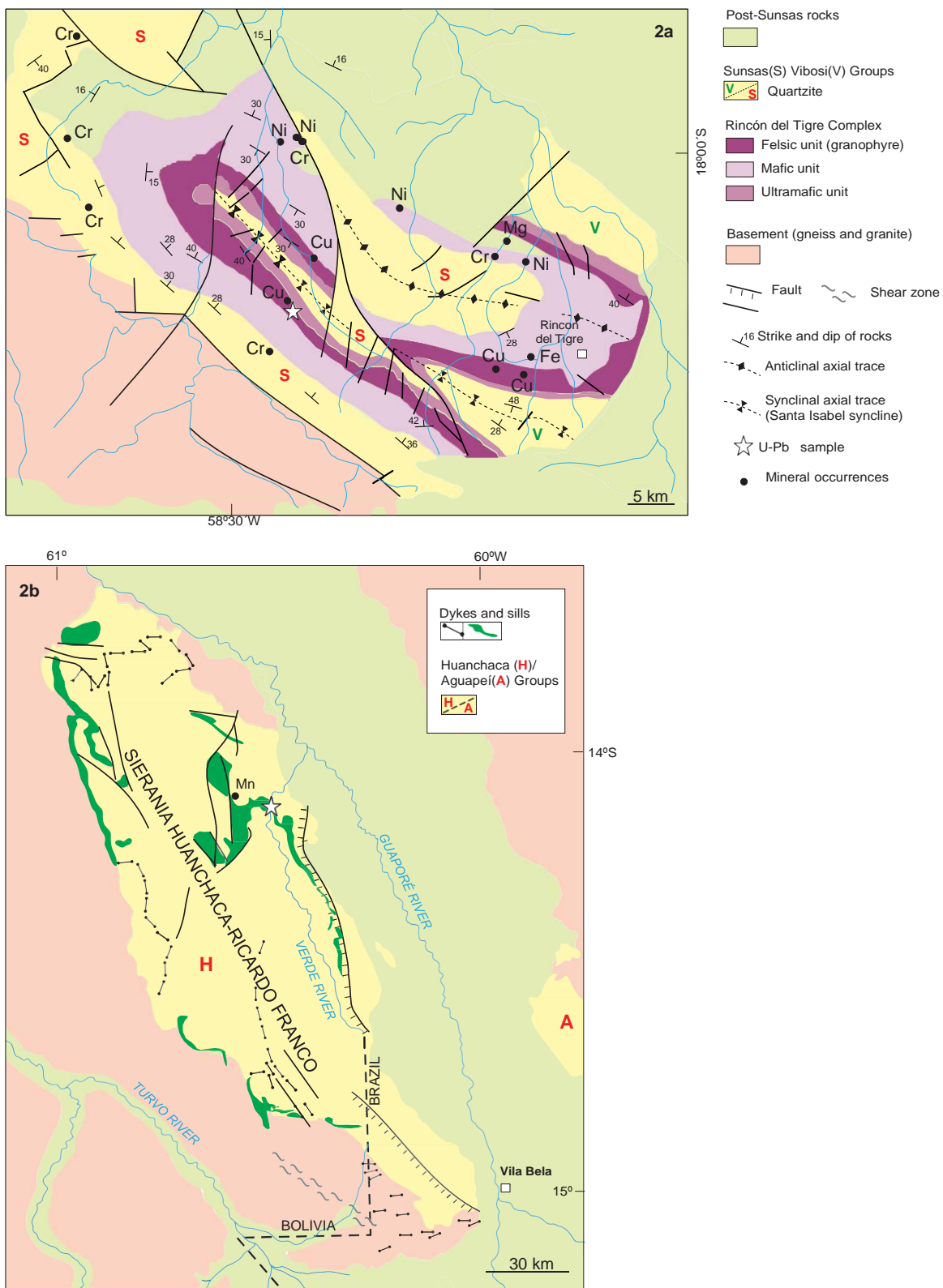


Fig. 2. (a) Geological outline of the Rincón del Tigre complex (after Litherland et al., 1986). The local NW-SW trending structural framework is also shown, as for the entire Sunsas collisional belt; (b) geologic outline of the Huanchaca/Aguapeí Group at the Serrania Huanchaca-Ricardo Franco. This tableland is extensively covered by Cenozoic units (not shown). The morphology of the main sills and dykes as well as the location of the studied sample is also shown. See text for details.

Adapted from Litherland and Power (1989) and Lima et al. (2011).

Table 1

Main geologic and tectonic characteristics of the Sunsas-Aguapeí province, southwestern fringe of the Amazonian Craton (adapted Teixeira et al., 2010). *Keys:* RSI (Rondonian-San Ignacio province; 1.56–1.30 Ga), RNJ (Rio Negro-Juruena province; 1.78–1.60 Ga). See text and Fig. 1 for details.

Characteristics of the Province	Major tectonic features	Main regional units, including syn- to late orogenic granitoids	Post-tectonic and anorogenic intrusions
<i>Sunsas orogeny</i> (1100–1000 Ma): collisional arc (allochthonous type) at the southern margin of the Paraguá terrane. Widespread inboard effects (over the RSI and RNJ provinces)*	Rio Negro, Santa Catalina and San Diablo fronts.	Granitoid rocks (1.10–1.07 Ga). Passive margin sequences: Sunsas and Vibosi Groups (<1.17 Ga). Platform covers: Huanchaca and Aguapeí Groups (inside the Paraguá terrane) and Pacaás Novos Fm. (<1.20 Ga) and coeval rift units over the RSI and RNJ provinces.	Santa Clara suite (1.08–1.07 Ga). Hunchaca intrusive suite and Rincón del Tigre complex (1.10 Ga). [#]
	Reactivation and magmatism overprinting the RSI: (i) crustal shortening with granite emplacement (Rio Pardo suite (1.05 Ga) in the Nova Brasilândia belt (1.13–1.00 Ga); (ii) Aguapeí aulacogen and nearby mylonite belts (0.95–0.91 Ga).		Granitic suites (Rondonian Tin Province; Rio Pardo): 0.99–0.90 Ga. Guapéí granitic suite (0.95–0.92 Ga).

[#] This work.

that unconformably overlies the Pensamiento Granitoid Complex (e.g., Souza and Hildred, 1980; Litherland et al., 1986; Ruiz, 2005; Santos et al., 2005; Vargas-Mattos et al., 2007; Lima et al., 2012). This granitoid complex is not affected by the Sunsas deformation and metamorphism, as indicated by the much older K–Ar ages (1.34–1.27 Ga; Litherland et al., 1986) than the 1118 Ma metamorphic age of the Sunsas belt (see above).

The Huanchaca Group, which contains thick basic sills (see below), forms an elongated 30° N–40° W trending tableland known as Serrania Huanchaca (see Fig. 1) about 150 km long and 50 km wide. It comprises flat-lying or low-dipping strata of sandstones and minor orthoquartzitic conglomerates, siltstones, and mudstones that have been divided into four formations: the Arco Iris (basal), Cuatro Carpas, Buena Vista and Rio Verde (uppermost). Much of this basin is covered by Cretaceous sandstones. Of note, manganese mineralization has been reported in one of these reefs (e.g., Litherland and Power, 1989; Boger et al., 2005; Matos et al., 2009). The Huanchaca Group is correlative with the Aguapeí Group that crops out in the Brazilian sector. The latter cover sequence consists (from base to top) of the Fortuna, Vale do Promissão and Morro Cristalino formations. The whole package can be considered as a transgressive–regressive platform sequence comprising a basal sandstone–conglomerate unit, an intermediate pelitic one and an upper sandstone unit (Saes et al., 1992). Laser ablation – ICPMS geochronology on detrital zircons from siliciclastic rocks of lower Fortuna Formation yielded ²⁰⁷Pb/²⁰⁶Pb ages as young as 1167 ± 27 Ma (Vargas-Mattos et al., 2009). A U–Pb SHRIMP age on xenotime (1149 ± 7 Ma), extracted from a pelite of the Vale do Promissão Formation, constrains the time of a post-depositional diagenetic episode within the Aguapeí basin (Santos et al., 2005). Possible correlatives of the Huanchaca Group occur further north within the Rondonian-San Ignacio province, as suggested by a similar extensional/cratonic depositional setting and equivalent lithologies. One of these tectonic basins – the Pacaás Novos Formation (see Fig. 1) – is floored by the Nova Floresta gabbroic sills (not shown) that yield ⁴⁰Ar/³⁹Ar plateau ages of 1198 ± 3 Ma and 1201 ± 3 Ma (Tohver et al., 2002).

According to Teixeira et al. (2010), the Sunsas orogeny induced widespread transpression and crustal shortening inside the already stable continental foreland, with high grade metamorphism overprinting the country rocks. For instance, the Nova Brasilândia supracrustal belt (see Fig. 1), which includes 1.13–1.00 Ga syn- to late-tectonic felsic and mafic intrusions (Rizzotto et al., 2002), exhibits major transcurrent structures related to lateral mass escape due to the outboard Sunsas collision (e.g., Tohver et al., 2004, 2005). To the southeast of the Nova Brasilândia belt, folded siliciclastic strata originated in an initial extensional setting locally known as the Aguapeí aulacogen, as well as nearby mylonite-shear

zones dated at ca. 1.0 Ga (Santos, 2003; Ruiz, 2005; Fernandes et al., 2006) are good indicators of the late collisional offshoots of the Sunsas orogeny (Teixeira et al., 2010 and references therein).

Finally, the Sunsas orogeny has been considered a representative example of the progressive outgrowth from an originally Late Mesoproterozoic, active continental margin – the Grenville Orogeny – that eventually produced the Rodinia supercontinent, as conceived by the seminal work of Hoffman (1991) among others. Table 1 summarizes the geologic and tectonic characteristics of the Sunsas belt.

3. Geology and age background of the Rincón del Tigre igneous complex

The Rincón del Tigre complex is a mafic–ultramafic layered sill (4.5 km thick; e.g., Litherland et al., 1986; Annells et al., 1986a,b; Prendergast et al., 1998; Prendergast, 2000). This complex crops out in the southeast tip of the Sunsas belt (see Figs. 1 and 2a), and shows local intrusive relationships with both the Sunsas (below) and Vibosi (above) groups. Both the Rincón del Tigre complex and the Sunsas/Vibosi metasedimentary envelope were subjected to a similar low grade metamorphism (see previous section). Moreover, they both exhibit gentle folds. The observed axial trace of the anticlinal/synclinal structures is parallel to the general strike of both the metasedimentary rocks and layering of the igneous rocks. The structural framework matches well with the NW–SE trend of the Sunsas shear zones and the overprinting deformation in the basement rocks (see above). According to the interpretations of Fletcher (1979) and Adamek et al. (1996), the Rincón del Tigre Complex was emplaced during a precursor extensional phase of the Sunsas orogeny.

The Rincón del Tigre mafic–ultramafic rocks outcrop over about 720 km² but probably extend eastwards underneath the cover sequences (Litherland et al., 1986). For instance, two small mafic–ultramafic occurrences have been described within the so-called San Diablo block (see Fig. 1), namely the Chaquipoc basic complex (hornblendite, diorite) and two nearby layered gabbroic intrusions (not shown) that occur ca. 90 km away from the town of Rincón del Tigre (Mitchell, 1979; Landivar et al., 1996). Although the ages of these intrusions are unknown, their NW-trending strikes are parallel to the structure of the Rincón del Tigre complex, and suggest a common link.

The composition of the Rincón del Tigre rocks varies from ultrabasic (serpentinized dunite, harzburgite, olivine bronzitite, bronzite picrite), mafic (norite, gabbro) through to granophyre (Annells et al., 1986a). However, no geochemical data are available up to now. According to these authors the geologic relationships for the mafic–ultramafic complex allow the division into a lower

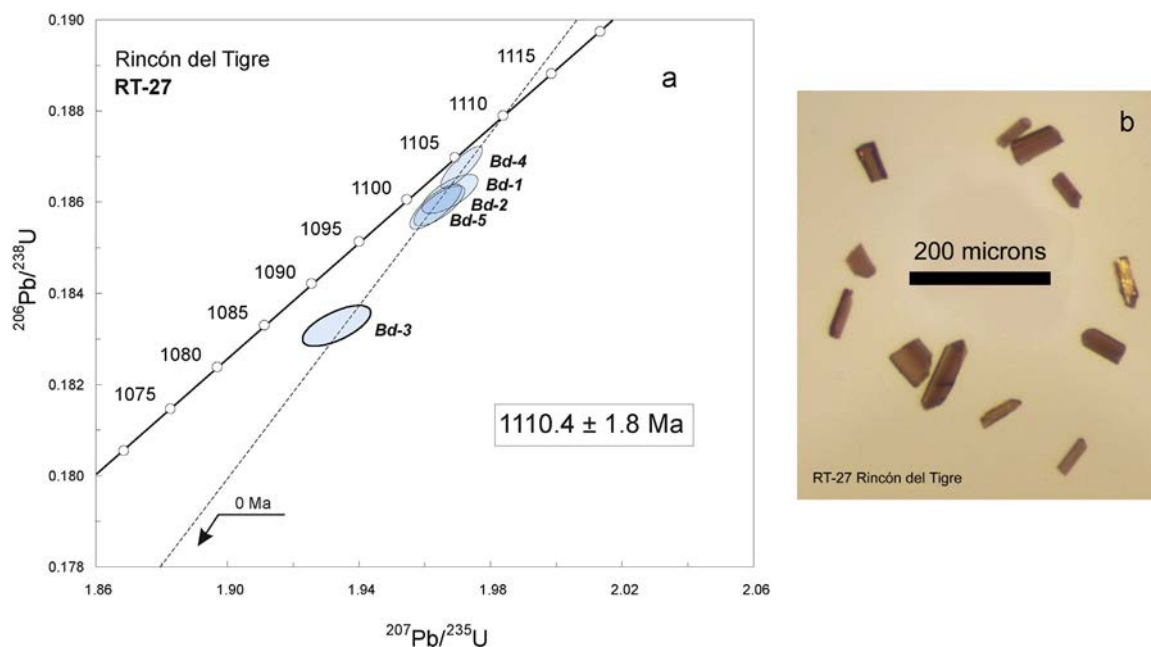


Fig. 3. (a) Concordia diagram showing ID-TIMS U–Pb isotopic results and (b) image of separated baddleyites from RT-27 granophyre (Rincón del Tigre layered complex). Error ellipses reflect 2 σ level of uncertainty. Regression MSWD (Mean Square of Weighted Deviates) = 0.4; probability of fit = 82%. Upper intercept age is based on a linear regression anchored through the origin (0 Ma) and fit through all data points.

Ultramafic Unit (Fig. 2a), an intermediate Mafic Unit and an upper Felsic Unit. According to Litherland et al. (1986), the Felsic Unit is found between the Mafic Unit and the Vibosi roof rocks, and is composed of a dark pink, medium-grained granophyre (300–750 m thick), for which a precise U–Pb age is reported below. Associated with the base of the magnetite gabbro portion, there occurs a low-grade sulfide rich zone 80–185 m thick, containing sub-economic platinum-group elements and gold mineralization. Cu, Mn, Cr, Fe and Ni are the main economic ores in the area (Prendergast, 2000 and references therein). A geophysical survey has delineated a significant gravity high along the northern edge of the Rincón del Tigre Complex suggesting the presence of a feeder dyke (Fig. 3 from Litherland et al., 1986). Fig. 2a presents a geologic sketch of the layered complex with its main economic ore occurrences, and the sampling site of the new U–Pb dating.

Table 2 summarizes previously published age determinations for the Rincón del Tigre complex. Most results have large uncertainties including the Rb/Sr whole rock determination with an age of 993 ± 139 Ma (2 σ ; MSWD = 4.6; $^{87}\text{Sr}/^{86}\text{Sr}_i = 0.7153 \pm 0.0074$) employing several lithologies from the complex (basic and

ultrabasic rocks and granophyres). Indeed, there are appreciable difficulties in the interpretation, given that the analyzed samples may represent one or more injections of the magma, which although coeval, probably have different initial $^{87}\text{Sr}/^{86}\text{Sr}$ ratios, most of which cluster at an elevated level of about 0.71 (Litherland et al., 1986). The Sr isotopic signature implies that magma evolution involved crustally-derived melts, and the high errors attached to both the age and initial ratio reflect a limited spread in Rb/Sr ratios of the analyses. Therefore, the initial ratio is not considered useful in terms of understanding potential mantle source characteristics. K–Ar ages for a granophyre (1067 ± 23 Ma), for a coeval gabbro (1099 ± 37 Ma) and for a nearby dyke (1002 ± 22 Ma) are of similar age but also have large uncertainties. In summary, the published Rb–Sr and K–Ar studies suggest a broadly 1 Ga age but do not allow a precise time of emplacement for the Rincón del Tigre complex. The age range of these samples is also similar to ages of syn- and post-orogenic granitic suites that are scattered across the Sunsas-Aguapeí province in Bolivia and Brazil (see previous section and Table 1). These granitic suites are discussed again in Section 6.1.

4. Geology and age background on the Huanchaca intrusive suite

Huanchaca mafic magmatism, here termed the Huanchaca intrusive suite (Ruiz et al., 2010; Lima et al., 2011, 2012; Sécoco et al., 2011), was previously termed the Huanchaca Dolerite Suite (Litherland et al., 1986). It is characterized by prominent mafic sills and related dykes that crosscut the Huanchaca platform cover (“Serranía Huanchaca-Ricardo Franco”) and/or the Pensamiento Granitoid Complex and older rocks of the Paraguá terrane at the Bolivia–Brazil border, nearby the town of Vila Bela (see Fig. 2b). Overall, the area of the sills and dykes associated with the Huanchaca intrusive suite is ca. 150 km².

According to Litherland and Power (1989), the largest sills (50 and 200 m thick; 30NW trending; 12SW dip) as well as most of the dolerite dykes (N70–90E trending, usually subvertical) penetrate the Arco Iris (mainly sandstones) and Cuatro Carpas (mainly quartzites) formations of the lower part of the Huanchaca Group.

Table 2

Previous age determinations for the Rincón del Tigre (RdT) and Huanchaca (HS) igneous complexes. (1) Litherland et al. (1986); (2) Darbyshire (1979); (3) Santos et al. (1979); (4) Lima et al. (2012). Keys: RdT, Rincón del Tigre complex; HU, Huanchaca Intrusive suite. See text for details.

Unit	Method	Material	Obs	Age (Ma)	Refs.
RdT	Rb–Sr	Whole rock	Granophyre	993 ± 139	1
RdT	K/Ar	Whole rock	Granophyre*	1067 ± 23	2
RdT	K/Ar	Whole rock	Gabbro	1099 ± 37	1
RdT	K/Ar	Whole rock	Dyke	1002 ± 22	1
HU	K/Ar	Whole rock	Dolerite sill	918 ± 20	1
HU	K/Ar	Whole rock	Dolerite dyke	845 ± 19	1
HU	K/Ar	Whole rock	Dolerite dyke	888 ± 20	1
HU	K/Ar	Whole rock	Microgabbro	936 ± 20	3
HU (LG-70)	Ar/Ar	Amphibole	Gabbro sill*	$1040 \pm 40^{**}$	4
HU (LG-70)	Ar/Ar	Plagioclase	Gabbro sill	$948 \pm 5^{**}$	4

* Rocks also dated by the U–Pb method (this work).

** Plateau age.

Table 3

Main petrographic and chemical characteristics of the Huanchaca Intrusive Suite (after Lima et al., 2012). See text for details.

Intrusive type	Lithology	Texture	Essential Minerals	Accessory minerals	Geochemical affinity
Dykes	Diabase, basalt	inequigranular, subophitic, ophitic, porphyritic, vitrophyric, hialophytic	Plagioclase, pyroxene, olivine	Amphibole, titanite, opaque minerals, apatite, K-feldspar, quartz	Subalkaline, tholeiite, andesitic basalts, intraplate
Sills	Diabase	Subophitic to ophitic, rarely intergranular	Plagioclase, pyroxene, amphibole	Titanite, apatite, biotite, chlorite, K-feldspar, quartz	Subalkaline, tholeiite, andesitic basalts, intraplate

Outcrops of the Huanchaca intrusive suite (dykes and sills) are composed of fine- to medium grained rocks (massive gabbro and gabbro-norite) that exhibit diverse igneous textures in thin sections (Table 3). However, minor olivine melanorite differentiates and monzonite and quartz diorite hybrids related to contamination locally occur in the Huanchaca suite (Litherland et al., 1986). According to Litherland et al. (1986), both sills and dykes correspond to the structural pattern of continental-type magmatism. For instance, the sills are geochemically consistent with quartz tholeiitic basalts and andesitic basalts of subalkaline character. Lima et al. (2012) report that these sills have mg# values (0.25–0.39), significant FeO_t enrichment, moderate LREE-enrichment (La/Yb ~5–7) and positive Ba anomalies, coupled with negative anomalies for Nb, Sr, Eu, and Ti in multielement diagrams. Combined with coherent clustering in Zr/Y vs. Zr space (Lima et al., 2012), the geochemical data suggest that the sills were derived from evolved basaltic magmas in a within-plate setting (Table 3). Furthermore, these authors conclude from correlations among LREE and high field strength elements that the Huanchaca sills were derived from a LILE enriched, Nb–Ti depleted, homogeneous mantle source (Lima et al., 2012).

Near the town of Vila Bela (see Fig. 2b), the Huanchaca dykes are subvertical to vertical and mainly N 70°–90° E trending, and have thicknesses from 0.5 to 25 m. According to Sécoco et al. (2011) who detailed the petrography and geochemistry of the dykes, some preserve igneous textures. Chemically, they can be classified as diabbases and basalts of subalkaline, tholeiitic affinity, whereas the FeO_t enrichment and Zr vs. Zr/Y characteristics are similar to intraplate basalts, like the Huanchaca sills. The dykes show REE patterns comparable to E-MORB, but with slightly higher La/Yb ratios (Sécoco et al., 2011).

Litherland et al. (1986) report three K–Ar whole rock ages for the Huanchaca mafic rocks (see Table 2): one sill yields an age of 918 ± 20 Ma, whereas two dolerite dykes yield ages of 888 ± 19 and 845 ± 20 Ma. In the Brazilian sector, one microgabbro gives a K–Ar age of 936 ± 20 Ma (Santos et al., 1979). In addition, the sill chosen for our U–Pb geochronological study (see below) yields a ⁴⁰Ar/³⁹Ar amphibole plateau age of 1040 ± 40 Ma whereas its plagioclase age is significantly younger (948 ± 5 Ma) possibly due to argon loss (Lima et al., 2012). This sill also occurs in the Brazilian sector, and is injected into flat-lying pelites and sandstones of the Vale da Promissão Formation of the Aguapeí Group that is coeval with the Huanchaca Group in Bolivia (see previous section). In general, these intrusions show sharp contacts with the host rocks, parallel to the bedding (Lima et al., 2012).

According to Ruiz et al. (2010) and Lima et al. (2012), the Huanchaca intrusive suite could mark an extensional, anorogenic episode, as suggested by conspicuous sills and mafic dykes located along the Bolivian–Brazilian frontier, displaying roughly comparable K–Ar (940–850 Ma; whole rock and plagioclase) and ⁴⁰Ar/³⁹Ar (plagioclase; amphibole) ages (950–1040 Ma). Nevertheless all these dates (see Table 2) must be considered as minimum estimates for the time of emplacement of these rocks, and are dependent on the argon retention and chemical composition of the respective mineral systems, or both.

5. ID-TIMS U–Pb methodology and results

Grains of baddeleyite (ZrO₂) were successfully recovered from both the Rincón del Tigre and Huanchaca intrusions, allowing, for the first time, precise ID-TIMS U–Pb isotopic measurements to constrain magmatic crystallization ages for these bodies. Despite its generally fine grain size (20–150 μm) and thin, delicate, blade-like forms, baddeleyite is widely recognized as the principal mineral suitable for accurate and precise dating of the emplacement and crystallization of gabbro and dolerite dykes and sills because of its near-ubiquitous occurrence in these compositions (Heaman and LeCheminant, 1993). In each case, a procedure was followed similar to that described by Söderlund and Johansson (2002), in which between 100 and 200 g of sample was finely ground and passed over a shaking water (Wilfley) table until a heavy mineral concentrate was produced. Best quality baddeleyite crystals were then hand-picked under alcohol using a binocular microscope, and selected for analysis. Fractions were washed and loaded into Teflon capsules along with hydrofluoric acid and a ²⁰⁵Pb–²³⁵U isotopic tracer, and dissolved at 200 °C over 3–4 days following the general procedures reported by Krogh (1973). Estimates of fraction weights were made using measurements from digital imaging and the density of baddeleyite. Ion exchange purification of Pb and U was not carried out. Samples were converted to salts using 3N HCl, and loaded on outgassed Re filaments into a VG354 mass spectrometer using Sigel and phosphoric acid. Isotope ratios were measured using a Daly detector equipped with digital ion counting. System deadtime corrections during this period were 20 ns for Pb and U. Corrections for Daly mass bias were 0.07% / AMU, and thermal mass discrimination was taken to be 0.10% / AMU. Uranium–lead blanks in the laboratory normally average about 0.5 pg for Pb and 0.1 pg for U. Plotting and data regressions were carried out using the algorithms and software (Isoplot3.0) developed by Ludwig (2003). All errors described here and in the plots (including error ellipses and calculated ages) are provided at the 2-σ level of uncertainty. More complete details of the separation and analytical details are provided in Teixeira et al. (2013) and Reis et al. (2013).

A sample of granophyre (RT-27; 58.732.94 W, 18.11329 S; see Fig. 2a) from the upper unit of the Rincón del Tigre complex yielded abundant, good quality grains of baddeleyite. They comprised small to large (up to ~100 μm), typically fresh, striated blades and blade fragments (Fig. 3b). Five separate fractions, consisting of between 3 and 5 grains each, were analyzed and yielded ²⁰⁷Pb/²⁰⁶Pb ages ranging from 1108 to 1112 Ma, with minor discordance (0.6–2.3%; Table 4). Ratios of Th/U are uniformly low (0.05–0.09), consistent with values for fresh, igneous baddeleyite. The isotopic data for the Rincón del Tigre granophyre are essentially collinear (Fig. 3a), and free regression of the data yields an upper intercept of 1110.8 Ma, with a lower intercept within error of the origin (55 ± 550 Ma). Therefore, we have chosen to assume zero-aged Pb-loss and anchored a regression at the origin, yielding an upper intercept age of 1110.4 ± 1.8 Ma (2σ; MSWD = 0.4; 82% probability of fit). We interpret the 1110 ± 2 Ma as a robust estimate of the age of emplacement and crystallization of the granophyre, and by extension, the Rincón del Tigre layered complex.

Table 4
Baddeleyite U–Pb isotopic data for RT-27 granophyre (Rincón del Tigre layered complex) and LG-70 gabbroic sill (Huanchaca suite). See text for details.

Fraction	Description	Weight (μg)	U (ppm)	PbT (pg)	PbC (pg)	Th/U	$^{206}\text{Pb}/$ ^{204}Pb	$^{206}\text{Pb}/$ ^{238}U	$\pm 2\sigma$	$^{207}\text{Pb}/$ ^{235}U	$\pm 2\sigma$	$^{207}\text{Pb}/$ ^{206}Pb	$\pm 2\sigma$	Ages (Ma)						
														$^{206}\text{Pb}/$ ^{238}U	$\pm 2\sigma$	$^{207}\text{Pb}/$ ^{235}U	$\pm 2\sigma$	$^{237}\text{Pb}/$ ^{206}Pb	$\pm 2\sigma$	Disk. (%)
RT-27 ($18^{\circ}12'03''\text{S}$; $58^{\circ}26'14''\text{W}$) – Rincon del Tigre complex																				
Bd-1	4 dark-brn bl frag	0.3	221	56.07	1.25	0.052	3090	0.186167	0.000352	1.96744	0.00697	0.076647	0.000199	1100.6	1.9	1104.4	2.4	1112.0	5.2	1.12
Bd-2	5 medium-brn bl frag	0.3	182	31.88	0.59	0.073	3700	0.185895	0.000365	1.96428	0.00642	0.076636	0.000168	1099.1	2.0	1103.3	2.2	1111.7	4.4	1.24
Bd-3	5 medium-brn bl frag	0.3	144	25.10	0.77	0.092	2234	0.183246	0.000366	1.93286	0.00853	0.076500	0.000265	1084.7	2.0	1092.5	3.0	1108.2	6.9	2.30
Bd-4	3 dark-brn bl frag	0.5	265	58.30	0.56	0.051	7173	0.186751	0.000384	1.97114	0.00524	0.076552	0.000110	1103.7	2.1	1105.7	1.8	1109.5	2.9	0.57
Bd-5	3 medium-brn bl & frag	0.5	166	23.22	0.39	0.049	4042	0.185887	0.000409	1.96315	0.00646	0.076596	0.000158	1099.1	2.2	1103.0	2.2	1110.7	4.1	1.14
Sample LG-70 ($14^{\circ}12'50.8''\text{S}$; $60^{\circ}26'36.4''\text{W}$) – Huanchaca suite																				
Bd-1	1 medium-br long blade*	0.1	97	20.83	1.36	0.060	1062	0.185349	0.000491	1.96084	0.01642	0.076727	0.000558	1096.1	2.7	1102.2	5.6	1114.1	14.5	1.76
Bd-2	3 medium-brn bl frag	0.2	149	70.28	0.42	0.150	11,104	0.186957	0.000673	1.97498	0.00772	0.076616	0.000082	1104.9	3.7	1107.0	2.6	1111.2	2.1	0.62
Bd-3	3 medium-brn bl frag*	0.2	140	68.34	1.34	0.106	3444	0.184868	0.000354	1.95454	0.00655	0.076680	0.000179	1093.5	1.9	1100.0	2.3	1112.9	4.7	1.89

Notes: All analyzed fractions represent best quality, fresh grains of baddeleyite.

Abbreviations: brn – brown; bl – blade; frag – fragment.

PbT is total amount (in picograms) of Pb.

PbC is total measured common Pb (in picograms) assuming the isotopic composition of laboratory blank: $^{206}\text{Pb}/^{204}\text{Pb}$ – 18.221; $^{207}\text{Pb}/^{204}\text{Pb}$ – 15.612; $^{208}\text{Pb}/^{204}\text{Pb}$ – 39.360 (errors of 2%).

Pb/U atomic ratios are corrected for spike, fractionation, blank, and, where necessary, initial common Pb; $^{206}\text{Pb}/^{204}\text{Pb}$ is corrected for spike and fractionation.

Th/U is model value calculated from radiogenic $^{208}\text{Pb}/^{206}\text{Pb}$ ratio and $^{207}\text{Pb}/^{206}\text{Pb}$ age, assuming concordance.

Disk. (%) – percent discordance for the given $^{207}\text{Pb}/^{206}\text{Pb}$ age.

Uranium decay constants are from Jaffey et al. (1971).

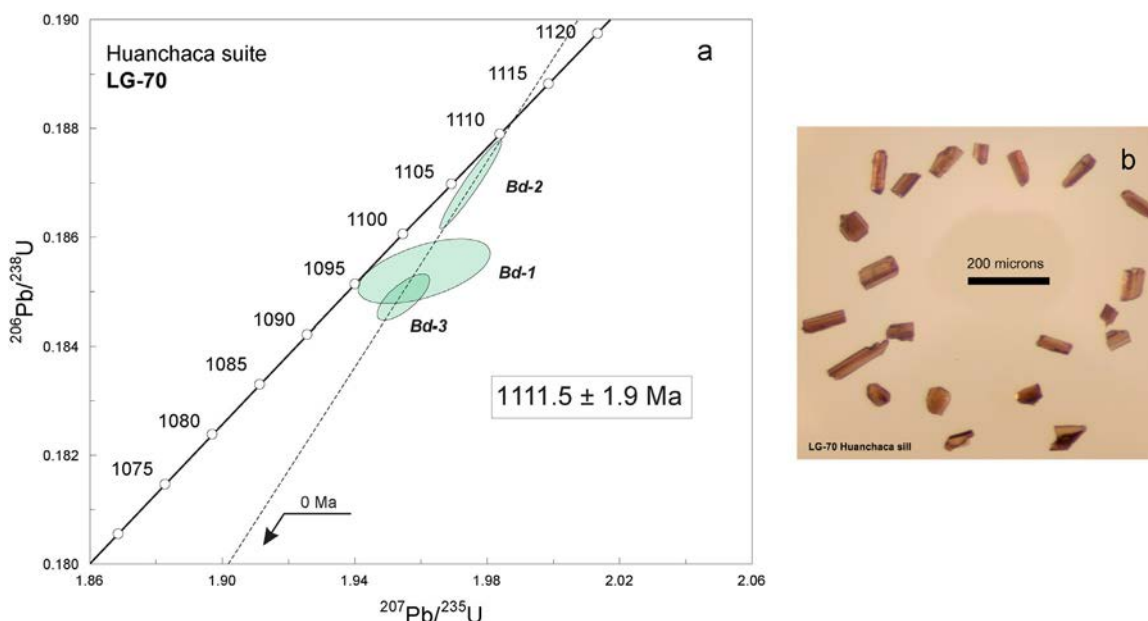


Fig. 4. (a) Concordia diagram showing ID-TIMS U–Pb isotopic results and (b) image of separated baddeleyites from LG-70 gabbroic sill (Huanchaca intrusive suite). Error ellipses reflect 2σ level of uncertainty. Regression MSWD = 0.3; probability of fit = 76%. Upper intercept age is based on a linear regression anchored through the origin (0 Ma) and fit through all data points.

Medium-grained gabbro from the Huanchaca sill (sample LG-70; 60.44345 W, 14.21416 S; see Fig. 2b) yielded a modest amount of medium-brown baddeleyite blades and blade fragments, ranging in size up to approximately 100 μm in the longest dimension (Fig. 4b). Three fractions of baddeleyite grains were prepared, comprising 1–3 grains each. Isotopic results are provided in Table 4, and are presented in graphical form in Fig. 4a. The $^{207}\text{Pb}/^{206}\text{Pb}$ ages for these fractions range from 1111–1114 Ma, again with minor discordance (0.6–1.9%; Table 4). Th/U ratios range from 0.06 to 0.15, higher values possibly reflecting the minor presence of a fine, microscopic coating of zircon on the baddeleyites, though its presence could not be confirmed optically (Table 4). Results for individual fractions are dispersed slightly below Concordia and slightly clustered (Fig. 4a). Resultingly, free regression of the data yields an upper intercept age of 1110.4 Ma, but projects to a negative lower intercept with a large error (-254 ± 780 Ma), again within error of 0 Ma. The data are thus better fit to a regression anchored at the origin (0 Ma), which yields an upper intercept age of 1111.5 ± 1.9 Ma (2σ ; MSWD = 0.3; 76% probability of fit). We interpret 1112 ± 2 Ma to represent the primary age of emplacement and high-temperature crystallization of the Huanchaca sill.

6. Discussion and tectonic implications

6.1. Regional distribution of the Rincón del Tigre–Huanchaca LIP in Amazonia

The age for the Rincón del Tigre granophyre is identical to the age of the Huanchaca mafic sill, which is located some 500 km away (see Fig. 1), and both units have similar intraplate chemistry. Such a precise age match suggests that these two units belong to the same intraplate magmatic event. If so, then this anorogenic (intraplate) event would be regionally significant in the SW portion of the Amazonian Craton. Intraplate magmatism of large scale and potential short duration should be termed a large igneous province (LIP) and would be predicted to be associated with the arrival of a mantle plume (e.g., Bryan and Ernst, 2008; Bryan and Ferrari, 2013; Ernst, 2014). If our interpretation is correct that these two intrusive suites (1110–1112 Ma), 500 km apart, belong to a single

intraplate magmatic episode (a LIP), then it can be expected that other mafic–ultramafic units and also silicic units in the region may also belong to this event.

Several other suites of mafic sills and dykes are present in the SW Amazonian Craton, some of which are undated and some of which have very poorly constrained K–Ar and $^{40}\text{Ar}/^{39}\text{Ar}$ such as the dykes located to the south of Serrania Huanchaca–Ricardo Franco, nearby Vila Bela (see Fig. 2 and Table 1) and the Nova Floresta sills (ca. 1200 Ma) of the Pacaás Novos basin. Some of these units may also belong to the 1110–1112 Ma Rincón del Tigre–Huanchaca LIP as they show geochemistry similar to the Huanchaca sills (Sécoco et al., 2011). However, this needs to be tested by further U–Pb dating. In addition, possibly related silicic magmatism in the SW Amazonian Craton includes the 1.13–1.00 Ga felsic–mafic plutons emplaced into the Nova Brasilândia collisional belt as well as scattered granitic plutons in Bolívia, and potentially including the Sn–Mo anorogenic granites of Rondônia Tin Province (see previous section and Fig. 1). As is now widely realized, silicic magmatism can often be associated with LIPs and be generated by partial melting of the lower crust due to thermal input from a magmatic underplate associated with a mantle plume (e.g., Bryan and Ernst, 2008; Bryan and Ferrari, 2013; Ernst, 2014).

LIPs are characteristically associated with the arrival of mantle plumes although non-plume origins certainly apply in some situations (see discussion in Ernst, 2014; also see Foulger, 2010 for an emphasis on non-plume models). In addition, plumes or hotspots are associated with rifting and breakup of continents (see next section). However, the location of a plume center can be difficult to determine. Plume-related LIP events can extend over areas of greater than several million square kilometers (e.g., the 200 Ma CAMP, 250 Ma Siberian Trap, 1267 Ma Mackenzie LIP events; Ernst, 2014). Given such a scale, the extent represented by the Rincón del Tigre–Huanchaca event could be a fraction of the original scale of the event, which may potentially have even wider distribution in Amazonia and also be present on formerly adjacent blocks (see below). Thus the spatial association of the Rincón del Tigre–Huanchaca LIP with the late Mesoproterozoic accretionary belt of SW Amazonia may not have any tectonic significance. On the other hand, a link with this margin may be suggested by the

spatial association with the precursor Aguapeí aulacogen (now folded) where the original sediments have maximum depositional age of 1067 Ma according to the available detrital zircon U–Pb ages (see previous section).

Numerous LIPs are also known which are associated with mantle plumes ascending into a zone undergoing orogenic shortening (e.g., the 1240 Ma Sudbury, and 1880 Ma Circum-Superior LIPs; Ernst, 2014). These are interpreted to reflect a plume ascending from depth with no link to the overlying plate tectonic environment into which it randomly ascends (see Section 14.3 in Arndt et al., 2008). Further U–Pb geochronology work is required on the numerous undated and poorly dated mafic and ultramafic units (and silicic magmatism) of Amazonia to determine the full extent of this Rincón del Tigre–Huanchaca LIP event, the location of its plume center and any tectonic association with the accretionary SW margin of Amazonia.

This is the second LIP of Proterozoic age recognized within the Amazonian Craton. Reis et al. (2013) document a 1790 Ma LIP widespread in the northern Amazonian Craton, characterized by magmatism of the Avanavero event. We believe that both the 1790 Ma and the 1110 Ma igneous activities represent major intraplate episodes in the growing Nuna and Rodinia supercontinents, respectively. Aspects of the reconstruction history of 1790 Ma LIP are considered in Teixeira et al. (2013) where the link with similar age magmatism of the Uruguayan swarm in the Rio de la Plata Craton is discussed in the context of the Nuna (Columbia) supercontinent. Below we consider the significance of the 1110 Ma LIP in terms of the breakup history of the supercontinent Rodinia.

6.2. Summary and reconstruction implications

Several authors (e.g., Cordani et al., 2003, 2009; Kröner and Cordani, 2003; Pisarevsky et al., 2003; Tohver et al., 2006; D'Agrella-Filho et al., 2008) envisage a large oceanic domain separating Laurentia (plus Amazonia and West Africa) from landmasses such as the Congo–São Francisco, Rio de La Plata and Kalahari during the assembly of Rodinia. Alternatively, this supercontinent would include all continental blocks that existed at ca. 1.0 Ga (e.g., Li et al., 2008). In this regard, the accretionary belts of the SW Amazon region that formed the Rondonian–San Ignacio province (1.56–1.30 Ga) and the adjoining 1.13–1.10 Ga Sunsas belt (see Fig. 1) are all witnesses of successive episodes of plate convergence along an active Mesoproterozoic continental margin. For instance, Cordani et al. (2010) explore the tectonic link of intraplate episodes of Grenville-type age overprinting large portions of the Amazonian Craton, such as the Nova Floresta sills (1.18–0.95 Ga), the 995–974 Ma ‘cratogenic’ granites of the Rondônia Tin Province (see above), and the so-called KMudku mylonitic episode (1.20 ± 0.10 Ga). According to these authors, these geological features could be related to inboard reactivations of the Sunsas collision occurring at the south-western cratonic margin.

The Sunsas belt has been considered to be equivalent of the ultimate stages of the Grenvillian orogeny in northeastern North America, developed parallel to the younger Appalachian margin of Laurentia. It is marked by successive episodes of plate convergence and terrane accretion from about 1250 Ma to 1000 Ma (e.g., Bartholomew and Hatcher, 2010). Grenvillian-age processes have been recorded in isolated metamorphic basement inliers within the Andean region from Colombia to southern Peru and northern Chile, in Mexico, and exotic terranes accreted to Amazonia during the assembly of Rodinia (e.g., Cordani et al., 2003, 2005; Chew et al., 2011). Whereas these segments provide key tectonic tracers for Amazonia–Laurentia interactions within Rodinia reconstructions, the initial relative locations of such segments of the Grenville orogeny and their internal structures are still subject

to large uncertainties. See the special issue of Journal of South American Earth Sciences, v. 29 (2010) for a comprehensive review concerning events of Grenvillian age in Central and South America.

A key question for the model is the timing of when SW Amazonia and Eastern Laurentia joined. If they had joined by 1110 Ma then it might be expected that the 1110–1120 Ma Rincón del Tigre–Huanchaca LIP would extend into adjacent Laurentia. Although such LIP magmatism has not been recognized within the eastern Grenville margin of Laurentia (e.g., Ernst and Buchan, 2001; Ernst, 2014), central Laurentia does host similar age magmatism. For instance, the Keweenaw (Mid-Continent) LIP has an age range of 1115–1085 Ma (e.g., Heaman et al., 2007), which at the older end of the age range would overlap with the 1112–1110 Ma age of the Rincón del Tigre–Huanchaca LIP. Thus, if eastern Laurentia was attached to SW Amazonia at this time, a tectonic relationship between the Rincón del Tigre–Huanchaca LIP and the older end of the Keweenaw LIP must be considered.

Furthermore, if a reconstructed link between western Amazonia and eastern Laurentia is correct, then perhaps the oldest anorogenic mafic magmatism in Amazonia, dated at ca. 1200 Ma (e.g., Nova Floresta mafic sills; see above), can be spatially juxtaposed with the widespread anorogenic magmatism of this age along the Grenville margin of Laurentia (event 97 in Ernst and Buchan, 2001). These potential Laurentian equivalents include the Davy Group sills of the Wakeham terrane (1177 ± 5/–4 Ma), the coronitic gabbros in the Baie de Nord segment of the Tshenukutish domain (U–Pb 1170 ± 5 Ma), and Algonquin metagabbros in the Central Gneiss belt (1170 ± 30 Ma). As a corollary, this implies that the two landmasses could have been close enough to share a coeval intraplate event.

Nevertheless, there are potentially other crustal blocks that can be linked with Amazonia on the basis of an exact age match with the 1110 Ma Rincón del Tigre–Huanchaca LIP, specifically: 1110 ± 3 Ma gabbro-norite dykes of the Angola portion of the Congo Craton (Ernst et al., 2013b), the 1112–1106 Ma Umkondo event of the Kalahari Craton (Hanson et al., 1998, 2004a,b, 2006) and the 1113 ± 7 Ma Mahoba dykes of the northern Indian Craton (Pradhan et al., 2012). Ernst et al. (2013b) offered a preliminary reconstruction that juxtaposed all these blocks and their LIPs along with the West African Craton, which is considered to have been attached to Amazonia in its Gondwana fit from about 2 Ga to ca. 130 Ma, after which Africa and South America separated. Paleomagnetic constraints that support a close relationship of these blocks only exist for Kalahari and Indian cratons at this time (e.g., Ernst et al., 2013a and references therein). Paleomagnetic data from the 1110 Ma units in the Amazonia and Congo cratons are still needed to test whether these blocks could have been near to Kalahari and India at this time.

As a final point, we take into account links between Amazonia and Baltica which have been considered to form a coherent landmass during most of the Proterozoic eon (from ca. 1.8 Ga to ca. 800 Ma), during two supercontinent cycles encompassing both the Nuna and Rodinia supercontinents, according to the SAMBA reconstruction of Johansson (2009, 2014). However, several possible alternative Mesoproterozoic–Neoproterozoic reconstructions involving Amazonia have been proposed (e.g., Cordani et al., 2009, 2010 and references therein), and a detailed assessment of the implications for reconstructions based on our new U–Pb geochronology must be tested with well constrained paleomagnetic data in the future. If Amazonia and Baltica were in the SAMBA reconstruction through 1110 Ma to younger ages, then we predict 1110 Ma magmatism should also be present in Baltica. However, a 1110 Ma LIP has not yet been identified in Baltica (Ernst et al., 2008), and from a LIP ‘barcoding’ perspective, the continuation of the SAMBA reconstruction to 1110 Ma therefore remains inconclusive.

6.3. Economic potential

LIPs can host a range of major ore deposits (e.g., Ernst, 2007, 2014; Ernst and Jowitt, 2013): Ni–Cu–PGE deposits can be associated with mafic to ultramafic intrusions, IOCG (iron-oxide–copper–gold) deposits can be linked with associated A-type granites, associated carbonatites can host Nb–Ta–REE ores, and diamondiferous kimberlites are associated with many LIPs. In addition, some VMS (volcanic massive sulphide), IFs (iron formations), SEDEX (sedimentary exhalative) and other commodity types can result from the thermal input from LIP magmatism into the crust over wide areas, driving hydrothermal systems that concentrate metals. The Rincón del Tigre intrusion of this new 1110 Ma LIP is already known to host Ni–Cu–PGE mineralized zones and therefore the potential is high for additional Ni–Cu–PGE occurrences in other mafic portions of this LIP such as in the Huanchaca sills. As discussed above, the Rondonia Tin province may also be related. The potential for other associated commodities should be considered.

7. Conclusions

High quality U–Pb (ID-TIMS) geochronology has provided the first precise ages for the Rincón del Tigre layered complex (granophyre; 1110 ± 2 Ma) and a Huanchaca mafic sill (1112 ± 2 Ma). The identical ca. 1110–1112 Ma crystallization ages obtained for each intrusion and the large distance between them (about 500 km), suggests that these belong to a previously unrecognized LIP in Amazonia. Additional dolerite sills and dykes are postulated to belong to this LIP, as well as related silicic magmatism with associated tin mineralization. Specifically the Rincón del Tigre intrusion has significant Ni–Cu–PGE mineralization increasing the potential for similar mineralization in other mafic–ultramafic units of this LIP.

In models in which the Sunsas orogeny of SW Amazonia is linked with the Grenville orogeny of eastern Laurentia, the Rincón del Tigre–Huanchaca LIP of SW Amazonia does not have matching 1110 Ma in adjacent Laurentia, but there is a match with the major Keweenaw LIP of Central Laurentia. In addition, ca. 1170–1200 Ma anorogenic mafic dykes and sills of Amazonia would correlate with scattered ca. 1170–1180 Ma intraplate magmatism of eastern Laurentia. So it is possible, from a LIP perspective, that SW Amazonia and eastern Laurentia were juxtaposed at ca. 1110 Ma and even ca. 1170–1200 Ma, i.e. prior to the main Grenville (and Sunsas) collision. Paleomagnetic data are equivocal as to whether SW Amazonia was adjacent or not to eastern Laurentia at ca. 1000 Ma (see Fig. 3 in Evans, 2013).

The newly identified 1110–1120 Ma Rincón del Tigre–Huanchaca LIP in the SW Amazonian Craton also has a remarkable “barcode match” with several other LIP events around the world (cf. Ernst et al., 2008). For instance, identical-aged ca. 1110 Ma intraplate magmatism is found in several other blocks: the Congo, Kalahari, and Indian cratons (e.g., Ernst et al., 2013b) and a nearest neighboring relationship is suggested, in which case the 1110 Ma units of these various blocks would be combined into a overall LIP of huge scale (potentially covering several million sq. km).

Acknowledgements

The first author thanks the Brazilian National Research Council (CNPq) for its continuous support for the research projects. This is publication no. 36 of “The Large Igneous Provinces – Continental Reconstruction – Metallogeny, Industry Consortium Project (www.supercontinent.org)”. Finally the authors are grateful to the

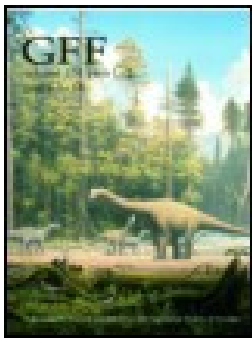
reviewers and the Editor-in-Chief for offering constructive comments and improvements in the early version of the manuscript.

References

- Adamek, P.M., Troeng, B., Landivar, G., Llanos, A., Matos, R., 1996. Evaluación de los recursos minerales del Distrito San Ramón. *Boletín del Servicio Geológico de Bolivia* 10, 77.
- Anells, R.N., Fletcher, C.J.N., Styles, M.T., Burton, C.C.J., Evans, R.B., Harding, R.R., 1986a. The Rincón del Tigre Igneous Complex: a major layered ultramafic–mafic intrusion of Proterozoic age in the Precambrian shield of eastern Bolivia. Part I. Geology and mineral potential (with 1:100,000 scale geological map). *British Geological Survey, Overseas Geology and Mineral Resources*, pp. 63.
- Anells, R.N., Fletcher, C.J.N., Styles, M.T., Appleton, J.D., Burton, C.C.J., Evans, R.B., Harding, R.R., 1986b. Mineral potential of the Rincón del Tigre Igneous Complex: a major Upper Proterozoic layered intrusion in the shield of eastern Bolivia. In: Gallagher, M.J., Ixer, R., Neary, C.R., Prichard (Eds.), *Metallogeny of Basic and Ultrabasic Rocks*. Institution of Mining and Metallurgy, London, pp. 487–498.
- Arndt, N.T., Leshner, C.M., Barnes, S.J., 2008. *Komatiites*. Cambridge University Press, pp. 467.
- Bartholomew, M.J., Hatcher Jr., R.D., 2010. The Grenville orogenic cycle of southern Laurentia: unraveling sutures, rifts, and shear zones as potential piercing points for Amazonia. *J. S. Am. Earth Sci.* 29, 4–20.
- Berrangé, J.P., 1982. The Eastern Bolivia mineral exploration project “Proyecto Precambrico”. *Episodes* 4, 3–8.
- Bettencourt, J.S., Tosdal, R.M., Leite Jr., W.B., Payolla, B.L., 1999. Mesoproterozoic rapakivi granites of Rondonia Tin Province, southwestern border of the Amazonian Craton, Brazil-I. Reconnaissance U–Pb geochronology and regional implications. *Precambrian Res.* 95, 41–67.
- Bettencourt, J.S., Leite Jr., W., Payolla, B., Ruiz, A.S., Matos, R.S., Tosdal, R.M., 2010. The Rondonian–San Ignacio Province in the SW Amazonian Craton: an overview. *J. S. Am. Earth Sci.* 29, 28–46.
- Bispo-Santos, F., D’Agrella-Filho, M.S., Pacca, I.I.G., Janikian, L., Trindade, R.I.F., Elming, S.-Å., Silva, J.A., Barros, M.A.S., Pinho, F.E.C., 2008. Columbia revisited: paleomagnetic results from the 1790 Ma Colider volcanics (SW Amazonian Craton, Brazil). *Precambrian Res.* 164, 40–49.
- Bispo-Santos, F., D’Agrella-Filho, M.S., Trindade, R.I.F., Elming, S.-Å., Janikian, L., Vasconcelos, P.M., Perillo, B.M., Pacca, I.I.G., Silva, J.A., Barros, M.A.S., 2012. Tectonic implications of the 1419 Ma Nova Guarita mafic intrusives paleomagnetic pole (Amazonian Craton) on the longevity of Nuna. *Precambrian Res.* 196–197, 1–22.
- Boger, S.D., Raetz, M., Giles, D., Etchart, E., Fanning, C.M., 2005. U–Pb age from the Sunsas region of eastern Bolivia, evidence for allochthonous origin of the Paragua Block. *Precambrian Res.* 139, 121–146.
- Bryan, S.E., Ernst, R.E., 2008. Revised definition of large igneous provinces (LIPs). *Earth – Sci. Rev.* 86, 175–202.
- Bryan, S.E., Ferrari, L., 2013. Large igneous provinces and silicic large igneous provinces: progress in our understanding over the last 25 years. *Geol. Soc. Am. Bull.* 125, 1053–1078, <http://dx.doi.org/10.1130/B30820.1>.
- Casquet, C., Cordani, U.G., Pankhurst, R.J., 2010. Editorial foreword. *J. S. Am. Earth Sci.* 29, 1–3.
- Cawood, P.A., Kröner, A., Collins, W.J., Kusky, T.M., Mooney, W.D., Windley, B.F., 2009. *Accretionary Orogens Through Earth History*. Geological Society, Special Publications, London, pp. 1–36, <http://dx.doi.org/10.1144/SP318.1>.
- Chew, D.M., Cardona, A., Mis’kovic’, A., 2011. Tectonic evolution of western Amazonia from the assembly of Rodinia to its break-up. *Int. Geol. Rev.* 53 (11–12), 1280–1296, <http://dx.doi.org/10.1080/00206814.2010.527630>.
- Condie, K.C., 2007. Accretionary orogens in space and time. In: Hatcher Jr., R.D., Carlson, M.P., McBride, J.H., Martínez Catalan, J.R. (Eds.), *4-D Framework of Continental Crust*, Memoir, vol. 200. Geological Society of America, pp. 145–158, [http://dx.doi.org/10.1130/2007.1200\(09\)](http://dx.doi.org/10.1130/2007.1200(09)).
- Cordani, U.G., Teixeira, W., 2007. Proterozoic Accretionary belts in the Amazonian Craton. In: Hatcher Jr., R.D., Carlson, M.P., McBride, J.H., Martínez Catalan, J.R. (Eds.), *The 4D Framework of Continental Crust*, GSA Memoir, vol. 200. Geological Society of America Book Editors, Boulder, Colorado, pp. 297–320.
- Cordani, U.G., Neves, B.B.B., D’Agrella-Filho, M.S., 2003. From Rodinia to Gondwana: a review of the available evidence from South America. *Gondwana Res.* 6 (2), 275–284.
- Cordani, U.G., Cardona, A., Jimenez, D.M., Liu, D., Nutman, A.P., 2005. Geochronology of Proterozoic basement inliers in the Colombian Andes: tectonic history of remnants of a fragmented Grenville Belt. Terrane processes at the margins of Gondwana. *J. Geol. Soc. Lond. Special Publication* 246, 329–346.
- Cordani, U.G., Teixeira, W., D’Agrella-Filho, Trindade, R.I., 2009. The position of the Amazonian Craton in supercontinents. *Gondwana Res.* 15, 396–407.
- Cordani, U.G., Fraga, L.M., Reis, N., Tassinari, C.C.G., Brito-Neves, B.B., 2010. On the origin and tectonic significance of the intra-plate events of the Grenvillian-type age in South America: a discussion. *J. S. Am. Earth Sci.* 29, 143–159.
- D’Agrella-Filho, M.S., Tohver, E., Santos, J.O.S., Elming, S.A., Trindade, R.I.F., Pacca, I.G., Geraldes, M.C., 2008. Direct dating of paleomagnetic results from Precambrian sediments in the Amazon Craton: evidence for Grenvillian emplacement of exotic crust in SE Appalachians of North America. *Earth Planet. Sci. Lett.* 267, 188–199, <http://dx.doi.org/10.1016/j.epsl.2007.11.030>.
- D’Agrella-Filho, M.S., Trindade, R.I.F., Elming, S.-Å., Teixeira, W., Yokoyama, E., Tohver, E., Geraldes, M.C., Pacca, I.I.G., Barros, M.A.S., Ruiz, A.S., 2012. The 1420 Ma Indivaí Mafic Intrusion (SW Amazonian Craton): paleomagnetic

- results and implications for the Columbia Supercontinent. *Gondwana Res.* 22 (3–4), 956–973, <http://dx.doi.org/10.1016/j.gr.2012.02.022>.
- Darbyshire, D.P.F., 1979. Results of the age determination programme. Unpublished Report Eastern Bolivia Mineral Exploration Project, phase I, p. 9. Unpublished Open file in Bolivia (Geobol) and the United Kingdom (BGS).
- Darbyshire, D.P.F., 2000. The Precambrian of Eastern Bolivia – a Sm–Nd isotope study. In: 31st International Geologic Congress – 2000, Rio de Janeiro, Brazil, Abstract Volume, CD-ROM.
- Ernst, R.E., 2007. Large igneous provinces (LIPs) in Canada through time and their metallogenic potential. In: Goodfellow, W.D. (Ed.), *Mineral Deposits of Canada: A Synthesis of Major Deposits Types, District Metallogeny, the Evolution of Geological Provinces and Exploration Methods*, vol. 5. Geological Association of Canada, Mineral Deposits Division Special Publication, pp. 929–937.
- Ernst, R.E., 2014. *Large Igneous Provinces*. Cambridge University Press, pp. 630 (in press).
- Ernst, R.E., Buchan, K.L., 2001. Large mafic magmatic events through time and links to mantle plume heads. In: Ernst, R.E., Buchan, K.L. (Eds.), *Mantle Plumes: Their Identification Through Time*. Geological Society of America Special Paper, vol. 352, pp. 483–575.
- Ernst, R.E., Jowitz, S.M., 2013. Large Igneous Provinces (LIPs) and metallogeny, vol. 17. Society of Economic Geologists Special Publication, pp. 17–51.
- Ernst, R.E., Wingate, M.T.D., Buchan, K.L., Li, Z.X., 2008. Global record of 1600–700 Ma Large Igneous Provinces (LIPs): implications for the reconstruction of the proposed Nuna (Columbia) and Rodinia supercontinents. *Precambrian Res.* 160, 159–178.
- Ernst, R.E., Bleeker, W., Söderlund, U., Kerr, A.C., 2013a. Large Igneous Provinces and supercontinents: toward completing the plate tectonic revolution. *Lithos* 174, 1–14, <http://dx.doi.org/10.1016/j.lithos.2013.02.017>.
- Ernst, R.E., Pereira, E., Hamilton, M.A., Pisavevsky, S.A., Rodrigues, J., Tassinari, C.C.G., Teixeira, W., Van-Dunem, V., 2013b. Mesoproterozoic intraplate magmatic ‘barcode’ record of the Angola portion of the Congo Craton: newly dated magmatic events at 1505 and 1110 Ma and implications for Nuna (Columbia) supercontinent reconstructions. *Precambrian Res.* 230, 103–118, <http://dx.doi.org/10.1016/j.precamres.2013.01.010>.
- Evans, D.A.D., 2013. Reconstructing pre-Pangean supercontinents. *Geol. Soc. Am. Bull.* 125 (11–12), 1735–1751, <http://dx.doi.org/10.1130/B30950.1>.
- Fernandes, C.J., Kuyumjian, R.M., Pulz, G.M., Geraldes, M.C., Pinho, F.E.C., 2006. Geologia estrutural e idade $^{40}\text{Ar}/^{39}\text{Ar}$ do depósito de ouro Pau-a-Pique, Faixa Móvel Aguapé, sudoeste do Estado do Mato Grosso. *Revista Brasileira de Geociências* 36, 3–15.
- Fletcher, C.J.N., 1979. La geología y potencial de minerales del área de Concepción (Cuadrante SE 20-3 con parte de SE 20-2). Informe inédito British Geological Survey – Servicio Geológico de Bolivia. (1 map), Santa Cruz de la Sierra, pp. 72.
- Foulger, G.R., 2010. *Plates vs. Plumes: A Geological Controversy*. Wiley-Blackwell, Chichester, pp. 328.
- Fuck, R.A., Brito-Neves, B.B., Schobbenhaus, C., 2008. Rodinia descendants in South America. *Precambrian Res.* 160 (1–2), 108–126.
- Geraldes, M.C., Van Schmus, W.R., Condie, K.C., Bell, S., Teixeira, W., Babinski, M., 2001. Proterozoic geologic evolution of the SW part of the Amazonian Craton in Mato Grosso state, Brazil. *Precambrian Res.* 111, 91–128.
- Hanson, R.E., Martin, M.W., Bowring, S.A., Munyanyiwa, H., 1998. U–Pb zircon age for the Umkondo dolerites, eastern Zimbabwe: 1.1 Ga large igneous province in southern Africa–East Antarctica and possible Rodinia correlations. *Geology* 26 (816), 1143–1146.
- Hanson, R.E., Crowley, J.L., Bowring, S.A., Ramezani, J., Gose, W.A., Dalziel, I.W.D., Pancake, J.A., Seidel, E.K., Blenkinsop, T.G., Mukwakwami, J., 2004a. Coeval large-scale magmatism in the Kalahari and Laurentian cratons during Rodinia assembly. *Science* 304, 1126–1129.
- Hanson, R.E., Crowley, J.L., Bowring, S.A., Ramezani, J., Gose, W.A., Dalziel, I.W.D., Pancake, J.A., Seidel, E.K., Blenkinsop, T.G., Mukwakwami, J., 2004b. Coeval large-scale magmatism in the Kalahari and Laurentian cratons during Rodinia assembly. *Science* 304, 1126–1129.
- Hanson, R.E., Harmer, R.E., Blenkinsop, T.G., Buller, D.S., Dalziel, I.W.D., Gose, W.A., Hall, R.P., Kampunzu, A.B., Key, R.M., Mukwakwami, J., Munyanyiwa, H., Pancake, J.A., Seidel, E.K., Ward, E.K., 2006. Mesoproterozoic intraplate magmatism in the Kalahari craton: a review. *J. Afr. Earth Sci.* 46, 141–167.
- Heaman, L.M., LeCheminant, A.N., 1993. Paragenesis and U–Pb systematics of baddeleyite (ZrO_2). *Chem. Geol.* 110, 95–126.
- Heaman, L.M., Easton, R.M., Hart, T.R., Hollings, P., MacDonald, C.A., Smyk, M., 2007. Further refinement of the timing of Mesoproterozoic magmatism, Lake Nipigon region, Ontario. *Can. J. Earth Sci.* 44, 1055–1086, <http://dx.doi.org/10.1139/E06-117>.
- Hoffman, P.F., 1991. Did the breakup of Laurentia turn Gondwanaland inside-out? *Science* 252, 1409–1412.
- Jaffey, A.H., Flynn, K.F., Glendenin, L.E., Bentley, W.C., Essling, A.M., 1971. Precision measurement of half-lives and specific activities of ^{235}U and ^{238}U . *Phys. Rev. C* 4, 1889–1906.
- Jesus, G.C., Sousa, M.Z.A., Ruiz, A.S., Matos, J.B., 2010. Petrologia e geocronologia (U/Pb–Sm/Nd) do Granito Passagem, Complexo Granitóide Pensamiento, SW do Cráton Amazônico (MT). *Revista Brasileira de Geociências* 40, 392–408.
- Johansson, A., 2009. Baltica, Amazonia and the SAMBA connection – 1000 million years of neighbourhood during the Proterozoic? *Precambrian Res.* 175, 221–234.
- Johansson, A., 2014. From Rodinia to Gondwana with the ‘SAMBA’ model – a distant view from Baltica towards Amazonia and beyond. *Precambrian Res.* 244, 226–235, <http://dx.doi.org/10.1016/j.precamres.2013.10.012>.
- Krogh, T.E., 1973. A low contamination method for hydrothermal decomposition of zircon and extraction of U and Pb for isotopic age determinations. *Geochim. Cosmochim. Acta* 37, 485–494.
- Kröner, A., Cordani, U.G., 2003. African, southern Indian and South American cratons were not part of the Rodinia supercontinent: evidence from field relationships and geochronology. *Tectonophysics* 375, 325–352, [http://dx.doi.org/10.1016/S0040-1951\(03\)00344-5](http://dx.doi.org/10.1016/S0040-1951(03)00344-5).
- Landivar, G., Gonzalez, R., 1997. Mapa Geológico del Área Serranías San José – San Diablo. Servicio Nacional de Geología y Minería, escala 1:100.000.
- Landivar, G., Roca, J., Carvajal, R., Barroso, E., 1996. Mapa Geológico Serranías San José – San Diablo. Servicio Nacional de Geología y Minería, SERGEOMIN, 1 sheet (1: 250,000 scale).
- Li, Z.X., Bogdanova, S.V., Collins, A.S., Davidson, A., De Waele, B., Ernst, R.E., Fitzsimons, I.C.W., Fuck, R.A., Gladkochub, D.P., Jacobs, J., Karlstrom, K.E., Lul, S., Natapovm, L.M., Pease, V., Pisarevsky, S.A., Thrane, K., Vernikovsky, V., 2008. Assembly, configuration, and break-up history of Rodinia: a synthesis. *Precambrian Res.* 160, 179–210.
- Lima, G.A., Sousa, M.Z.A., Ruiz, A.S., Século, D.B., 2011. Enxame de Diques e Sills Máficos da Suíte Intrusiva Huanchaca: evidências da ruptura do Supercontinente Rodinia no SW do Cráton Amazônico. In: 8th National Symposium on Tectonics, Campinas, São Paulo, Brazil, CD-ROM.
- Lima, G.A., Sousa, M.Z.A., Ruiz, A.S., D’Agrella Filho, M.S., Vasconcelos, P., 2012. Sills máficos da Suíte Intrusiva Huanchaca – SW do Cráton Amazônico: registro de magmatismo fissural relacionado à ruptura do Supercontinente Rodinia. *Revista Brasileira de Geociências* 42, 111–129.
- Litherland, M., Bloomfield, K., 1981. The Proterozoic history of eastern Bolivia. *Precambrian Res.* 15, 157–179.
- Litherland, M., Power, P.E.J., 1989. The geologic and geomorphologic evolution of Serrania Huanchaca, eastern Bolivia: the legendary ‘Lost World’. *J. S. Am. Earth Sci.* 2 (1), 1–17.
- Litherland, M., Annels, R.N., Appleton, J.D., Berrangé, J.P., Bloomfield, K., Burton, C.C.J., Darbyshire, D.P.F., Fletcher, C.J.N., Hawkins, M.P., Klinck, B.A., Llanos, A., Mitchell, W.I., O’Connor, E.A., Pitfield, P.E.J., Power, G., Webb, B.C., 1986. The Geology and Mineral Resources of the Bolivian Precambrian Shield, vol. 9. British Geological Survey Overseas Memoir, pp. 153.
- Litherland, M., Annels, R.N., Darbyshire, D.P.F., Fletcher, C.J.N., Hawkins, M.P., Klinck, B.A., Mitchell, W.I., O’Connor, E.A., Pitfield, P.E.J., Power, G., Webb, B.C., 1989. The Proterozoic of Eastern Bolivia and its relationship to the Andean Mobile Belt. *Precambrian Res.* 43, 157–174.
- Ludwig, K.R., 2003. *Isoplot/EX 3. A Geochronological Toolkit for Microsoft Excel*. Special Publication 4. Berkeley Geochronological Center.
- Matos, R., 2010. Geocronologia e evolução paleo-mesoproterozóica do Oriente Boliviano, região sudoeste do Cráton Amazônico (Bolívia) (Unpublished Doctoral thesis). Instituto de Geociências, pp. 240.
- Matos, R., Teixeira, W., Geraldes, M.C., Bettencourt, J.S., 2009. Geochemistry and Nd–Sr isotopic signatures of the Pensamiento Granitoid Complex, Rondonian–San Ignacio Province, Eastern Precambrian shield of Bolivia: petrogenetic constraints for a Mesoproterozoic magmatic arc setting. *Revista Geologia USP série científica* 9 (2), 89–117.
- Mitchell, W.I., 1979. La geología y potencial de minerales del área de Santo Corazón – Rincón del Tigre (Cuadrantes SE 21-5, con parte de SE 21-9 y SE 21-6 con parte de SE 21-10). British Geological Survey – Servicio Geológico de Bolivia (1 map), Santa Cruz de la Sierra, pp. 131.
- Nalon, P.A., Sousa, M.Z.A., Ruiz, A.S., Macambira, M.B., 2013. Batólito Guaporeí uma extensão do Complexo Granitóide Pensamiento em Mato Grosso, SW do Cráton Amazônico. *Revista Brasileira de Geociências* 43, 85–100.
- Nance, R.D., Murphy, J.B., Santosh, M., 2014. The supercontinent cycle: a retrospective essay. *Gondwana Res.* 25 (1), 4–29, <http://dx.doi.org/10.1016/j.gr.2012.12.026>.
- Pisarevsky, S.A., Wingate, M.T.D., Harris, L.B., 2003. Late Mesoproterozoic (ca 1.2 Ga) palaeomagnetism of the Albany–Fraser orogen: no pre-Rodinia Australia–Laurentia connection. *Geophys. J. Int.* 155, F6–F11.
- Pradhan, V.R., Meert, J.G., Pandit, M.K., Kamenov, G., Mondal, M.E.A., 2012. Paleomagnetic and geochronological studies of the mafic dyke swarms of Bundelkhand craton, central India: implications for the tectonic evolution and paleogeographic reconstructions. *Precambrian Res.* 198–199, 51–76, <http://dx.doi.org/10.1016/j.precamres.2011.11.011>.
- Prendergast, M.D., 2000. Layering and precious metals mineralization in the Rincón del Tigre Complex, Eastern Bolivia. *Econ. Geol.* 95, 113–130, <http://dx.doi.org/10.2113/gsecongeo.95.1.113>.
- Prendergast, M., Bennett, M., Henicke, O., 1998. Platinum Exploration in the Rincón del Tigre Complex, Eastern Bolivia, ROYAUME-UNI. *Institution of Mining and Metallurgy*, pp. B39–B47.
- Reis, N.J., Teixeira, W., Hamilton, M.A., Bispo-Santos, F., Almeida, M.E., D’Agrella-Filho, M.S., 2013. Avanço de magmatismo, a late Paleoproterozoic lip in the Guiana Shield, Amazonian Craton: U Pb ID-TIMS baddeleyite, geochemical and paleomagnetic evidence. *Lithos* 174, 175–195, <http://dx.doi.org/10.1016/j.lithos.2012.10.011>.
- Rizzotto, G.J., Hartmann, L.A., 2012. Geological and geochemical evolution of the Trincheira Complex, a Mesoproterozoic ophiolite in the southwestern Amazon craton, Brazil. *Lithos* 148, 277–295.
- Rizzotto, G.J., Bettencourt, J.S., Teixeira, W., Pacca, I.G., D’Agrella-Filho, M.S., Vasconcelos, P.M., Basei, M.A.S., Onoe, A.T., 2002. Geologia e geocronologia da Suíte Metamórfica Colorado e suas encaixantes SE de Rondônia: implicações para a evolução paleo-mesoproterozóica do SW do Cráton Amazônico, Geologia USP. *Série Científica* 2, 41–55.

- Rizzotto, G.J., Hartmann, L.A., Santos, J.O.S., McNaughton, N.J., 2014. Tectonic evolution of the southern margin of the Amazonian craton in the late Mesoproterozoic based on field relationships and zircon U–Pb geochronology. *Anais da Academia Brasileira de Ciências* 86 (1), 57–84.
- Ruiz, A.S., 2005. Evolução geológica do sudoeste do Craton Amazônico, região limítrofe Brasil-Bolívia-Mato Grosso (Unpublished Ph.D. thesis). State University of São Paulo, UNESP – Rio Claro, SP, Brazil, pp. 260.
- Ruiz, A.S., D'Agrella-Filho, M.S., Sousa, M.Z.A., Lima, G.A., 2010. Tonian sills and mafic dike swarms of the S-SW Amazonian craton, records of Rodinia Supercontinent break-up?, vol. 91, no. 26. Meeting of the Americas, EOS Transactions American Geophysical Union, pp. 3.
- Sadowski, G.R., 2002. The fit between Amazonia, Baltica and Laurentia during the mesoproterozoic assemblage of the supercontinent rodinia. *Gondwana Res.* 5, 101–107.
- Sadowski, G.R., Bettencourt, J.S., 1996. Mesoproterozoic tectonic correlations between eastern Laurentia and the western border of the Amazonian Craton. *Precambrian Res.* 76, 213–227.
- Saes, G.S., Leite, J.A.D., Alvarenga, C.J.S., 1992. Evolução tectono-sedimentar do Grupo Aguapeí, Proterozóico Médio na porção meridional do Cráton Amazônico: Mato Grosso e Oriente Boliviano. *Revista Brasileira de Geociências* 23 (1), 31–37.
- Santos, J.O.S., 2003. Geotectônica dos Escudos das Guianas e Brasil Central. In: Bizzi, L.A., Schobbenhaus, C., Vidotti, R.M., Gonçalves, J.H. (Eds.), *Geologia, Tectônica e Recursos Minerais do Brasil – CPRM, Brasília IV (II)*, pp. 169–226.
- Santos, R.O.B., Pitthan, J.H.L., Barbosa, E.S., Fernandes, C.A.C., Tassinari, C.C.G., Campos, D.A., 1979. Folha SD.20 – Guaporé. *Geologia, Rio De Janeiro, Ministério das Minas e Energia-Secretaria Geral, Projeto RADAMBRASIL – Geologia*, vol. 19, pp. 21–123.
- Santos, J.O.S., Hartmann, L.A., Gaudette, H.E., Groves, D.I., McNaughton, N.J., Fletcher, I.R., 2000. A new understanding of the provinces of the Amazon craton based on integration of field mapping and U–Pb and Sm–Nd geochronology. *Gondwana Res.* 3 (4), 453–488.
- Santos, J.O.S., Rizzotto, G., Easton, M.R., Potter, P.E., Hartmann, L.A., McNaughton, N.J., 2002. The Sunsás Orogen in Western Amazon Craton, South America and correlation with the Grenville Orogen of Laurentia, based on U–Pb isotopic study of detrital and igneous zircons. *Geological Society of America, Precambrian Geology*, pp. 122–128.
- Santos, J.O.S., McNaughton, N.J., Hartmann, L.A., Fletcher, I.R., Matos, R.S., 2005. The age of deposition of the Aguapeí Group, western Amazon Craton, based on U–Pb study of diagenetic xenotime and detrital zircon. In: 12th Congresso Latinoamericano de Geologia, Quito, Ecuador, CD-ROM.
- Santos, J.O.S., Rizzotto, G.J., McNaughton, N.J., Matos, R., Hartmann, L.A., Chemale Junior, F., Potter, P.E., Quadros, M.L.E.S., 2008. The age and autochthonous evolution of Sunsás Orogen in West Amazon Craton. *Precambrian Res.* 165, 120–152.
- Século, D.B., Ruiz, A.S., Souza, M.Z.A., Lima, G.A., 2011. Geologia, petrografia e geoquímica do enxame de diques máficos da região de Vila Bela da Santíssima Trindade (MT) – suite intrusiva Huanchaca – SW do Cráton Amazônico. *Geociências* 30 (4), 561–573.
- Söderlund, U., Johansen, 2002. A simple way to extract baddeleyite (ZrO₂). *Geochem. Geophys. Geosyst.* 3 (2), <http://dx.doi.org/10.1029/2001GC000212>.
- Souza, E.P., Hildred, P.R., 1980. Contribuição ao estudo da geologia do Grupo Aguapeí, oeste de Mato Grosso. In: *Anais, XXXI Congresso Brasileiro de Geologia*, vol. 2, Camburiu, Brazil, pp. 813–820.
- Sparrenberger, I., Bettencourt, J.S., Tosdal, R.M., Wooden, J.L., 2002. Datações U–Pb convencional versus SHRIMP do Maciço Estanífero Santa Bárbara, Suite Granitos Últimos de Rondônia, Brasil. *Revista Geologia USP série científica* 2, 79–94.
- Teixeira, W., Geraldes, M.C., Matos, R., Ruiz, A.S., Saes, G., Vargas-Mattos, G.L., 2010. A review of the tectonic evolution of the Sunsás belt, SW Amazonian Craton. *J. S. Am. Earth Sci.* 29, 47–60.
- Teixeira, W., D'Agrella-Filho, M.S., Hamilton, M.A., Ernst, R.E., Girardi, V.A.V., Mazzucchelli, M., Bettencourt, J.S., 2013. U–Pb (ID-TIMS) baddeleyite ages and paleomagnetism of 1.79 and 1.59 Ga tholeiitic dyke swarms, and position of the Rio de la Plata Craton within the Columbia supercontinent. *Lithos* 174, 157–174.
- Tohver, E., Pluijm, B.A.V.D., Voo, R.V.D., Rizzotto, G.J., Scandolaro, J.E., 2002. Paleogeography of the Amazon Craton at 1.2 Ga: early Grenvillian collision with the Llano segment of Laurentia. *Earth Planet. Sci. Lett.* 199, 185–200.
- Tohver, E., Van der Pluijm, B.A., Mezger, K., Essene, E., Scandolaro, J.E., Rizzotto, G.J., 2004. Significance of the Nova Brasilândia metasedimentary belt in western Brazil: redefining the mesoproterozoic boundary of the Amazon Craton. *Tectonics* 23, TC6004, <http://dx.doi.org/10.1029/2003TC001563>.
- Tohver, E., Pluijm, B.V.D., Mezger, K., Scandolaro, J.E., Essene, E., 2005. Two stage tectonic history of the SW Amazon craton in the late Mesoproterozoic: identifying a cryptic suture zone. *Precambrian Res.* 137, 35–59.
- Tohver, E., Teixeira, W., van der Pluijm, B., Geraldes, M.C., Bettencourt, J.S., Rizzotto, G., 2006. Restored transect across the exhumed Grenville orogen of Laurentia and Amazonia, with implications for crustal architecture. *Geology* 34 (8), 669–672.
- Vargas-Mattos, G.L., 2006. Geocronología U/Pb en granitos post y sin-tectónicos de la Orogenia Sunsás en el Cráton Amazonico de Bolivia (M.Sc. dissertation). Universidade do Estado do Rio de Janeiro, Rio de Janeiro, Brazil, pp. 107p.
- Vargas-Mattos, G.L., Geraldes, M.C., Schmitt, R.S., Matos, R., Teixeira, W., Valencia, V., Ruiz, J., 2007. Geocronología U–Pb de zircões detríticos do Grupo Aguapeí (Serras Ricardo Franco, Santa Bárbara e Salto do Céu): Implicações na evolução geológica do SW do Cráton Amazônico. In: XI Congresso Brasileiro de Geoquímica, Atibaia, Brazil, CD-ROM.
- Vargas-Mattos, G.L., Geraldes, M.C., Matos, R., Teixeira, W., 2009. Resultados parciais U–Pb de alguns corpos intrusivos gerados na orogênesis Sunsás, SW do Cráton Amazônico na Bolívia. In: *Anais do XI Simpósio de Geologia do Centro-Oeste, Cuiabá, Brazil*, p. 62.



GFF

ISSN: 1103-5897 (Print) 2000-0863 (Online) Journal homepage: <http://www.tandfonline.com/loi/sgff20>

Widespread ca. 1.4 Ga intraplate magmatism and tectonics in a growing Amazonia

Wilson Teixeira, Richard E. Ernst, Mike A. Hamilton, Gabrielle Lima, Amarildo S. Ruiz & Mauro C. Geraldés

To cite this article: Wilson Teixeira, Richard E. Ernst, Mike A. Hamilton, Gabrielle Lima, Amarildo S. Ruiz & Mauro C. Geraldés (2015): Widespread ca. 1.4 Ga intraplate magmatism and tectonics in a growing Amazonia, GFF, DOI: [10.1080/11035897.2015.1042033](https://doi.org/10.1080/11035897.2015.1042033)

To link to this article: <http://dx.doi.org/10.1080/11035897.2015.1042033>



Published online: 24 Sep 2015.



Submit your article to this journal [↗](#)



Article views: 4



View related articles [↗](#)



View Crossmark data [↗](#)

Full Terms & Conditions of access and use can be found at
<http://www.tandfonline.com/action/journalInformation?journalCode=sgff20>

Widespread ca. 1.4 Ga intraplate magmatism and tectonics in a growing Amazonia

WILSON TEIXEIRA¹, RICHARD E. ERNST^{2,3}, MIKE A. HAMILTON⁴, GABRIELLE LIMA⁵,
AMARILDO S. RUIZ⁶ and MAURO C. GERALDES⁷

TEIXEIRA, W., ERNST, R.E., HAMILTON, M.A., LIMA, G., RUIZ, A. & GERALDES, M.C., 2015: Widespread ca. 1.4 Ga intraplate magmatism and tectonics in a growing Amazonia. *GFF*, Vol. 00 (Pt. 1), pp. 1–14. q Geologiska Föreningen. doi: <http://dx.doi.org/10.1080/11035897.2015.1042033>.

Abstract: High-quality U–Pb (Isotope Dilution-Thermal Ionisation Mass Spectrometry; ID-TIMS) baddeleyite ages were obtained for the Salto do Céu (SC) gabbroic sill (1439 ± 4 Ma) and Nova Lacerda mafic dyke swarm (1387 ± 17 Ma) located ca. 150 km apart in the Jauru terrane (Paleo- to Mesoproterozoic) – SW Amazonia. From a geodynamic perspective, the new ages mark widespread Mesoproterozoic extensional tectonics and associated magmatism (e.g. dolerite dykes and rapakivi suites) in a growing continental margin. The SC sill is coeval with the nearby Rio Branco anorogenic rapakivi granite. Intermittent extensional tectonics (1.44 and 1.39 Ga) is widespread in the central and northern portions of the Amazonian Craton, given by co-magmatic charnockites and rapakivi granites, and mafic–ultramafic complexes. On a global scale, this activity may be coeval with a major intra-continental-related igneous event in Laurentia and Fennoscandia, as well as with mafic dykes in NW West African Craton. This suggests large igneous province (LIP)-scale magmatism. A further aspect is that the 1.4 Ga magmatism is age-equivalent with convergent-margin processes (Alto Guapore´ orogen and the related Rio Alegre oceanic remnant) that evolved outboard the active margin of the proto-Amazonian Craton. This may represent a coincidence in time between intraplate rifting, LIP magmatism (plume related) and subduction. Other causal mechanisms are also considered such as pulses of back-arc extension behind the accreting arcs. Our data provide new clues as to the longevity of the Columbia (or Nuna) supercontinent, and are consistent with previously published paleomagnetic poles from Mesoproterozoic intraplate magmatism in Amazonia, Laurentia and Baltica (South America-Baltica model).

Keywords: U–Pb baddeleyite ages; mafic sills and dykes; Mesoproterozoic; Amazonian Craton; Columbia supercontinent

¹*Instituto de Geociências, Universidade de São Paulo, Rua do Lago 562, São Paulo, São Paulo 05508-080, Brazil; wteixeir@usp.br*

²*Department of Earth Sciences, Carleton University, Ottawa, Canada K1S 5B6*

³*Faculty of Geology and Geography, Tomsk State University, Tomsk 634050, Russia*

⁴*Jack Satterly Geochronology Laboratory, Department of Earth Sciences, University of Toronto, Toronto, Ontario, Canada M5S 3B1*

⁵*Programa de Pós-Graduação, Universidade Federal do Pará, Belém, Pará 66075-110, Brazil*

⁶*Departamento de Geologia Geral, Universidade Federal de Mato Grosso, Cuiabá, Mato Grosso 78060-900, Brazil*

⁷*Faculdade de Geologia, Universidade do Estado do Rio de Janeiro, Rio de Janeiro, Rio de Janeiro 20550-013, Brazil*

Manuscript received 13 January 2015. Revised manuscript accepted 14 April 2015.

1. Highlights

- First U–Pb baddeleyite ages for the Salto do Céu (SC) sills and Nova Lacerda (NL) dykes.
- These ages define two intraplate igneous events active in Mesoproterozoic Amazonia.
- The studied rocks have age matches with dykes and rapakivi suites over the craton.
- There is a tight age match between plume-related magmatism and subduction.

2. Introduction

The southwestern portion of the Amazonian Craton records a polycyclic Proterozoic crustal history, distinguished by tectonic provinces that young successively toward the SW. They are the product of assembly of multiple NW–SE trending accretionary belts, supported by a coherence in the U–Pb age patterns from igneous and metamorphic rocks and related chemical and isotopic constraints within each given belt or province. In this regard, the respective timing of cratonization (minimum ages) can be inferred by precise ages of diachronic variation of the anorogenic activity such as rapakivi suites, mafic–ultramafic

complexes, mafic dyke swarms and sequences of undeformed volcanic-sedimentary cover within or across the province (s) (e.g. Geraldes et al. 2004a, 2014; Tassinari & Macambira 2004; Cordani & Teixeira 2007; Teixeira et al. 2011, 2015; Girardi et al. 2012). Notably, regional spatial and temporal correlations in the intraplate magmatism coupled with paleomagnetic evidence have provided constraints on the role of large igneous provinces (LIPs) during Proterozoic time, particularly related to Amazonia's potential relationships in supercontinent cycles such as the assembly and breakup of Columbia (or Nuna) and Rodinia (e.g. Rogers & Santosh 2002; Tohver et al. 2006; Bispo-Santos et al. 2008, 2012; Li et al. 2008; Cordani et al. 2009; Elming et al. 2009; D'Agrella-Filho et al. 2012; Reis et al. 2013; Roberts 2013; Teixeira et al. 2014).

This paper presents the first Isotope Dilution-Thermal Ionisation Mass Spectrometry (ID-TIMS) U–Pb baddeleyite ages for two regionally important intrusive suites in the Mato Grosso region (SW Amazonian Craton) – the SC gabbroic sills, and NL mafic dyke swarm, located some 150 km apart in the Jauru terrane (e.g. Bettencourt et al. 2010a). The new age data, together with a compilation of tracer isotopic and published geochemical information reveal hitherto unrecognized, but tectonically significant intervals of anorogenic magmatism related to a broadening Amazonia during the Mesoproterozoic. These data are discussed in the framework of developing a robust LIP barcode (Bleeker & Ernst 2006; Ernst 2014) for this crustal block, and for testing of global reconstructions and the long-lived history of supercontinent Columbia.

3. Geologic– tectonic framework

We provide an overview of the geologic and tectonic setting of SW Amazonian Craton with a focus on the Mesoproterozoic Rondonian-San Ignacio (RSI) province; the role of coeval magmatic activity within the already cratonized immediate NE, as well as over the central and northern portions of the craton.

The SW Amazonian Craton, including portions of the Brazilian states of Rondonia and Mato Grosso and the counterparts in Bolivia, comprises three roughly parallel segments of the Rio Negro-Juruena (RNJ; 1790–1550 Ma), the RSI (1560–1300 Ma) and the Sunsas-Aguapeí (1250–950 Ma) tectonic provinces (Fig. 1). These provinces show a protracted geologic history that youngs toward the SW fringe of the craton (e.g. Cordani & Teixeira 2007 and references therein). From a geodynamic perspective, this reflects a long-lived soft-accretion regime producing multiple magmatic arcs and progressive amalgamation of the accretionary edges outboard from an Archean/Paleoproterozoic continental core. Notably, the Proterozoic stepwise crustal growth was accompanied by extensional-related magmatism over the previously stable provinces, such as anorogenic rapakivi suites, mafic dyke swarms and sills, along with tectonic basins (Cordani et al. 2010 and references therein). For instance, much of the igneous activity crops out along regional structures, first recognized by radar imagery (Teixeira et al. 1989 and references therein). Final tectonic stability of the Amazonian Craton occurred in the late Mesoproterozoic (Sadowski & Bettencourt 1996; Teixeira et al. 2010; Bettencourt et al. 2010a; Rizzotto et al. 2013).

The Proterozoic provinces have been sub-divided into distinct terranes and belts, based on regional geologic grounds (e.g. metamorphic episodes, shear zones, tectonic fronts), supported by geochronology, among other tools (e.g. Litherland et al.

1986; Teixeira et al. 1989; Geraldes et al. 2001; Boger et al. 2005; Ruiz 2005; Tohver et al. 2006; Cordani & Teixeira 2007; Bettencourt et al. 2010a; Rizzotto & Hartmann 2012; Rizzotto et al. 2013). For instance, the Jauru terrane (Fig. 1), in the state of Mato Grosso – where the studied rocks crop out – comprises Paleoproterozoic basement rocks that include relicts of greenstone belts (Alto Jauru Group) and a mafic–ultramafic suite (Co'rego Dourado). These rocks have been collectively ascribed to the RNJ province (Tassinari et al. 1996). The country rocks were largely remobilized during the Mesoproterozoic as shown by granitoid rocks that are ascribed to the Cachoeirinha and Santa Helena orogenies. The Cachoeirinha and Santa Helena plutons are genetically linked with the 1.56–1.30 Ga RSI composite orogeny – see Bettencourt et al. (2010a) for review. However, in this same time range Mesoproterozoic anorogenic felsic and mafic magmatism, as well as mafic dykes and sills are conspicuous over the Jauru terrane (Geraldes et al. 2004a, 2004b; Corre' da Costa et al. 2009; Teixeira et al. 2011; Girardi et al. 2012). The mafic sills and dykes that occur in the vicinity of the Rio Branco and NL towns, respectively, are the focus of our work.

According to Bettencourt et al. (2010a), the evolution of the RSI orogeny lasted ca. 260 million years, and included successive slab subduction events, accretion and stacking of the magmatic arcs. The proposed model involves an ocean closure now recognized as the Guaporé suture (Rizzotto et al. 2013) and final docking between the Paragua' terrane (allochthonous) and the RNJ province. Hence, several orogenic compartments with particular tectonic–magmatic histories can be distinguished within the RSI province, with extensive exposures in the Brazilian Rondonia and Mato Grosso states, such as in the Jauru terrane and in the Paragua' terrane in Bolivia, as summarized later (e.g. Geraldes et al. 2001; Boger et al. 2005; Bettencourt et al. 2010a; Rizzotto et al. 2013 and references therein; see Fig. 1):

(1) The Cachoeirinha (1587–1522 Ma) orogen comprises calc-alkaline volcanic and plutonic (tonalite, granodiorite, granite) rocks evolved during the Cachoeirinha orogeny (Geraldes et al. 2001). These rocks are peraluminous to weakly metaluminous, subalkaline to calc-alkaline in chemistry (e.g. 1.56–1.52 Ga Santa Cruz suite), and have been considered as the roots of a continental margin Andean-type arc built upon Paleoproterozoic basement (Jauru crust). This geologic setting is also suggested by the $^{147}\text{Sm}/^{143}\text{Nd}(t)$ values (2.0 to 21.3) and T_{DM} ages (1.9–1.7 Ga), reported for the Cachoeirinha rocks (Geraldes et al. 2001; Ruiz et al. 2004; Bettencourt et al. 2010a; see Table 1).

(2) The Santa Helena orogen (1485–1420 Ma), comprising syn- to late-tectonic plutons such as the Santa Helena (1.44–1.42 Ga), the Pindaituba (1.46–1.42 Ga) and the Águas Claras (1.44–1.42 Ga) suites occurring over the Jauru terrane. These suites evolved during the Santa Helena orogeny (Geraldes et al. 2001), and are mainly composed of monzonites, granodiorites and tonalites that have a large areal extent in the central portion of the Jauru terrane (Ruiz 2005; Bettencourt et al. 2010a). The reported $^{147}\text{Sm}/^{143}\text{Nd}(t)$ values (from CHUR to 24.0), T_{DM} ages from 1.5 to 1.8 Ga (Geraldes et al. 2001; Ruiz 2005), and the sub-alkaline and calc-alkaline composition suggest the parental magmas of the granitoid rocks derived in oceanic/continental arc settings. In particular, the less evolved facies of the Santa Helena suite is slightly metaluminous, whereas the most fractionated is weakly peraluminous (Geraldes et al. 2001). The NL dyke swarm (a

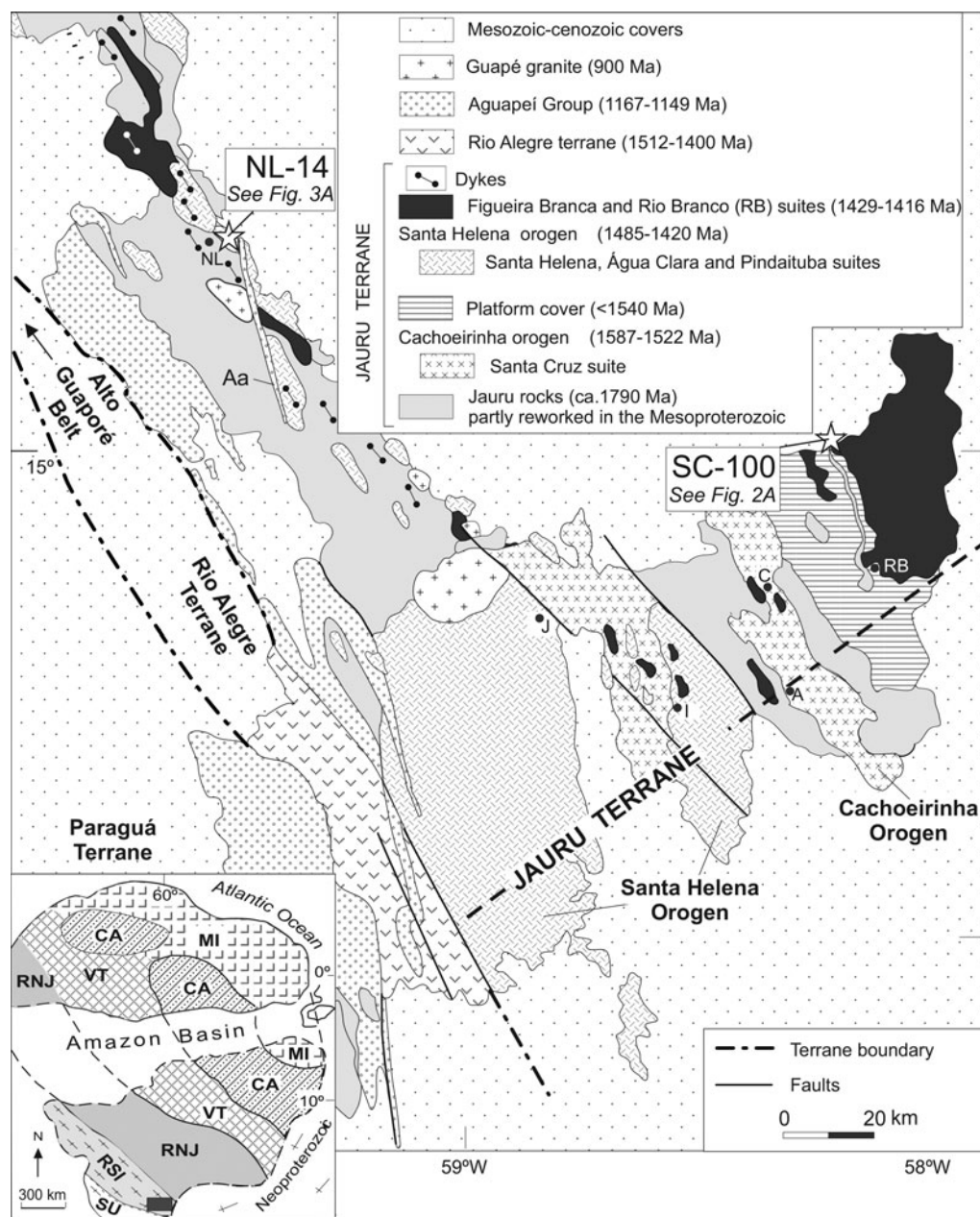


Fig. 1. Geologic outline of the SW portion of the Amazonian Craton showing the major boundaries between tectonic units in the Jauru terrane – Mato Grosso region (adapted from Geraldès et al. 2001; Bettencourt et al. 2010a). Aa, Aguapeí aulacogen. Inset shows the internal crustal provinces of the Amazonian Craton (after Cordani & Teixeira 2007). Key locations in the geologic sketch: RB, Rio Branco; C, Cachoeirinha; I, Indiavaí; J, Jauru; NL, Nova Lacerda. See text for details.

focus of our paper) crosscuts the basement rocks and plutons of the Pindaituba suite (see previous point).

It is worth mentioning that anorogenic magmatism age-equivalent with the timing of the Santa Helena rocks is conspicuous across the Jauru terrane (see Fig. 1) units, such as the Figueira Branca mafic–ultramafic complex that includes the Indiavaí gabbro and felsic-mafic plugs that occur in the Jauru-Indiavaí region (U–Pb ages of 1429 ± 3 to 1416 ± 7 Ma; Teixeira et al. 2011; D’Agrella-Filho et al. 2012). In a similar manner, the Nova Guarita intrusive suite geotectonically inserted in the Paleoproterozoic Ventuari-Tapajós province (see Fig. 1 inset) yields an age (Ar–Ar plateau) of 1418.5 ± 3.5 Ma (Bispo-Santos et al. 2012). The latter suite comprises profuse NW-trending dykes of gabbro, microgabbro and diabase occurring about 600 km northward from the SC sills.

In the easternmost portion of the Jauru terrane (see Fig. 1) where the SC sills crop out there is the Rio Branco anorogenic suite (Geraldès et al. 2001, 2004a,b) which comprises a felsic member with syenites to rapakivi granites, and a mafic member (gabbro, tholeiitic diabase dykes and porphyritic basalt). Hybrid felsic-mafic rocks are also present. Trace element abundances (e.g. Rb, Y and Nb) suggest a common petrogenesis for both the mafic and felsic rocks, whilst a within-plate affinity is also apparent from the chemical data. The felsic member (granophyre) yielded an ID-TIMS U–Pb zircon age of 1423 ± 2 Ma, whereas the mafic member (porphyritic gabbro) yielded a significantly older U–Pb age of 1471 ± 31 Ma (Geraldès et al. 2001). These authors noted that the zircons recovered from this gabbro may have a small inherited component, and we consider thereby that the U–Pb age of granophyre (1423 Ma) probably defines the crystallization of the

Table 1. Summary of geologic–tectonic characteristics of the SW portion of the Amazonian Craton with emphasis on the RSI province (adapted from Bettencourt et al. 2010a; Teixeira et al. 2010; Rizzotto et al. 2013).

Province	Dynamics and orogenic events	Main regional units	Anorogenic intrusions (Ga)
RSI (1.56–1.30 Ga); stable cratonic area for the Sunsas collisional (SA) orogeny	Accretionary tectonics (RSI composite orogeny): Rio Alegre (1.51–1.48 Ga), Cachoeirinha (1.56–1.52 Ga), Alto Guapore´ (1.47, 1.44–1.43 and 1.35–1.33 Ga), Santa Helena (1.44–1.42 Ga), San Ignacio (1.37–1.33 Ga) belts. High-grade metamorphism accompanying emplacement of collisional-related plutonism (ca. 1.35 Ga)	Trincheira ophiolite. Orthogneisses, supracrustal associations. Syn- to late-tectonic plutons genetically associated with a given event of the RSI orogeny. Coeval rocks in the Paragua´ terrane (Bolivian counterpart)	A-type and rapakivi granites (0.99–0.90), mafic dykes and sills, tectonically related with the SA collision
RNJ (1.79–1.55 Ga); tectonically stable basement for the adjoining RSI and SA orogenies	Juvenile accretion with recurrent volcano-plutonic pulses. Metamorphic imprints and inboard anorogenic magmatism due to the RSI orogeny. Tectonic reactivation related to the SA collision	Granite-greenstone terrane (Jauru terrane). Correlative medium- to high-grade units in Rondônia (Brazil) and in the Paragua´ terrane, intruded by distinct Mesoproterozoic granitoid rocks related to RSI	Rio Branco (1.43) and Nova Guarita (1.41) suites. Figueira Branca layered complex (1.43–1.42). Santo Antônio (1.38) and Teotônio (1.39) suites. Alvorada granite (1.39), tectonically related with the syn- to late-orogenic phase (1.44–1.43) of outboard Alto Guapore´ arc

Notes: RO, Rondônia state; MT, Mato Grosso state. See text for details.

Rio Branco suite. The Rio Branco suite yields T_{DM} ages between 1.7 and 2.0 Ga, whereas the $1_{Nd(1.42\text{ Ga})}$ values (data recalculated from Geraldès et al. 2001) vary from 0.8 to 21.4 (gabbros) 20.1 to 1.2 (monzosyenites) and 20.3 to 22.2 (granophyres). As a whole, these data suggest that the magma source was slightly contaminated by a Paleoproterozoic continental component such as the Jauru crust, as expected for its intraplate setting.

(3) The Rio Alegre oceanic remnant (1512–1400 Ma) composed of an oceanic-like metavolcano-sedimentary association (basic to ultrabasic volcanic rocks, subvolcanic rocks associated with chert and banded iron formation), as well as coeval granitoid plutons occupies a large area between the Jauru terrane to the east and the Paragua´ terrane to the west (see Fig. 1). The calc-alkaline tonalite and granodiorite to granite plutons are predominant within the Rio Alegre terrane (Geraldès et al. 2001; Matos et al. 2004; Ruiz 2005). U–Pb crystallization ages for the volcanic and plutonic rocks range between 1512 ± 9 and 1465 ± 4 Ma, whereas the gabbroic rocks give U–Pb zircon ages ranging from 1509 ± 10 to 1494 ± 11 Ma. The volcanic and plutonic rocks disclose positive $1_{Nd(t)}$ values (ρ_4 , ρ_5) with T_{DM} ages of about 1.5 Ga (see Table 1), and together with the geochemical signatures demonstrate that they originated in an evolved Mesoproterozoic oceanic setting (back-arc basin or ocean ridge and island arc; Matos et al. 2004; Ruiz 2005; Bettencourt et al. 2010a). Metamorphism under greenschist to lower amphibolite facies and mylonitization producing a N20W foliation were associated with collision of the arc against the proto-Amazonian Craton during the Mesoproterozoic (Matos et al. 2004).

As a corollary, considering that the basement of both the Paragua´ terrane and the RNJ continental margin is late Paleoproterozoic in age (Boger et al. 2005; Santos et al. 2008; Matos et al. 2009), the Rio Alegre orogen could be interpreted as an exotic terrane that was eventually juxtaposed onto the proto-Amazonian Craton margin triggered by the collision of the Paragua´ terrane (Geraldès et al. 2001; Bettencourt et al. 2010a and references therein).

More recently, juvenile crust (1470–1430 Ma) has been described in portions of the RSI province, mainly attributed to the WNW–ESE trending Alto Guapore´ belt (not shown in Fig. 1). The main belt is largely exposed from the NW sector of

Rondônia to the SE and to the SW portion of Mato Grosso, assuming that it includes rocks previously ascribed to the Rio Alegre terrane. Notably the Alto Guapore´ belt preserves a paleosuture zone mirrored by the ophiolitic Trincheira complex and associated oceanic-like chemical and clastic metasedimentary assemblages and metamafic rocks. Coeval dioritic–tonalitic complex and granitoid rocks are also present. From a tectonic point of view, this framework marks the suturing of the proto-Amazonian Craton and the Paragua´ terrane in the 1470–1320 Ma time interval (Rizzotto & Hartmann 2012; Rizzotto et al. 2013).

The available SHRIMP U–Pb datings indicate that the Trincheira ophiolite formed during the accretionary phase at 1.47 Ga, and was succeeded by the syn- to late-tectonic tonalitic–plagiogranitic plutons (1.44–1.43 Ga) whilst overprinted by upper amphibolite–granulitic metamorphism. The ophiolitic rocks show Nd–Sr juvenile isotopic signatures in coherence with derivation from a depleted mantle source in an island-arc/back-arc setting (Rizzotto et al. 2013). On a regional scale, the history of the Alto Guapore´ belt is consistent with the ages of scattered plutonic rocks such as in the Bolivian counterpart (Paragua´ terrane) where the San Ramón tonalite yields a U–Pb age of 1431 ± 4 Ma (Santos et al. 2008). In addition, in the Rio Alegre terrane, Matos et al. (2004) characterized two generations of intrusive plutons given by U–Pb crystallization ages of 1412 ± 5 and 1384 ± 40 Ma, but their setting (arc, back-arc or intraplate) is unclear.

A latter collisional phase, given by the emplacement of gabbro and granite plutons (1.35–1.34 Ga) in the Alto Guapore´ belt, marks the impingement of the Paragua´ terrane against the proto-Amazonian Craton (Rizzotto et al. 2013). This was accompanied by regional high-grade metamorphism, including deformation of the Trincheira ophiolitic complex and other granitoid units. In a similar manner, in the Bolivian counterpart, the San Ignacio orogeny (1.35 ± 0.2 Ga) largely remobilized the Paragua´ terrane by means of deformation, high-grade metamorphism and emplacement of collisional-type granitic plutons – the Pensamiento Granitoid Complex (e.g. Litherland et al. 1986; Boger et al. 2005; Santos et al. 2008; Matos et al. 2009; Jesus et al. 2010; Nalon et al. 2013; Franc, a et al. 2014). All the above-mentioned highlight the final stage of the RSI composite orogeny given by juxtaposition of the Paragua´ terrane to the

proto-RSI province (e.g. Rio Alegre and Jauru terranes) at ca. 1.35 – 1.30 Ga ago (Bettencourt et al. 2010a; Rizzotto & Hartmann 2012; Rizzotto et al. 2013; Franc, a et al. 2014). In a general manner, this dynamic model is consistent with most previous published ideas about the evolution of the RSI orogeny (e.g. Cordani & Teixeira 2007 and references therein).

It is worthwhile to mention that anorogenic suites (rapakivi granites and coeval mafic and ultramafic rocks), coeval with the Alto Guaporé rocks, mark a stage of cratonic activity over the adjoining RNJ and RSI provinces such as the Santo Antônio suite (1373 ± 15 Ma and associated diabase dykes and the cospatial Teotônio suite (1387 ± 16 Ma; Bettencourt et al. 2010b). These intrusions crop out close to the town of Porto Velho (not shown), ca. 720 km away to the northwest from the NL dykes in the state of Mato Grosso. In a similar manner, the Jauru terrane contains significantly younger plutons such as the Alvorada undeformed granite (1389 ± 3 Ma; Ruiz 2005). Hence, from a tectonic perspective, these particular suites may represent discrete extensional episodes accompanying the terminal stages of the RSI orogeny (e.g. Bettencourt et al. 1999 and references therein).

Subsequently, the RSI province was affected by deformation, metamorphism, magmatism and basin tectonics due to the 1130 – 1000 Ma SA orogeny (Fig. 1). This allochthonous-type orogeny, as shown by the coherent tectonic fronts and metamorphism overprinting the RSI rocks, developed outboard from the southern edge of the Paraguaí terrane (Litherland et al. 1986; Litherland & Power 1989). The SA belt comprises the Sunsas/Vibosi supracrustal sequences, granitic suites (1105 – 1004 Ma), and the undeformed Huanchaca/Aguapé groups (Litherland et al. 1986; Santos et al. 2005; Geraldès et al. 2014). Collectively, these units characterize the Sunsas-Aguapé province (Teixeira et al. 2010 and references therein). Notably, this province includes the Aguapé Group (1167–1149 Ma; Santos et al. 2005), a transgressive–regressive platform sequence (Alvarenga & Saes 1992; Saes & Leite 1993) that unconformably overlies the plutonic–volcanic rocks of the Rio Alegre terrane (Brazil). This sequence occurs discontinuously along more than 500 km between the NE and eastern margins of the Paraguaí terrane in Bolivia (see Section 3), where it is locally named as the Huanchaca Group (Litherland & Power 1989; see Fig. 1). Additional U–Pb provenance studies for the Aguapé Group indicated a wide age range for the main sources of the sedimentary protholiths, compatible with the geologic framework of the RNJ and RSI provinces (Geraldès et al. 2014; Rizzotto et al. 2014). It is worth mentioning that the Huanchaca Group is intruded by mafic sills that are part of the 1.11 Ga

Rincón del Tigre-Huanchaca LIP (Teixeira et al. 2015) that marks the youngest mantle plume activity in Amazonia predating Rodinia breakup (Lima et al. 2012; Teixeira et al. 2015).

Finally, the SA collision is age correlative with anorogenic igneous activity, deformation and metamorphic imprints over the already tectonically stable crust (Jauru terrane) such as the 0.90 Ga Guapé granite (see Fig. 1) and shear zones (not shown) active between 0.93 and 0.91 Ga. In a similar manner the Rondonian Tin Granites (0.97 – 0.92 Ga), and contemporary mafic dykes and rift basins in the state of Rondônia (RSI province) are also tectonically related with the outboard SA event (Bettencourt et al. 1999; Ruiz 2005; Teixeira et al. 2010). In a global context, the SA orogeny is continuation of the Grenville collision associated with the assembly of Rodinia (e.g. Teixeira et al. 2010 and references therein). However,

alternative views concerning the position of Amazonia in this time frame have been proposed (e.g. Sadowski & Bettencourt 1996; Boger et al. 2005; Tohver et al. 2006; Cordani et al. 2009; Elming et al. 2009; Johansson 2009).

Table 1 presents a summary of the tectonic–magmatic evolution of the SW portion of the Amazonian Craton, with particular emphasis on the Mesoproterozoic igneous activity within the Jauru terrane that has important bearing on our work.

4. Methodology

Sample processing for the SC and NL was carried out in the Jack Satterly Geochronology Laboratory at the University of Toronto. In each case, all aspects of the analytical procedure were followed similar to that described by Söderlund & Johansen (2002), in which a small amount of sample (approximately 200 g) was finely ground and passed over a shaking water (Wilfley) table until a heavy mineral concentrate was produced. Best quality baddeleyite crystals were then handpicked under alcohol using a binocular microscope, and selected for analysis. Fractions were washed and loaded into Teflon capsules along with hydrofluoric acid and a ^{205}Pb – ^{235}U isotopic tracer, and dissolved at 200°C over 3–4 days following the general procedures reported by Krogh (1973). Estimates of fraction weights were made using measurements from digital imaging and the density of baddeleyite. The samples were converted to salts using 3N-HCl, and loaded on outgassed Re filaments into a VG354 mass spectrometer using Si gel and phosphoric acid. Isotope ratios were measured using a Daly detector equipped with digital ion counting. System deadtime corrections during this period were 20 ns for Pb and U. Corrections for Daly mass bias were 0.07%/AMU (atomic mass unit), and thermal mass discrimination was taken to be 0.10%/AMU. Uranium–lead blanks in the laboratory normally average about 0.5 pg for Pb and 0.1 pg for U. Plotting and data regressions were carried out using the algorithms and software (Isoplot 3.0) developed by Ludwig (2003). All errors described here and in the plots (including error ellipses and calculated ages) are provided at the two-sigma level of uncertainty. More complete details of the separation and analytical details are provided in Reis et al. (2013).

Baddeleyite blades and fragments occur as a very rare, trace accessory phase in both samples, and the recovered yield from each diabase/gabbro was low. Moreover, as shown in Table 2, isolated baddeleyite crystals from these samples have very low concentrations of uranium, and, combined with their age, consequently very low levels of radiogenic Pb (ca. 20 pg for all fractions). Measured $^{207}\text{Pb}/^{235}\text{U}$ ratios are disproportionately affected by these factors and as a result have relatively large uncertainties.

5. Geologic setting of the SC mafic sills

Profuse tholeiitic sills intrude a local flat-lying sedimentary sequence that is formed by non-deformed pelites, sandstones, as well as conglomerates (Fig. 2(A)). This cratonic sequence overlies the NE fringe of the Jauru terrane nearby the towns of Rio Branco and SC. This local sedimentary sequence has been traditionally considered age equivalent with the westward Aguapé Group (SHRIMP U–Pb age of ca. 1.15 Ga in diagenetic xenotime; Santos et al. 2005). Geraldès et al. (2014) studied (by means of U–Pb zircon detrital ages) one outcrop of the pelitic-sandstone sequence occurring nearby the towns of SC and Rio

Table 2. ID-TIMS U–Pb baddeleyite isotopic data for SC-100 and NL-14 samples.

Fraction	Description	Weight (mg)	U (ppm)	Pb ⁱ (pg)	Pb _c (pg)	Th/U	²⁰⁶ Pb/ ²⁰⁴ Pb	²⁰⁶ Pb/ ²³⁸ U	²⁰⁷ Pb/ ²³⁵ U	²⁰⁷ Pb/ ²⁰⁶ Pb	Ages (Ma)		Disc (%)								
											²⁰⁶ Pb/ ²³⁸ U	²⁰⁷ Pb/ ²³⁵ U		²⁰⁷ Pb/ ²⁰⁶ Pb	²⁰⁷ Pb/ ²³⁵ U						
SC-100	SC gabbroic sill																				
Bd-1	11 Medium-brn bl and frags	0.1	7	17.65	0.4	0.139	2698	0.240107	0.0013	3.00076	0.01844	0.090641	0.00028	1387.3	6.8	1407.8	4.	1439.1	5.	4	
Bd-2	15 Medium-brn bl and frags	0.2	6	15.76	3	0.144	1841	0.237539	0.000631	2.96791	0.0146	0.090618	0.000336	1373.9	3.3	1399.4	6	1438.6	8	5	
Bd-3	15 Pale brn bl and frags	0.2	6	14.27	0.5	0.213	1334	0.241873	0.000709	3.02427	0.01956	0.090684	0.000481	1396.4	3.7	1413.8	3.	1440	7.	3	
NL-14	NL diabase dyke																				
Bd-1	6 Medium-brn bl and frags	0.1	5	12.88	0.7	0.065	1216	0.245799	0.00236	2.98949	0.11261	0.088209	0.002904	1416.8	12.2	1404.9	4.	1387	10.	4	
Bd-3	20 Medium-brn bl and frags	0.1	9	16.57	0.9	0.085	1643	0.229857	0.00115	2.79917	0.0344	0.088522	0.000904	1333.8	6	1355.3	9	1389.5	1	4	
Bd-4	20 Medium-brn bl and frags	0.1		13.63	0.9	0.063	1269	0.239975	0.001809	2.90034	0.08485	0.087656	0.002239	1386.6	9.4	1382		1375		–	

Notes: All analyzed fractions represent best quality, fresh grains of baddeleyite. Abbreviations: brn, brown; bl, blades; frags, fragments. Pbⁱ is total amount (in picograms) of Pb. Pb_c is total measured common Pb (in picograms) assuming the isotopic composition of laboratory blank: 206/204 = 15.612; 208/204 = 39.360 (errors of 2%). Pb/U atomic ratios are corrected for spike, fraction, blank and, where necessary, initial common Pb. ²⁰⁶Pb/²³⁸U is corrected for spike and fractionation. Th/U is model value calculated from radiogenic ²⁰⁶Pb/²⁰⁶Pb ratio and ²⁰⁷Pb/²⁰⁶Pb age, assuming concordance. Disc. (%) is percent discordance for the given ²⁰⁷Pb/²⁰⁶Pb age. Uranium decay constants are from Jaffey et al. (1971).

Branco (see above) in the attempt to compare with the westward Aguapeí Group. According to these authors, this local sedimentary unit is significantly older than the Aguapeí Group, as supported by the youngest age mode at 1.54 Ga, though the detrital population includes zircon grains as old as 1.9 Ga. The 1.54-Ga age mode is a match with the nearby

Cachoeirinha rocks (see Section 3). It is important to mention that the maximum age of deposition for the pelitic-sandstone sequence is also consistent with the local intrusive relationships of the 1.42-Ga Rio Branco rapakivi suite (see Section 3), given by a xenolith (pelite) in a granite outcrop (Ruiz 2005; Fig. 2(B)).

The SC sills are 1 – 5 m thick and regionally have intrusive contacts that are concordant to the bedding of the local sedimentary sequence (Fig. 2(C),(D)). The grain size ranges from fine to medium (Fig. 2(E)), and the bulk composition varies from gabbro to quartz-monzodiorite (Elming et al. 2009 and references therein). Cumulate and ophitic textures may be present. Plagioclase (labradorite-andesine) occurs commonly in the matrix as tabular euhedral to subhedral crystals and less commonly as phenocrysts up to 5 cm. The primary mineralogy consists of plagioclase, orthoclase, clinopyroxene (augite/titanoaugite or pigeonite), quartz and, rarely, olivine. Hornblende and tremolite-actinolite result from alteration of pyroxene, and biotite and chlorite from alteration of both minerals. Sericite and saururite result from alteration of plagioclase. Accessory minerals are frequently represented by titanite, magnetite, ilmenite and pyrite, zircon and as utilized here, baddeleyite (Elming et al. 2009). Geochemical data indicate the sills can be classified as tholeiitic basalts. From a tectonic point of view, the available trace element data are consistent with their interpretation as intraplate continental basalts (Ruiz 2005; Lima 2013). K–Ar dating on plagioclase and whole rock of the sills yielded ages between 1015 ± 17 and 875 ± 21 Ma (Ruiz 2005 and references therein). Previously published ⁴⁰Ar/³⁹Ar determinations for the sills yielded ages of 1035 ± 3, 1025 ± 8 and 981 ± 2 Ma. The latter (well-defined plateau age) was interpreted to represent the cooling age of the intrusive episode (Elming et al. 2009). These authors also report a paleomagnetic pole for these rocks, suggesting a possible tectonic reconstruction in which NW Amazonia was attached to eastern Laurentia (close to Greenland) at 981 Ma. However, the SC sills are more likely part of the older Rio Branco bimodal suite, as observed by hybrid magma mixtures between the rapakivi rocks, granophyres and gabbros (see above). Given these uncertainties, we obtained a U–Pb baddeleyite age for one SC sill (SC-100 sample) in order to define a precise igneous crystallization age (discussed later).

6. Geologic setting of the NL dyke swarm

The NNW trending NL mafic dyke swarm (100 km long and 20 km wide), originally named as Rancho de Prata intrusive suite (Ruiz 2005) occurs along the eastern side of the 0.96 – 0.91 Ga Aguapeí aulacogen (see Fig. 1). The latter unit and nearby shear zones (not shown) as old as 0.93 – 0.91 Ga have been considered as the late tectonic imprints of the SA collision over the Jauru crystalline basement – the proto-cratonic margin (see Teixeira et al. 2010 for review). Some NL dykes transect the NL syntectonic pluton dated at 1462 ± 12 Ma (Fig. 3(A),(B)) which is ascribed to the Pindaituba suite. This suite is widespread in the central area of the Jauru terrane. Furthermore, the Pindaituba suite is age-equivalent with the Santa Helena batholith to the

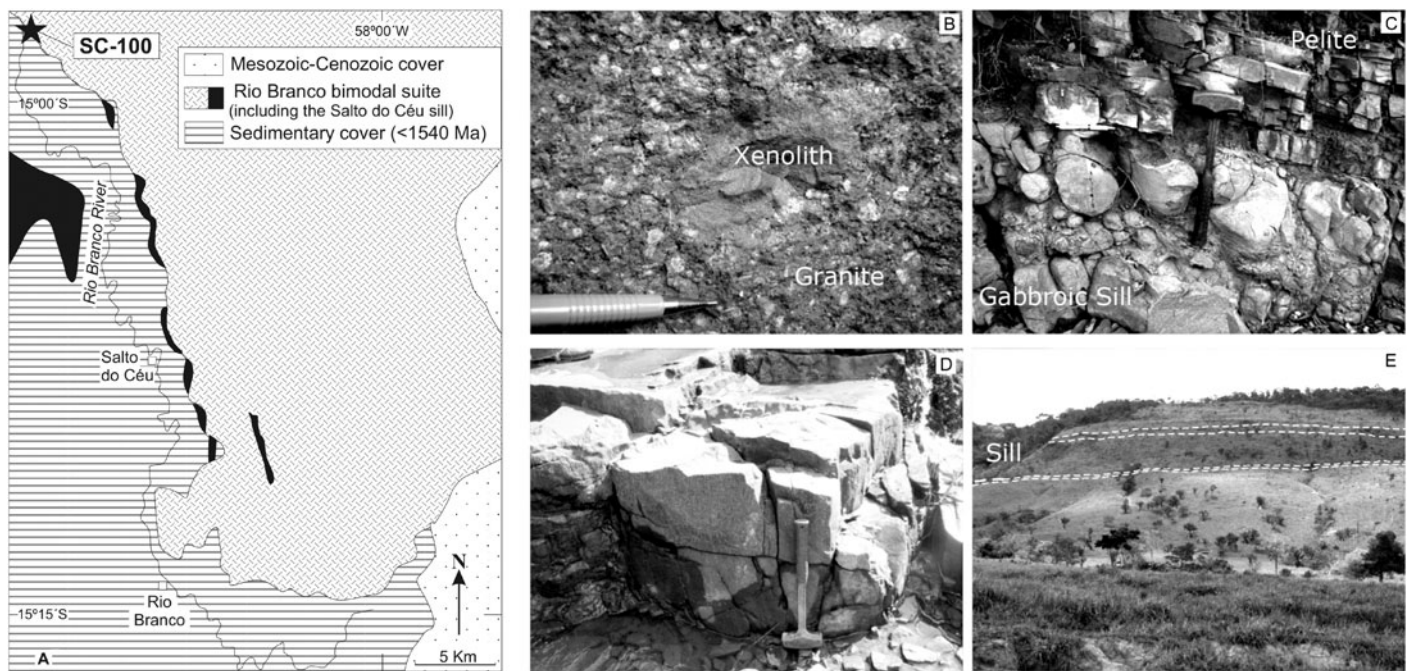


Fig. 2. A. Geologic framework of the Rio Branco region showing the areal extent of the SC mafic sills, the adjoining platform cover and the Rio Branco rapakivi suite. The sampling site is also shown (star). B. Pelitic xenolith in rapakivi granite (Rio Branco suite). C. Outcrop of the SC sill (bottom) with sharp contact with an undeformed pelitic-sandstone sequence nearby the town of SC. D. Overview of the SC sills in the Rio Branco area. The hill contains intercalations of the sills (dashed lines) that are concordant to the bedding of the local metasedimentary sequence. Rapakivi rocks of the Rio Branco suite occurs on the top of the hill. See text for details.

east, and both were geotectonically inserted into the RSI province (Geraldes et al. 2001, 2014; Bettencourt et al. 2010a).

According to Girardi et al. (2012), the NL dykes display an N30–40W trend, though many outcrops are aligned boulders or blocks (Fig. 3(C)). The dykes have thickness ranging from 50 cm to 30 m (most of them are about 3 m thick), and show vertical to subvertical dips. The NL dykes are classified into three coeval petrographic groups of basaltic composition (diabase, metadiabase and amphibolite) due to the emplacement mechanism under transpression according to field observations (Correˆa da Costa et al. 2009). The diabase dykes present intergranular, subophitic to ophitic textures, and are constituted by plagioclase, augite and minor enstatite. Quartz, primary amphibole, apatite, biotite, titanite, epidote and opaque minerals are common accessory phases. The metadiabases are mineralogically similar to the diabases, but the latter present granophyric intergrowths whereas pyroxene uralitization is typical for the metadiabases.

The dykes have tholeiitic affinity, and are basaltic in composition. Rb–Sr whole rock analyses using all petrographic groups of the swarm yielded a best-fit isochron age of 1380 ± 32 Ma (Correˆa da Costa et al. 2009). $^{40}\text{Ar}/^{39}\text{Ar}$ analyses in biotite from one amphibolite dyke intruding the NL granite yielded plateau ages ranging from 1360 to 1385 Ma interpreted as the approximate time of emplacement (M.S. D’Agrella-Filho, written communication, 2009). More recently, SHRIMP U–Pb zircon ages for two metadiabase dykes of this swarm yielded 1440 ± 13 and 1432 ± 20 Ma (M.S. D’Agrella-Filho, written communication, 2010). Considering that zircons in mafic rocks are not common and may be inherited, we instead focused on

recovering baddeleyite crystals for TIMS U–Pb dating of one pristine diabase dyke of the NL swarm.

From a tectonic perspective, Girardi et al. (2012) interpreted the NL dykes to be coeval with the accretion of the Alto Guaporé belt (1.47 and 1.43 Ga; Rizzotto & Hartmann 2012), as a result from the outboard slab subduction below the Jauru crust. In other words, the NL dyke swarm may mark a contemporary inboard extensional activity induced by a NW–SE extensional/compressional stress (intraplate conditions) over the thickened and rigid Paleoproterozoic crust. Indeed, the reported trace element patterns and ratios are consistent with fractional crystallization of evolved melts derived from heterogeneous, enriched mantle sources in a slab subduction-metasomatic mixing model, in coherence with the $^{143}\text{Nd}/^{147}\text{Sm}$ values ranging from $\text{p}0.9$ to $\text{p}2.6$ and coupled $^{147}\text{Sm}/^{143}\text{Nd}$ values between $\text{p}2$ and $\text{p}6$ (Girardi et al. 2012).

7. Results and discussion

We selected one sample each of the SC sills (SC-100; $14858^{\circ}06.200\text{S}$; $58810^{\circ}06.100\text{W}$) and NL dykes (NL-14; $14832^{\circ}42.00\text{S}$; $59828^{\circ}25.00\text{W}$) for U–Pb dating on baddeleyite fractions. Both samples were relatively fine grained (see Fig. 1).

Maximum dimensions of baddeleyites recovered from the SC gabbro sill (SC-100 sample; $14858^{\circ}06.200\text{S}$; $58810^{\circ}06.100\text{W}$) were equally small and challenging to manipulate (average ≈ 25 microns). Nonetheless, three fractions comprising 11–15 crystals each yield consistent U–Pb results, with model $^{207}\text{Pb}/^{206}\text{Pb}$ ages ranging narrowly between 1438.6 and

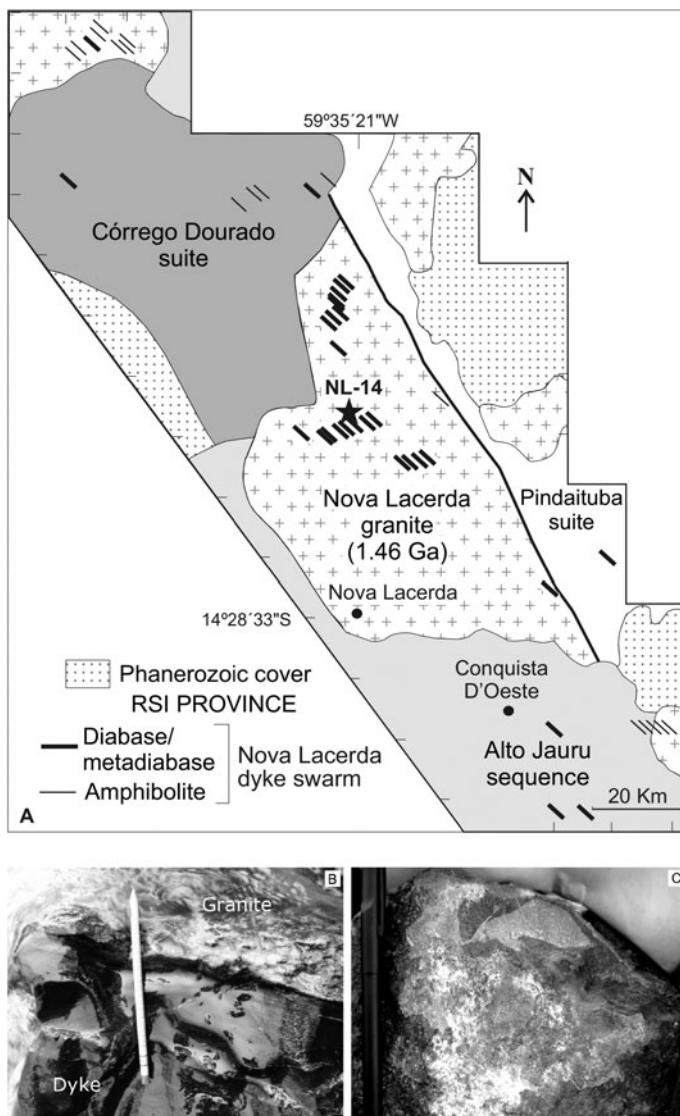


Fig. 3. A. Geological sketch of the NL dyke swarm in the Jauru terrane (adapted from Girardi et al. 2012). Most dykes crosscut the Alto Jauru metasedimentary–metavolcanic sequence, the Córrego Dourado suite (mafic–ultramafic rocks) and the NL granite (Pindaituba suite). The sampling site is also shown (star). B, C. Field aspects of the NL dyke swarm. A key outcrop shows the sharp intrusive contact between a NL dyke and the NL granite (C). RSI, Rondonian–San Ignacio province (1.56–1.30 Ga). See text for details.

1440.0 Ma. A weighted average age for all three fractions of baddeleyite is 1439 ± 4 Ma (Table 2, Fig. 4(A)), which we infer to date the age of emplacement of this gabbro sill. Minor discordance displayed by these analyses may result partly from alpha-recoil effects (e.g. Romer, 2003), or from the incorporation of thin rims of zircon, which are more susceptible to alteration and Pb-loss than baddeleyite. Optically, most of the baddeleyites have a dull lustre (see Fig. 4(A)), which would support the notion of rims, but the small grain sizes preclude a confirmation of this without detailed scanning electron microscope study. Th/U ratios for these fractions (0.14–0.21) are elevated compared to most pure baddeleyites (typically < 0.10), and offer further support of this conclusion. Furthermore, the uniformity of the model $^{207}\text{Pb}/^{206}\text{Pb}$ ages

(Table 2) implies a near zero-aged Pb-loss rather than a secondary Pb-loss event during, for example, Mesoproterozoic docking of the Paragua block or during SA orogeny to the west of the study area [notably this hypothesis is suggested from the Ar–Ar ages reported by Elming et al. (2009) – see Section 5]. Consequently, any zircon rims on baddeleyite may have simply developed during late magmatic stages of igneous crystallization, as local silica activities increased.

Four individual fractions were analyzed for the NL diabase, comprising between 6 and 20 crystals each whose average maximum dimension was only 20 microns. One fraction (Bd-2) contained unacceptably high levels of common Pb and the results were discarded. Three other fractions yielded slightly discordant to slightly reverse discordant results (Table 2, Fig. 4(B4)). The data provide a weighted average $^{207}\text{Pb}/^{206}\text{Pb}$ age of 1387 ± 17 Ma, which is interpreted to represent the best estimate of the primary age of emplacement and crystallization of this NL dyke.

7.1. Intraplate events (1.44–1.42 and 1.39 Ga): global implications

High-quality baddeleyite ID-TIMS U–Pb ages for the SC sill (1439 ± 4 Ma) and the NL dyke (1387 ± 17 Ma) provide clues for two distinct intraplate episodes active in Mesoproterozoic Amazonia, given the age matches with scattered mafic dykes and anorogenic suites in Mato Grosso and Rondônia states. From a tectonic point of view, both episodes affected the proto-

RSI province, as inboard extensional magmatism akin to continental margin collapse, accompanying the syn- to late-orogenic stage of the Alto Guaporé oceanic arc (see Section 3).

In particular, the SC sill is age equivalent with the Rio Branco bimodal suite that crops out nearby (see Fig. 2), and then can be regarded as a mafic component of this suite which is now stated as 1.44–1.43 Ga old. Indeed, according to tectonic discrimination diagrams (Geraldes et al. 2001) both the mafic and felsic rocks indicate a within-plate affinity, whilst they are emplaced into a local pelitic-sandstone platform cover sequence according to field relationships (see Section 4). Anorogenic activity likely coeval with the SC sill within the Jauru terrane are the Figueira Branca mafic–ultramafic complex and the coeval Indivaí gabbro (1429 ± 3 to 1416 ± 7 Ma), as well as the Nova Guarita dyke swarm (1418.5 ± 3 Ma). The latter occurs to the north, ca. 700 km away from the studied area.

The significantly younger NL dyke (1387 Ma) is compatible within error with a previous published Rb–Sr isochron (1380 ± 32 Ma) using several outcrops of the NL dyke swarm. Notably the 1387 Ma age is match with the anorogenic Teotônio and Santo Antônio suites that occur in the state of Rondônia, again far away from the study area – see Section 3. However, the NL dykes show trace element patterns and ratios that are consistent with fractional crystallization of evolved melts derived from heterogeneous, enriched mantle sources in a slab subduction-metasomatic mixing model (Girardi et al. 2012). This agrees well with the previously published $^{143}\text{Nd}/^{147}\text{Sm}$ values (0.9 to 2.6) and coupled $^{147}\text{Sm}/^{143}\text{Nd}$ values (2 to 26; Corrêa da Costa et al. 2009). Alternatively, the bulk isotopic signature could also be consistent with lithospheric mantle or crustal contamination of an intraplate magma.

7.1.1 Back-arc model. – From a geodynamic perspective, a back-arc model could explain the profuse 1.44–1.42 and 1.38 Ga magmatic episodes observed over the Jauru terrane, given the

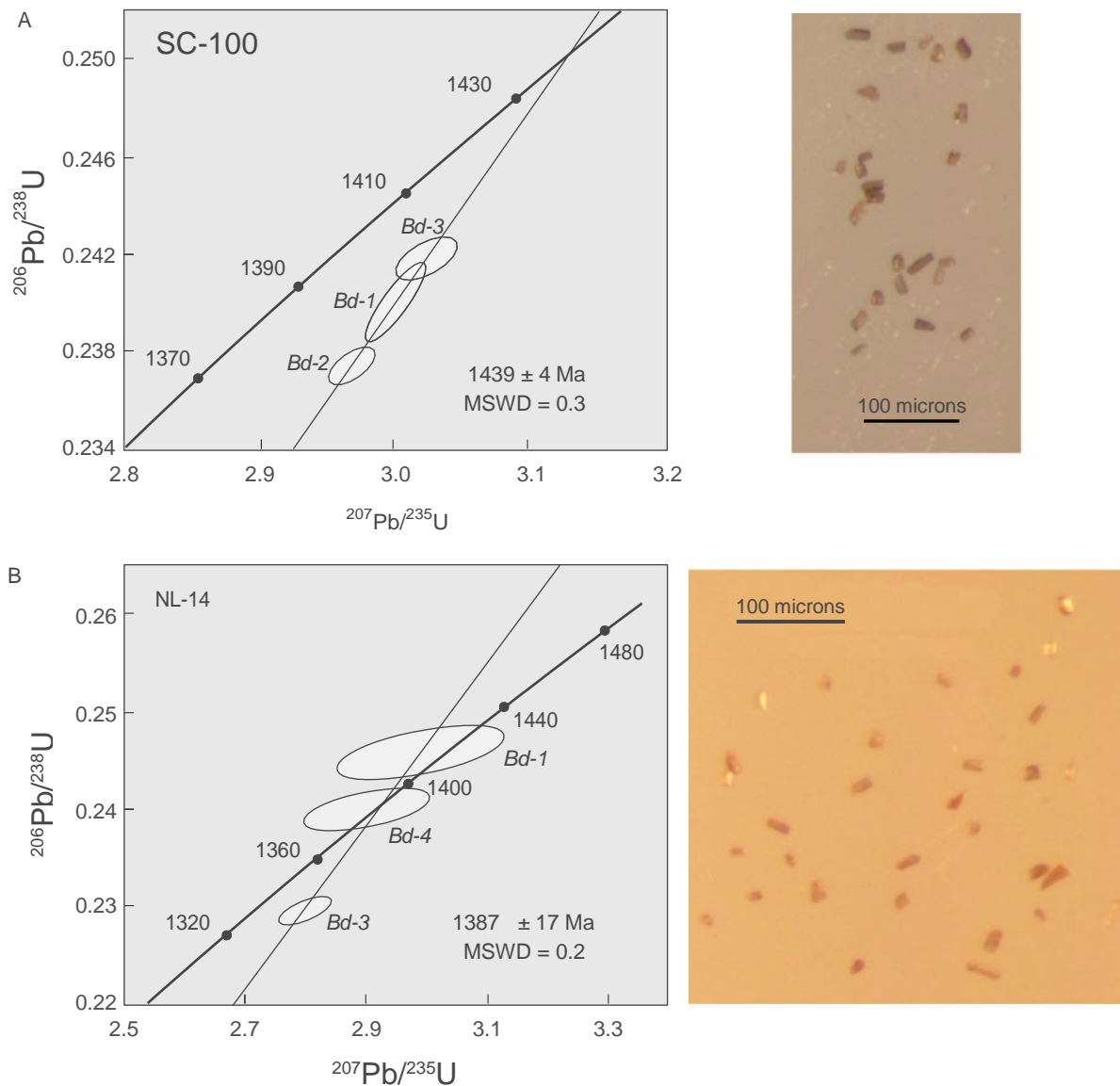


Fig. 4. U–Pb Concordia diagrams showing analytical results for baddeleyites from the selected samples. Respective photographs of the baddeleyites under binocular microscope are also shown: (A) SC gabbroic sill (SC-100); (B) NL diabase dyke (NL-14).

concomitant evolution of the Alto Guapore/Rio Alegre oceanic arc and the coeval Pindaituba and Santa Helena syn-tectonic batholiths occurring in the Jauru terrane. In particular, the back-arc model is consistent with the geochemistry of the Santa Helena batholith which parental magma was probably contaminated by subducted slab fluids (e.g. Girardi et al. 2012). For instance, the Alto Guapore and the Rio Alegre terranes have been collectively interpreted as a result of subduction-related phenomena with concurrent juvenile accretion, highlighted by the Trincheira ophiolite (1470 Ma) and syn- to late-tectonic plutonism (1439–1432 Ma). Notably the latter U–Pb ages are identical to those of the SC sills and nearby anorogenic rocks (e.g. rapakivi rocks) emplaced into the already cratonized continental crust of SW Amazonia (e.g. Rondônia state), including examples in the Paraguá terrane. Therefore, a causal relationship among the subduction-related magmatism and the 1.44–1.42 Ga extension-like igneous episodes is likely. In such a tectonic context, the NL dykes (ca. 1387 Ma) might be a second pulse of back-arc

extension probably formed by evolved melts derived from heterogeneous, enriched mantle sources akin to the Alto Guapore arc, as an inherited feature. This hypothesis is again consistent with the slab subduction-metasomatic mixing model of Girardi et al. (2012) – see Section 6. However, the shape of the subducted slab that could trigger of such episodes inboard the continental margin is still not clear, due to the lack of geophysical information and heat flow simulations among other tools.

7.1.2 Related 1.44–1.42 Ga magmatism extends to central and northern Amazonia. – The ca. 1.44–1.42 Ga magmatism of SW Amazonia is age equivalent with a widespread anorogenic pulse in the central and northern part of the Amazonian Craton (CA; see Fig. 1 inset), ca. 2000 km away from the studied area (Table 3), where, however, earlier rapakivi suites (Mesoproterozoic) are also present (Fraga et al. 2009 and references therein). For instance, the Serra Grande suite (Fig. 5) which is formed by co-magmatic charnockites and rapakivi granites yields U–Pb SHRIMP ages between 1434 ± 11 and 1425 ± 6 Ma (Santos et al. 2011). The

Tapuruquara gabbro complex 500 km away to the southwest could be coeval with this intraplate episode, as suggested by a previously published Rb/Sr mineral isochron age of 1427 ± 189 Ma (Santos et al. 2000). According to these authors, the Tapuruquara intrusion is the westernmost occurrence of a string of 14 gabbro–anorthosite–ultramafite complexes, circular like, that are located in the northwest fringe of the Tapajos-Parima province of Santos et al. (2000). This region is also known as the northwest portion of the RNJ province of Cordani & Teixeira (2007). It is worth mentioning that scattered mafic dykes at the 1.43–1.35 Ga age interval crop over the Amazonian Craton (Fig. 5; see Table 3), as suggested K–Ar apparent ages (Teixeira 1978), although this remains to be proved by precise U–Pb geochronology. Of note the emplacement of these dykes is tectonically controlled by NW and NE trending structures as delineated in Fig. 5. In particular, if the 1.44–1.42 Ga magmatism in central and northern Amazonia is coeval to the Rio Branco rapakivi suite, the SC sill and related intraplate magmatism near the active margin in SW Amazonia (see Fig. 5). Thus, the LIP scale of this event (2000 km across) would not be consistent with standard back-arc origin. Conversely, it could represent more unusual circumstances that caused a much wider zone of back-arc extension, or could suggest the role of a mantle plume; both models are discussed in more detail later.

7.1.3 1.44 – 1.42 Ga magmatism also in Baltica, Eastern Laurentia and West Africa. – There is a remarkable geologic–tectonic correspondence between Mesoproterozoic orogenic events in SW Amazonia, Laurentia (e.g. Pinwarian, early Elsonian), Finland and Sweden – Fennoscandia (e.g. Hallandian–Danopolonian) including the timing of anorthosite–mangerite–charnockite–rapakivi granite (AMCG) magmatism and associated tectonism (e.g. Bogdanova et al. 2001; Söderlund et al. 2002). In particular, the term Hallandian has been addressed for a regional orogenic event (1.47–1.44 Ga) related to convergent processes and coeval mafic and felsic magmatism, outside the 1.1–0.92 Ga Sveconorwegian orogeny in Fennoscandia (e.g. Brander & Söderlund 2009; Ulmius et al., 2015). Collectively the Mesoproterozoic activity is intrusive into a proposed

Paleoproterozoic, global-scale orogen known as Yavapai–Penokean–Svecofennian orogeny (cf. Condie 2007). However, some orogenic segments remain poorly known such as in Amazonia, and the tectonic significance for particular Mesoproterozoic extensional-like intrusive magmatism (i.e. orogenic link, anorogenic) remains unclear. In any case, the global Proterozoic framework is in broad coherence with reconstruction models of the Columbia supercontinent (e.g. Rogers & Santosh 2002; Zhao et al. 2004).

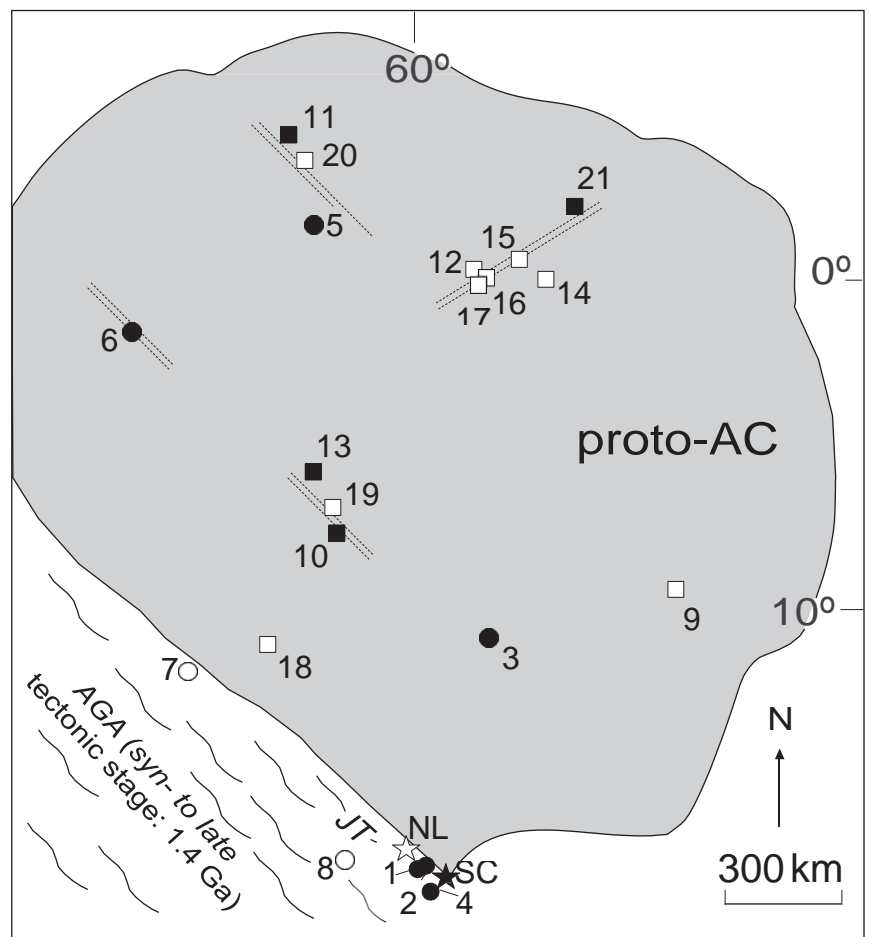
Notably diachronic variation of A-type granitic plutons and mafic dykes (1.6 – 1.1 Ga age span) is outstanding over the Amazonian and Canadian shields (e.g. McLelland 1989; Gower & Krogh 2002; Payolla et al. 2002; Cordani & Teixeira 2007) and the Fennoscandia where the older AMCG complexes (1.65–1.55 Ga) have been interpreted as anorogenic because they typically intrude crustal terranes more than 50 m.y. earlier (e.g. Rämö & Haapala 2005; Dall’Agnol et al. 2012). From the above, the nature and tectonic significance of AMCG suites have long been a key issue for Mesoproterozoic lithosphere dynamics, including dynamic aspects of supercontinent cycles. Regarding Fennoscandia, for example, thermal doming, local lithosphere extension and thinning with consequent partial melting of the lower crust have been suggested as a link for generation of rapakivi magmas (Rämö & Haapala 1995; Andersson et al. 1999). Åhäll et al. (2000) noted the temporal correlation between each stage of younging convergent-margin orogenic events (i.e. continuous active Baltica-Laurentia continental margin) and Mesoproterozoic intracratonic magmatism that was echoed by a phase of rapakivi suite farther inside the cratonic foreland. Alternative views considered that accretion of new crust and collision with concomitant upper mantle disturbance as the causal relationship for such peculiar magmatic episodes that are present in several segments of Columbia (e.g. Bingen et al. 2008; Bogdanova et al. 2008 and references therein). Brander & Söderlund (2009), based on new and compiled data from the widespread mafic and felsic intrusions including anorthosites (1.47 – 1.44 Ga) in the Fennoscandia, interpreted this younger suite of intra-continental intrusions time related

Table 3. Compilation of rapakivi suites, mafic–ultramafic complexes and mafic dykes over the Amazonian Craton time related to the Mesoproterozoic Alto Guaporé belt.

N	Unit/sample	Rock	Material	Age (Ma)	Method	Reference
1	Figueira Branca	Gabbro	Zircon	1425 ± 8 ; 1416 ± 7	U–Pb	Teixeira et al. (2011)
2	Indiavaí	Gabbro	Zircon	1416 ± 7	U–Pb	D’Agrella-Filho et al. (2012)
3	Nova Guarita	Diabase	Biotite	1418 ± 3	Ar–Ar	Bispo-Santos et al. (2012)
4	Rio Branco	Granophyre	Zircon	1423 ± 2	U–Pb	Geraldes et al. (2001)
5	Serra Grande	Granite; Charnokite	Zircon	1434 ± 11 ; 1425 ± 6	U–Pb	Santos et al. (2011)
6	Tapuruquara	Gabbro	Minerals + whole rock	1427 ± 189	Rb–Sr	Santos et al. (2000)
7	Santo Antônio + Teotônio	Granite	Zircon	1373 ± 15 ; 1387 ± 16	U–Pb	Bettencourt et al. (2010b)
8	Alvorada	Granite	Zircon	1389 ± 3	U–Pb	Ruiz (2005)
9	23A66	Gabbro	Whole rock	1439 ± 38	K–Ar	Teixeira (1978)
10	PT26.2	Diabase	Whole rock	1429 ± 16	K–Ar	Teixeira (1978)
11	PT292D	Diabase	Plagioclase	1420 ± 58	K–Ar	Teixeira (1978)
12	PT J8	Diabase	Plagioclase	1420 ± 32	K–Ar	Teixeira (1978)
13	PT36	Diabase	Whole rock	1420 ± 22	K–Ar	Teixeira (1978)
14	TR79	Diabase	Whole rock	1408 ± 50	K–Ar	Teixeira (1978)
15	PT17	Diabase	Plagioclase	1385 ± 39	K–Ar	Teixeira (1978)
16	PT J7	Diabase	Whole rock	1376 ± 19	K–Ar	Teixeira (1978)
17	PT21B	Diabase	Plagioclase	1375 ± 37	K–Ar	Teixeira (1978)
18	PT26.1	Basalt	Whole rock	1366 ± 18	K–Ar	Teixeira (1978)
19	PT18.1	Diabase	Plagioclase	1366 ± 15	K–Ar	Teixeira (1978)
20	CUJ-1	Diabase	Whole rock	1336 ± 65	K–Ar	Teixeira (1978)
21	IMM30C	Basalt	Whole rock	1333 ± 67	K–Ar	Teixeira (1978)

Note: See text for details.

Fig. 5. Cartoon of Mesoproterozoic Amazonia (AC, proto-Amazonian Craton), showing the distribution of selected anorogenic magmatism such as the 1.49 Ga SC sill and the 1.38 Ga NL dykes – black and open stars, respectively. JT, Jauru terrane; AGA, Alto Guapore´ arc. 1, Figueira Branca complex; 2, Indiava´ gabbro; 3, Nova Guarita dyke; 4, Rio Branco rapakivi suite; 5, Serra Grande rapakivi suite; 6, Tapuruquara complex; 7, Santo Anto´nio and Teoto´nio suites; 8, Alvorada granite. Keys: black symbols (1.44–1.42 Ga); open symbols (1.38 Ga). 9–21, roughly contemporary dykes: 1.43 Ga (black squares), 1.35 Ga (open squares). Regional structures (dashed lines) that highlight the tectonic-related dyke emplacement are also shown. See text for details.



with southward convergent-margin processes – highlighted by the Hallandian (ca. 1.45 Ga) events. In other words, these contributions considered an orogenic character for these igneous pulses due to their temporal relationship with distal convergent processes. In particular for the Eastern Grenville province, Gower & Krogh (2002) envisaged that the inboard AMCG plutons, contemporary with the early Elsonian orogeny (1.46–1.42 Ga), was induced by a distal slab flattening event akin to an overridden spreading center, in coherence with the inland absence of calc-alkaline rocks of early Elsonian age.

Regarding Amazonia, furthermore, a model coupling a plume with subduction-related processes could also be plausible to explain the origin of the 1.44-Ga SC sills and coeval rapakivi rocks, such as some analogues that has been described in the world (e.g. see Stott & Mueller 2009 for reference). Indeed such peculiar dynamics could induce contemporary regional extension accompanied by profuse magmatism over the continental margin, as hypothesized here. In this context, the new and compiled data for rapakivi suites and mafic dykes in SW Amazonia (see Fig. 5) suggest that these rocks emplaced as response of an outboard active supra-subduction zone – the Alto Guapore´ oceanic arc (Rizzotto et al. 2014). In this sense, the rapakivi suites and coeval rocks could be considered as an “orogenic link”. Alternatively, when one considers that these rocks were injected into tectonically stable crust they could be interpreted as “anorogenic” from this point of view.

In a global-scale perspective, there is evidence for a growing proto-continental margin (SW Amazonia – Eastern Laurentia – Baltica) during the Mesoproterozoic time frame (e.g. Sadowski &

Bettencourt 1996; Geraldès et al. 2001, 2004a; Tohver et al. 2005; Cordani et al. 2009; So´derlund et al., 2002 and references therein), with consequent inboard (back-arc) intraplate tectonics in Columbia (Nuna) per the mechanisms discussed earlier. This also implies the longevity of this supercontinent during most of the Mesoproterozoic (e.g. Ernst et al. 2008; Bispo-Santos et al. 2012; D’Agrella-Filho et al. 2012). In such model, the SC sills (1.44 Ga) and the NL dyke swarm (1.39 Ga) investigated here could be tectonically linked to a worldwide compressional-related magmatism (on the SW side of Amazonia), where the coeval rocks inside the proto-craton (central and northern Amazonia) could be similarly associated to breakup or attempted breakup of the continental crust. Alternatively the origin of this widespread LIP scale ca. 1.44–1.42 Ga activity over Amazonia could be suggestive of a plume origin and that a portion of the plume spread along the base of the lithosphere and ascended and partially melted in the vicinity of the subduction zone to explain the coeval 1.44–1.42 Ga magmatism near the active margin of SW Amazonia (see discussion of models in Bright et al. 2014; Ernst 2014).

The ca. 1.44–1.42 Ga activity of Amazonia does not have an age match with other crustal blocks except in the NW West African Craton (WAC) where two dated dykes in one Anti-Atlas inlier yielded *in situ* baddeleyite ages of ca. 1416 Ma age (So´derlund et al. 2013). It was concluded that the earlier U–Pb ID-TIMS baddeleyite ages reported for these same dykes (El Bahat et al. 2013) had been biased to an incorrect younger 1380 Ma age by processes related to younger regional overprinting events. Consequently, there is a match between

the 1.42 Ga magmatism of NW-WAC and the ca. 1.44–1.42 Ga magmatism in Amazonia, and these plausibly could be part of the same igneous event. This is in agreement with the reconstruction of WAC and Amazonia assuming the Gondwana fit (e.g. Cordani et al. 2009 and references therein), as well as with the South America-Baltica (SAMBA) reconstruction (Johansson 2009, 2014). Around the world, it has been noticed that there are major LIP events at ca. 1.46–1.45 Ga marking a major breakup stage of Columbia or Nuna (Ernst et al. 2008, 2013). In the context of the conclusion from this paper that the 1.44–1.42 Ga magmatism is widespread in Amazonia, and linked to magmatism in West Africa, Eastern Laurentia and Fennoscandia then a 1.44–1.42 Ga magmatism may also be important a growing Columbia (Nuna) and its breakup.

The significant younger NL dykes yielded an emplacement age with a large uncertainty (1387 ± 17 Ma); therefore, it is uncertain whether it should be correlated with global ca. 1.38 Ga magmatism recognized in many crustal blocks, as summarized in Ernst et al. (2008). If a correlation is made, there is a strong suggestion of a global age match with 1.38–1.39 Ga magmatism in NE Laurentia (northern Greenland), NW Laurentia, northern Siberia (Anabar shield), SE Baltica (southern Urals), Antarctica (Vestfold Hills), Kalahari Craton. It was further proposed that the regions having ca. 1.38 Ga magmatism were originally clustered into nodes: a western Laurentia node possibly linked with the Vestfold Hills (Antarctica) and Kalahari Craton, and a NE Laurentia node linked with northern Siberia and eastern Baltica, and possibly the Congo-Saõ Francisco Craton (Ernst et al. 2008, 2013). In any case, the NL age has the better match with the NE Laurentia node, given the inferred Mesoproterozoic proximity in the SAMBA reconstruction.

7.1.4 Paleomagnetic inferences. – Regarding the Mesoproterozoic paleogeography of Amazonia, D’Agrella-Filho et al. (2012) presented a paleomagnetic pole for the 1415.9 \pm 6.9 Ma Indiavaí gabbro, and considering that this gabbro is coeval to the 1425.5 \pm 8.0 Ma Figueira Branca mafic-ultramafic complex (Teixeira et al. 2011). In this sense, Bispo-Santos et al. (2012) reported a similar paleomagnetic pole for the Nova Guarita dyke swarm (^{40}Ar – ^{39}Ar age of 1418.5 \pm 3.5 Ma) that occurs ca. 600 km to the northwest (10.358S/55.368W; not shown) from the SC sills. Consequently, this implies not only a similar tectonic framework for both paleomagnetic poles but also the bulk rigidity of the continental crust at that time, as hypothesized here. Of note, these two paleomagnetic poles are more consistent with the 1470–1380 Ma poles for Baltica and Laurentia, and consequently are compatible again with the South America (Amazonia) – Baltica “SAMBA” model (Johansson 2009, 2014; Bispo-Santos et al. 2012; Reis et al. 2013). Finally a similar scenario is suggested using the previously published paleomagnetic pole of SC sills and the new 1.44 Ga U–Pb age for the SC sill (D’Agrella-Filho; oral communication 2014). However, additional paleomagnetic studies in Amazonia are still needed to better constrain its position in the Mesoproterozoic frame.

Acknowledgements – The authors acknowledge the support of the National Council of Scientific and Technological Development (# 302917/2009-8; # 479779/2011-2) and the Research Foundation of State of Saõ Paulo, Brazil (# 07/59531-4). The authors thank N. Reis and J.S. Bettencourt for the helpful suggestions that helped the elaboration of the early version of the manuscript. The authors are also grateful to Guest Editor U. Soëderlund, reviewer L. Hartmann and an anonymous reviewer for the final constructive comments that improved this paper. This is a contribution no. 43 of LIPs Supercontinent Reconstruction – Resource Exploration project (<http://www.supercontinent.org>; see also <http://www.camiro.org/exploration/ongoing-projects>).

Disclosure statement

No potential conflict of interest was reported by the authors.

References

- Ahàll, K.-I., Connely, J.N. & Brewer, T.S., 2000: Episodic rapakivi magmatism due to distal orogenesis? Correlation of 1.69–1.50 Ga orogenic and inboard, anorogenic events in the Baltic Shield. *Geology* 28, 823–826.
- Alvarenga, C.J.S. & Saes, G.S., 1992: Stratigraphy and sedimentology of Middle and Late Proterozoic units in the Southeast of the Amazonian Craton. *Revista Brasileira de Geociências* 22: 493–499.
- Andersson, J., Soëderlund, U., Cornell, D., Johansson, L. & Moëller, C., 1999: Sveonorwegian (Grenvillian) deformation, metamorphism and leucosome formation in SW Sweden, SW Baltic Shield: constraints from a Mesoproterozoic granite intrusion. *Precambrian Research* 98, 151–171. doi:10.1016/S0301-9268(99)00048-0.
- Bettencourt, J.S., Leite Jr., W., Ruiz, B., Matos, A.S., Payolla, R.S. & Tosdal, R. M., 2010a: The Rondonian-San Ignacio Province in the SW Amazonian Craton: an overview. *Journal of South American Earth Sciences* 29, 28–46. doi:10.1016/j.jsames.2009.08.006.
- Bettencourt, J.S., Payolla, B.L., Leite Júnior, W.B., Fuck, R.A. & Dantas, E.L., 2010b: LA-MC-ICP-MS U–Pb zircon geochronology and Sm–Nd isotopes of granites of the Teotônio and Santo Antônio intrusive suites, SW Amazonian Craton, Rondônia, Brazil: new insights about crystallization ages and tectonic implications. In *South American Symposium on Isotope Geology*, 6th, Short Papers, CPRM–Brazilian Geologic Survey, Brasília, Brazil, 4 p.
- Bettencourt, J.S., Tosdal, R.M., Leite Jr., W.B. & Payolla, B.L., 1999: Mesoproterozoic rapakivi granites of the Rondônia Tin Province, southwestern border of the Amazonian craton, Brazil – I. Reconnaissance U–Pb geochronology and regional implications. *Precambrian Research* 95, 41–67. doi:10.1016/S0301-9268(98)00126-0.
- Bingen, B., Andersson, J., Soëderlund, U. & Moëller, C., 2008: The Mesoproterozoic in the Nordic countries. *Episodes* 31, 29–34.
- Bispo-Santos, F., D’Agrella-Filho, M.S., Pacca, I.I.G., Janikian, L., Trindade, R.I. F., Elming, S.A., Silva, J.A., Barros, M.A.S. & Pinho, F.E.C., 2008: Columbia revisited: paleomagnetic results from the 1790 Ma Colider volcanics (SW Amazonian Craton, Brazil). *Precambrian Research* 164, 40–49. doi:10.1016/j.precamres.2008.03.004.
- Bispo-Santos, F., D’Agrella-Filho, M.S., Trindade, R.I.F., Elming, S.-Å., Janikian, L., Vasconcelos, P.M., Perillo, B.M., Pacca, I.I.G., Silva, J.A. & Barros, M.A.S., 2012: Tectonic implications of the 1419 Ma Nova Guarita mafic intrusives paleomagnetic pole (Amazonian Craton) on the longevity of Nuna. *Precambrian Research* 196–197, 1–22.
- Bleeker, W. & Ernst, R., 2006: Short-lived mantle generated magmatic events and their dyke swarms: The key unlocking earth’s paleogeographic record back to 2.6 Ga. In E. Hanski, S. Mertanen, T. Råimo & J. Vuollo (eds): *Dyke swarms – indicators of crustal evolution*, 3–26 Taylor and Francis Balkema, London.
- Bogdanova, S.V., Bingen, B., Gorbatshev, R., Kheraskova, T.N., Kozlov, V.I., Puchkov, V.N. & Volozh, Yu.A., 2008: The East European Craton (Baltica) before and during the assembly of Rodinia. *Precambrian Research* 160, 23–45. doi:10.1016/j.precamres.2007.04.024.
- Bogdanova, S.V., Page, L.M., Skridlaite, G. & Taran, L.N., 2001: Proterozoic tectonothermal history in the western part of the east european craton: ^{40}Ar – ^{39}Ar geochronological constraints. *Tectonophysics* 339, 39–66. doi:10.1016/S0040-1951(01)00033-6.
- Boger, S.D., Raetz, M., Giles, D., Etchart, E. & Fanning, C.M., 2005: U–Pb age data from the Sunas region of eastern Bolivia, evidence for the allochthonous origin of the Paragua Block. *Precambrian Research* 139, 121–146. doi:10.1016/j.precamres.2005.05.010.
- Brander, L. & Soëderlund, U., 2009: Mesoproterozoic (1.47–1.44 Ga) orogenic magmatism in Fennoscandia; baddeleyite U–Pb dating of a suite of massif-type anorthosite in S. Sweden. *International Journal of Earth Sciences* 98, 499–516. doi:10.1007/s00531-007-0281-0.
- Bright, R.M., Amato, J.M., Denyszyn, S.W. & Ernst, R.E., 2014: U–Pb geochronology of 1.1 Ga diabase in the southwestern United States: testing models for the origin of a post-Grenville Large Igneous Province. *Lithosphere* 6, 135–156. doi:10.1130/L335.1.
- Condie, K.C., 2007: Accretionary orogens in space and time. In R.D. Hatcher Jr., M.P. Carlson, J.H. McBride & J.R. Martinez Catalan (eds.): *4-D framework of continental crust: Geological Society of America, Memoir* 200, 145–158. Geological Society of America, Boulder, CO.
- Cordani, U.G., Fraga, L.M., Reis, N., Tassinari, C.C.G. & Brito-Neves, B.B., 2010: On the origin and tectonic significance of the intra-plate events of Grenvillian-type age in South America: a discussion. *Journal of South American Earth Sciences* 29, 143–159. doi:10.1016/j.jsames.2009.07.002.
- Cordani, U.G. & Teixeira, W., 2007: Proterozoic accretionary belts in the Amazonian Craton. In R.D. Hatcher Jr., M.P. Carlson, J.H. McBride & J. R. Martinez Catalan (eds.): *The 4D framework of continental crust. GSA memoir*, 297–320. Geological Society of America Book Editors 200, Boulder, CO.
- Cordani, U.G., Teixeira, W., D’Agrella-Filho, M.S. & Trindade, R.I.F., 2009: The position of the Amazonian Craton in supercontinents. *Gondwana Research* 15, 396–407. doi:10.1016/j.gr.2008.12.005.
- Corrêa da Costa, P.C., Girardi, V.A.V., Ruiz, A.S. & Matos, J.B., 2009: Geocronologia Rb-Sr e características geoquímicas dos diques máficos da região de Nova Lacerda e Conquista D’Oeste (MT), porção sudoeste do Craton Amazônico [Rb-Sr geochronology and geochemical characteristics of

- mafic Dykes in the Nova Lacerda and Conquista D'Oeste region, Mato Grosso, SW Amazonian Craton]. *Geologia USP: Série Científica* 9, 115 – 132.
- D'Agrella-Filho, M.S., Trindade, R.I.F., Elming, S.-A., Teixeira, W., Yokoyama, E., Tohver, E., Geraldes, M.C., Pacca, I.I.G., Barros, M.A.S. & Ruiz, A.S., 2012: The 1420 Ma Indivavaí Mafic Intrusion (SW Amazonian Craton): paleomagnetic results and implications for the Columbia Supercontinent. *Gondwana Research* 22, 956 – 973.
- Dall'Agnol, R., Frost, C.D. & Ra'mo', O.T., 2012: IGCP Project 510 A-type granites and related rocks through time: project vita, results, and contribution to granite research. *Lithos* 151, 1 – 16. doi:10.1016/j.lithos.2012.08.003.
- El Bahat, A., Ikenne, M., So'derlund, U., Cousens, B., Youbi, N., Ernst, R., Soulaïmani, A., El Janati, M. & Hafid, A., 2013: U–Pb baddeleyite ages and geochemistry of Dolerite Dykes in the Bas Dra' Inlier of the Anti-Atlas of Morocco: newly identified 1380 Ma event in the West African Craton. *Lithos* 174, 85–98. doi:10.1016/j.lithos.2012.07.022.
- Elming, S.-A., D'Agrella-Filho, M.S., Page, L.M., Tohver, E., Trindade, R.I.F., Pacca, I.I.G., Geraldes, M.C. & Teixeira, W., 2009: A palaeomagnetic and ⁴⁰Ar/³⁹Ar study of Late Precambrian sills in the SW part of the Amazonian Craton: Amazonia in the Rodinia reconstruction. *Geophysical Journal International* 178, 106 – 122. doi:10.1111/j.1365-246X.2009.04149.x.
- Ernst, R.E., 2014: *Large igneous provinces*. Cambridge, UK: Cambridge University Press.
- Ernst, R.E., Pereira, E., Hamilton, M.A., Pisarevsky, S.A., Rodrigues, J., Tassinari, C.C.G., Teixeira, W. & Van-Dunem, V., 2013: Mesoproterozoic intraplate magmatic “barcode” record of the Angola portion of the Congo Craton: newly dated magmatic events at 1505 and 1110 Ma and implications for Nuna (Columbia) supercontinent reconstructions. *Precambrian Research* 230, 103 – 118. doi:10.1016/j.precamres.2013.01.010.
- Ernst, R.E., Wingate, W.T.D., Buchan, K.L. & Li, Z.X., 2008: Global record of 1600 – 700 Ma large igneous provinces (LIPs): implications for the reconstruction of the proposed Nuna (Columbia) and Rodinia supercontinents. *Precambrian Research* 160, 159 – 178. doi:10.1016/j.precamres.2007.04.019.
- Fraga, L.M.B., Dall'Agnol, R., Costa, J.B.S. & Macambira, M.J.B., 2009: The Mesoproterozoic Mucajai anorthosite–mangerite–rapakivi granite complex, Amazonian Craton, Brazil. *The Canadian Mineralogist* 47, 1469 – 1492. doi:10.3749/canmin.47.6.1469.
- Franca, O., Ruiz, A.S., Sousa, M.Z.A., Batata, M.E.F. & Lafon, J.M., 2014: Geology, petrology, U–Pb (shrimp) geochronology of the Morrinhos granite – Paragua terrane, SW Amazonian craton: implications of magmatic evolution of the San Ignacio orogeny. *Brazilian Journal of Geology* 44, 415 – 432.
- Geraldes, M.C., Bettencourt, J.S., Teixeira, W. & Matos, J.M., 2004b: Geochemistry and isotopic constraints on the origin of the Mesoproterozoic Rio Branco anorogenic plutonic suite, SW of Amazonian Craton, Brazil: high heat flow and crustal extension behind the Santa Helena arc? *Journal of South American Earth Sciences* 16, 1 – 14.
- Geraldes, M.C., Heilbron, M.C.P. & Teixeira, W., 2004a: Lithospheric versus asthenospheric source of the SW Amazonian craton A-type granites: the role of the Paleo- and Mesoproterozoic accretionary belts for their coeval continental suites. *Episodes* 27, 1 – 5.
- Geraldes, M.C., Nogueira, C.C., Vargas-Matos, G.L., Matos, R., Teixeira, W., Valencia, V. & Ruiz, J., 2014: U–Pb detrital zircon ages from the Aguapeí Group (Brazil): implications for the geological evolution of the SW border of the Amazonian Craton. *Precambrian Research* 1, 1 – 26.
- Geraldes, M.C., Van Schmus, W.R., Condie, K.C., Bell, S., Teixeira, W. & Babinski, M., 2001: Proterozoic geologic evolution of the SW part of the Amazonian Craton in Mato Grosso state, Brazil. *Precambrian Research* 111, 91 – 128. doi:10.1016/S0301-9268(01)00158-9.
- Girardi, V.A.V., Corre' da Costa, P.C. & Teixeira, W., 2012: Petrology and Sr–Nd characteristics of the Nova Lacerda mantle swarm, SW Amazonian Craton: new insights regarding its subcontinental dike source and Mesoproterozoic geodynamics. *International Geology Review* 54, 165 – 182. doi:10.1080/00206814.2010.510238.
- Gower, C. & Krogh, T.E., 2002: A U–Pb geochronological review of the Proterozoic history of the eastern Grenville Province. *Canadian Journal of Earth Sciences* 39, 795 – 829. doi:10.1139/e01-090.
- Jaffey, A.H., Flynn, K.F., Glendenin, L.E., Bentley, W.C. & Essling, A.M., 1971: Precision measurement of half-lives and specific activities of ²³⁵U and ²³⁸U. *Physics Reviews C* 4, 1889 – 1906.
- Jesus, G.C., Sousa, M.Z.A., Ruiz, A.S. & Matos, J.B., 2010: Petrologia e geocronologia U–Pb e Sm–Nd do Granito Passagem, Complexo Granitoide Pensamiento, SW do Craton Amaz'nico – MT [Petrography and U–Pb and Sm/Nd geochronology of the Passagem Granite, Pensamiento Granitoid Complex, Paragua Terrane, SW Amazonian Craton, Mato Grosso, Brazil]. *Revista Brasileira de Geoci'ncias* 40, 392 – 408.
- Johansson, A., 2009: Baltica, Amazonia and the SAMBA connection – 1000 million years of neighbourhood during the Proterozoic?. *Precambrian Research* 175, 221 – 234. doi:10.1016/j.precamres.2009.09.011.
- Johansson, A., 2014: From Rodinia to Gondwana with the “SAMBA” model—a distant view from Baltica towards Amazonia and beyond. *Precambrian Research* 244, 226 – 235. doi:10.1016/j.precamres.2013.10.012.
- Krogh, T.E., 1973: A low-contamination method for hydrothermal decomposition of zircon and extraction of U and Pb for isotopic age determinations. *Geochimica et Cosmochimica Acta* 37, 485–494. doi:10.1016/0016-7037(73)90213-5.
- Li, Z.X., Bogdanova, S.V., Collins, A.S., Davidson, A., De Waele, B., Ernst, R. E., Fitzsimons, I.C.W., Fuck, R.A., Gladkochub, D.P., Jacobs, J., Karlstrom, K.E., Lu, S., Natapov, L.M., Pease, V., Pisarevsky, S.A., Thrane, K. & Vernikovsky, V., 2008: Assembly, configuration, and break-up history of Rodinia: a synthesis. *Precambrian Research* 160, 179 – 210. doi:10.1016/j.precamres.2007.04.021.
- Lima, G.A., 2013: Magmatismo máfico fissural relacionado à ruptura do Supercontinente Rodínia na porção sul do sudoeste do Craton Amaz'nico. Exame de Qualificação de Doutorado (Unpublished internal report) [Mafic magmatism in the SW portion of the Amazonian Craton: constraints for the Rodinia break-up]. Universidade Federal do Para', Bele'm, Brazil. 78p.
- Lima, G.A., Souza, M.Z.A., Ruiz, A.S., D'Agrella-Filho, M.S. & Vasconcelos, P., 2012: Sills máficos da Suíte Intrusiva Huanchaca – SW do cra'ton Amaz'nico: registro de magmatismo fissural relacionado a ruptura do Supercontinente Rodínia [Mafic sills of the Huanchaca Intrusive Suite (SW Amazonian Cra'ton): record of fissural magmatism related to the break-up of Rodinia]. *Revista Brasileira de Geoci'ncias* 42, 111 – 129.
- Litherland, M., Annells, R.N., Appleton, J.D., Berrange', J.P., Bloomfield, K., Burton, C.C.J., Darbyshire, D.P.F., Fletcher, C.J.N., Hawkins, M.P., Klinck, B.A., Llanos, A., Mitchell, W.I., O'Connor, E.A., Pitfield, P.E.J., Power, G. & Webb, B.C., 1986: The geology and mineral resources of the Bolivian Precambrian shield. *British Geological Survey Overseas Memoir* 9, 153 p.
- Litherland, M. & Power, P.E.J., 1989: The geologic and geomorphologic evolution of Serranía Huanchaca, eastern Bolivia: the legendary “Lost World”. *Journal of South American Earth Sciences* 2, 1 – 17. doi:10.1016/0895-9811(89)90023-0.
- Ludwig, K.R., 2003: *Isoplot/EX 3. A geochronological toolkit for Microsoft Excel*. Special Publication, 4. Berkeley Geochronological Center, Berkeley, CA.
- Matos, J.B., Schorscher, J.H.D., Geraldes, M.C., Sousa, M.Z.A. & Ruiz, A.S., 2004: Petrografia, geoquímica e geocronologia das rochas do Or'geno Rio Alegre, Mato Grosso: um registro de crosta oceânica mesoproterozoica no SW do Cra'ton Amaz'nico [Petrography, geochemistry and geochronology of Rio Alegre orogenic rocks, Mato Grosso: Record of Mesoproterozoic oceanic crust in the SW Amazonian Craton]. *Geologia USP, Série Científica* 4, 75–90. Matos, R., Teixeira, W., Geraldes, M.C. & Bettencourt, J.S., 2009: Geochemistry and Nd–Sr isotopic signatures of the Pensamiento Granitoid Complex, Rondonian–San Ignacio Province, Eastern Precambrian shield of Bolivia: petrogenetic constraints for a mesoproterozoic magmatic arc setting, geologia USP. *Série Científica* 9, 89–117.
- McLelland, J.M., 1989: Crustal growth associated with anorogenic, mid-Proterozoic anorthosite massifs in northeastern North America. *Tectonophysics* 161, 331 – 341. doi:10.1016/0040-1951(89)90163-7.
- Nalon, A.P., Sousa, M.Z.A., Ruiz, A.S. & Macambira, M.B., 2013: Bato' lito Guapore': uma extensa'õ do Complexo Granitoide Pensamiento em Mato Grosso, SW do Cra'ton Amaz'nico [The Guapore' Batholith: an extension of the Pensamiento Granitoid Complex in Mato Grosso, SW Amazonian Craton]. *Brazilian Journal of Geology* 43, 85 – 100. doi:10.5327/Z2317-48892013000100008.
- Payolla, B.L., Bettencourt, J.S., Kozuch, M., Leite, W.B., Fetter, A.H. & Van Schmus, W.R., 2002: Geological evolution of the basement rocks in the east-central part of the Rondonia Tin Province, SW Amazonian Craton, Brazil: U–Pb and Sm–Nd isotopic constraints. *Precambrian Research* 119, 141 – 169. doi:10.1016/S0301-9268(02)00121-3.
- Ra'mo', O.T. & Haapala, I., 1995: One hundred years of Rapakivi Precambrian basement of the Gulf of Finland and granite. *Mineralogy Petrology* 52, 129 – 185.
- Reis, N.J., Teixeira, W., Hamilton, M.A., Bispo-Santos, F., Almeida, M.E. & D'Agrella-Filho, M.S., 2013: Avanavero mafic magmatism, a late Paleoproterozoic LIP in the Guiana Shield, Amazonian Craton: U–Pb ID-TIMS baddeleyite, geochemical and paleomagnetic evidence. *Lithos* 174, 175–195. doi:10.1016/j.lithos.2012.10.014.
- Rizzotto, G.J. & Hartmann, L.A., 2012: Geological and geochemical evolution of the Trinchera Complex, a Mesoproterozoic ophiolite in the southwestern Amazon craton, Brazil. *Lithos* 148, 277 – 295. doi:10.1016/j.lithos.2012.05.027.
- Rizzotto, G.J., Hartmann, L.A., Santos, J.O.S. & McNaughton, N.J., 2014: Tectonic evolution of the southern margin of the Amazonian craton in the late Mesoproterozoic based on field relationships and zircon U–Pb geochronology. *Anais da Academia Brasileira de Ciências* 86, 57 – 84. doi:10.1590/0001-37652014104212.
- Rizzotto, G.J., Santos, J.O.S., Hartmann, L.A., Tohver, E., Pimentel, M.M. & McNaughton, N.J., 2013: The Mesoproterozoic Guapore' suture in the SW Amazonian Craton: geotectonic implications based on field geology, zircon geochronology and Nd–Sr isotope geochemistry. *Journal of South American Earth Sciences* 48, 271 – 295. doi:10.1016/j.jsames.2013.10.001.
- Roberts, N.M.W., 2013: The boring billion? – lid tectonics, continental growth and environmental change associated with the Columbia supercontinent. *Geoscience Frontiers* 4, 681 – 691. doi:10.1016/j.gsf.2013.05.004.
- Rogers, J.J.W. & Santosh, M., 2002: Configuration of Columbia, a mesoproterozoic supercontinent. *Gondwana Research* 5, 5 – 22. doi:10.1016/S1342-937X(05)70883-2.
- Romer, R.L., 2003: Alpha-recoil in U–Pb geochronology: effective sample size matters. *Contributions to Mineralogy and Petrology* 145, 481 – 491. doi:10.1007/s00410-003-0463-0.

- Ruiz, A.R., 2005: Evolução geológica do sudoeste do Craton Amazônico, região limítrofe Brasil-Bolívia e Mato Grosso [Geologic evolution of the SW Amazonian Craton, Brazil-Bolivia border and Mato Grosso] (PhD thesis). State University of São Paulo, Rio Claro, São Paulo, Brazil.
- Ruiz, A.S., Geraldes, M.C., Matos, J.B., Teixeira, W., Van Schmus, W.R. & Schmitt, R., 2004: The 1590 – 1520 Ma Cachoeirinha magmatic arc and its tectonic implications for the Mesoproterozoic. SW Amazonian Craton crustal evolution. *Anais da Academia Brasileira de Ciências* 76, 807 – 824.
- Sadowski, G.R. & Bettencourt, J.S., 1996: Mesoproterozoic tectonic correlations between eastern Laurentia and the western border of the Amazon Craton. *Precambrian Research* 76, 213–227. doi:10.1016/0301-9268(95)00026-7.
- Saes, G.S. & Leite, J.A.D., 1993: Evolução tectono-sedimentar do Grupo Aguapeí, Pro-terozóico Médio na porção meridional do Cráton Amazônico: Mato Grosso e oriente boliviano [Tectono-sedimentary evolution of the Aguapeí Group (Middle Proterozoic) in the southern portion of Amazonian Craton: Mato Grosso and Eastern Bolivia]. *Revista Brasileira de Geociências* 23, 31 – 37.
- Santos, J.O.S., Hartmann, L.A., Gaudette, H.E., Groves, D.I., McNaughton, N.J. & Fletcher, I.R., 2000: A new understanding of the provinces of the Amazon Craton based on integration of field mapping and U–Pb and Sm–Nd geochronology. *Gondwana Research* 3, 453 – 488. doi:10.1016/S1342-937X(05)70755-3.
- Santos, J.O.S., McNaughton, N.J., Hartmann, L.A., Fletcher, I.R. & Salinas, R. M., 2005: The age of the deposition of the Aguapeí Group, Western Amazon Craton, based on U–Pb study on diagenetic xenotime and detrital zircon. In *Latin American Congress, Quito, Ecuador, extended abstracts*, 1–4. Ministerio de Energia y Minas, Quito, Ecuador.
- Santos, J.O.S., Pinto, V., McNaughton, N.J. & Silva, L.C., 2011: Magmatismo Serra Grande em Roraima: formação cognética de granito rapakivi e charnockito em ca. 1430 Ma [Serra Grande anorogenic suite (Roraima state, Brazil): coeval rapakivi granite and charnockite at ca. 1430 Ma]. In *128 Simpósio de Geologia da Amazônia – Boa Vista – Roraima*. CDROM.
- Santos, J.O.S., Rizzotto, G.J., Potter, P.E., McNaughton, N.J., Matos, R.S., Hartmann, L.A., Chemale, F. & Quadros, M.E.S., 2008: Age and autochthonous evolution of the Sunsás Orogen in West Amazon Craton based on mapping and U–Pb geochronology. *Precambrian Research* 165, 120–152. doi:10.1016/j.precamres.2008.06.009.
- Söderlund, U. & Johanssen, U., 2002: A simple way to extract baddeleyite (ZrO₂). *Geochemistry, Geophysics, and Geosystems* 3, 1 – 7. doi:10.1029/2001GC000212.
- Söderlund, U., Ibanez-Mejia, M., El Bahat, A., Ikenne, M., Soullaimani, A. & Youbi, N., 2013: Reply to comment on U–Pb baddeleyite ages and geochemistry of dolerite dykes in the Bas-Draâ Inlier of the Anti-Atlas of Morocco: newly identified 1380 Ma event in the West African Craton by André Michard and Dominique Gasquet. *Lithos* 174, 101 – 108.
- Söderlund, U., Moller, C., Andersson, J., Johansson, L. & Whitehouse, M., 2002: Zircon geochronology in polymetamorphic gneisses in the Sveconorwegian orogen, SW Sweden: ion microprobe evidence for 1.46–1.42 and 0.98–0.96 Ga reworking. *Precambrian Research* 113, 193–225.
- Stott, G. & Mueller, W., 2009: Superior province: the nature and evolution of the Archean continental lithosphere. *Precambrian Research Special Publication (Preface)* 168, 1–3.
- Tassinari, C.C.G., Cordani, U.G., Nutman, A.P., Van Schmus, W.R., Bettencourt, J.S. & Taylor, P.N., 1996: Geochronological systematics on basement rocks from the Rio Negro-Juruena Province (Amazonian Craton) and tectonic implications. *International Geology Review* 38, 161 – 175. doi:10.1080/00206819709465329.
- Tassinari, C.C.G. & Macambira, M.J.B., 2004: A evolução tectônica do Craton Amazônico [Tectonic evolution of the Amazonian Craton]. In V. Mantesso-Neto, A. Bartorelli, C.R. Carneiro & B.B. de Brito-Neves (eds.): *Geologia do Continente Sul-Americano – Evolução da Obra de Fernando Flávio Marques de Almeida*, 471–485. Editora Beca, São Paulo.
- Teixeira, W., 1978: Significação tectônica do magmatismo básico e alcalino na região amazônica (Unpublished master dissertation) [Basic and alkaline magmatism in the Amazon region: tectonic implications]. Institute of Geosciences, University of São Paulo.
- Teixeira, W., Geraldes, M.C., D'Agrella-Filho, M.S., Santos, J.O.S., Sant'Ana Barros, M.A., Ruiz, A.S. & Correia da Costa, P.C., 2011: Mesoproterozoic juvenile mafic-ultramafic magmatism in the SW Amazonian Craton (Rio Negro-Juruena province): SHRIMP U–Pb geochronology and Nd–Sr constraints of the Figueira Branca Suite. *Journal of South American Earth Sciences* 32, 309 – 323. doi:10.1016/j.jsames.2011.04.011.
- Teixeira, W., Geraldes, M.C., Matos, R., Ruiz, A.S., Saes, G. & Vargas-Mattos, G., 2010: A review of the tectonic evolution of the Sunsás belt, SW Amazonian Craton. *Journal of South American Earth Sciences* 29, 47 – 60. doi:10.1016/j.jsames.2009.09.007.
- Teixeira, W., Hamilton, M.A., Lima, G., Ruiz, A.S., Matos, R. & Ernst, R.E., 2015: Precise ID-TIMS U–Pb baddeleyite ages (1110 – 1112 Ma) for the Rincón del Tigre-Huanchaca large igneous province (LIP) of the Amazonian Craton: implications for the Rodinia supercontinent. *Precambrian Research* 265, p. 273 – 285.
- Teixeira, W., Tassinari, C.C.G., Cordani, U.G. & Kawashita, K., 1989: A review of the geochronology of the Amazonian Craton: tectonic implications. *Precambrian Research* 42, 213–227.
- Tohver, E., Teixeira, W., Van Der Pluijm, B.A., Geraldes, M.C., Bettencourt, J.S. & Rizzotto, G., 2006: Restored transect across the exhumed Grenville orogen of Laurentia and Amazonia, with implications for crustal architecture. *Geology* 34, 669–672. doi:10.1130/G22534.1.
- Tohver, E., van der Pluijm, B., Scandola, J.E. & Essene, E.J., 2005: Late Mesoproterozoic deformation of SW Amazonia (Rondonia, Brazil): geochronological and structural evidence for collision with southern Laurentia. *The Journal of Geology* 113, 309 – 323. doi:10.1086/428807.
- Ullius, J., Andersson, J. & Möller, C., 2015: Hallandian 1.45 Ga high temperature metamorphism in Baltica: P–T evolution and SIMS U–Pb zircon ages of aluminous gneisses, SW Sweden. In N. Roberts, G. Viola & T. Slagstad (eds.): *The structural, metamorphic and magmatic evolution of Mesoproterozoic orogens*. *Precambrian Research* 265, 10 – 39.
- Zhao, G.C., Sun, M., Wilde, S.A. & Li, S.Z., 2004: A Paleo-Mesoproterozoic supercontinent: assembly, growth and breakup. *Earth-Science Reviews* 67, 91–123. doi:10.1016/j.earscirev.2004.02.003.



UNIVERSIDADE FEDERAL DO PARÁ
INSTITUTO DE GEOCIÊNCIAS
PROGRAMA DE PÓS-GRADUAÇÃO EM GEOLOGIA E GEOQUÍMICA

PARECER

Sobre a Defesa Pública da Tese de Doutorado de
GABRIELLE APARECIDA DE LIMA

A banca examinadora da Tese de Doutorado de **GABRIELLE APARECIDA DE LIMA** orientanda do Prof. Dr. Moacir José Buenano Macambira (UFPA) e coorientanda da Profa. Dra. Maria Zélia Aguiar de Sousa (UFMT), composta pelos professores doutores Ângela Beatriz de Menezes Leal (UFBA), Leila Soares Marques (USP), Jean Michel Lafon (UFPA), e Claudio Nery Lamarão (UFPA), após apresentação da sua tese intitulada “**SOLEIRAS E ENXAMES DE DIQUES MÁFICOS DO SUL E SUDOESTE DO CRÁTON AMAZÔNICO**” emite o seguinte parecer:

A candidata apresentou contribuição relevante ao conhecimento do tema. O documento está bem apresentado na forma de três artigos submetidos e dois publicados. A apresentação oral foi bem estruturada e de conteúdo relevante para a área de estudo da pesquisa. A candidata mostrou capacidade de síntese e na arguição defendeu positivamente sua tese, demonstrando maturidade científica.

Com base no exposto, a banca examinadora decidiu por unanimidade aprovar a tese de doutorado.

Belém, 19 de agosto de 2016.

Moacir José Buenano Macambira (Orientador – UFPA)

Ângela Beatriz de Menezes Leal (UFBA)

Leila Soares Marques (USP)

Jean Michel Lafon (UFPA)

Claudio Nery Lamarão (UFPA)